University of Southampton

THE MIGRATION AND ACCUMULATION OF RADIONUCLIDES IN THE RAVENGLASS SALTMARSH, CUMBRIA, UK

December 1999

A thesis submitted for the degree of Doctor of Philosophy

Jung-Suk Oh (BSc, MSc)

Faculty of Science

School of Ocean and Earth Science

Southampton Oceanography Centre

ABSTRACT

Profiles of ^{241}Am, ^{137}Cs, ^{238}Pu, $^{239240}Pu$ & ^{241}Pu have been studied in four cores collected from the Ravenglass saltmarsh, Cumbria and one core collected from the Irish Sea, near the effluent pipeline of the Sellafield nuclear reprocessing plant. Major and trace elements have also been measured to look at the effects of sediment composition and any redox controls on element redistribution. In addition, almost one hundred surface scrape samples were collected from the Ravenglass saltmarsh and the same radionuclides were measured to study the lateral distribution of radionuclides. Three of the Ravenglass cores have well preserved the history of Sellafield discharge since the plant became operational in 1952. There are no significant post depositional processes and redox changes for all the cores studied. However, one of the saltmarsh cores collected from the front of the marsh shows that surface erosion has occurred. Surface scrape sample results also show that erosion is a significant process which results in the redistribution of sediments within the marsh.

The core collected from the Irish Sea adjacent to the effluent pipeline shows sediment mixing has operated and these mixed sediments are the main source of material to the saltmarsh. Using the Sellafield discharge records from 1952 onwards, sediment mixing rates have been estimated using a simple mathematical model and they are inferred to be between 80 % and 90 %. Isotopic ratios of Pu isotopes have been compared to those estimated ratios corresponding to particular sediment mixing rates and show good agreement up to 30 cm below the surface. There is less correlation between Sellafield discharge ratios and measured ratios in cores below 30 cm and this may be due to unreliable discharge data or more likely the advective redistribution of material in the saltmarsh. A contribution of ^{241}Am originating from the decay of ^{241}Pu in cores was determined. The ingrown ^{241}Am contributes significantly to the total ^{241}Am measured. Based on the Sellafield discharge record, it is estimated that approximately 46 % of total ^{241}Am in the system has originated from the decay of ^{241}Pu discharged from the plant since 1952. Spatial distribution of radionuclides in the Ravenglass saltmarsh is controlled by sediment accumulation associated with tidal inundation frequency and the clay content in the sediments. Surface erosion also plays a major role in redistributing saltmarsh sediment labelled with older Sellafield discharge within the marsh together with the sediments originated from the River Esk.

ACKNOWLEDGMENTS

I would like to acknowledge the guidance and help of Dr. Ian Croudace, Dr. Phillip Warwick and Dr. Arthur Sanchez during this project. They are not only my supervisors but also good friends. I also thank Mrs. Sonia Bryant (formerly of the Geosciences Advisory Unit) and Mrs. Wink Janes in every aspect while I was in the Geology Department (Sadly, it does not exist anymore). Dr. Rex Taylor, Dr. Andy Milton, Dr. Andy Cundy, Mr. Frank Wigley and Mr. Thorsten Warneke have provided me with every help I needed while I was carrying out this project. There are some Koreans I would like to thank for their wonderful friendship. Dr. Ki-Hong Shin, Mr. Young-Seog Kim, Mr. Kyu-Yong Choi & Mr. Jae-Kyoon Kang are those Koreans always willing to drink a couple of pints with me whenever I was happy or depressed. I am also grateful to my parents for their financial assistance, and grandmother and two lovely sisters for their encouragement. In addition, the support from my parents-in-law and my wife's two sisters and a brother is also very appreciated. All my friends in Korea working hard in their areas have given me motivation to pursue the PhD. Finally, very special thanks to my wife, Ok-Kyung, who always encouraged and supported me in all aspects. She devoted herself to look after three kids (?), me and our lovely two children, Sang-Hoon & Seung-Yeon. Without her support, I would not have completed this project.

감사의 글

Radionuclides 라는 단어조차 생소했던 저를 제자로 삼아 오늘의 결실을 맺도록 모든 면에서 도움을 주신 지도 교수 세 분 (Dr. Ian Croudace, Dr. Phil Warwick & Dr. Arthur Sanchez) 께 우선 감사를 드립니다. 지난 4년 동안 훌륭한 스승이자 좋은 친구였던 세 분에게 무어라 감사의 말씀을 드려야 할지 모르겠습니다. Geosciences Advisory Unit 의 Mrs. Sonya Bryant, Mrs. Wink Janes, Dr. Andy Cundy 그리고 ICP-MS LAB의 Dr. Andy Milton, TIMS LAB의 Dr. Rex Taylor, 같이 실험실에서 동고동락 했던 Frank, Thorsten, 모두들 제 기억 속에 평생 남아있을 분들입니다. 5년이 조금 넘는 Southampton의 생활에서 항상 도움을 주셨던 많은 한국 분들도 잊을 수가 없을 것입니다. 즐거울 때나 우울할 때 함께 술 잔을 기울이며 좋은 충고를 아끼지 않았던 신 기홍 박사, 김 영석 학형, 최 규용 군에게도 깊은 감사를 드립니다. 그리고 같이 학위를 시작했으나 개인적인 사정으로 일찍 귀국해야만 했던, 그리고 철 없던 저에게 공부하는 자의 마음가짐을 깨우쳐 주었던 강 재균 학형에게도 미안한 마음과 감사한 마음을 같이 전합니다. 비록멀리 떨어져 있었지만 항상 마음 속 한 구석을 차지하고 있었던 한국의 친구들과 학부시절의 교수님들께도 고마움을 표하고 싶습니다. 못난 자식 걱정을 하시면서 모든 면에서 도와주신 부모님과 할머님 그리고 정수, 현수 두 동생들에게도 무엇으로 감사함을 전해야 할지 모르겠습니다. 항상 보잘것 없는 사위를 걱정해 주신 장인, 장모님과 은경, 옥 처제 그리고 늦게나마 공부에 재미를 붙인 처남 태영에게도 감사한 마음을 전합니다. 끝으로 자신을 희생하며 못난 남편을 보살펴 준 사랑하는 아내와 상훈, 승연 두 아이들에게 이 부족한 논문을 바칩니다.

CONTENTS

LIST OF FIGURES

LIST OF TABLES

Chapter 1. Introduction

CHAPTER 1

1. Introduction

1.1. Introduction to the study

This project is concerned with an examination of the spatial and vertical distribution of anthropogenic radionuclides (such as ^{241}Am, ^{137}Cs, Pu & U isotopes etc.) and their migration and accumulation in saltmarsh surface sediments and sediment cores of a macrotidal estuary. One subtidal core collected from the Irish Sea adjacent to the effluent pipeline is also analysed for comparison purposes. The Ravenglass saltmarsh (see Figure 1-1), which is ungrazed and located at the mouth of the Esk estuary, west Cumbria, was chosen as a research site since it is well known to have significant activities of various radionuclides originating from the Sellafield reprocessing plant. Many studies have been carried out on this particular saltmarsh, the Irish Sea, the Scottish coasts and surrounding areas of Sellafield in Cumbria in order to estimate the levels of contamination and determine the radiological significance of those artificial radionuclides originated from Sellafield. These studies have shown that radionuclides have accumulated in these environments (Hetherington, 1978 ; Aston & Stanners, 1981a,b,c ; Hamilton & Clifton, 1980 ; Hamilton, 1981 ; Aston & Rae, 1982 ; Aston & Stanners, 1982 a,b,c ; MacKenzie & Scott, 1982 ; Peirson *et al.*, 1982 ; Horrill, 1983 ; Stanners & Aston, 1984 ; Aston *et al.*, 1985 ; Hamilton & Stevens, 1985 ; Hamilton, 1989 ; McDonald *et al.*, 1990, 1992 ; Assinder *et al.*, 1993 ; Livens *et al.*, 1994 ; MacKenzie *et al.*, 1994 ; Pattenden & McKay, 1994). Some of these studies are summarised in Table 1-1. From the results of these works, it is well known that the bottom residual currents and associated particulate matter (i.e. suspended sediments) are the main mechanism responsible for the transportation of particle-associated radionuclides, ^{241}Am and Pu isotopes in particular, to the estuarine and coastal areas.

Although the levels of radionuclide discharge from the Sellafield site are within the authorised limits, large amounts of radiologically important radionuclides have been released from the Sellafield nuclear reprocessing plant (Table 1-2). As shown in Table 1-2, radionuclide discharges from Sellafield are similar or lower (except for ^{241}Am & ^{238}Pu) than releases from atmospheric weapons testing fallout. Nevertheless, since the radionuclides discharged from the Sellafield site are distributed over a smaller area, it is useful to understand how they migrate and accumulate after being introduced into the environment in

Authors	Research sites	Determinants	Objectives
Hetherington (1978)	Ravenglass estuary (Newbiggin)	Pu isotopes	Study of general Pu interaction with factors such as grain size, organic contents, interstitial water etc.
Aston & Stanners (1981a)	East Irish Sea, River Esk, Ravenglass estuary	Pu isotopes	Understanding the behaviour of Pu in the intertidal sediments
Aston & Stanners (1982c)	Ravenglass estuary (40 loactions)	Ce, Cs, Ru & Zr/Nb	Study of gamma emitting fission products in association with particle sizes in surface sediments
MacKenzie & Scott (1982)	Southern Scotland intertidal areas	Cs, Pu, Al, Mn and $CaCO_3$	Study of Cs & Pu behaviour in the intertidal sediments in conjunction with processes such as physical & biological mixing, redox reactions etc.
Peirson *et al.* (1982)	Cumbrian coast & 30 locations in Cumbria grassland	Cs & Pu isotopes	Determination of the pathways and transfer mechanisms of radionuclides
Stanners & Aston (1984)	Ravenglass Estuary (Newbiggin)	Cs & Pu isotopes	The use of Sellafield derived radionuclides for interpreting the geochronology of recent sedimentary deposits
McDonald *et al.* (1990)	Irish Sea	Am, Cs & Pu isotopes, Particle sizes	Assessing the source terms and mechanisms of transport for radionuclides in the Irish Sea
McDonald *et al.* (1992)	Southwest Scotland (46 locations)	Am, Cs & Pu isotopes, Particle sizes	Extending the database on dispersion of Sellafield derived radionuclides to the coast of Southwest Scotland
Assinder *et al.* (1993)	Cumbrian coast	13 determinants including Am, Cs & Pu	Determination of the spatial distributions of studied determinants in Cumbrian coastal sediments
Livens *et al.* (1994)	Ravenglass saltmarsh	Pu isotopes	Understanding the relationship between Pu in the sediment phases and the interstitial waters (K_d determination)
MacKenzie *et al.* (1994)	Saltmarsh on the Solway Coast	Am, Cs, Pu isotopes & ^{210}Pb	Understanding the mechanisms of Sellafield radionuclide dispersal in the Irish Sea, mixing in particular

Table 1-1. Summaries of several works on the Sellafield-derived radionuclides in various environments

order to develop predictive models which could be used to assess their fate in the environment. This modelling can then be used to assess the radiological impact.

(Unit : TBq)

	^{241}Am	^{137}Cs	^{238}Pu	^{239,240}Pu	^{241}Pu
Sellafield 1952-1996* (Gray *et al.*, 1995)	0.5×10^3	4.1×10^4	0.1×10^3	0.6×10^3	2.2×10^4
Weapons testing (Choppin *et al.*, 1996)	0.37	9.1×10^5	3.3×10^2	1.3×10^5	1.7×10^5
Chernobyl accident (IAEA, 1986)	2.0×10^4	3.8×10^4	0.3×10^2	0.6×10^2	5.1×10^3

* The data are not decay-corrected.

Table 1-2. Radionuclides released from different sources

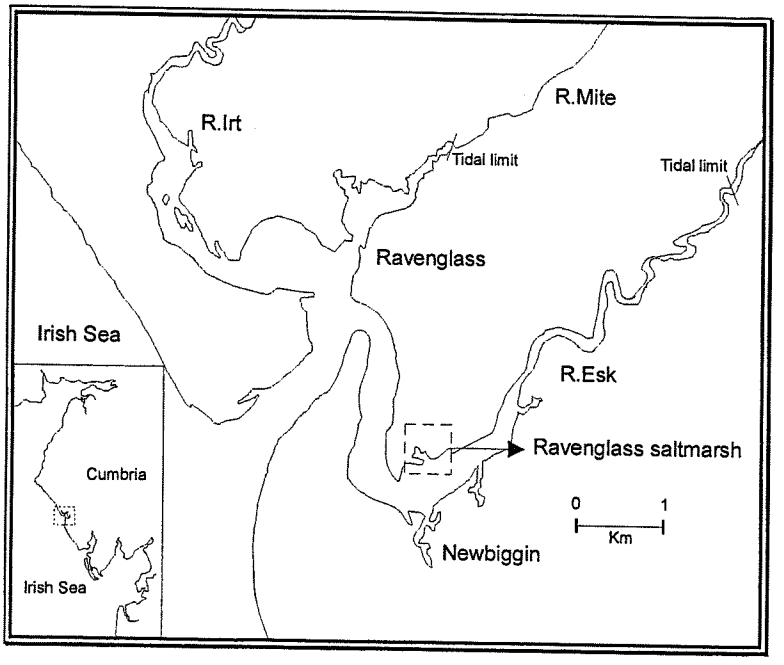

Figure 1-1. Location of the research site (Ravenglass saltmarsh)

1.2. Aims of the study

The first objective of this study is to estimate the scale of any mixing in the sediment source prior to accumulation in the saltmarsh. Sellafield discharges, Am and Pu isotopes in particular, are scavenged by marine sediments and these sediments undergo mixing. A simple mathematical model will be introduced to estimate the mixing of sediments labelled with Sellafield-derived radionuclides from the effluent until they arrive at the Ravenglass saltmarsh. Estimated sediment mixing rates will be applied to calculate sediment accumulation rates using the radionuclides measured (such as ^{241}Am, ^{137}Cs and Pu isotopes). Knowing the sediment accumulation rates in the saltmarsh, ingrown ^{241}Am from the decay of ^{241}Pu will be estimated.

The second objective is to investigate the behaviour of radionuclides after the sediments labelled with Sellafield-derived radionuclides are deposited onto the saltmarsh (post-depositional processes). The influence of oxic and anoxic changes (early diagenesis), bioturbation, tidal inundation and erosion on vertical and spatial radionuclide distributions will be evaluated.

The last objective of this study is to investigate the vertical and spatial distribution of anthropogenic radionuclides (^{241}Am, ^{137}Cs and Pu isotopes including ^{241}Pu) in the ungrazed saltmarsh. Saltmarshes are subject to less physical reworking and bioturbation and therefore tend to record historical events occurring in the environment. By studying the vertical and spatial distributions of radionuclides in the saltmarsh, the behaviour of anthropogenic radionuclides can be understood. In addition, the determination of ^{241}Pu activities is important since its daughter ^{241}Am is one of the major radionuclides contributing to the radiological dose to the general public. There are only limited data reported for ^{241}Pu in the literature. The spatial distribution data for ^{241}Am and ^{137}Cs are compared with those reported in a DOE-funded study by Horrill (1983) to look at the spatial distribution changes of such nuclides over a 17 year period and to identify what controls the spatial distribution of radionuclides in the saltmarsh. Although the levels of discharged radionuclides are well below the authorised limits, it is important to monitor the environment so that the data can be used to verify the safety of the discharges in terms of public health and the quality of the natural environment.

1.3. Background information to the study

1.3.1. Radionuclides of interest in this study

The average life of nuclear fuel in a reactor is about four years and after this time the fuel efficiency decreases because of the accumulation of fission and activation products. As an example, Figure 1-2 shows the consumption of fissile ^{235}U and production of fission products as well as other actinide elements during the fuel utilisation. The consumption of fissile ^{235}U produces new fissile ^{239}Pu and ^{241}Pu from ^{238}U through the neutron capture. Therefore, after an enriched U fuel has operated for some time, both ^{239}Pu and ^{241}Pu contribute to the energy production. Consequently, the ^{235}U consumption rate decreases for the same power production in an ageing fuel. This will help to understand how the radionuclides released in the liquid waste are produced. Most used nuclear fuel is not a waste. It is only 3 % becoming waste after reprocessing. What is left (96 % uranium and 1 % plutonium) can be recycled and reused to make more nuclear fuel. Such reprocessing of spent nuclear fuel is carried out at the Sellafield nuclear reprocessing plant. Radioactive liquid waste containing fission products (such as ^{134}Cs, ^{137}Cs, ^{129}I, ^{90}Sr, ^{99}Tc) as well as transuranic elements has been discharged. There are two major sources of liquid waste from the plant. The one is the process liquors from reprocessing operations and the other is the purge water used in the fuel storage ponds. The nuclides studied here have relatively long half-lives and, therefore, it is necessary to study carefully the fate of such highly persistent elements when they are discharged into the environment. Some brief information on these nuclides is given below.

1.3.1.1. ^{241}Am

^{241}Am, discovered in 1944 by Seaborg *et al.* (1949), is formed from the decay of ^{241}Pu which originates from successive (multiple) neutron captures by ^{239}Pu.

$$^{239}Pu \xrightarrow{n\,r} {}^{240}Pu \xrightarrow{n\,r} {}^{241}Pu \xrightarrow{Beta^{-}\,(14.4\,yr)} {}^{241}Am$$

^{241}Am is both an alpha and gamma emitter with alpha energies at 5.44 MeV (12.8% yield) and 5.49 MeV (85.2% yield), and gamma energy at 59.5 keV (36% abundance) (Browne &

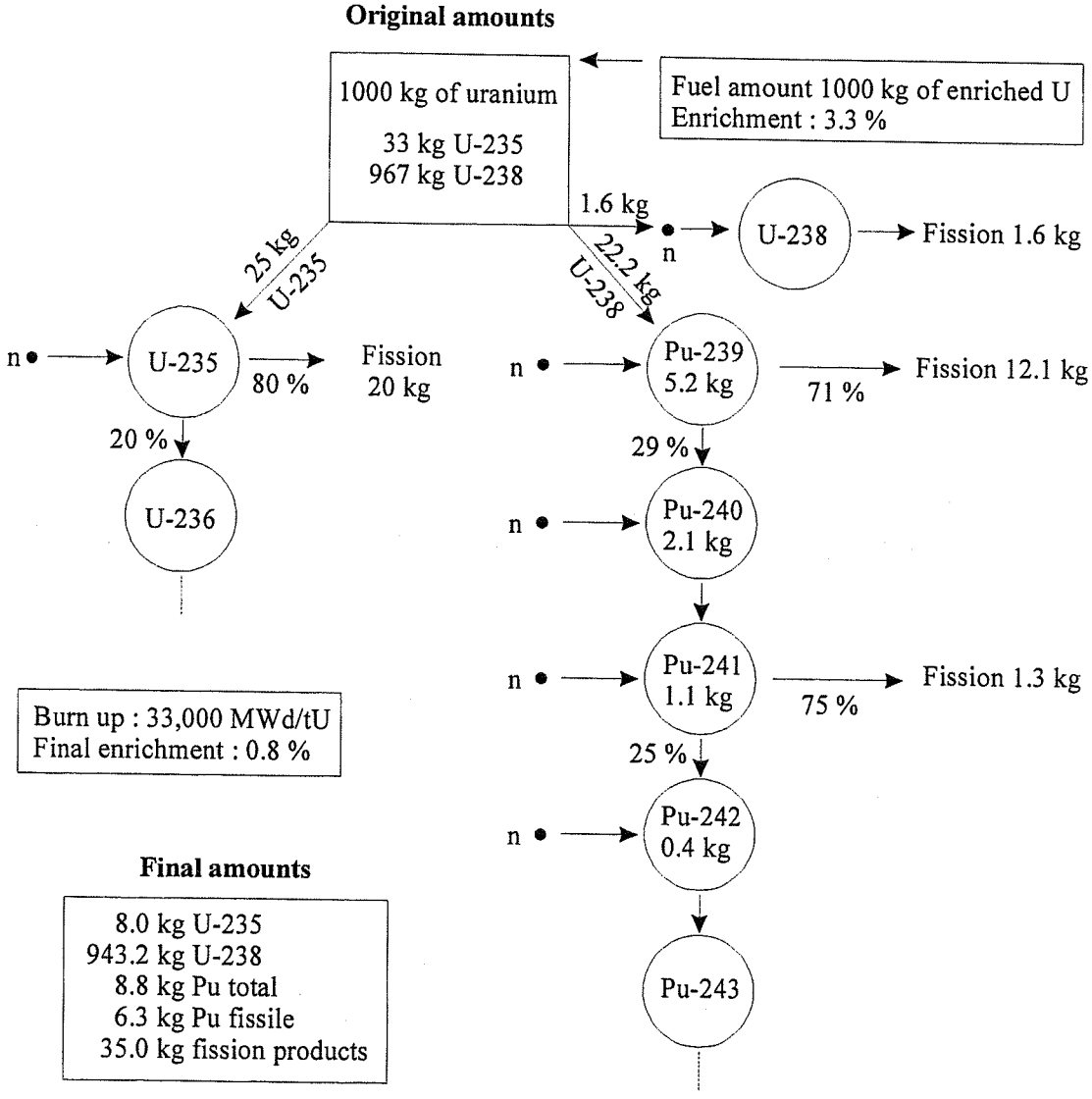

Figure 1-2. Production of radionuclides in a light water power reactor (Choppin *et al.*, 1996)

Firestone, 1986). Am(III) is the major oxidation state stable both in oxidising and reducing environments.

As already mentioned, ^{241}Am is a daughter element of ^{241}Pu which has a relatively short half life (14.4 years). After 5 half lives (approx. 70 years), more than 95% of ^{241}Pu will have decayed to ^{241}Am. Day & Cross (1981) reported the importance of ^{241}Am originating from the decay of ^{241}Pu in the Sellafield discharges. They estimated that approximately 27 % of total ^{241}Am in 1980 had originated from the decay of ^{241}Pu *in situ* in the Irish Sea area based on the discharges from Sellafield. It now is estimated approximately 46 % of the total ^{241}Am is ingrown ^{241}Am. A contribution also occurs from weapons testing. Since large discharges of ^{241}Pu are made to the environment, (for example, discharges of ^{241}Pu from the Sellafield site are approximately 1-2 orders of magnitude higher than for other Pu isotopes (Gray *et al.*, 1995)), it is important to monitor the concentration of ^{241}Pu that eventually will decay to ^{241}Am in the environment. Table 1-3 shows nuclear properties of ^{241}Am and ^{137}Cs.

	^{241}Am	^{137}Cs
Half-life (year)	433	30.3
Method of Production	^{241}Pu daughter Multiple n capture	Fission product
Main Radiation	5.44 MeV, 5.49 MeV (α) 59.5 keV (γ)	661.7 keV (γ) $E_{Ave.}$: 188 keV (β)

Table 1-3. Nuclear properties of ^{241}Am and ^{137}Cs

1.3.1.2. ^{137}Cs

^{137}Cs is a product of nuclear fission (~ 6% fission yield) occurring either within a reactor or during detonation of atomic weapons and has a half life of 30 years. Most ^{137}Cs introduced into the environment originates from weapons testing carried out during the 1950s and 1960s and from discharges from nuclear facilities. A significant recent release of ^{137}Cs in the northern hemisphere, especially Europe was the Chernobyl accident which occurred on 26 April 1986. Since these releases represent distinctive spikes (see Table 1-2), they have been used for chronological applications which depend on minimal post-depositional migration (Ritchie & McHenry, 1990 ; Croudace & Cundy, 1995).

1.3.1.3. Plutonium isotopes

Plutonium is the most important radionuclide among the radionuclides studied since it has three major isotopes (^{238}Pu, ^{239,240}Pu and ^{241}Pu) which show significant activity concentrations in the environments. What makes Pu isotopes more important is their relatively long half-lives and their extreme radiotoxicity. Pu isotopes are classified as the most toxic radionuclides along with ^{90}Sr, Ra and Pa isotopes. The first artificially produced isotope of plutonium was ^{238}Pu. ^{238}Pu has been used as a fuel for satellites because of its power density of 6.8 - 7.3 W/cm^3 (Choppin *et al.*, 1996). ^{239}Pu was discovered in 1941 as the decay product of ^{239}Np. ^{239}Pu is the isotope of major importance because of its potential as a nuclear energy source. ^{239}Pu exhibits high fissibility with both thermal and fast neutrons which means that the sufficient amount of ^{239}Pu will experience an instantaneous nuclear explosion like ^{235}U. Therefore, ^{239}Pu has been used as both nuclear fuel and in nuclear weapons. In addition, Pu isotopes are produced in spent nuclear fuel and can be recycled after being reprocessed. Table 1-4 shows several important plutonium isotopes and their nuclear properties.

Plutonium isotopes found in the environment are mostly anthropogenic, although minute amounts are present in natural uranium. The major source of plutonium isotopes is the atmospheric nuclear weapons testing performed from 1944 to 1963. Approximately 2 × 10^{20} Bq of fission products and smaller amounts of plutonium isotopes were released (Choppin *et al.*, 1996). A second source is the release from nuclear facilities including nuclear power plants and fuel reprocessing plant. In the UK, the Sellafield site is one of the biggest sources of anthropogenic plutonium isotopes into the natural environment. For example, 10.4 kg of plutonium (0.16 kg americium and 0.48 kg neptunium) is produced from one tonne of spent uranium fuel after 10 years cooling time (Morse & Choppin, 1991). Table 1-2 compares the plutonium isotopes released in atmospheric nuclear weapons testing, in the Irish Sea discharged from the Sellafield site and from the Chernobyl accident in 1986. Other sources of plutonium isotopes in the environment are accidental releases from various incidents. One of them is the release of 600 TBq of ^{238}Pu in the Southern Hemisphere when the SNAP-9 satellite's power source burned up in 1964. Pattenden *et al.* (1989) reported that the typical ratio of ^{238}Pu/^{239,240}Pu in soils of the UK that is characteristic of nuclear weapons testing and the satellite burn-up is 0.045. Typical ratios of ^{238}Pu/^{239,240}Pu in the Sellafield

discharges in recent years are in the range of 0.3 - 0.4. Such ratios can be used to identify the sources of Pu isotopes at particular locations. Although the activities of plutonium isotopes released from the nuclear facilities and various incidents do not exceed those of atmospheric nuclear weapons testing, they are much more important since most of those releases are carried out in the localised areas. Therefore, it is essential to understand their fate and behaviour in such localised environments after being released from the source.

	^{238}Pu	^{239}Pu	^{240}Pu	^{241}Pu	^{242}Pu
Half-life (year)	87.74	24100	6563	14.4	376000
Method of Production	^{242}Cm, ^{238}Np daughter	^{239}Np daughter, n capture	Multiple n capture	Multiple n capture	Multiple n capture
Main Radiation	5.457 MeV 5.499 MeV (α)	5.143 MeV 5.155 MeV (α)	5.123 MeV 5.168 MeV (α)	21 KeV (E_{Max}) (β)	4.857 MeV 4.901 MeV (α)

Table 1-4. Nuclear properties of plutonium isotopes

Pu has four major oxidation states (III, IV, V and VI) and behaves differently in the environments with different oxidation states. Reduced Pu (III & IV) is readily associated with particulate matter and oxidised Pu (V & VI) tends to remain in solution. For example, Nelson & Lovett (1978) reported that more than 75 % of the Pu in the Irish Sea water (< 0.22 μm), and less than 10 % of the Pu on particulate matter (> 0.22 μm) was Pu (V & VI). These behaviours are shown in oxic and anoxic water systems (Sanchez *et al.*, 1986, 1991, 1994 ; Choppin & Kobashi, 1990). It is believed that Pu (IV) is the predominant species in the Irish Sea water. It is supported by the findings that more than 95 % of Pu released from the Sellafield site to the Irish Sea are rapidly removed to the seabed, in association with particulate matter (Heatherington, 1978). Pu (III) may be present but Pu (III) shows fast oxidation to Pu (IV) in the presence of carbonate (Nelson *et al.*, 1989). Aston (1980) reported that the hydrolysis of Pu (IV) followed by the irreversible polymerisation to colloidal $Pu(OH)_4$ is potentially the major control of Pu speciation in seawater. He also reported that Pu (VI) may occur as $PuO_2CO_3OH^-$ species.

1.3.2. Distribution coefficients (K_d)

The distribution coefficient (K_d) is used to describe the equilibrium distribution of species between the dissolved and particulate-associated phases. It can be summarised as ;

$$K_d = \left(\frac{\text{Activity per unit mass of particulate}}{\text{Activity per unit mass of solution}} \right)$$

Several authors have reported K_ds for different radionuclides and they are shown in Table 1-5. The K_ds show quite a large variability between authors. Those differences result from the different chemical and physical conditions of each sampling locations. There are concerns over the use of K_d values because of these variations. Sholkovitz (1983) suggested several questions about the use of K_ds and they are summarised by Morse & Choppin (1991). More recently Hamilton (1998) also criticised the concept of K_ds. The summaries by Morse and Choppin (1991) are ;

1. The concept that a K_d represents an equlibrium constant in natural systems generally has not been demonstrated and must be considered highly questionable at best.
2. Natural waters contain particles of various sizes, mineralogies, organic matter content, and skeletal components, the organic matter may be living, partly decomposed, or a residue of decomposition ; skeletal matter may also be in various stages of formation or dissolution.
3. The chemical composition and particle size distribution in coastal waters can show large spatial and temporal variations.
4. In practice the measured K_d values incorporate a suite of geochemical, biochemical, and sedimentological processes including adsorption-desorption, remineralisation, precipitation, redox transformations, bioaccumulation, and ion-exchange etc.

5. Pu can exist in a particular system in as many as three, possibly four, oxidation states, each capable of having very different solubility, complexing, and adsorption properties.
6. Ligands formed in the environments, such as phosphate, bicarbonate, and organic complexants, may alter K_ds.
7. K_d provides a static picture at a point in time of a dynamic set of complex and not necessarily interrelated processes.

	^{241}Am	^{137}Cs	Pu isotopes
Heatherington (1978)	-	-	1.5×10^5
IAEA (1985)	2.0×10^6	1.0×10^3	-
Burton (1986)	2.0×10^6	-	1.1×10^6
Howorth (1989)	2.0×10^6	-	3×10^5
McKay & Pattenden (1989)	-	1.3×10^3	-
Livens *et al.* (1994)	-	-	6.1×10^5
Mitchell *et al.* (1991)	2.3×10^5	-	2.1×10^5
Nelson & Lovett (1978)	-	-	1.0×10^6 (III & IV) 1.0×10^4 (V & VI)
Morse & Choppin (1991)	2.0×10^6	-	1.0×10^5
Pulford *et al.* (1998)	-	2×10^5	-

Table 1-5. K_ds of radionuclides reported in the literature

The use of K_ds has to be subject to the samples being collected from the same environment since they can vary with samples from different locations. In other words, it depends very much on the system being investigated. As suggested above, K_ds are not absolute values but can be used to understand general behaviour of radionuclides in the environments as a first approximation.

1.3.3. Behaviour of ^{137}Cs in saline and freshwater environment

It has been reported that ^{241}Am and Pu isotopes associated with sediments are not readily remobilised by salinity changes between 3 ‰ and 35 ‰ (Burton, 1986). However, the effect of salinity on K_d of ^{137}Cs is not certain as it will vary in freshwater and seawater. This is because when ^{137}Cs is released to a marine environment, it has to compete with

seawater cations for sorption sites and the sorption may take place very slowly. However, when ^{137}Cs is discharged into a freshwater environment, it may easily and quickly sorb onto clay particles (Jacobs & Tamura, 1960). Applying this hypothesis to this work, when ^{137}Cs is released from the Sellafield site, it competes with seawater cations for sorption sites and, at the same time, transports to the possible sinks subject to the surface, bottom and tidal currents. The Ravenglass saltmarsh is one of the sinks for the radionuclides released from the Sellafield site. Some of the ^{137}Cs will sorb onto clay particles during transport. When they are introduced into the estuarine system, the waterbody becomes less saline because of dilution with freshwater. Consequently, there are fewer cations to compete with the sorption sites. More ^{137}Cs is adsorbed onto the clay particles and those ^{137}Cs-tagged clay particles arrive at the Ravenglass saltmarsh and accumulate. With time (months to years), the fixation of ^{137}Cs into clay lattices occurs and ^{137}Cs becomes non-exchangeable. Therefore, if there is no chemically driven redistribution of ^{137}Cs such as redox reactions and diffusion, ^{137}Cs is not mobile in the sediment column. This may be one of the possible explanations for the lower K_d (1.0×10^3) estimated in the Irish Sea and higher K_d (2×10^5) measured in the saltmarsh environment (Pulford *et al.*, 1998).

1.3.4. Behaviour of redox sensitive elements

The majority of chemical changes in saltmarsh environments are redox driven and such reactions can cause element migration to occur in marine and estuarine sediments during early diagenesis. In other words, they strongly depend on the redox environment in the interstitial water - sediment system. The redox environment is largely controlled by the degree to which organic carbon is preserved and subsequently undergoes decomposition by bacterial action (Chester, 1990).

There is a diagenetic sequence of catabolic processes in the sediments, the nature of which depends on the specific oxidising agent that "burns" the organic matter. As organic matter is mobilised in the sediments, it donates electrons to several oxidised components in the interstitial water-sediment complex. Where oxygen is present, it is the preferred electron acceptor. During the diagenetic sequence the terminal electron accepting species alter as the oxidants are consumed in the order of decreasing energy production per mole of organic carbon oxidised. During diagenesis, there is a general sequence so as to utilise the following

electron acceptors (oxidising agents) : oxygen > nitrate > manganese oxides > iron oxides > sulphate (Berner, 1980). The redox processes for Mn are shown in Fig. 1-3. as an example.

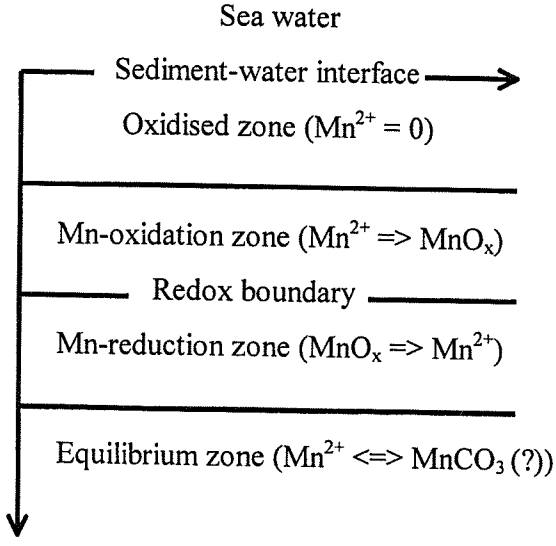

Figure 1-3. Schematic representation of the zonation of marine sediments with respect to Mn diagenesis (Burdige & Gieskes, 1983)

As dissolved oxygen is consumed in the interstitial water, the sediments become reducing and can ultimately become anoxic. The depth at which the oxic/anoxic change occurs depends on the rate of organic carbon supplied and the rate at which it is buried. Therefore the thickness of the surface sediment oxic layer increases from nearshore to pelagic regions as the accumulation rate decreases. The redox boundary which can be used as an indicator of the change between oxidising and reducing conditions in sediments is often accompanied by a colour change, which is generally from red-brown (oxidised) to grey-green or black (reduced). Therefore a range of redox environments in marine sediments can be expressed on the basis of the increasing thickness of the surface oxic layer. For example, under deeper water, the thickness of the surface oxic layer increases so that the progress of the diagenetic sequence decreases. In pelagic sediments, the thickness of the surface oxic layer can extend downwards for several tens of metres (Chester, 1990).

In nearshore sediments that are not deposited under an anoxic or intermittently anoxic water column, diagenesis is dependent on local environmental conditions. Diagenesis can be influenced by some factors such as bioturbation and bottom stirring (Rosental *et al.*, 1986). A major characteristic of nearshore sediments is that the surface oxic layer is usually very thin, and in the anoxic sediment below, diagenesis often progresses to the sulphate reduction stage (Malcolm *et al.*, 1986).

Radionuclide	Half life (yr)	Dating range (yr)	Applications to
^{137}Cs	30	0 - 30	Sediments
$^{239,240}Pu$	2.4×10^4,6.6×10^3	0 - 30	Sediments
^{90}Sr	28	0 - 30	Corals
$^{210}Pb/^{226}Ra$	$22/1.6\times10^3$	0 - 150	Sediments
^{14}C	5730	10^2 - 4×10^4	Sediments, trees, corals, bones
$^{4}He/U$	-	10^2 - 10^5	Corals, groundwater, fossils
$^{230}Th/^{234}U$	$7.5\times10^4/2.5\times10^5$	5 - 10^5	Sediments, nodules, shells, bones, teeth
$^{230}Th/^{232}Th$	$7.5\times10^4/1.4\times10^{10}$	5 - 5×10^5	Sediments, nodules, shells, bones, teeth
$^{231}Pa/^{230}Th$	$3.4\times10^4/7.5\times10^4$	10^4 - 5×10^5	Sediments, nodules, shells, bones, teeth
$^{231}Pa/^{235}U$	$3.4\times10^4/7.1\times10^3$	10^4 - 1.5×10^5	Sediments, nodules, shells, bones, teeth
$^{234}U/^{238}U$	$2.5\times10^5/4.5\times10^9$	10^4 - 10^6	Sediments, corals
^{26}Al	7.4×10^5	10^5 - 3×10^6	Sediments
^{10}Be	1.5×10^6	10^5 - 10^7	Sediments
^{36}Cl	3.1×10^5	Up to 10^6	Nodules, glaciers, meteorites, groundwater
$^{40}K/^{40}Ar$	1.3×10^9	4×10^5 - 10^{10}	Volcanic ash in sediments
^{41}Ca	1.0×10^5	10^4 - 10^6	Fe-meteorites
^{53}Mn	3.7×10^6	10^5 - 10^7	Meteorites
$^{238}U/^{206}Pb$	4.5×10^9		Zircon, uraninite, monazite, lava
$^{235}U/^{207}Pb$	0.7×10^9	10^7 - 10^{10}	Sedimentary rocks, intrusive
$^{232}Th/^{208}Pb$	1.4×10^{10}		Igneous or metamorphic rocks
$^{87}Rb/^{86}Sr$	$4.7\times10^{10}/4.9\times10^9$	10^7 - 10^{10}	Rb-rich minerals
$^{129}I/^{129}Xe$	1.64×10^6	10^6 - 10^{10}	Meteorites, ocean sediments

Table 1-6. Radionuclides used for geochronological purposes (Santschi & Honeyman, 1989)

1.3.5. Establishing a chronology for the marshes

Radioisotopes are widely used for dating purposes in the environmental science. Some of the methods used are given in Table 1-6. The ^{210}Pb method is one of the techniques that can be used for dating sediments within the last 100 - 150 years and this method has been used to estimate the accumulation rates in various environments (Krishnaswami *et al.*,

1971 ; Koide *et al.*, 1972 ; Nittrouer *et al.*, 1979 ; Carpenter *et al.*, 1984 ; DeMaster *et al.*, 1985 ; Siverberg *et al.*, 1986 ; Edgington *et al.*, 1991 ; Chung & Chang, 1995). In addition, artificial radionuclides with well-defined inputs, such as fallout radionuclides from the atmospheric nuclear weapons' testing, the Chernobyl reactor accident and the localised discharge from nuclear facilities, have also been used for dating purposes.

1.3.5.1. ^{210}Pb method

The use of ^{210}Pb was first introduced by Goldberg (1963) for determining the accumulation rate of glacial ice. The decay series of ^{238}U includes gaseous ^{222}Rn, which escapes into the atmosphere from the Earth's surface (Figure 1-4), and eventually form the short-lived lead isotope ^{210}Pb ($t_{1/2}$ = 22.3 yr). The combination of long and short half-lives of the parent ^{226}Ra isotope and its daughters (such as ^{222}Rn, ^{210}Pb) tends to produce a secular equilibrium. However, they are not in equilibrium in the natural environment because of the contribution of ^{210}Pb formed by the decay of ^{222}Rn escaped from the Earth's surface. This is called unsupported ^{210}Pb or excess ^{210}Pb. It has been known that the residence time of ^{210}Pb originated from the ^{222}Rn in the atmosphere is days to months before it is precipitated on the Earth's surface by both wet and dry deposition. Once ^{210}Pb is precipitated on the Earth's surface, it is adsorbed on to the sedimentary particles, deposited on the seabed or surface soil and finally buried. Based on the assumptions that ;

the sediment accumulation is constant over several half-lives
the constant input of excess ^{210}Pb
no significant sediment mixing occurs after deposition

it is possible to estimate the sediment accumulation rates from the decay of excess ^{210}Pb. However, this method only works well if the accumulation rates are greater than 0.03 cm/yr (Appleby & Oldfield, 1992).

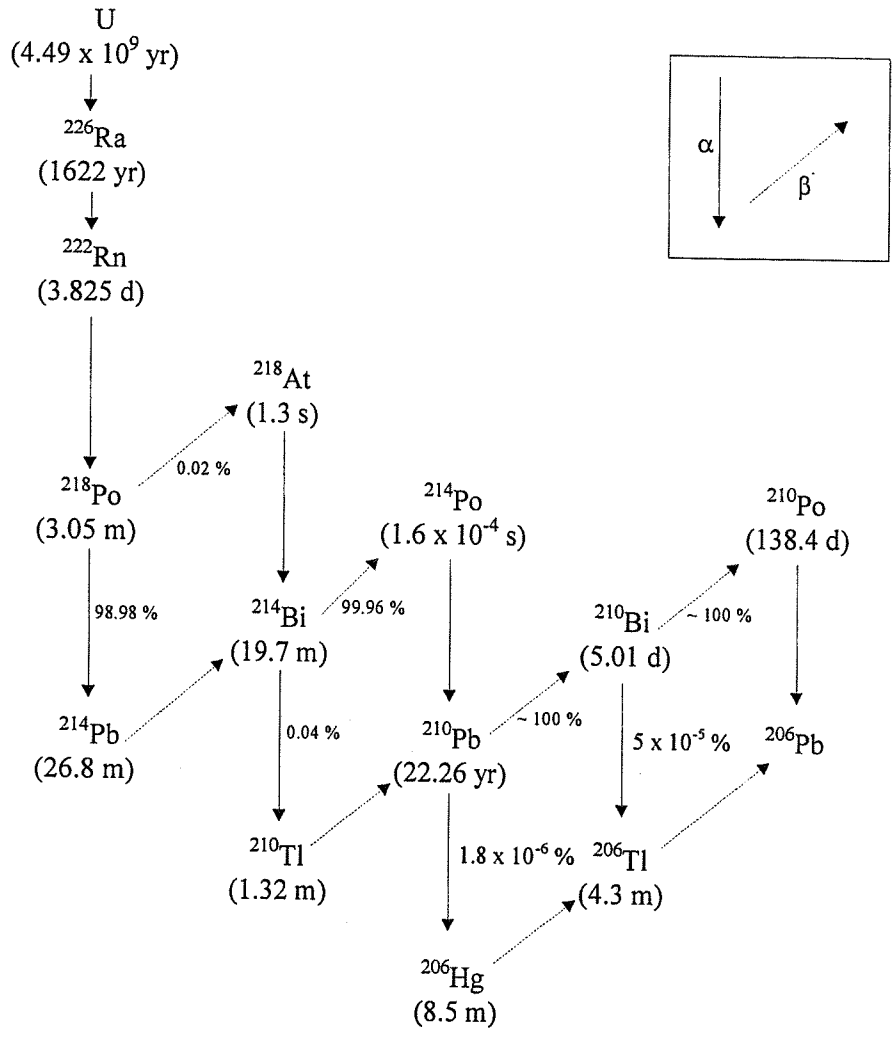

Figure 1-4. Decay scheme of ^{238}U leading to the generations of ^{210}Pb

1.3.5.2. The use of artificial radionuclides in dating

Fallout radionuclides originated from nuclear weapons' testing in the atmosphere, the Chernobyl accident in 1986 and the burn-up of a satellite power source in 1964 have been used for the estimation of sediment accumulation rates. These radionuclides can be used for dating where there are well-defined pulse inputs and no other sources of the artificial radionuclide in the system. Several radionuclides show a distinct single peak in the sediment profiles unless they are involved in post-depositional processes. However, releases from nuclear facilities are being carried out since the operation commenced. Radionuclides from

such sources can only be used when all the discharge data are available and annual discharges show distinctive features (peaks or abrupt changes in discharge). If the annual discharges are almost constant over the years, they cannot be used for geochronological applications. One of the typical examples is the Sellafield nuclear fuel reprocessing plant in Cumbria, UK. There are clear discharge peaks for most radionuclides released from Sellafield which represent 1970s. The artificial radionuclides discharged from the Sellafield site, therefore, have been used for the determination of sediment accumulation rates in many studies (Aston & Stanners, 1979 ; Stanners & Aston, 1981a,b ; Aston & Rae, 1982 ; Clifton & Hamilton, 1982 ; Hamilton & Clark, 1984 ; Stanners & Aston, 1984 ; Radakovitch *et al.*, 1999). Various techniques have been used such as the use of $^{134}Cs/^{137}Cs$ ratios, Cs/Pu ratios and the vertical activity profiles of Cs and Pu isotopes with different apparent diffusion coefficients and lag-time. ^{241}Am, ^{137}Cs and Pu isotopes are the radionuclides most easily and widely used on account of their relatively long half-life. In the case of ^{134}Cs & ^{137}Cs, because they are more soluble than the other two radionuclides they may be associated with different mixing and transport processes. Therefore, the safest way of using these artificial radionuclides for dating purposes is comparing the results acquired by several different radionuclides.

1.3.6. Estuaries

Estuaries are "semi-enclosed coastal bodies of water which have a free connection with the open sea and within which sea water is measurably diluted with fresh water derived from land drainage" (Pritchard, 1967).

Fairbridge (1980) elaborated on this definition with "an inlet of the sea reaching into a river valley as far as the upper limit of the tidal rise". Estuaries are divided into three distinct zones (Fairbridge, 1980 ; Chester, 1990) in terms of their geological settings.

1) A lower (marine) estuary, which is connected with the sea
2) A middle estuary, which is subject to strong mixing of sea water & fresh water
3) An upper (fluvial) estuary, which is characterised by fresh water inputs but which is subjected to daily tidal action

Estuaries also can be categorised into three different types, characterised by their circulation patterns. They are :

1. Salt wedge (micro tidal) estuaries
2. Partially mixed (meso tidal) estuaries
3. Well mixed (macro tidal) estuaries

This categorisation is mainly derived from variations in tidal range and river discharge. Salt wedge type estuaries are where river discharges are dominant with virtually no tidal variation. Partially mixed estuaries develop where rivers discharge into a sea with a moderate tidal range. Finally, where tidal flow is completely dominant with minor river input, well mixed estuaries occur.

Estuaries are associated with the mixing of sea water, fresh water and particulate matter (both organic and inorganic) which are transported with the two water bodies during the tidal cycles. The two water bodies have different compositions including particulate matter which plays an important role in transporting pollutants from both sea and land. Estuaries are often described as regions of high sediment accumulation and of traps for materials transported both seaward and inland by tidal currents and rivers. It is necessary to determine the contributions of those two source inputs for predicting and manipulating their fate. It will help us in understanding the behaviour of pollutants released into the marine or terrestrial environments.

1.3.7. Saltmarshes

The definition of a saltmarsh is "a relatively flat area of the shore where fine-grained sediment is deposited and where salt-tolerant grasses grow and represent a biologically active ecosystem" (Libes, 1992). Saltmarshes cover only a small area in the UK, 0.12% or 27000 ha (Horrill, 1983). However, as Horrill (1983) indicated, the importance of saltmarshes in areas subject to contaminated by radioactive material is that they can be a source of radionuclide contaminated aerosols carried inland by wind and they could be reclaimed for agricultural land or incorporated into water supply schemes. In the case of grazed saltmarshes, they can be a direct pathway of pollutants (radionuclides in this case) to

human beings via meat and dairy products. Therefore it is very important to understand the levels of pollution in the saltmarshes. Recently, Sanchez *et al.* (1998) carried out work to look at the radionuclide concentrations in saltmarshes along the coastline of the Eastern Irish Sea and reported levels of radionuclide contamination in those saltmarshes. They found that the levels of radionuclide decreased with increasing distance from Sellafield ranging over 4 orders of magnitude between the Esk estuary and the estuaries in southern Wales. Their results showed that saltmarshes are one of the environments where radionuclides accumulate and can preserve the history of Sellafield discharges.

1.3.8. Transportation and interaction of Sellafield radionuclides

Low level liquid wastes have been discharged from the nuclear fuel reprocessing plant in Sellafield. Once released from the site they interact with both seawater and particulate matter (sediments) where they undergo adsorption, desorption, deposition and resuspension etc., until they finally reach possible sinks (e.g. sea floor sediment, saltmarsh etc.). Figure 1-5 shows those processes. This is supported by the findings that a major fraction (approx. 95%) of the Pu released is lost from the water to the sediment immediately after its discharge from the pipeline (Hetherington, 1978). This Pu is believed to be transported in association with the general transport processes in the region. The interaction depends on the chemical behaviour of each element and the extent of this is represented by the K_d (see section 1.3.2.). Radionuclides with high K_ds (such as ^{241}Am, Pu isotopes etc.) will be associated with particulate matter and those having lower K_ds (e.g. Cs isotopes) will be mixed with seawater and transported. This can be described by the conservative and non-conservative behaviour of elements during the mixing process. If the distribution of a dissolved radionuclide is controlled only by physical mixing process its concentration will linearly decrease along a salinity gradient, and its behaviour is described as conservative. However, if the dissolved radionuclide is involved in any reactions resulting in its loss from or its addition to the dissolved state it is described as non-conservative. ^{137}Cs shows conservative behaviour and ^{241}Am and Pu isotopes behave non-conservatively during the mixing process (Assinder *et al.*, 1984). These interactions are continuously occurring during transportation. Two important factors in controlling the interactions of radionuclides during transportation may be resuspension (reworking) of labelled particulate and adsorption/desorption of radionuclides from particulates. The former is a mechanical

process and the latter is a physico-chemical process. These processes will involve the mixing of radionuclides discharged at different time periods. Radionuclides discharged from the source and associated with both seawater and particulate matter are transported by marine (both surface and bottom) and tidal currents. However, tidal currents and river inputs predominantly control the transportation and the mixing of such radionuclides in the estuarine environment. Although the activities are lower than those measured in the samples from the south of Sellafield, Sellafield-derived radionuclides are found along the coasts of south-west Scotland (McDonald *et al.*, 1990, 1992 ; Kim *et al.*, 1992 ; Assinder *et al.*, 1993). Pu isotopes and other radionuclides' isotopic ratio comparisons were used to identify the source terms. Tidal currents are believed to play a major role transporting radionuclides to south-west Scotland coasts.

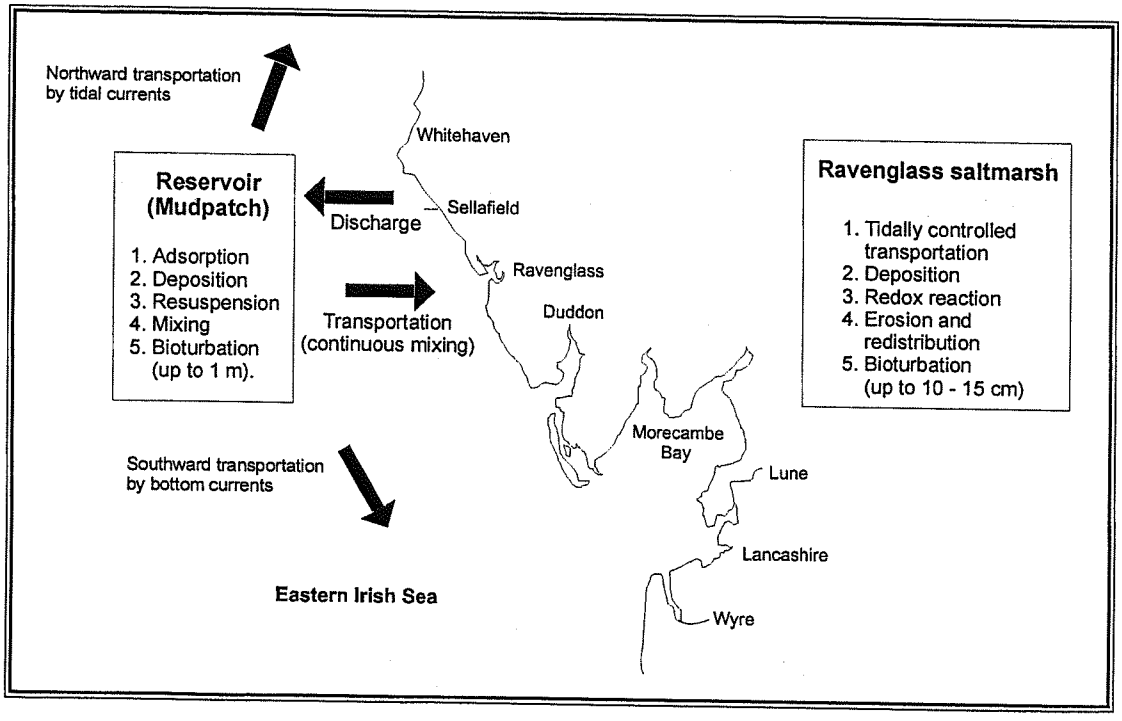

Figure 1-5. Simplified diagram of radionuclide pathways and possible processes during the transportation

1.3.9. Bioturbation

One of the factors which can affect the distribution of pollutants (radionuclides in this case) in the sediment is bioturbation. It is caused by the burrowing and feeding activities of

benthic organisms resulting in biological stirring of the sediments. These biological activities have been used to explain the post-depositional migration of radionuclides in various environments (Kershaw *et al.*, 1983,1984 ; McMurtry *et al.*, 1985 ; Pentreath, 1987 ; Woodhead, 1988). Care must be taken when the concept of bioturbation is applied to interpret the data. For example, in sediments from the coastal areas, bioturbation can take place as deeply as 1 m below the surface since there are marine animals (such as crabs) big enough to cause such deep bioturbation. Kershaw *et al.* (1984) reported that bioturbation is responsible for the redistribution of radionuclides to depth of up to 140 cm in cores collected from the Irish Sea. However, for core samples taken from saltmarshes, bioturbation is most active in the top few centimetres (Hetherington, 1978 ; Libes, 1992). Animals like small crabs and polychaete worms are responsible for the bioturbation in saltmarsh environment. In addition, saltmarshes usually have high sediment accumulation rates making it unlikely that bioturbation could be responsible for the post-depositional migration of radionuclides to a deeper depth. Hamilton & Clarke (1984) also reported that bioturbation in the Ravenglass saltmarsh may take place in the top few centimetres and it does not seem to alter the vertical distribution of radionuclides. Laminations often found in the saltmarsh core also imply the limited mixing. Overall, bioturbation is an important process in mud flats but not in saltmarshes where plant roots stabilise the sediments.

Chapter 2. Areas under investigation

2. Areas under investigation

2.1. Overview of study area

2.1.1. Sellafield site

The Sellafield complex is the largest as well as oldest nuclear site in the United Kingdom (Fig.2-1). The site was first used as a conventional munitions factory during the Second World War. After the War, in 1947, two air cooled reactors were constructed for plutonium production, known as the Windscale Piles. They were closed following a fire in Pile I in October 1957 which released significant activities of both fission products and actinides (Table 2-1). A prototype Advanced Gas Cooled Reactor was also operated on the site between 1963 and 1981. There are two major operational facilities on the Site now. The first is a cluster of four Magnox reactors at Calder Hall. All four reactors are still in operation with the first reactor having started operation in 1956. Fuel from Calder Hall and other Magnox reactors operating throughout the UK was originally stored in an open fuel storage pond but storage of spent fuel was transferred to an enclosed pond in 1985. The second group of facilities on site is the spent fuel reprocessing plant including SIXEP (site ion exchange effluent plant), EARP (enhanced actinide removal plant) and THORP (thermal oxide reprocessing plant) which began operation in 1985, 1994 and 1994, respectively. This reprocessing plant is the second largest spent nuclear fuel reprocessing facility in the world in terms of its reprocessing throughput (La Hague in N. France being the largest).

	^{3}H	^{137}Cs	^{131}I	^{239}Pu	U
Activities (TBq)	5000	22	740	1.6	Approx. 20 kg

Table 2-1. Activities of key radionuclides released from the fire in Pile I (Gray *et al.*, 1995)

The Sellafield site has discharged radioactive effluents into the NE Irish Sea since 1952 through submerged pipelines terminating about 2.5 km below the high water mark (Nelson & Lovett, 1978 ; Gray *et al.*, 1995). The discharge is carried out under authorisations from the Ministry of Agriculture, Food and Fisheries (MAFF). The annual discharge records of various radionuclides in liquid effluent from the Sellafield plant since it

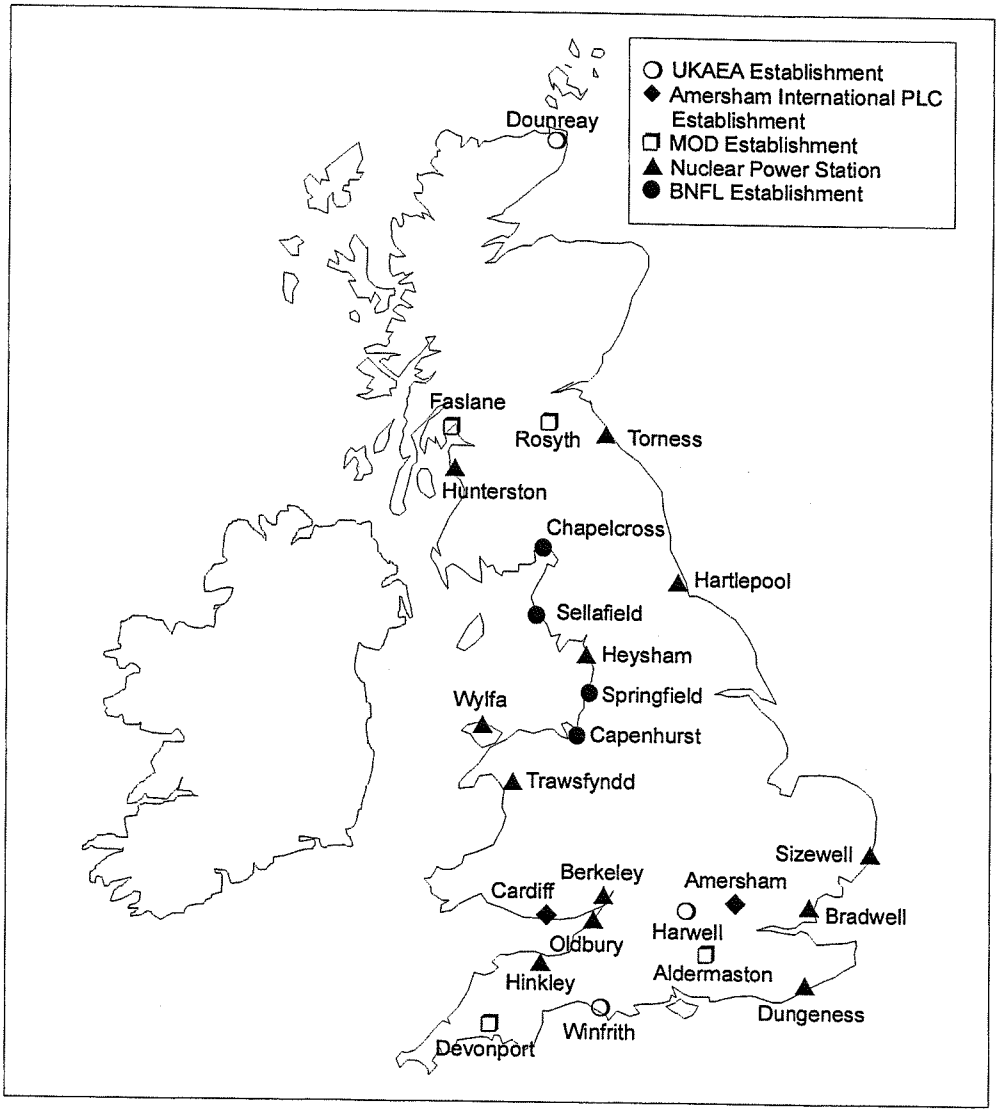

Figure 2-1. Locations of nuclear facilities in United Kingdom (after MAFF, 1993)

Year	^{3}H	^{90}Sr	^{134}Cs	^{137}Cs	^{144}Ce	^{238}Pu	$^{239,240}Pu$	^{241}Pu	^{241}Am
1996	3000	16	0.27	10	0.78	0.06	0.15	4.4	0.07
1995	2700	28	0.51	12	1.1	0.08	0.23	7.7	0.11
1994	1700	29	0.61	14	0.84	0.17	0.50	14	0.38
1993	2300	17	1.18	22	2.5	0.36	0.97	38	0.87
1992	1200	4.2	0.83	15	1.7	0.24	0.69	25	0.54
1991	1800	4.1	0.76	16	1.7	0.26	0.82	30	0.74
1990	1700	4.2	1.2	24	2	0.29	0.84	32	0.75
1989	2100	9.2	1.7	29	3.8	0.31	0.9	30	1.1
1988	1700	10	0.95	13	3.2	0.38	1	36	0.75
1987	1400	15	1.2	12	3.9	0.35	0.97	32	0.65
1986	2200	18	1.3	18	3.3	0.62	2	63	1.3
1985	1100	52	30	330	5	0.8	2.6	81	1.6
1984	1600	72	35	430	9	2.6	8.3	350	2.3
1983	1800	200	89	1200	24	2.9	8.7	330	2.2
1982	1800	320	140	2000	22	4.7	16	480	6.4
1981	2000	280	170	2400	17	5	15	600	8.8
1980	1300	350	240	3000	37	6.9	20	730	8.2
1979	1200	250	240	2600	83	12	38	1500	7.8
1978	1000	600	400	4100	100	12	46	1800	7.9
1977	910	430	600	4500	150	7.5	29	980	3.7
1976	1200	380	740	4300	150	8.8	38	1300	12
1975	1400	470	1100	5200	210	8.8	35	1800	36
1974	1200	390	1000	4100	240	8	38	1700	120
1973	740	280	170	770	540	11	54	2800	110
1972	1200	560	220	1300	500	9.9	47	1900	80
1971	1200	460	240	1300	640	9.3	46	1800	38
1970	1200	230	220	1200	460	3.8	31	1000	19
1969	870	110	62	440	500	2.8	27	730	14
1968	790	50	48	370	370	2.1	28	630	21
1967	590	52	15	150	510	1.2	17	290	17
1966	460	34	16	180	250	0.66	13	170	7.5
1965	330	56	10	110	140	0.3	6.9	81	8.1
1964	290	36	6.1	100	120	0.22	5.5	62	4.5
1963	140	20	6.1	85	52	0.25	8.1	55	0
1962	250	38	3.9	74	89	0.2	6.6	37	0
1961	250	18	1.8	40	80	0.14	4.6	18	0
1960	250	19	1.4	34	33	0.08	2.7	6.2	0
1959	250	57	2.7	73	260	0.06	2.1	4.4	0
1958	250	93	5.7	230	220	0.06	1.9	3.9	0
1957	250	61	3.5	140	96	0.05	1.6	3.4	0
1956	250	71	4.1	160	47	0.06	1.8	3.7	0
1955	250	9.3	0.52	21	35	0.02	0.7	1.9	0
1954	250	19	1.2	46	66	0.02	0.6	2.3	0
1953	250	36	1.2	46	66	0.02	0.5	1	0
1952	250	33	1.2	46	66	0.02	0.54	2	0

Table 2-2. Discharges of key radionuclides to the Irish Sea from Sellafield (Units : TBq/yr) (Gray et al., 1995 ; BNFL, 1997)

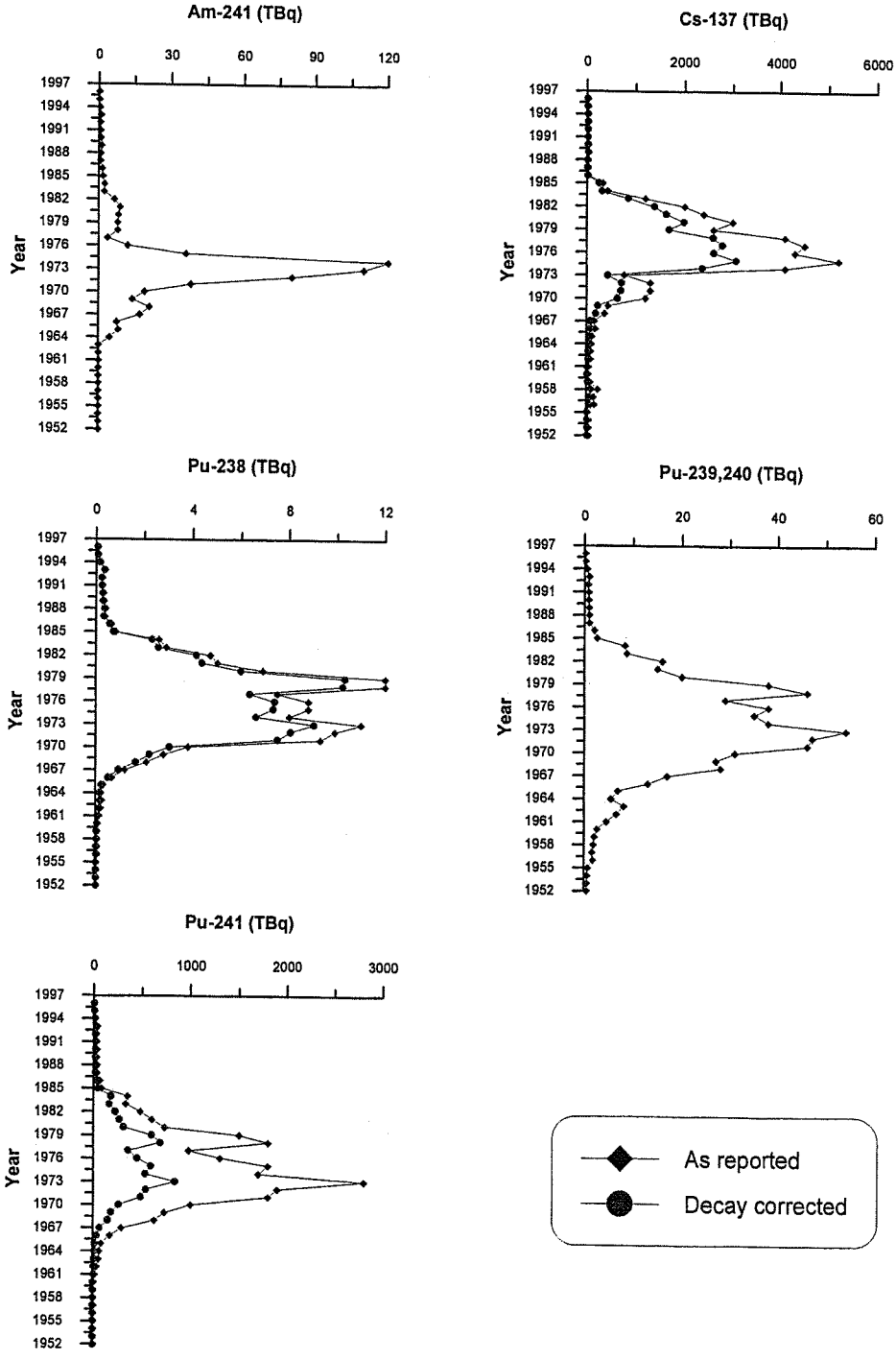

Figure 2-2. Annual discharges of radionuclides from Sellafield (decay-corrected to 1998)

started operating are shown in Table 2-2 and Figure 2-2. Currently, there are two major sources of liquid effluent. The first are the liquors from reprocessing of spent fuel elements which involves separating uranium, plutonium and highly radioactive fission products by several solvent extraction stages, and the other is purge water used in the fuel storage pond including the THORP Receipt and Storage area. The fuel storage pond water was initially discharged from the site to the Irish Sea without treatment until the late 1970s. Discharges peaked in the mid- to late 1970s due to increased throughputs, the processing of stored residues (Kershaw & Baxter, 1993) and the increased storage time and consequent corrosion of Magnox fuel (Gray *et al.* 1995). Discharges decreased markedly after the introduction of new treatment facilities in the plant such as SIXEP (Site Ion Exchange Effluent Plant) in 1985 which was successful in reducing discharges of ^{134}Cs, ^{137}Cs and ^{90}Sr and EARP (Enhanced Actinide Removal Plant) in 1994 which significantly reduced actinides in discharges. There are also some minor sources such as surface drainage water, laundry effluent and sewage (Gray *et al.*, 1995). Apart from those authorised routine discharges, there have been several incidents which resulted in the unauthorised release of radioactivity into the surroundings. The emission of uranium oxide from the Pile chimneys in 1954 (Mossop, 1960 ; Stather *et al.*, 1986) released considerable amounts of radionuclides and the Pile I fire in October 1957 also contributed to the accidental release of radionuclides from the site. Other incidents were the B30 fire in July 1979, the B242 release in September 1979 and the B241 sludge tank release in July 1984. These incidents released 21GBq, 1.6GBq, 1.4 MBq, 11 GBq and 10 MBq of $^{239,240}Pu$ to the environment, respectively (Gray *et al.*, 1995). Further details of the site and histories are well documented in a paper by Gray *et al.* (1995).

2.1.2. Nuclear fuel reprocessing at Sellafield

Once the spent nuclear fuel arrives at the Sellafield plant, it is placed in a storage pond and the short-lived fission products are allowed to decay. Following the storage and cooling, the main steps of reprocessing are :

1) The head end section (opening of the spent fuel)
2) The main fractionation of uranium, plutonium and fission products
3) The purification of uranium

4) The purification of plutonium
5) The waste treatment (flocculation, ion-exchange and sorption)

Solvent extraction is used for the separation of uranium, plutonium and fission products. At Sellafield, a technique called the "Purex process" (Plutonium Uranium Redox EXtraction) is used which uses tributyl phosphate (TBP) as the extractant. The distribution of uranium, plutonium and fission products between 30 % TBP - kerosene and HNO_3 varies depending on the acid concentration. Distribution coefficients (K_d) of Sr, Cs and many other fission products are < 0.01 for all concentrations of HNO_3. However, the K_ds of both U(VI) and Pu(IV and VI), are greater at higher HNO_3 concentrations so that extraction takes place. The K_ds of actinides are less than 1 at low HNO_3 concentrations and the back extraction of uranium and plutonium from the organic phase is carried out with dilute HNO_3. In the first cycle (see Figure 2-3) more than 99.8 % of U(VI) and Pu(IV & VI) are co-extracted from 3-4 M HNO_3 into 30% TBP - kerosene and more than 99 % of fission products remain in the HNO_3 fraction. Pu(IV) is reduced to Pu(III) by adding a reducing agent such as U(IV) nitrate or Fe(II) sulphamate and reduced Pu(III) stripped to a new aqueous phase. Uranium is then extracted from the organic phase by dilute HNO_3. The Purex process is repeated to obtain additional decontamination. Both separated uranium and plutonium fractions are transferred to the further purification sections. The aqueous solutions containing fission products are converted into vitrified form in the Waste Vitrification Plant on site. During these processes liquid wastes are produced such as high, medium and low level liquid wastes. They are subsequently cleaned by flocculation, ion exchange, sorption and, finally, low level liquid wastes (LLLW) are released to the Irish Sea as part of the authorised discharge. The LLLW contain fission products such as ^{90}Sr, ^{134}Cs, ^{137}Cs, ^{106}Ru, ^{99}Tc and actinides.

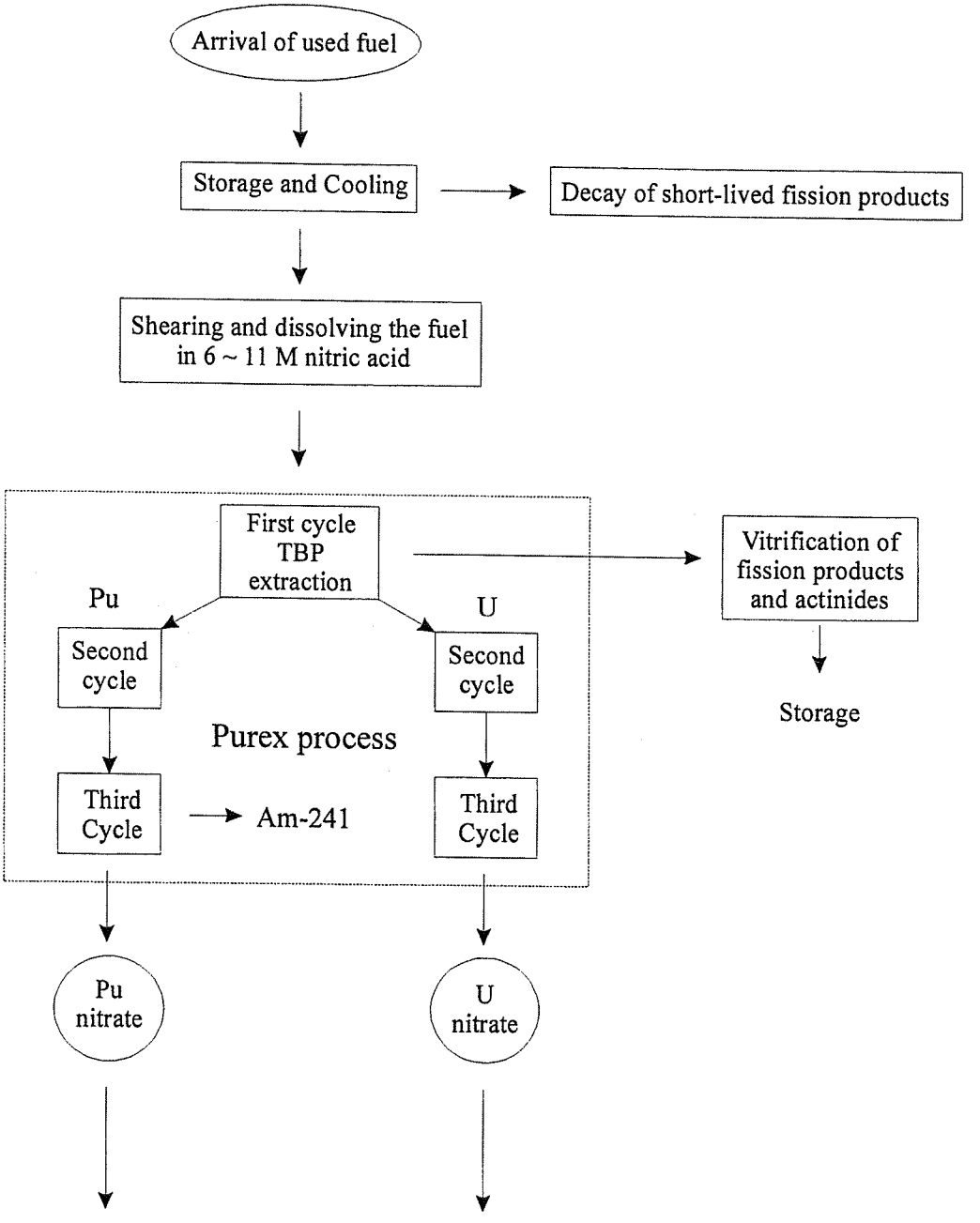

Figure 2-3. Schematic representation of the reprocessing of used fuel at Sellafield

2.1.3. Fate of radionuclides following discharge to the Irish Sea

Treated low level liquid wastes containing fission products and actinides are released into the Irish Sea through the effluent pipelines. Among those radionuclides, Pu isotopes in particular, are associated with particulate matter (sediments) shortly after their release from the Sellafield site (Hetherington, 1978), bottom currents in association with bed-loads will play a major role in transporting radionuclides from their source to the surrounding region. Figure 2-4 shows the direction of both surface and bottom currents in the Irish Sea. Radionuclides migrate to the southeast along the coastline by both surface and bottom currents until they join the currents to the North. In addition, as shown in Figure 2-5, the dominant type of sediment in the vicinity of the Sellafield outfall where the discharge is carried out is mud. Therefore, particle reactive radionuclides such as ^{241}Am and Pu isotopes will be associated with this muddy sediment and form a reservoir in the vicinity of the discharge point which may act as an additional source that can supply Sellafield-derived radionuclides to the surrounding areas (see Figure 1-5).

It is well known that the eastern Irish Sea and Cumbrian coast receive significant amounts of radionuclides discharged from Sellafield. As mentioned earlier the Ravenglass saltmarsh is one of the sinks which is mainly controlled by tidal currents since the river Esk is categorised as a macrotidal estuary. The sedimentation in macrotidal estuaries is dominated by fine marine sediment transported inland by estuarine circulation patterns involving net landward movement of seawater along the bottom of the estuary. The mixing of sediments with those labelled with previous years radionuclides during the transportation must be noted since they can behave as another source input to the sediment representing the most recent discharge from the Sellafield site. For example, Mackenzie & Scott (1993) reported that the comparatively small reductions in critical group exposure in the UK, compared with the two orders of magnitude decrease in the Sellafield discharge in the 1980s, was due to the radionuclides persisting in the environment from earlier discharges. The Irish Sea bottom sediments may act as another source term for the radionuclides dispersed to the estuaries, harbours and coasts (i.e. continual reworking and transportation of the Irish Sea mudpatch : see Figure 1-5).

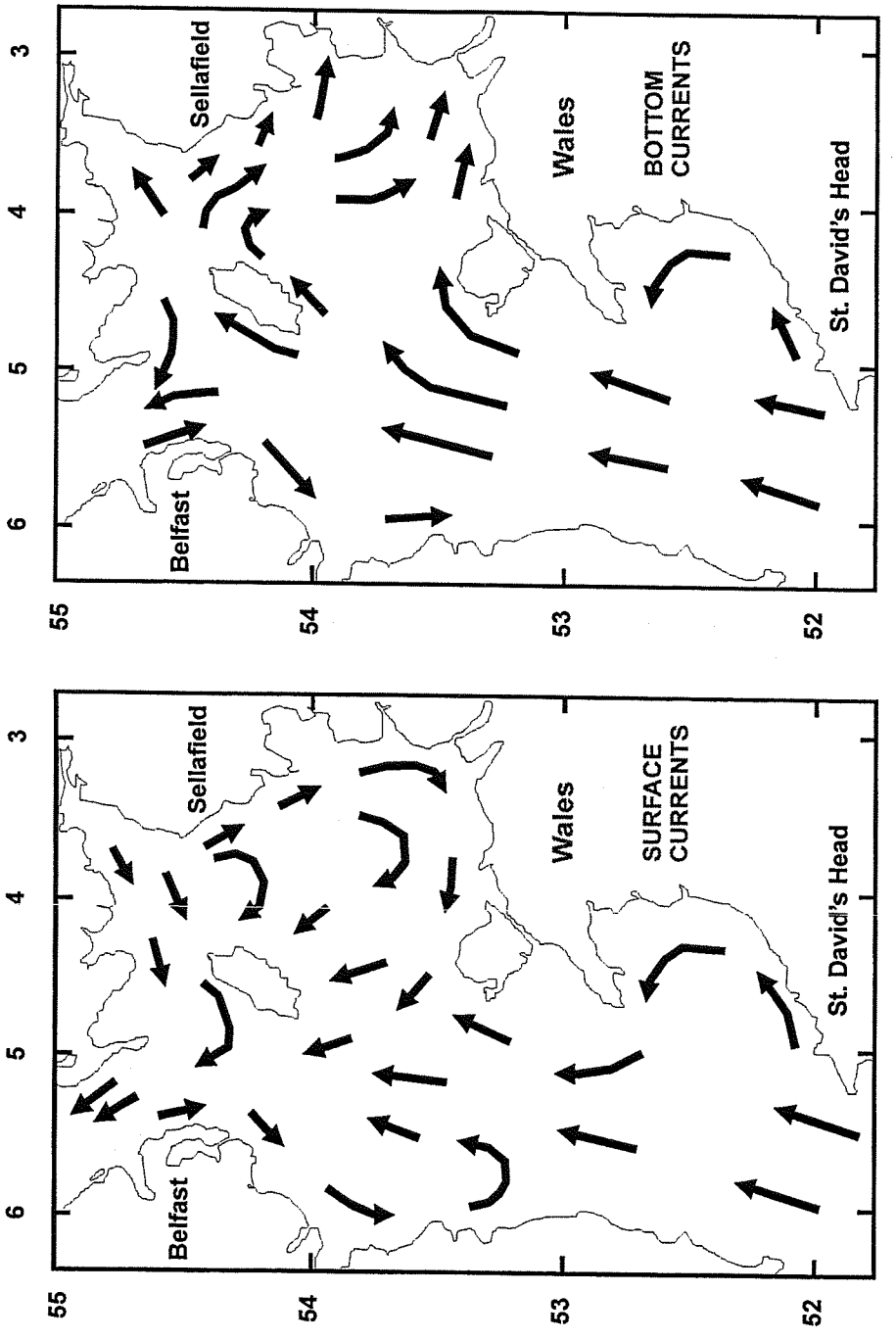

Figure 2-4. Surface and bottom mean residual currents in the Irish Sea (Kershaw *et al.*, 1992)

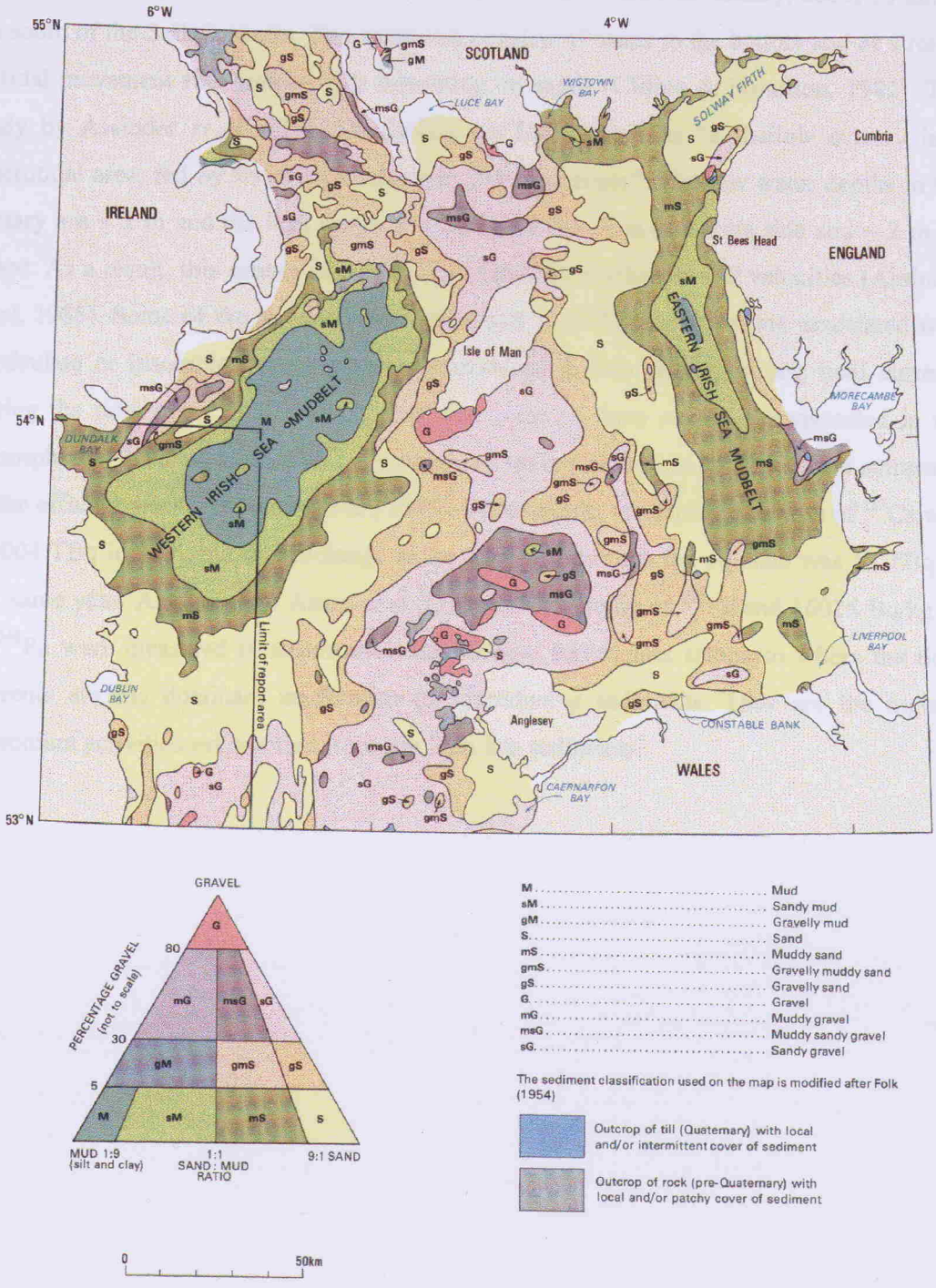

Figure 2-5. Composition of Irish Seabed sediments (after Jackson *et al.*, 1995)

2.2. Ravenglass saltmarsh

The Ravenglass saltmarsh is located at the mouth of the Esk Estuary, about 10 km to the south of the Sellafield site. This saltmarsh consists of sands in the bottom and as a result of tidal movement fine-grained silts depositing on sands (Clifton & Hamilton, 1982). The study by Assinder *et al.*, (1985) described the Esk estuary as "a shallow estuary in a macrotidal area, fed by rivers with relatively low discharges". The low water depths in the estuary are < 1 m and the tidal range at Ravenglass is ~ 4 m on spring tide and ~ 2 m on neaps. As a result, this estuary has relatively high tidal discharges and velocities (Assinder *et al*, 1985). Some of the radionuclides discharged from Sellafield that are associated with particulate or insoluble phases could be introduced to this area by strong tidal currents during the tidal cycle. It is also possible that some of them could be transported in the atmosphere. However, atmospheric discharges of radionuclides are not significant compared to the effluent discharges (Gray *et al.*, 1995). For example, atmospheric release of ^{137}Cs was 0.0004 TBq in 1992 but the discharge to the Irish Sea through the pipeline was 15 TBq in the same year. According to Aston *et al.* (1985), 4118 Bq/kg of ^{238}Pu and 16026 Bq/kg of $^{239,240}Pu$ were measured in sediments collected near Ravenglass saltmarsh where the tidal currents are the dominant mechanism for introducing sediments. They are the highest plutonium activities yet reported from any Irish Sea sediments.

Chapter 3. Sampling locations and methods used for the research

3. Sampling locations and methods used for the research

3.1. Sampling locations

Figures 3-1 & 3-2 show the sampling locations in the Irish Sea and on the Ravenglass saltmarsh (a panoramic view and the main channel of the saltmarsh is shown in Figure 3-3). The Irish Sea core was collected by MAFF during their 1995 cruise. Three saltmarsh sediment cores were taken from the front of the saltmarsh and one core was collected from the northwest of the saltmarsh. Surface scrape samples were also collected from the saltmarsh at pre-existing grid intersection points using the grid by Horrill (1983) as part of a DOE-funded research programme. Some points have become channels since Horrill set up the original grid so these samples could not be collected. Grid intersections located in the creeks or the channel were avoided for sample collection and in these instances samples were collected from the marsh closest to the original intersection points (see Appendix 1 for more sample details).

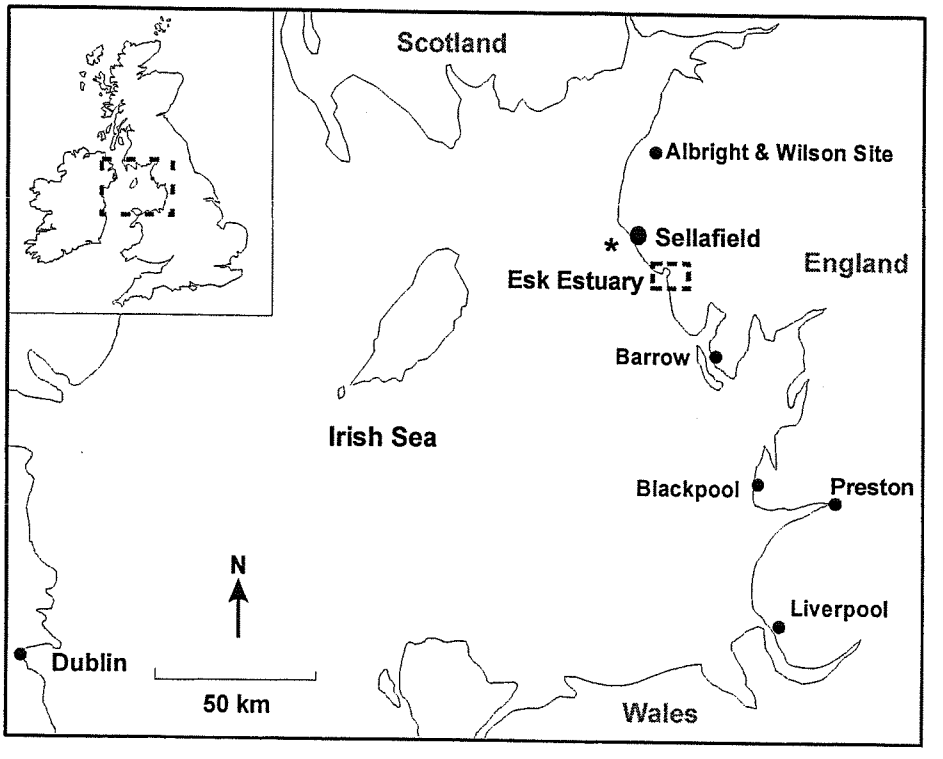

Figure 3-1. Irish Sea and the sampling location (* I-96-002 core)

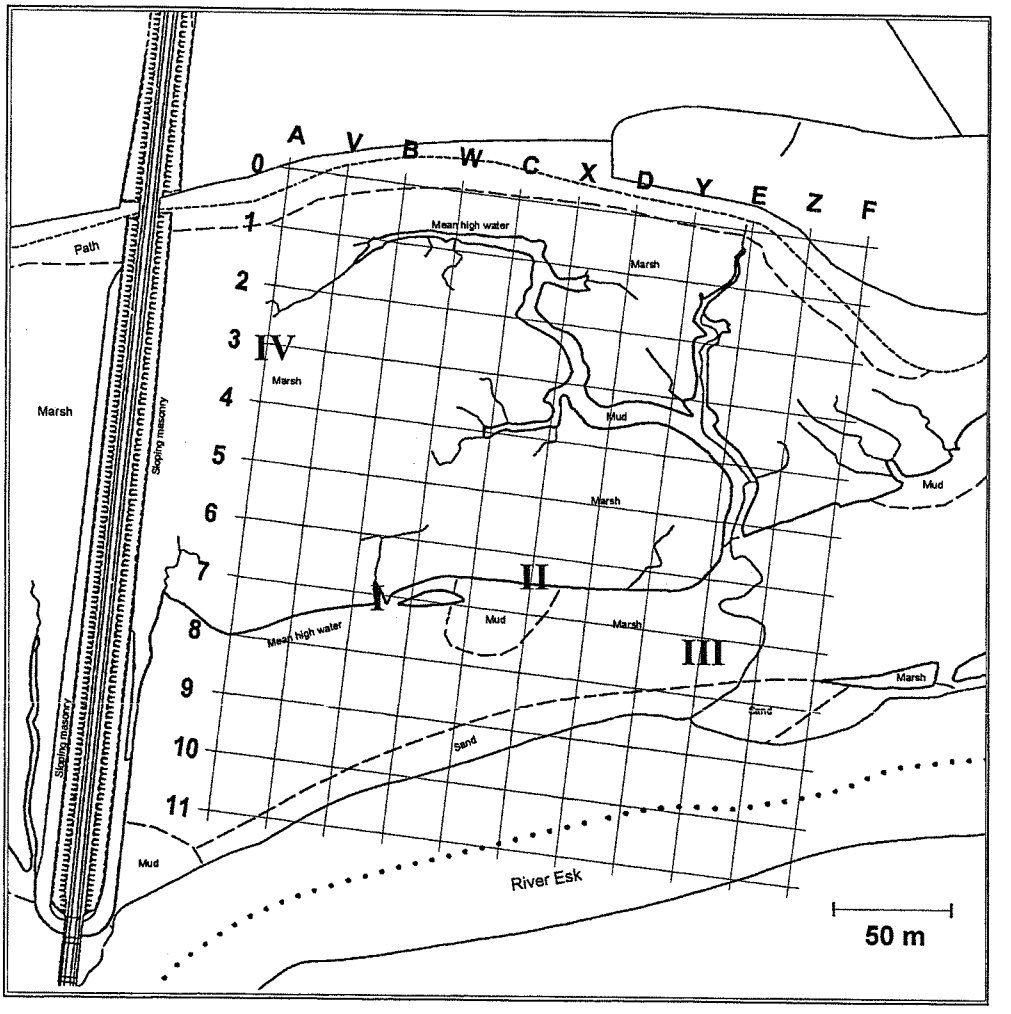

Figure 3-2. Sampling locations (I : R-96-000, II : R-96-007, III : R-96-008 & IV : R-97-003 core)

a) A panoramic view of the marsh

b) A photograph of the main channel

a) Looking southeast
b) Looking south towards Newbiggin

Figure 3-3. The views of the Ravenglass saltmarsh

3.2. Gamma spectrometry

Gamma spectrometry was used to determine ^{241}Am and ^{137}Cs. Approximately 20 g of dried samples were transferred into 22 ml polythene scintillation vials and counted for 8 hours using Canberra well-type HPGe detector (see Table 3-1). Acquired energy spectra were then analysed and the activity of radionuclides calculated using Fitzpeaks software. The gamma spectrometer was previously calibrated for both energy and efficiency against an Amersham QCY-48 mixed radioisotope standard adsorbed onto a sediment matrix using the method described by Croudace (1991). Figure 3-4 shows an efficiency curve for the detector. Limits of detection for both ^{241}Am and ^{137}Cs are 1 Bq/kg.

	Details	Note
Model	GCW 4523	
Type	Coaxial one open end	
Diameter	76 mm	
Active volume	239 cc	
Well depth	45 mm	
Resolution	FWHM (2.25 keV)	^{60}Co (1332 keV)
Peak/Compton	46.5 : 1	"
Efficiency	41.1 %	"

Table 3-1. Detector specification and performance data

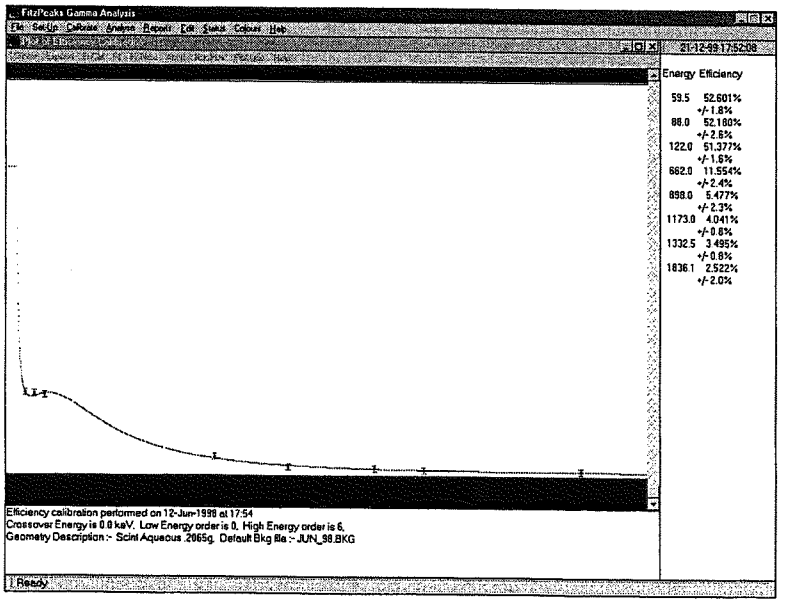

Figure 3-4. An efficiency curve for the gamma spectrometer

3.3. XRF analysis

3.3.1. Bead preparation

The beads were prepared by mixing 0.8g of ground, ignited (at 900°C for minimum 2 hours) sediment sample with 4g of a eutectic mixture of 80% Lithium metaborate & 20% Lithium tetraborate to produce a 5:1 ratio mix. The mixture of sample and flux was then fused in a platinum crucible for about 10 minutes at 1200°C, transferred to a casting dish and allowed to cool. The beads were then measured for major elements by a Phillips 1400 sequential X-ray fluorescence spectrometer.

3.3.2. Pellet preparation

Approximately 10g of ground sample was pressed to 12 tonnes to produce a pellet. A PVA binder was not needed for the clay rich sediments but was added to the sandy sediments. The pellets were then analysed for the trace elements by XRF.

3.4. Separation of plutonium

3.4.1. Introduction

Techniques such as ion exchange chromatography (Korkisch & Tera, 1961 ; Korkisch & Hazan, 1964 ; Nelson *et al.*, 1964 ; Krishnaswami & Sarin, 1976 ; Navratil *et al.*, 1979 ; Casella *et al.*, 1981 ; Kanai, 1986 ; Horwitz *et al.*, 1992, 1995 ; Parsa, 1992 ; Smith *et al.* 1995), and solvent extraction (Saito & Choppin, 1983 ; Yang *et al.*,1991 ; Pimpl *et al.*,1992 ; Shukla *et al.* 1993) have been commonly used for separating radionuclides in the environmental samples. However, since solvent extraction techniques are rather time consuming and produce relatively large volumes of organic wastes, techniques involving ion exchange (or extraction) chromatography are preferred. Separated radionuclides may then be measured using alpha spectrometry, liquid scintillation spectrometry or mass spectrometry.

As a preparation stage for ion exchange chromatography procedures, acid digestion has been used for leaching actinides from sediments. However, acid digestion does not always guarantee complete digestion, particularly when Pu is present as refractory PuO_2 in samples. As an alternative, fusion techniques have been used to achieve total dissolution of sediment and soil samples (Thomson, 1982 ; Kanai, 1986 ; Sill & Sill, 1995 ; Smith *et al.*, 1995). However, these fusion techniques also showed several problems such as an incomplete sample dissolution of insoluble siliceous material (sodium carbonate fusion), production of harmful gases such as HF and sulphuric acid fumes (mixed potassium fluoride and potassium pyrosulphate fusion) and damage of fusion vessels over repeated use which will be a significant cost issue (Croudace *et al.* 1998a,b). In addition, the general requirement for an effective complete dissolution limits sample sizes to around 3 grams. In this experiment, a borate fusion technique, which was developed by Croudace *et al.* (1998a,b) along with a separation of Pu using anion extraction chromatographic materials (EIChroM Industries, INC) was employed.

3.4.2. Experimental

Reagents

Concentrated hydrochloric acid
Concentrated nitric acid
9M hydrochloric acid
8M nitric acid
3M nitric acid
0.1M ammonium iodide/9M hydrochloric acid
0.2M PEG-2000 (polyethylene glycol, M.W.= 2000)
Electrolyte solution for electrodeposition

Sample preparation

Approximately 1g (0.5 g for LGC reference material) of dried and ground sample was transferred into a marked porcelain crucible. The crucible was then transferred into a furnace at 400°C for 10 minutes and the furnace temperature was increased to 600°C. The sample was ignited overnight. After the ignition, the crucible was removed from the furnace and allowed to cool. The sample was transferred into a clean Sterilin® pot and retained for the borate fusion stage.

Borate fusion

2.0 g of flux (80 % Lithium metaborate & 20 % Lithium tetraborate) was mixed with 1 g of sample and spiked with ^{242}Pu (approximately 50 mBq). The sample was transferred into a 35 ml grain-stabilised Pt - Au (95 % - 5 %) dish (Englehardt Industries) and placed in a furnace at approx. 1200 °C for 10 - 15 minutes. The crucible was gently swirled to ensure thorough mixing and dissolution of the sample. For each sample, a 250 ml beaker containing 50 ml of distilled water was prepared. The melt was carefully poured into water to quench the sample. The stirring bar was placed in the bottom of the beaker and 50 ml of concentrated nitric acid was added to the mixture in order to make the final acid strength of about 8M. The beaker was transferred to a 15-position multi-block heater/magnetic stirrer (Labortechnik, FRG), heated to 30 - 40°C and stirred overnight to effect dissolution. The heating was switched off and 1ml of PEG-2000 (0.2M Polyethylene glycol) was added.

Stirring was continued for another hour. The sample was filtered under suction through a 9 cm GF/A filter paper supported on a Whatman 540 filter. The filtrate was reserved for chemical separation. The filter residue consisting of silica and boric acid was discarded. This technique was developed to permit the analysis of a large number of samples over a short time.

Sequential separation of actinides

Anion exchange columns prepared with EIChrom anion resin 1 X 8, 100-200 mesh (6 cm high, 1 cm diameter) were prepared and pre-conditioned with 8M nitric acid. Anion columns were checked for any trapped air bubbles and the top of the column was plugged with cotton wool in order to avoid the resuspension of resin. 2 - 3 drops of concentrated hydrochloric acid were added to the sample solution to ensure Pu was present as Pu (IV). The sample solution was transferred onto the anion exchange column and allowed to percolate through column. The columns were washed with 20 ml of 8M nitric acid followed by 20 ml of 3M nitric acid which would wash Am, Th and U off the column. 3M nitric acid was used to wash U more effectively from the anion exchange column since U has a lower K_d in 3M nitric acid than in 8M nitric acid. The columns were washed with 50 ml of 9M hydrochloric acid to remove thorium. Plutonium was then eluted with 30 ml of freshly prepared ammonium iodide reagent (0.1M NH_4I/9M HCl). The eluent was evaporated to dryness and concentrated nitric acid was added to decompose iodide in the eluent. Evaporation was repeated until no further violet fumes of I_2 were produced. Eluents were then electrodeposited and Pu-alpha activities determined using an Octete alpha spectrometry (EG & G ORTEC). Details of electrodeposition used are reported in Appendices.

Standards

The standard reference materials used in this study were IAEA-135 (marine sediment from Irish Sea), LGC (River Esk sediment supplied by Laboratory of the Government Chemist), SRM-4357 (Pacific Ocean sediment) ; also analysed was a surface scrape sample (V7V) from the Ravenglass saltmarsh. Although V7V is not a standard reference material, it was analysed repeatedly to determine the reproducibility of the technique. The certified and

recommended values of nuclides in these standard materials are listed in Table 3-2 together with measured values.

(Bq/kg ± 2 S.D.)

	^{238}Pu	^{239,240}Pu	^{241}Pu
IAEA-135	41.5 ± 5.65	219 ± 20.5	2494 ± 162
Reference value	43 (41.6-45)	213 (205-225.8)	No data
LGC	207 ± 14	978 ± 70	13200 ± 1170
Reference value	211 ± 7.17	995 ± 37.8	13500 ± 1080
SRM-4357	2.56 ± 0.32	9.73 ± 1.94	154 ± 6.70
Reference value	2.29 ± 0.05	10.4 ± 0.20	No data
V7V	245 ± 10.1	1173 ± 74.4	14703 ± 312

Table 3-2. Reference and measured values of standard reference materials

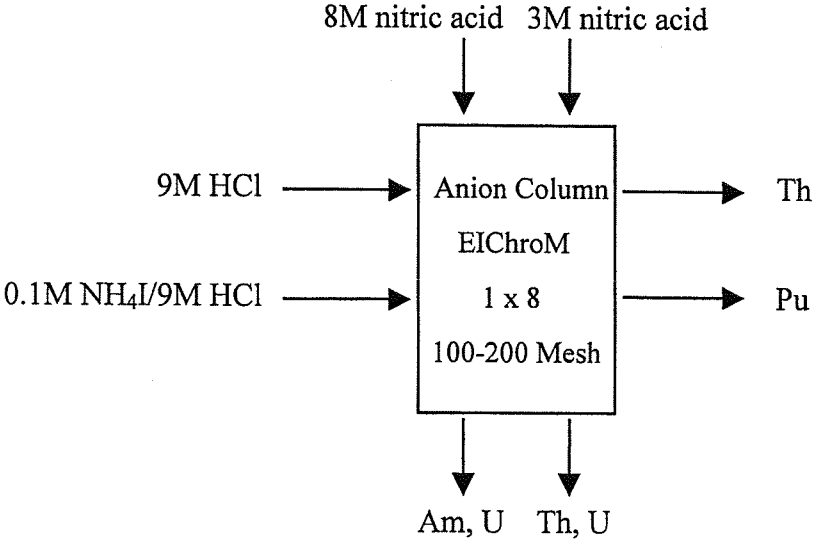

Figure 3-5. Schematic diagram of the separation.

3.5. Determination of ^{241}Pu in sediments

3.5.1. Introduction

Several isotopes of Pu are present in nuclear wastes (Table 3-3). Among the Pu isotopes, ^{241}Pu has been studied less extensively since it is a beta-emitter with a maximum energy of only 21 keV which represents less radiological significance than other alpha-emitting Pu isotopes. In addition, measuring ^{241}Pu requires additional separation and measurement procedures and instruments such as a mass spectrometer or liquid scintillation counter. However, ^{241}Am, the daughter element of ^{241}Pu, undergoes alpha decay with corresponding alpha energies at 5.443 MeV (13%) and 5.485MeV (85%) and a half-life of 433 yr. It was reported that ^{241}Am significantly contributes to the critical group dose for Sellafield (BNFL, 1997). It was estimated that approximately 27 % of total ^{241}Am originated from the *in situ* decay of ^{241}Pu in the Irish Sea area based on the discharges from Sellafield (Day & Cross, 1981). It now is estimated that approximately 46 % of the total ^{241}Am present is ingrown ^{241}Am. ^{241}Pu also has a relatively short half-life of 14.4 years compared to other Pu isotopes. Because of this short half-life, the ^{alphas}Pu/^{241}Pu ratios can be used in source apportionment studies (Livingston *et al.*, 1975) and potentially as a chronometer in determining the age of the deposited Pu. ^{241}Pu activities resulting from the recycling of MOX fuel are approximately 5 times higher than total Pu-alpha activities yielded by the same recycling process. It can be seen that ^{241}Pu discharges from the Sellafield site are 20 ~ 40 times higher than total Pu-alpha discharges since 1970. Consequently, ^{241}Pu is one of the major Pu isotopes released to the environment and, therefore, it will be beneficial to estimate ^{241}Pu activities for the above mentioned applications.

The short half-life and correspondingly high specific activity of ^{241}Pu favour its determination radiometrically. Livingston *et al.* (1975) determined ^{241}Pu activities in environmental samples by measuring ingrown ^{241}Am produced by the decay of ^{241}Pu previously plated on a disc for alpha spectrometer measurement of other Pu-alpha. However, it takes at least 1.5 - 2 years before measurable ingrown ^{241}Am is produced and an incomplete spectral separation of ^{241}Am from Pu isotopes will cause interferences in the determination of ^{241}Am by alpha spectrometry. The most widely used technique for the determination of ^{241}Pu in environmental samples is liquid scintillation counting (Horrocks &

Studier, 1958 ; Darral *et al.*, 1973 ; Pimpl, 1992 ; Ryan *et al.*, 1993 ; Paatero & Jaakkola, 1994). Developments in the application of alpha/beta discrimination in liquid scintillation counting has led to the application of this technique to the separation of ^{241}Pu and Pu-alpha counts during ^{241}Pu assay. The ^{241}Pu and Pu-alpha peaks are so well separated in conventional liquid scintillation counting that the peaks are readily distinguished through suitable windowing. Alpha / beta discrimination will effectively reduce the background in the Pu-alpha window but the background of the Wallac Quantulus is sufficiently low to make this unnecessary. Techniques have also been developed to count alpha spectrometry discs directly, with no further purification of the Pu, by placing the disc in the bottom of a liquid scintillation vial and adding the scintillant (Ryan *et al.*, 1993). Counting efficiencies are significantly lower as only a 2 π counting geometry is achievable. Variable deposition thickness on the alpha disc also leads to variable counting efficiencies for both ^{241}Pu and Pu-alpha which cannot be corrected for using conventional external standard quench correction techniques. Attempts have been made to use the liquid scintillation alpha peak to correct for quench but this introduces a further uncertainty in the measurement.

Pu Isotope	Half life	Decay mode	Decay energy MeV (yield)	Specific Activity Bq/g
^{236}Pu	2.90 y	α	5.72 (30.7%) 5.77 (69.1%)	1.9×10^{13}
^{238}Pu	87.7 y	α	5.46 (28.8%) 5.50 (71.0%)	6.3×10^{11}
^{239}Pu	24110 y	α	5.11 (11.5%) 5.14 (15.0%) 5.16 (73.3%)	2.3×10^{9}
^{240}Pu	6560	α	5.12 (27.0%) 5.17 (72.9%)	8.4×10^{9}
^{241}Pu	14.4 y	β	$E_{max} = 21$ keV	3.8×10^{12}
^{242}Pu	3.73×10^{5} y	α	4.86 (23.5%) 4.90 (76.5%)	1.5×10^{8}
^{244}Pu	8.0×10^{7} y	α	4.55 (19.4%) 4.59 (80.5%)	6.8×10^{5}

Decay data from Jef-PC v 2.0

Table 3-3. Plutonium isotopes present in nuclear fuel and wastes

To maximise the counting efficiency of ^{241}Pu whilst minimising measurement uncertainty, it was decided to develop a technique whereby Pu was leached from the alpha

disc and intimately mixed into the scintillant to produce a 4 π counting geometry source. Alpha/beta discrimination was not utilised as background count rates were sufficiently low and the ^{241}Pu and Pu-alpha peaks were sufficiently separated not to warrant further discrimination. As a certain amount of the steel disc is also leached with the Pu, a further purification of Pu was required. Yang *et al.* (1991) noted that Pu is extracted from nitric acid into a tri-octylphosphine oxide (TOPO) solution in toluene effecting an efficient separation of Pu from other elements found in steel. The toluene solution was ideal for liquid scintillation counting as primary and secondary fluors may be dissolved directly into the toluene or the solution may be mixed with commercial scintillants without significantly increasing the quench level of the sample. This latter approach was used as the basis of the technique described below.

3.5.2. Experimental

Reagents

^{241}Pu and ^{242}Pu standard solution
Gold Star scintillant
Glass and polythene scintillation vials
Concentrated nitric acid
4M nitric acid
Tri-octylphosphine oxide (TOPO)
Toluene
2,5-diphenyloxazole (PPO)
Naphthalene

Sample preparation

Stainless steel discs used for the determination of Pu-alpha activity by alpha-spectrometry were placed in glass beakers and 5ml of concentrated nitric acid was added. Beakers were then heated at 100°C for 10 minutes. Counting of some of the leached discs by alpha spectrometry confirmed that all Pu was leached under these conditions. The concentrated nitric acid was carefully transferred into glass scintillation vials and the acid was evaporated down to dryness. 2ml of 4M nitric acid was added to the glass scintillation vials for the extraction stage.

Extraction of Pu

2ml of 0.3M TOPO/toluene were added to glass scintillation vials and vials were shaken vigorously to extract Pu. The top organic layer was carefully transferred into polythene scintillation vials using disposable plastic pipettes. Care was taken to avoid the transfer of nitric acid which would increase quench during liquid scintillation counting. The extraction was repeated using another 2ml of 0.3M TOPO/toluene. 6ml of Gold Star scintillation cocktail were added to the vials containing a total of 4ml of 0.3M TOPO/toluene. Samples were then counted for 300 minutes.

Both commercial and laboratory-made scintillation cocktails were tested for the liquid scintillation measurement of ^{241}Pu and Pu-alpha. A disc previously analysed for Pu-alpha by alpha spectrometry was leached with 5ml concentrated nitric acid, and the nitric acid divided into two fractions containing the same activities of Pu isotopes. These two fractions were evaporated down to dryness. One fraction was dissolved in 2ml of 4M nitric acid and the other fraction was dissolved in 10ml 4M nitric acid. 2ml of 0.3M TOPO/toluene was added to the 2ml 4M nitric acid fraction and 10ml of 0.3M TOPO, 3% 2,5-diphenyloxazole (PPO) and 5% naphthalene/toluene were added to the other fraction. Both fractions were shaken for about two minutes to extract Pu. The organic layers were carefully transferred into polythene scintillation vials. The 10ml fraction was directly counted by liquid scintillation counting and the 2ml fraction was counted after adding 8ml of Gold Star scintillation cocktail. Solvent extraction using 0.3M TOPO, 3% PPO and 4M nitric acid was chosen since Pu can be selectively extracted from other elements such as fission products and Am in 4M nitric acid (Yang *et al.*, 1991). The ^{241}Pu counting efficiency using 0.3M TOPO, 3% PPO and 5% naphthalene/toluene is about factor of 10 lower than that obtained using 0.3M TOPO/toluene in Gold Star scintillation cocktail. Therefore, 0.3M TOPO/toluene in Gold Star scintillation cocktail was used for this experiment. Counting conditions are shown in Table 3-4 and the results of standard reference material are presented in Table 3-2. The ratios of Pu-alpha (particularly $^{239,240}Pu$)/^{241}Pu and the ^{241}Pu activities can be determined using the following equations :

$$\frac{^{239,240}Pu}{^{241}Pu} = R1 \times R2$$

$$^{241}Pu \text{ activity (Bq/kg)} = \left(\frac{\text{Added } ^{242}Pu \text{ in Bq}}{R1 \times R3} \times \frac{1000}{\text{Sample size in g}} \right)$$

Where ;

$$R1 = \frac{\text{CPM of Pu - alpha}}{\text{CPM of } ^{241}Pu \times \left(\frac{100}{\text{Counting efficiency of } ^{241}Pu} \right)} \text{ from the LSC}$$

$$R2 = \frac{\text{Counts of } ^{239,240}\text{Pu}}{\text{Counts of Pu - alpha}} \text{ from the alpha spectrometry}$$

$$R3 = \frac{\text{Counts of } ^{242}\text{Pu}}{\text{Counts of Pu - alpha}} \text{ from the alpha spectrometry}$$

	^{241}Pu	Pu-alpha
Window	1 - 300	560 - 710
Count time	300 min	300 min
Background cpm	1.7 - 2.0	0.30 - 0.35
Counting efficiency	32 - 35 %	100 %
Limit of detection*	3.5 Bq/kg	0.5 Bq/kg

*As defined by Currie (1968) ; sample size 5 g & chemical recovery approx. 75 %

Table 3-4. Liquid scintillation counting conditions

Chapter 4. Results

4. Results

4.1. Core samples

Figure 4-1 ~ 4-5 shows the geochemistry results and ^{241}Am, ^{137}Cs and Pu isotope results (including ^{241}Pu) for the cores analysed and their summaries for selected elements are listed in Table 4-1 along with loss on ignition data. This chapter only describes the results acquired. Interpretations on these results will be discussed in the following chapters.

		I-96-002 core	R-96-000 core	R-96-007 core	R-96-008 core	R-97-003 core
Al_2O_3 (wt.%)	Min.	7.09 (9 cm)	8.73 (36 cm)	9.64 (54 cm)	6.06 (58 cm)	11.37 (3 cm)
	Max.	8.62 (14 cm)	11.24 (top)	11.78 (28 cm)	9.53 (36 cm)	15.43 (19 cm)
	Mean	7.88	9.18	10.82	8.45	13.17
	Median	7.88	9.11	10.79	8.59	13.18
SiO2 (wt.%)	Min.	71.60 (14 cm)	60.73 (top)	62.75 (top)	69.70 (36 cm)	53.69 (3.5 cm)
	Max.	75.23 (9 cm)	71.79 (36 cm)	72.48 (54 cm)	81.39 (58 cm)	64.02 (30 cm)
	Mean	73.02	69.93	67.37	73.42	57.88
	Median	73.06	70.16	67.22	73.11	57.58
^{241}Am (Bq/kg)	Min.	1459 (top)	< 10	< 10	< 10	< 10
	Max.	13966 (28 cm)	8566 (19 cm)	24673 (18 cm)	14250 (top)	25080 (12 cm)
^{137}Cs (Bq/kg)	Min.	813 (6 cm)	< 10	< 10	93 (51 cm)	254 (27 cm)
	Max.	7159 (19 cm)	10011 (18 cm)	15224 (17 cm)	8961 (7 cm)	20676 (11 cm)
^{238}Pu (Bq/kg)	Min.	231 (top)	< 10	< 10	< 10	Not available
	Max.	2500 (28 cm)	1315 (17 cm)	2294 (18 cm)	1405 (12 cm)	"
$^{239,240}Pu$ (Bq/kg)	Min.	1093 (top)	147 (bottom)	< 10	< 10	Not available
	Max.	15780 (28 cm)	6074 (17 cm)	10824 (18 cm)	7400 (9 cm)	"
^{241}Pu (Bq/kg)	Min.	14305 (top)	244 (32 cm)	13 (42 cm)	39 (54 cm)	Not available
	Max.	152489 (28 cm)	78548 (17 cm)	114060 (18 cm)	85579 (9 cm)	"
LOI (wt.%)	Min.	6.9 (7 cm)	6.8 (33 cm)	6.0 (48)	3.9 (58 cm)	7.3 (30 cm)
	Max.	8.2 (2 cm)	11.0 (top)	11.7 (top)	7.4 (36 cm)	18.6 (2.5 cm)

Table 4-1. Summary of results in the core samples

4.1.1. Major and trace element results in cores

I-96-002 Core (Figure 4-1)

For all the major and trace elements, there are no significant changes throughout the core. The Al_2O_3 contents range from 7.09 to 8.62 (dry wt. %). The minimum values are 7.09 (9cm) and 7.12 (8 cm), whereas the maximum values are 8.48 (13 cm) and 8.62 (14 cm).

The average value of Al_2O_3 is 7.88 (dry wt. %). The SiO_2 contents lay a range of 71.60 to 75.23 with the average of 73.02 (dry wt. %). None of CaO, Fe_2O_3, MnO & S contents show significant changes with depth. Same pattern is observed for Loss on Ignition (LOI) data (6.9 ~ 8.2 %).

R-96-000 Core (Figure 4-2)

The Al_2O_3 contents are between 8.73 and 11.24 (dry wt. %). The average value is 9.18 (dry wt. %). With the average of 69.93, SiO_2 values vary from 60.73 to 71.79 (dry wt. %). The minimum value of Al_2O_3 is measured at 36 cm and that of the maximum is found at the top of the core. For SiO_2 results it is vice versa. The results of other elements show higher values at the top and become more or less constant throughout the core except for S contents. The S contents more or less increase with depth range from 0.16 to 0.45 (Wt. %). The LOI values lay between 6.8 and 11.0 %, where the highest one is found at the top.

R-96-007 Core (Figure 4-3)

The Al_2O_3 measurements range from 9.64 to 11.78 (dry wt. %) with its average of 10.82 (dry wt. %). The lowest value is measured at 54 cm and the highest one is found at 28 cm below the surface. For SiO_2 the highest measurement of 72.48 (dry wt. %) is found at 54 cm and that of the lowest is 62.75 (dry wt. %) at the top of the core. The average value of SiO_2 is 67.37 (dry wt. %). No dramatic changes are seen for S, however, MnO profile shows quite definite changes in this core. Top 1 ~ 3 cm show high CaO contents, although the rest of the core shows no major changes. LOI data are between 6.0 (52, 54 cm) and 12.0 % (top).

R-96-008 Core (Figure 4-4)

The highest value is 9.53 (dry wt. %) found at 36 cm and the lowest is 6.06 (dry wt. %) measured at 58 cm for Al_2O_3. The SiO_2 contents range from 69.70 to 81.39 (dry wt. %) and the lowest value (69.70) is found where that of the highest Al_2O_3 content is measured. The highest SiO_2 is detected where that of the minimum Al_2O_3 is found. The average values for Al_2O_3 and SiO_2 are 8.45 and 73.42 (dry wt. %), respectively. The S contents show dramatic changes in this core that increase sharply around 32 cm below the surface. The

similar changes are seen for MnO. Other elements such as Pb and Zn also show a decrease in the bottom of the core, although this decrease is not as sharp as that of S and MnO. LOI results vary between 3.9 and 7.4 % (58 and 36, 38 cm, respectively) with its average of 6.4 %.

R-97-003 Core (Figure 4-5)

This core was sub-sampled every 0.5 cm intervals to get higher resolution vertical profiles. The Al_2O_3 contents range from 11.37 to 15.43 (dry wt. %). The average value is 13.17 (dry wt. %). With the average of 57.88, SiO_2 values vary from 53.69 at 3.5 cm to 64.02 at 30 cm (dry wt. %). The minimum value of Al_2O_3 is measured at 3 cm and that of the maximum is found at 19 cm. The S contents range from 0.16 to 0.45 (Wt. %) and an increase is found at 3.5 cm. The LOI values lay between 7.3 and 18.6 %, where the highest one is found at 2.5 cm .

4.1.2. Radionuclide results in cores

I-96-002 Core (Figure 4-1)

The activities of ^{241}Am measured vary between 1459 ~ 13966 Bq/kg (dry weight). The highest activity is found at the bottom and the lowest value is measured at the top of the core. Activities of ^{241}Am in this core steadily increase with depth. The range of ^{137}Cs activities found is 813 ~ 7159 Bq/kg (dry weight). The highest activity is found at a depth of 19 cm below the surface and the lowest one is measured at a depth of 6 cm below the surface. Vertical profiles of ^{137}Cs in this core are very similar to those of ^{241}Am. The measured activities of Pu isotopes in this core are 1093 ~ 15780 Bq/kg (dry weight) for $^{239,240}Pu$, 231 ~ 2500 Bq/kg (dry weight) for ^{238}Pu and 14305 ~ 152489 Bq/kg (dry weight) for ^{241}Pu. It is the top of the core where the minimum values of all the Pu isotopes are measured. The maximum activities are found at the bottom of the core. Vertical profiles of Pu isotopes are quite similar to each other. For $^{239,240}Pu$ an elevated activity is seen at 3 cm below the surface which is not found for other Pu isotopes.

R-96-000 Core (Figure 4-2)

The maximum activities of ^{241}Am are 8566 and 8583 Bq/kg (dry weight) found at 18 and 19 cm below the surface. The lowest value is found at 35 cm below the surface and it is 2 Bq/kg. However, the uncertainty of the result is rather high. Another low activities (34 and 15 Bq/kg) are measured at 32 and 33 cm, respectively. Elevated levels of ^{241}Am are detected near the bottom (34 and 36 cm). The activities of ^{137}Cs found range from 4 to 10011 Bq/kg (dry weight). The general pattern of ^{137}Cs activities is increasing activities of ^{137}Cs up to 18 cm below the surface and smooth decrease in activities to the bottom of the core. Relatively higher activities are measured at 34 cm (258 Bq/kg) and 36 cm (352 Bq/kg) in depth. Vertical profiles of all Pu isotopes look very similar to each other as well in this saltmarsh core. ^{239,240}Pu activities are between 147 and 6074 Bq/kg (dry weight). For ^{238}Pu, activities range from 6 to 1315 Bq/kg (dry weight) and between 244 to 78548 Bq/kg (dry weight) for ^{241}Pu. The highest activities are found at 17 cm below the surface for all Pu isotopes and the lowest values are measured at 32 cm except for ^{239,240}Pu which the lowest activity is found at the bottom of the core.

R-96-007 Core (Figure 4-3)

The activities of ^{241}Am found range from 3 to 24673 Bq/kg (dry weight). Below 28 cm from the surface, either the uncertainties of the measured value become higher or it is not detected. Two ^{241}Am peaks are seen in this core. One is at 13 cm (10956 Bq/kg) and the other is 18 cm (24673 Bq/kg) where the highest value is measured. The highest ^{137}Cs activity is found at 17 cm below the surface and the measured activity is 15224 Bq/kg (dry weight). Below 39 cm from the surface, measured activities of ^{137}Cs are either relatively very low or undetectable. Uncertainties increase significantly below 30 cm from the surface for all Pu isotopes. The highest activities are 10824 Bq/kg for ^{239,240}Pu, 2294 Bq/kg for ^{238}Pu and 114060 Bq/kg for ^{241}Pu (dry weight). All those activities are measured at 18 cm below the surface. Although elevated activities are found at 46 cm, activities of Pu isotopes are relatively low in the deeper depths.

R-96-008 Core (Figure 4-4)

Unlike the other cores, the highest activity (14250 Bq/kg) is found at the top of the core. Other higher activities are 13029 and 13106 Bq/kg (dry weight) which are measured at 11 and 12 cm. Below 46 cm from the surface, ^{241}Am activities discontinue and uncertainties become higher. Similar to ^{241}Am, the activity of ^{137}Cs at the top is rather high. It is 4745 Bq/kg (dry weight) which is 4 ~ 5 times higher than the other three cores. The maximum value, however, which is 8961 Bq/kg (dry weight), is found 7 cm below the surface. Relatively higher activities of ^{137}Cs are measured in the bottom (below 50 cm) of the core that is not seen in the other three cores. The highest Pu activities are found at 9 cm (^{239,240}Pu and ^{241}Pu) and 12 cm (^{238}Pu) below the surface and they are 7400 Bq/kg, 1405 Bq/kg and 85579 Bq/kg (dry weight) for ^{239,240}Pu, ^{238}Pu and ^{241}Pu, respectively. Relatively higher activities are measured at the top of the core. The activity of ^{239,240}Pu at the top is 4970 Bq/kg, 1071 Bq/kg for ^{238}Pu and that of ^{241}Pu is 69884 Bq/kg (dry weight). Peaks of Pu isotopes are not as sharp as the other two Ravenglass saltmarsh cores.

R-97-003 Core (Figure 4-5)

The ^{241}Am activities vary from < 10 to 25080 Bq/kg (dry weight) in this core. The minimum values are measured at depth below 25 cm. The maximum activity is found at 12 cm. The activity range of ^{137}Cs found in this core is 254 ~ 20670 Bq/kg (dry weight). The highest activity is measured at 11 cm in depth. General shape of the profiles is very similar to that of the R-96-000 core and R-96-007 core.

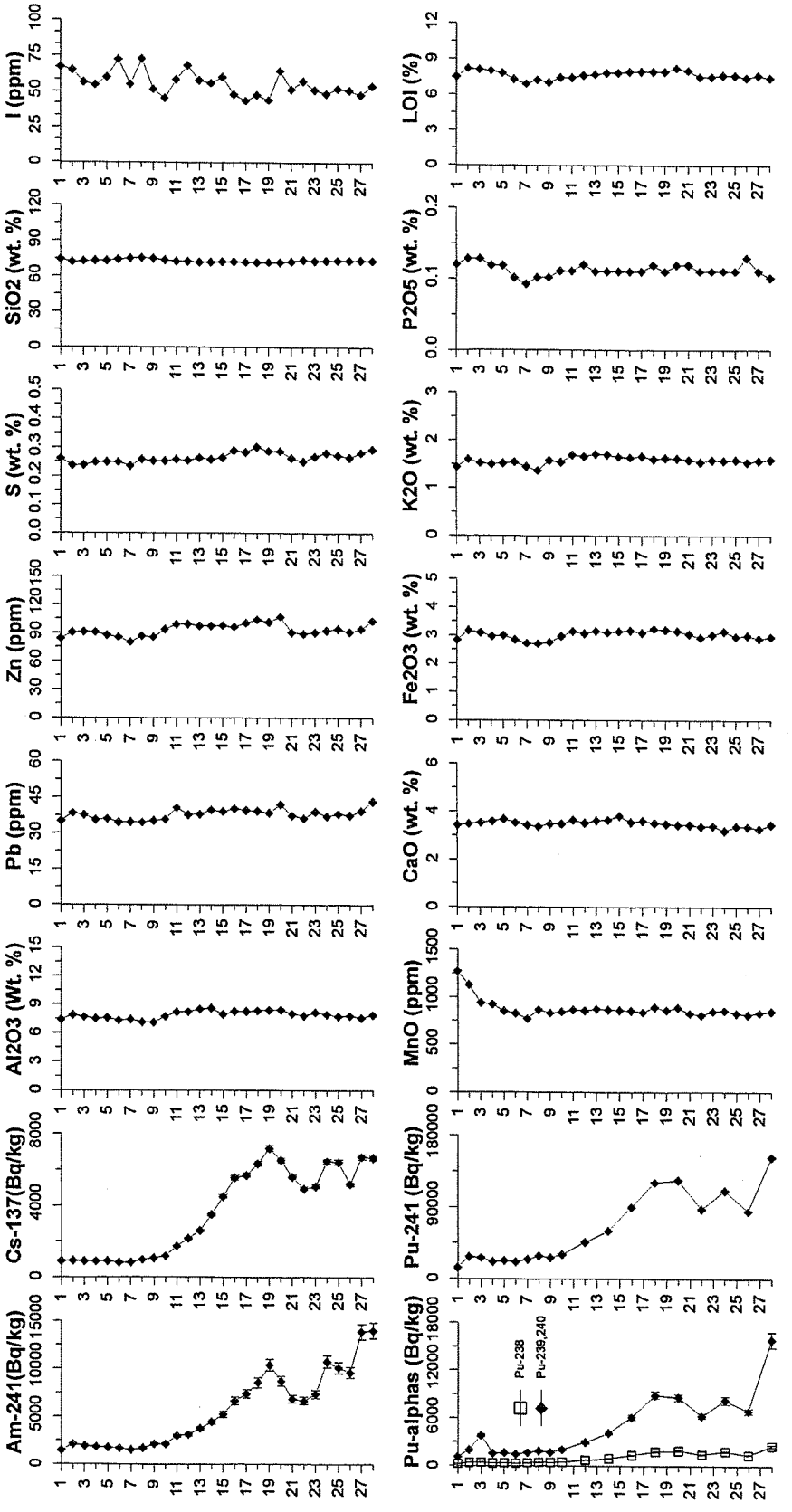

Figure 4-1. Geochemistry and radionuclide results for I-96-002 core

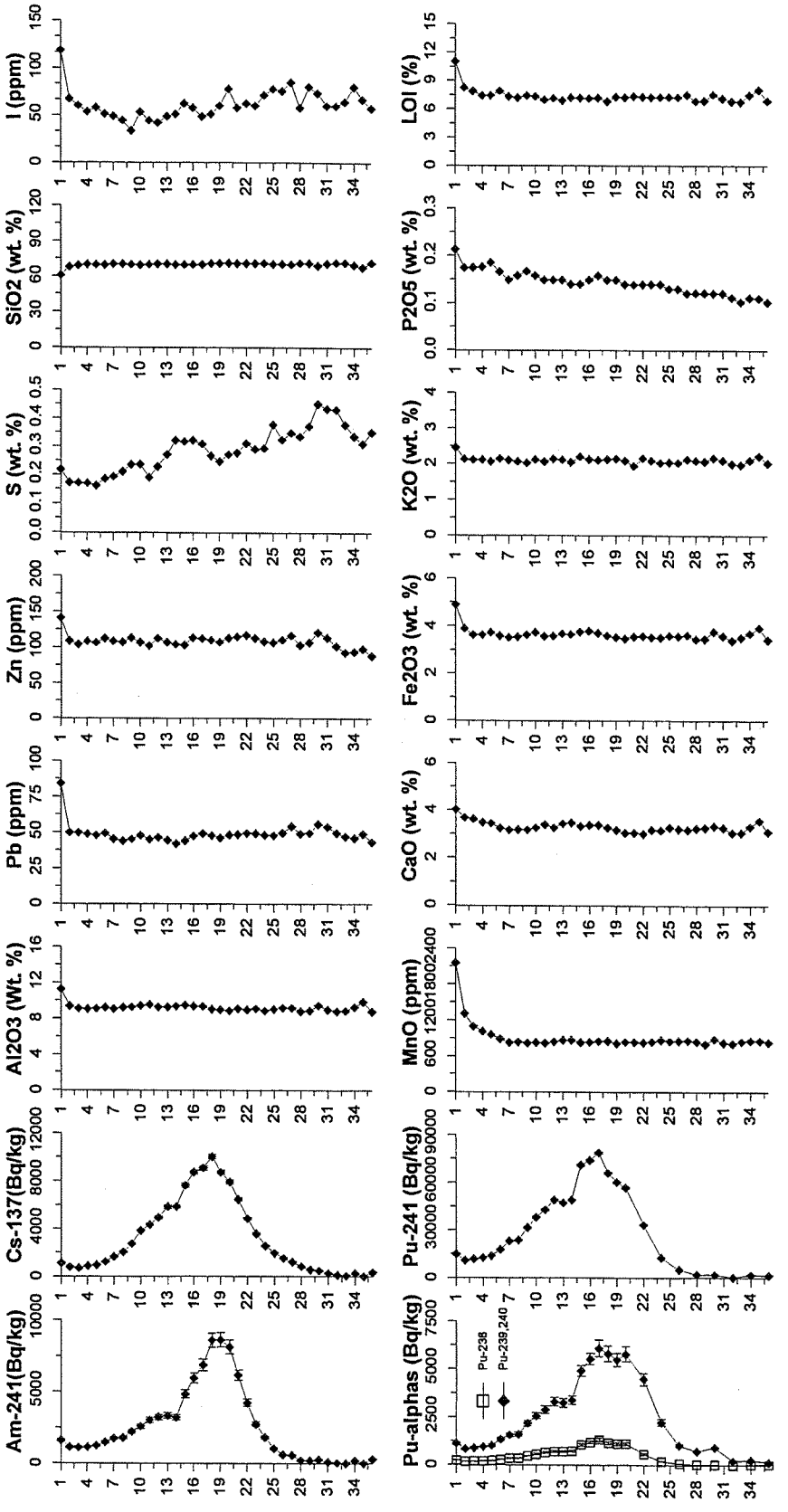

Figure 4-2. Geochemistry and radionuclide results for R-96-000 core

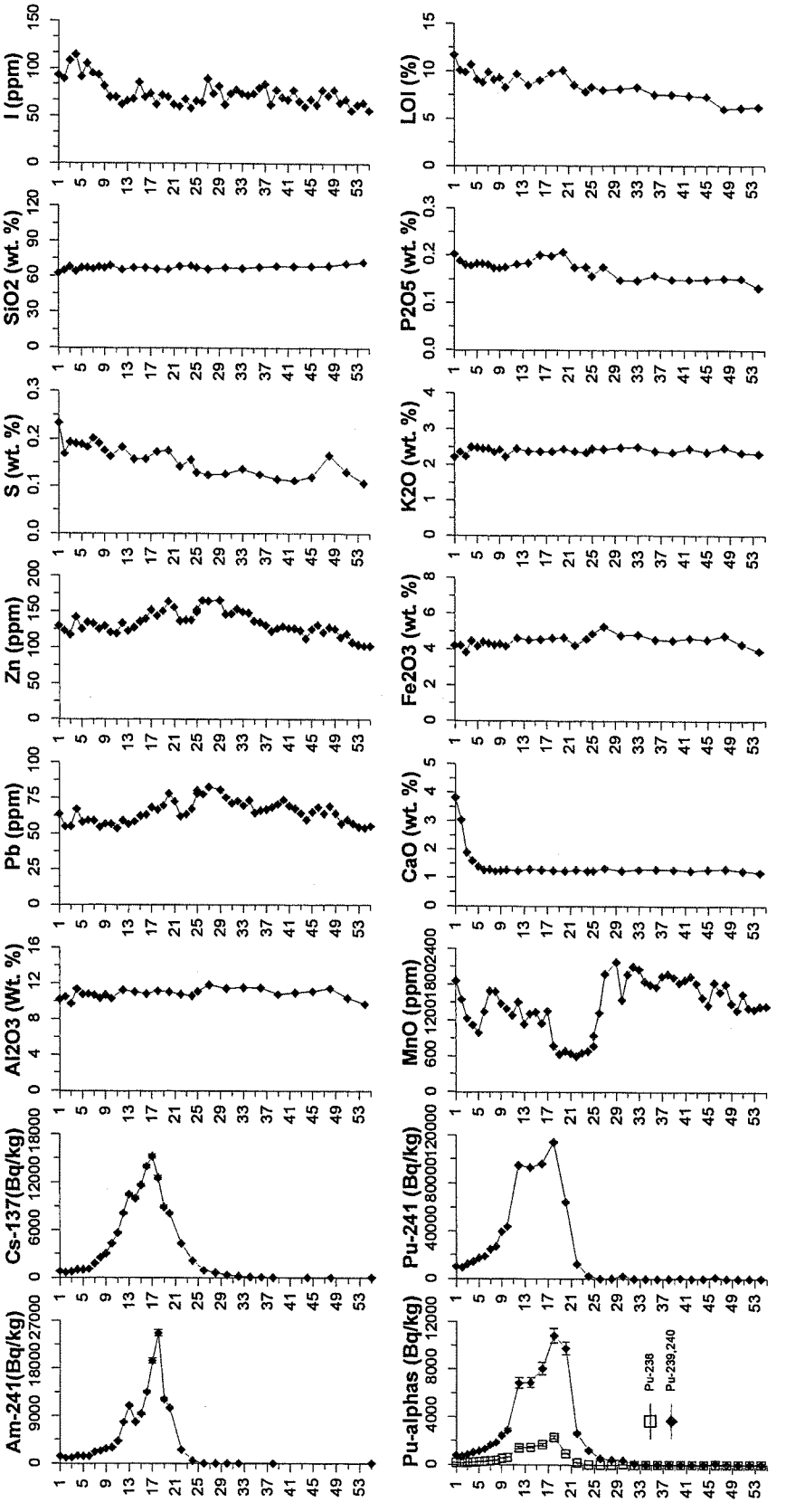

Figure 4-3. Geochemistry and radionuclide results for R-96-007 core

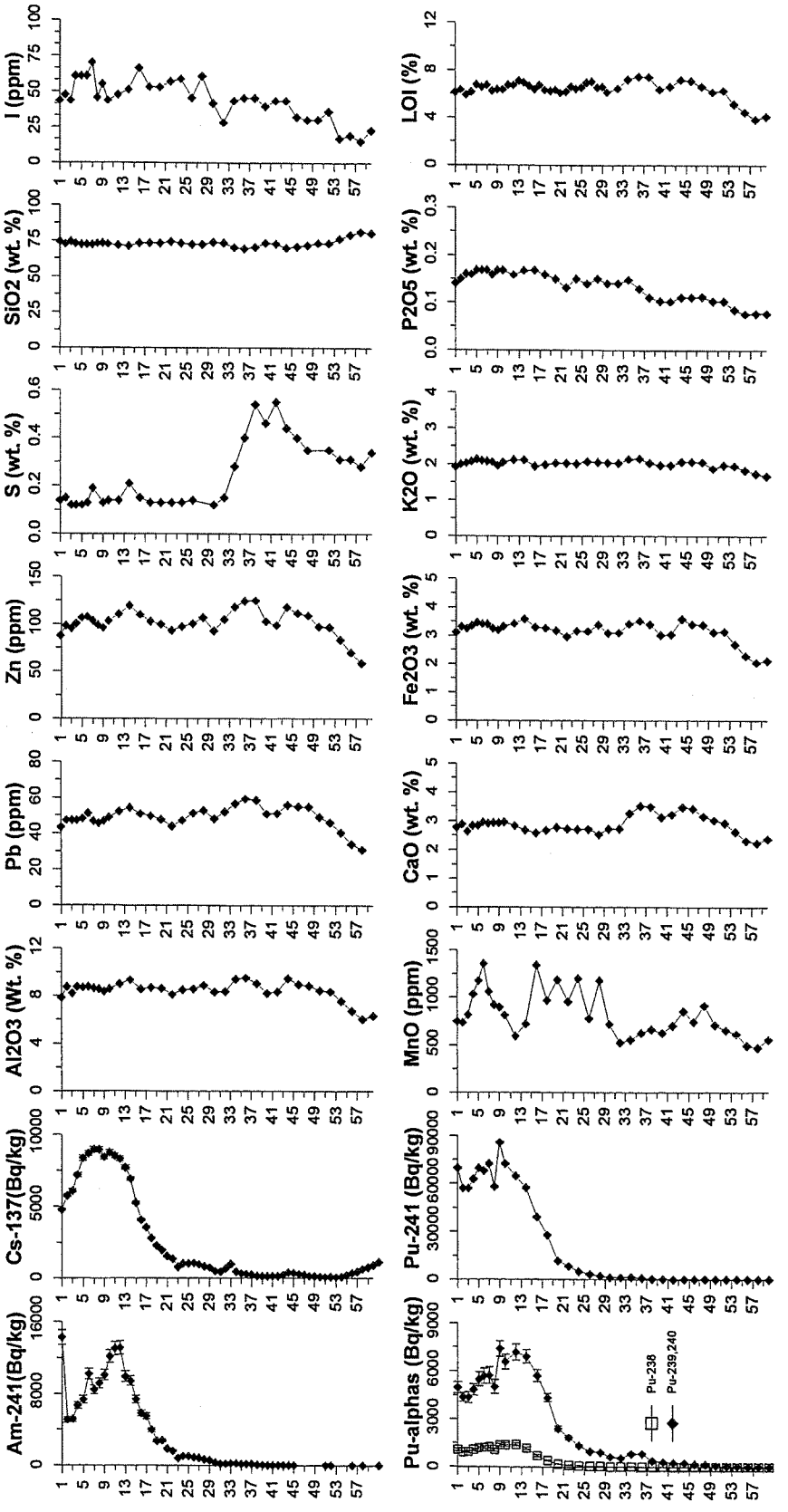

Figure 4-4. Geochemistry and radionuclide results for R-96-008 core

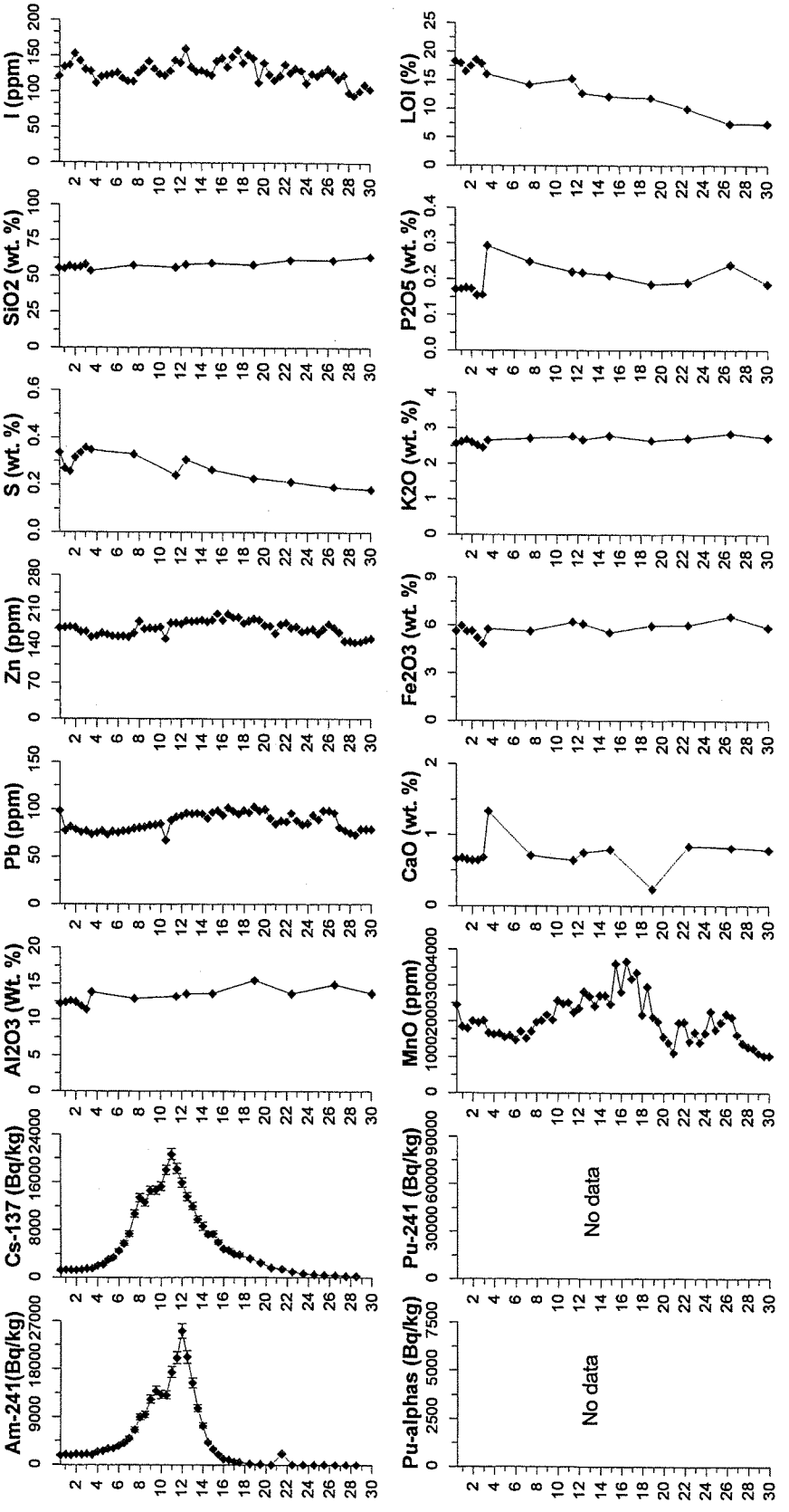

Figure 4-5. Geochemistry and radionuclide results for R-97-003 core

4.2. Surface scrape samples

4.2.1. ^{241}Am and ^{137}Cs activities in surface scrape samples (1980 and 1997)

^{241}Am activities for the 1980 surface scrape samples range from 603 to 11433 Bq/kg (dry weight) with the average of 5712 Bq/kg (dry weight). The highest ^{241}Am activity is found at X6 and the lowest value is measured at F7. Relatively higher activities are found around the edges and at some points in the middle of the marsh. For the 1997 samples, measured activities of ^{241}Am are between 807 and 3958 Bq/kg (dry weight). The average activity of the 1997 surface scrape samples is 1515 Bq/kg (dry weight). For 1997 ^{241}Am results, the lowest activity is measured from the sample collected at F5, and the highest activities of ^{241}Am are found at E0 and F6. Relatively higher activities of ^{241}Am (higher that 2000 Bq/kg) are measured from five different sampling locations which are B0, C9, E0, E6 and F6 (Figure 4-6).

^{137}Cs activities for the 1980 samples are between 509 and 29230 Bq/kg (dry weight). The average value for 1980 results is 16788 Bq/kg (dry weight). The highest activity is found at A6, and the lowest activity is measured at E0. For the 1997 results, ^{137}Cs activities lay between 494 and 5480 Bq/kg (dry weight) with the average activity of 1111 Bq/kg (dry weight). The highest activities of ^{137}Cs are measured at the same sampling points where the highest ^{241}Am are found, and the lowest activity is detected at W10 (Figure 4-7).

4.2.2. ^{238}Pu, ^{239,240}Pu and ^{241}Pu activities in surface scrape samples (1997)

The lowest activity of ^{238}Pu found is 101 Bq/kg (dry weight) at F5 and the highest activity is measured at F6 which is 823 Bq/kg (dry weight). Other higher activities (higher than 300 Bq/kg) are from the samples collected at B0, C9, E0, E6 and Z4 (Figure 4-8).

The activities of ^{239,240}Pu range from 499 to 3774 Bq/kg (dry weight). The sampling locations where the highest and the lowest activities measured are same as those of ^{238}Pu. Activities higher than 2000 Bq/kg are found at B0, E0 and E6 (Figure 4-9).

The range of measured ^{241}Pu activities are between 6670 and 55872 Bq/kg (dry weight). Like other Pu isotopes, it is F6 where the highest activity is found, however, the lowest activity is found at different location. It is W10 where the lowest value is detected. The activity (6681 Bq/kg) of ^{241}Pu from F5, where the lowest activities are found for other Pu isotopes, is very close to the lowest measurement. The results of ^{241}Pu are shown in Figure 4-10.

	A	V	B	W	C	X	D	Y	E	Z	F
0			*2975*	*1737*	*1772*	*1883*	*1785*	*1617*	*3958*		
			5476	7844	7955	5698	7881	9398	10656		
	1988	*1683*	*1170*	*1270*	*1338*	*1494*	*1484*	*1536*	*1339*	*1561*	*1661*
1	7955	8621	4625	6734	2031	6031	6623	3434	5735	6623	7511
	1777	*1536*	*1859*	*1698*	*1715*	*1083*	*1197*	*1396*	*1324*	*1675*	*1521*
2	6253	5365	6845	7030	6882	4810	3996	6623	6290	7289	6401
	1969	*1754*	*1763*	*1471*	*1178*	*1524*	*1232*	*1137*	*978*	*1372*	*1643*
3	8325	7178	6438	7030	3286	6179	2560	5069	2379	6253	5883
	1944	*1871*	*1947*	*1607*	*1549*	*1461*	*1709*	*1669*	*1636*	*1213*	*1433*
4	8214	3234	7178	4144	6623	6586	6475	8066	5920	6808	5032
	1550	*1712*	*1528*	*1695*	*1364*	*1540*	*1382*	*1332*	*1162*	*1060*	*807*
5	7215	10582	7622	7141	5513	6290	5402	6623	5846	3278	3263
	1256	*1621*	*1388*	*1254*	*1281*	*1219*	*1073*	*1029*	*2534*	*1003*	*3943*
6	7141	6882	6660	7955	6142	11433	4699	3149	1887	2945	1299
	1595	*1611*	*1460*	*1225*	*1172*	*897*	*875*				
7	6438	6882	8510	5402	1602	4255	3363	3027	2893	1310	603
	1477	*1422*	*1172*	*1300*	*1288*						
8	6031	2594	8473	5217	4625	4329	3774				
	1265	*1280*	*1050*	*1057*	*2059*						
9	4921	5032	5698	4921							
	1167	*1241*	*1466*	*850*							
10	4884	4810	4329								
	1168										
11	5069										

(1980 data are printed in normal and 1997 data are in Italics)

Figure 4-6. Surface scrape data for both 1980 and 1997 ^{241}Am (Bq/kg dry wt.)

	A	V	B	W	C	X	D	Y	E	Z	F
0			*3656*	*1684*	*1520*	*1221*	*1360*	*1155*	*5480*		
			20091	26307	18759	15947	17501	26048	509		
1	*1673*	*1106*	*900*	*854*	*814*	*1444*	*973*	*1000*	*871*	*1047*	*1178*
	28083	19203	12321	18241	7289	18463	21793	14208	18315	22237	19980
2	*1154*	*996*	*1155*	*1121*	*1027*	*656*	*735*	*997*	*872*	*1061*	*1015*
	18389	13653	16280	18093	16576	14319	12987	21238	19203	20165	17797
3	*1506*	*1225*	*1222*	*963*	*777*	*1253*	*795*	*753*	*956*	*1024*	*1366*
	21386	19425	18241	15318	10989	20313	7474	15688	5661	23717	18278
4	*1407*	*1316*	*1590*	*1065*	*957*	*1093*	*1229*	*1218*	*1399*	*872*	*1036*
	19129	9398	17723	13727	22533	20054	21682	23125	23865	21016	16058
5	*997*	*1178*	*1024*	*1067*	*989*	*1057*	*1020*	*841*	*782*	*710*	*575*
	19092	28601	22422	21349	16539	24309	18389	19240	18722	13172	10767
6	*931*	*1144*	*958*	*819*	*814*	*973*	*711*	*667*	*2538*	*660*	*3330*
	29230	23014	23088	21386	17945	21978	14578	11988	7326	7252	3700
7	*1117*	*1201*	*941*	*765*	*791*	*561*	*554*				
	27084	25567	21312	15540	6771	12210	11100	10397	9250	4514	1706
8	*948*	*876*	*731*	*818*	*773*						
	19166	5957	18315	15244	13653	14726	12691				
9	*877*	*852*	*693*	*653*	*1211*						
	16169	12506	16650	15244							
10	*749*	*771*	*873*	*494*							
	17612	14208	15170								
11	*742*										
	16391										

(1980 data are printed in normal and 1997 data are in Italics)

Figure 4-7. Surface scrape data for both 1980 and 1997 ^{137}Cs (Bq/kg dry wt.)

	A	V	B	W	C	X	D	Y	E	Z	F
0			411	222	230	252	226	215	546		
	241	205	160	166	187	171	205	237	184	198	233
1											
	230	211	242	237	234	170	172	195	178	217	184
2											
	246	245	239	202	154	231	183	158	148	178	247
3											
	255	236	287	219	220	212	228	230	253	332	219
4											
	202	208	186	194	180	196	192	198	143	155	101
5											
	241	212	201	186	176	169	149	143	452	150	823
6											
	215	231	188	179	162	135	115				
7											
	205	227	154	174	174						
8											
	166	189	165	171	304						
9											
	163	181	198	115							
10											
	165										
11											

Figure 4-8. Surface scrape data for ^{238}Pu in 1997 samples (Bq/kg dry wt.)

	A	V	B	W	C	X	D	Y	E	Z	F
0			2027	1038	1099	1203	1089	1044	2624		
1	1167	1067	801	823	879	856	999	1240	939	1010	1139
2	1149	1027	1211	1057	1102	848	866	920	909	1042	907
3	1249	1219	1220	1002	771	1082	912	775	938	875	1197
4	1262	1157	1445	1092	1018	1019	1122	1150	1187	1615	995
5	979	1035	1001	944	881	950	969	962	703	733	499
6	1164	1004	1013	889	854	797	715	701	2452	716	3774
7	1047	1122	878	871	759	647	588				
8	1041	1249	749	798	843						
9	831	943	812	840	1459						
10	808	896	963	566							
11	803										

Figure 4-9. Surface scrape data for ^{239,240}Pu in 1997 samples (Bq/kg dry wt.)

	A	V	B	W	C	X	D	Y	E	Z	F
0			27306	14016	14730	15796	14372	13678	37112		
1	15476	13623	10056	10458	10778	11068	12954	15385	11524	13155	15268
2	15410	13633	16857	13118	14932	10555	11044	12623	12322	14203	11901
3	16171	15334	16154	13015	10074	15032	11610	9958	10813	11979	16584
4	16635	15731	19652	13913	13658	14343	15624	14659	16238	21719	14627
5	12185	13181	11661	12281	11182	12748	13263	13057	9224	9816	6681
6	15617	12672	12520	10942	11175	10139	9729	9303	30781	9420	55872
7	13963	14703	11921	11583	9736	8910	7226				
8	13277	14565	9698	10491	11158						
9	11186	12304	10870	11165	20128						
10	10187	11763	12702	6670							
11	10455										

Figure 4-10. Surface scrape data for ^{241}Pu in 1997 samples (Bq/kg dry wt.)

Chapter 5. Estimation of the sediment mixing rates

5. Evaluation of sediment mixing

5.1. Introduction to sediment mixing

Various radionuclides discharged from the Sellafield nuclear site have been used to estimate the sediment accumulation rates in the saltmarsh environment (Aston & Stanners, 1979 ; Stanners & Aston, 1981a. ; Clifton & Hamilton, 1982). One of the approaches compares the isotopic ratios of the same elements (such as $^{134}Cs/^{137}Cs$ and $^{238}Pu/^{239,240}Pu$) to those of the Sellafield annual discharge. However, the mixing of discharged radionuclides with different ages and different isotopic ratios make the comparison of measured data with those of discharges from the Sellafield site problematic. In addition, as MacKenzie & Scott (1982) suggested, the use of isotopic ratios, particularly $^{238}Pu/^{239,240}Pu$, is subject to uncertainty because there are no ^{238}Pu discharge data from the Sellafield site prior to 1978. Therefore, it is necessary to find another approach of estimating the sediment accumulation rates to avoid these problems. It has been reported by numerous authors (Aston *et al.*, 1981 ; Aston & Stanners, 1982a ; MacKenzie *et al.*, 1987, 1994 ; Aston *et al.*, 1985 ; McDonald *et al.*, 1990 ; MacKenzie & Scott, 1993) that onshore transport of sediment labelled with Sellafield radionuclides is the major mechanism for transporting radionuclides to surrounding areas including intertidal, offshore and estuarine environments. Isotopic ratios have also been used in order to provide information on this onshore transport of sediment. An assumption of sediment mixing has been applied for these interpretations. Clifton & Hamilton (1982) suggested surface mixing occurred and MacKenzie & Scott (1982) and MacKenzie *et al.* (1994) modelled this mixing using a simple mathematical approach.

Figure 5-1 shows Pu isotopic ratios for Sellafield discharges, both as reported and decay corrected to 1998, and those measured in the core samples are shown in Figures 5-2 ~ 5-4. The ratios of Pu isotopes in the discharge and those measured in cores do not show any correlation. $^{238}Pu/^{239,240}Pu$ ratios in Sellafield discharge range from 0.25 to 0.40 between 1980 and 1996. However, $^{238}Pu/^{239,240}Pu$ ratios measured from the cores up to 30 cm below the surface are much lower than discharge ratios (around 0.2 in most cases). It appears that the other Pu isotopic ratios show the same pattern. In order to explain this discrepancy, a mathematical model has been developed based on the accumulation-plus-mixing model (MacKenzie & Scott, 1982).

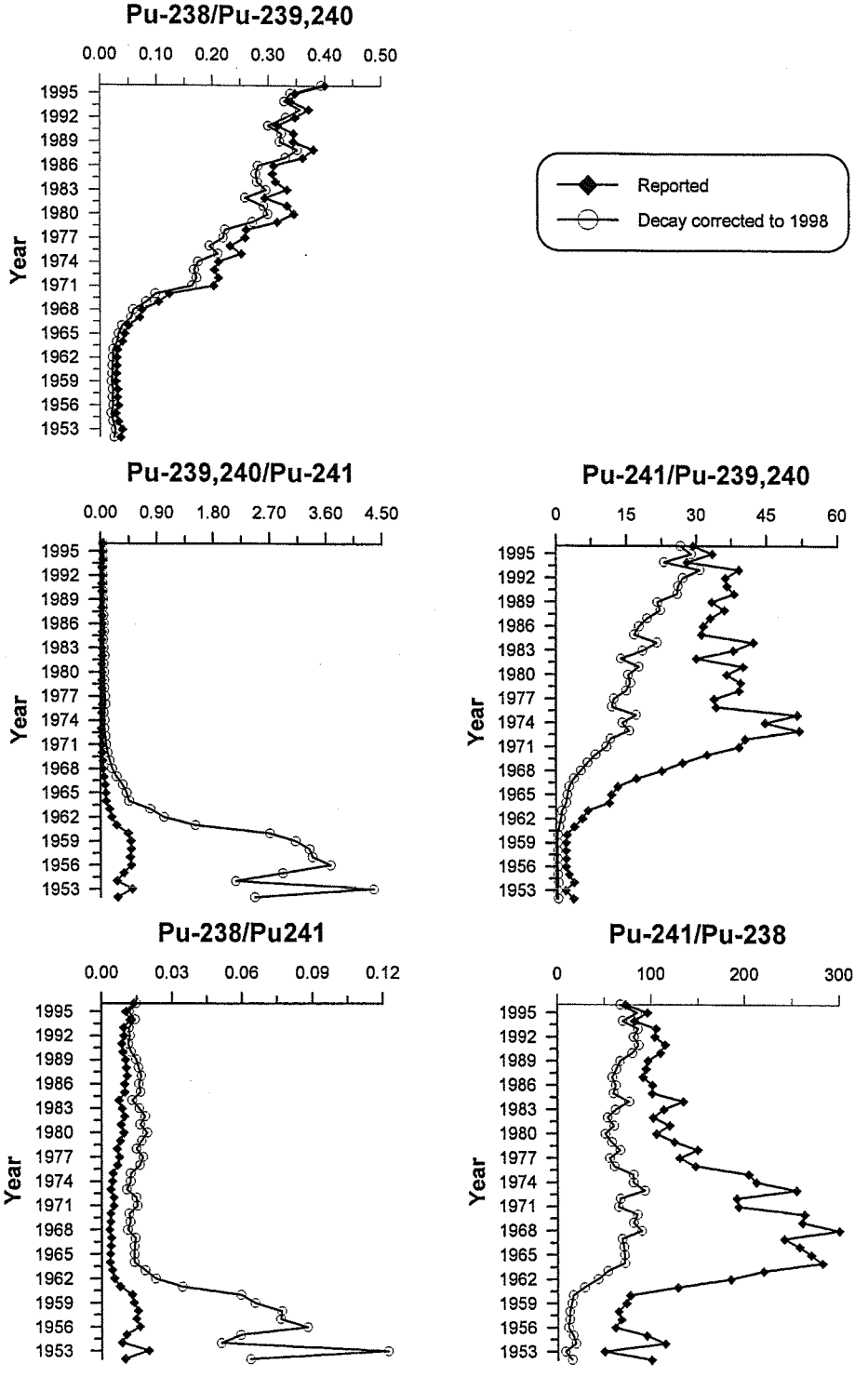

Figure 5-1. Isotopic ratios of Pu isotopes for the Sellafield discharges

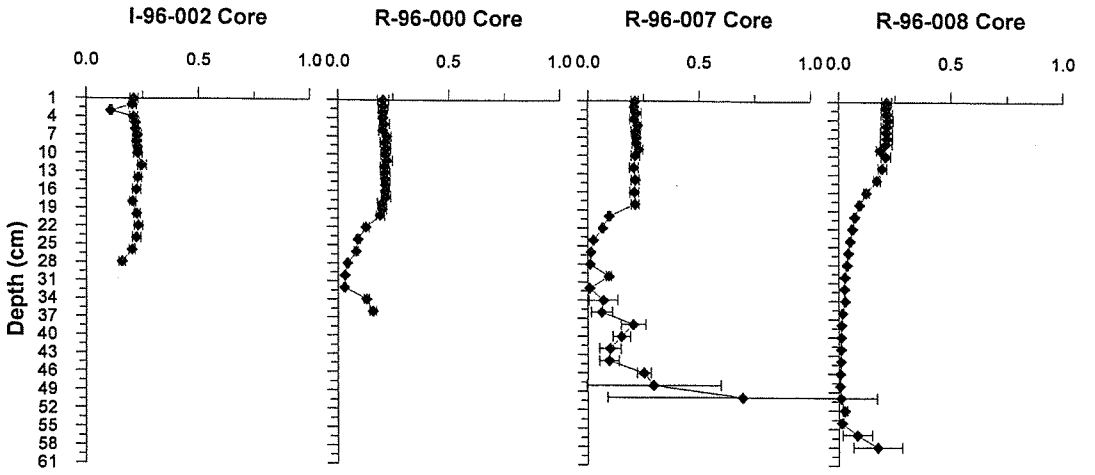

Figure 5-2. $^{238}Pu/^{239,240}Pu$ ratios in cores

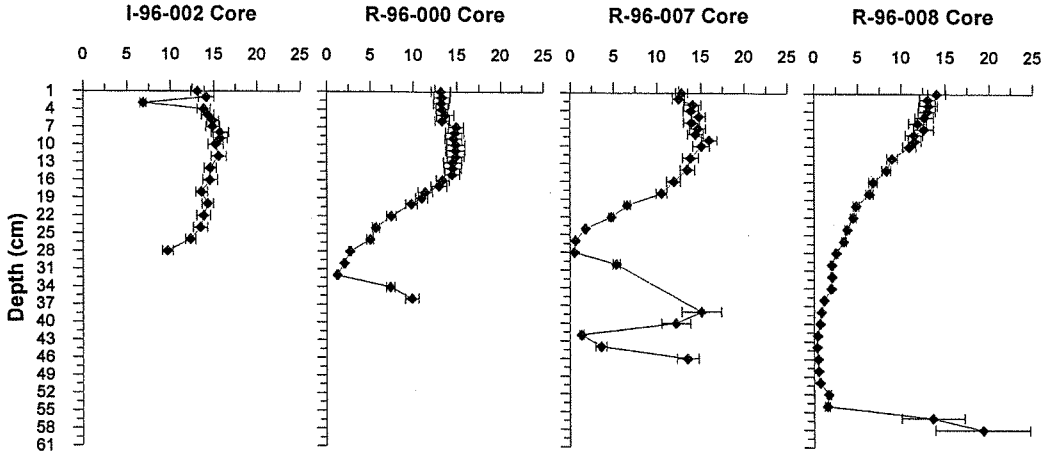

Figure 5-3. $^{241}Pu/^{239,240}Pu$ ratios in cores

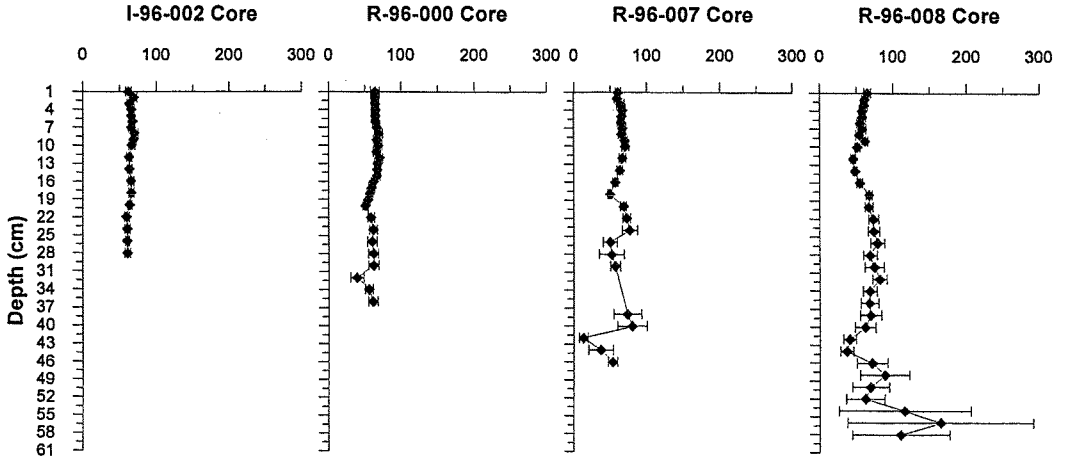

Figure 5-4. $^{241}Pu/^{238}Pu$ ratios in cores

The basis of the modelling by MacKenzie & Scott (1993) is best expressed by their statement "If the approximation is made that the sediment which is available for redistribution is subject to rapid total vertical mixing, then the radionuclide concentrations in the sediment would be determined by the time-integrated discharge, allowing for radioactive decay and ingrowth, and the radionuclide activity ratios would be equal to those of the time-integrated discharge". A similar approach was carried out by MacKenzie *et al.* (1994) using two cores collected close to Southwick Water, a small river in a saltmarsh on the Solway coast. They found that the ratio of the maximum measured radionuclide activity to that of the surface sample in cores has a value that is significantly different from that of the Sellafield discharge. They concluded that the mixing of sediments contaminated with Sellafield-derived radionuclides of different ages before deposition would be responsible for those discrepancies. However, it should be noted that they concluded that quantification of the degree of mixing was not possible because of the limited information for the Sellafield discharge. Recently, more accurate Sellafield discharge data have become available (Gray *et al.*, 1995) so it now is possible to estimate the degree of mixing. One of the recent publications by MacKenzie *et al.* (1998) concluded that the constant activity ratios of $^{238}Pu/^{239,240}Pu$ and $^{241}Am/^{239,240}Pu$ measured in three cores collected from the Irish Sea resulted from the mixing of sediments. As reported by Aston & Stanners (1981a), MacKenzie & Scott (1982), Sholkovitz & Mann (1984), Kershaw *et al.* (1990) and Malcolm *et al.* (1990), the dominant factors influencing the vertical distribution of radionuclides would be the variations in input, sedimentation and mixing.

It is necessary to briefly mention about the type of sediment mixing applied to this study. There may be several different types of mixing. The simplest type is complete mixing which is so thorough that no histories of source input are preserved. The second type is the mixing controlled by the annual deposition and diffusional migration. This kind of mixing can be predicted by a mathematical model. In this study, however, the mixing that has occurred before the sediment actually accumulates onto the saltmarsh (pre-depositional mixing) will be estimated. Figure 5-5 shows the possible process which can occur for such mixing. The basis of modelling for this study is that the surface sediments labelled with previous years discharge are resuspended and radionuclides in liquid waste discharged from Sellafield associated with the resuspended sediments and transported to the possible sinks. The assumptions and other features applied for the modelling are described in the following section.

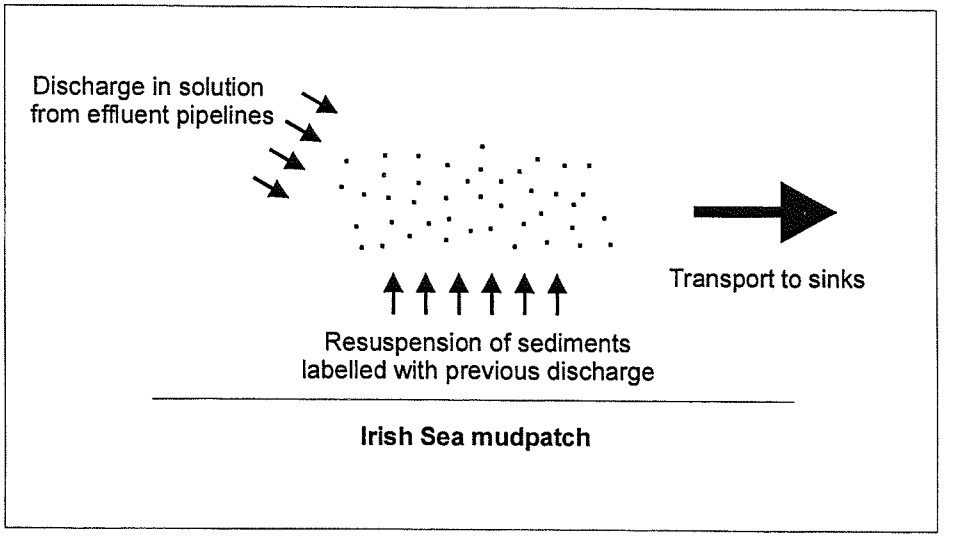

Figure 5-5. Schematic diagram of mixing process

5.2. Determination of the sediment mixing using core results

In order to estimate the sediment mixing, the following assumptions are made prior to mathematical modelling (see Figure 5-6).

1. Sediments contaminated with radionuclides from the Sellafield site in year (i) are mixed with sediments containing proportions of previous years (i-1) discharge: fractional bulk mixing
2. There is no direct input of year (i) sediment to the Ravenglass saltmarsh
3. Once introduced into and deposited onto the Ravenglass saltmarsh, there are no significant post-depositional processes (This assumption is supported by the ^{241}Am and ^{137}Cs found in the cores and the laminations found in the Ravenglass cores)
4. Sediment input into the Ravenglass saltmarsh is constant every year (supported by radionuclide distribution and the regularity of the laminations)
5. It is assumed that the calculated activities of ^{238}Pu before 1978 and other radionuclides by Gray *et al.* (1995) are correct
6. It should also be noted that all the data used are already decay-corrected to 1998 and ^{241}Am data used include ingrown ^{241}Am from the decay of ^{241}Pu

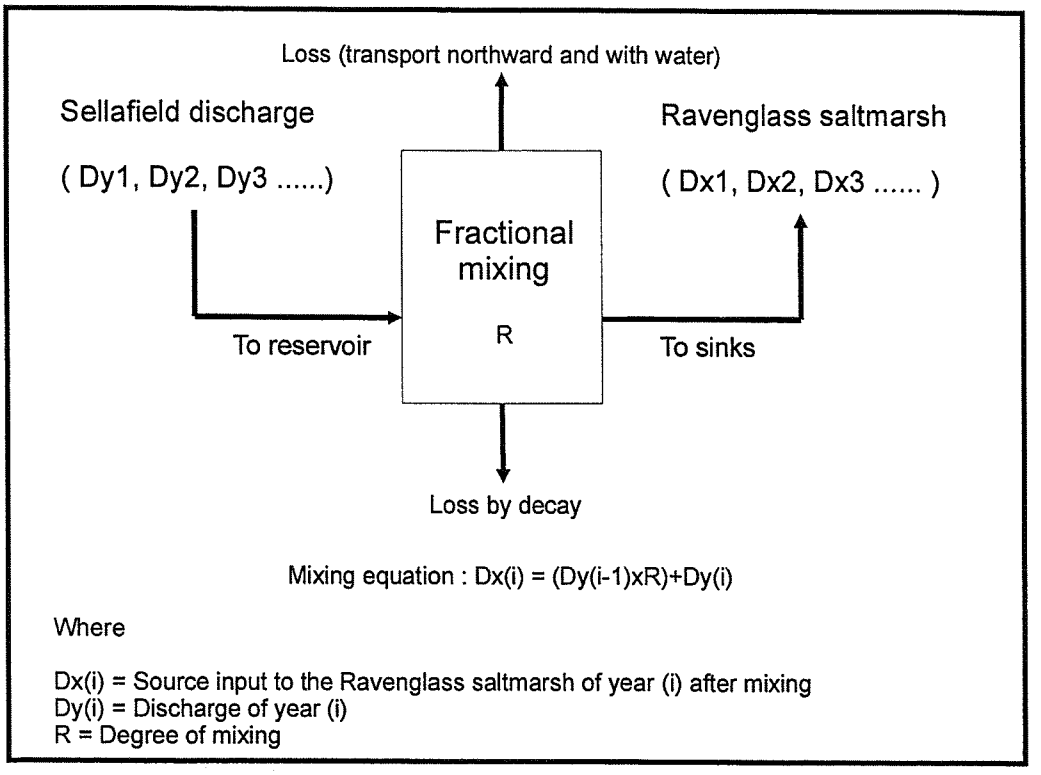

Figure 5-6. Schematic diagram of sediment mixing model

The results of the modelling are shown in Figure 5-7. It is the shape of the profiles with different degrees of mixing that are important (units in the X-axis are arbitrary). For example, consider the profiles of Pu isotopes. By comparing the vertical profiles of Pu isotopes in the R-96-000 and R-96-007 cores with those of discharges from the Sellafield site, it is immediately evident that the two clear peaks seen in a discharge profile (see Figure 7-5 ~ 7-7 for the Pu isotope discharges from Sellafield) are not manifest in the core samples. This can be explained with the help of modelling as shown in Figure 5-7. For the Pu isotopes, two discharge peaks still appear up to the mixing of 70-80 %. However, as observed in the core, the peaks become less clear at mixing higher than 80 %. It gives an indication that the mixing of sediments contaminated by Sellafield-derived radionuclides is higher than 80 %.

The second approach to estimate the mixing of sediments is through the comparison of the ratios of discharge peak activities over discharge activities in 1995 (corresponding to the top of the cores) for various radionuclides. For example, the peak ^{239,240}Pu activity from the Sellafield site as reported is 54 TBq in 1973 and that of 1995 is 0.23 TBq which gives the

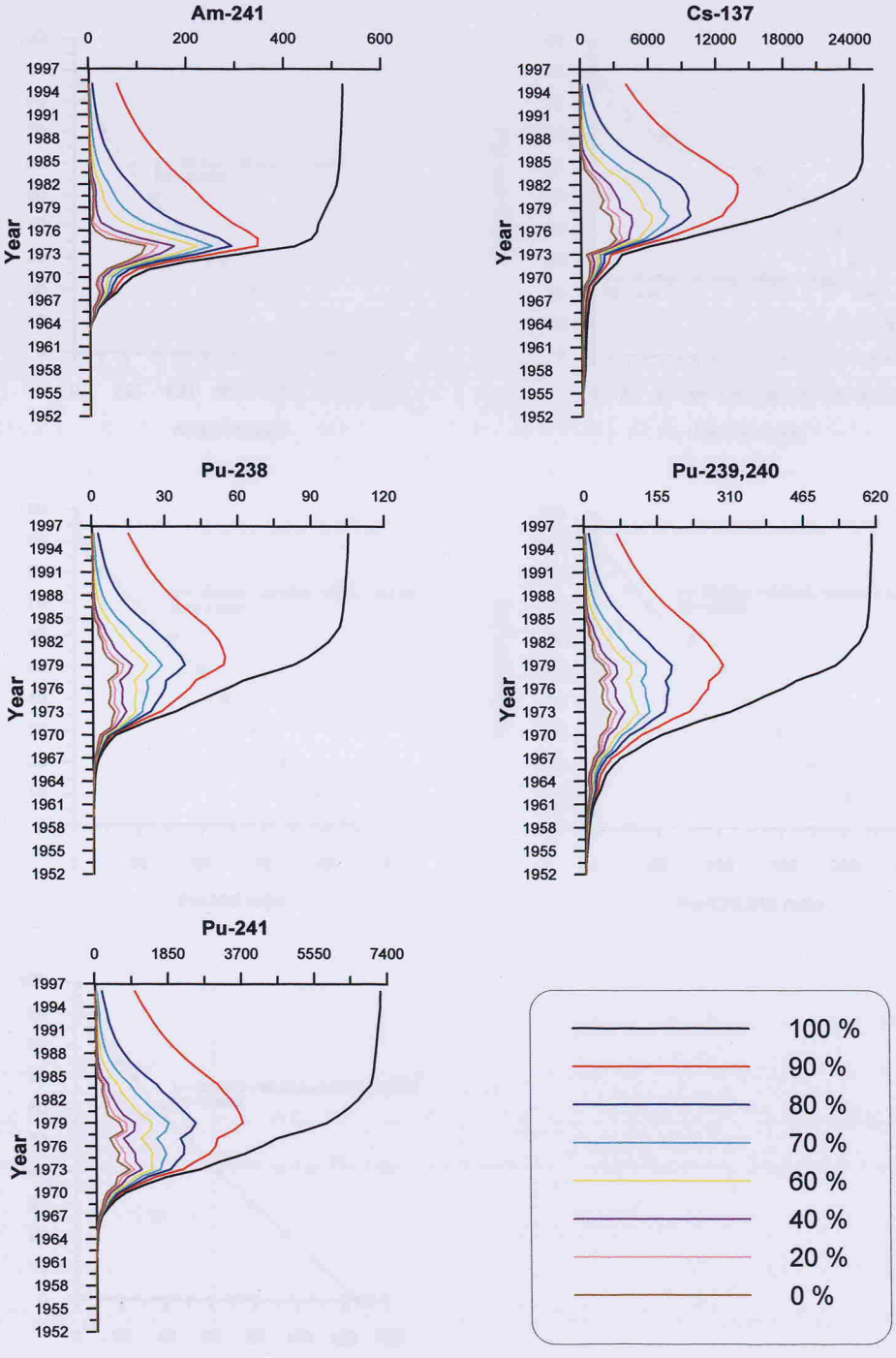

Figure 5-7. Profiles of radionuclides from Sellafield with various degrees of mixing

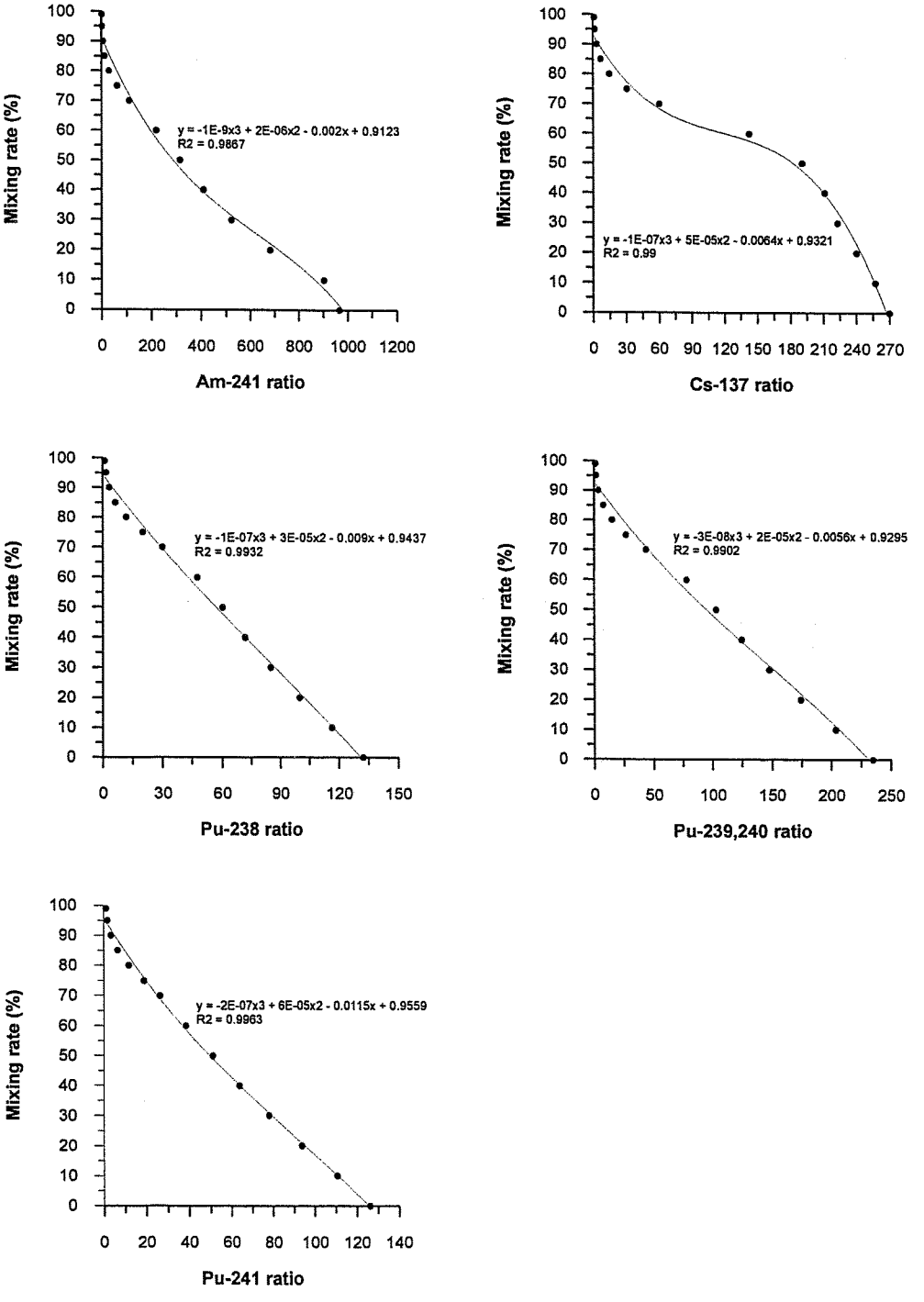

Figure 5-8. Ratios of peak discharge activities over discharge activities in 1995 with various degrees of mixing

ratio of 235. If the mixing is assumed to be 90 %, the peak cumulative ^{239,240}Pu activity is 293 TBq and that of 1995 is 77 TBq which generates the ratio of 3.8. Figure 5-8 shows the ratio of peak to 1995 in discharges for different degrees of mixing. (activities of discharges used are decay corrected arbitrarily to 1998 and ^{241}Am activities include the ingrowth by the decay of ^{241}Pu). It is therefore possible to estimate the sediment mixing from the discharge point until the contaminated sediments arrive at the Ravenglass saltmarsh using the equations in Figure 5-8. Table 5-1 shows the estimated sediment mixing using the R-96-000, R-96-007 and R-97-003 cores. In addition to the three cores from this work, results from (1) four Irish Sea intertidal cores studied by Aston & Stanners (1981a, 1982a), (2) the Maryport Harbour core studied by Kershaw *et al.* (1990), (3) two of the Ravenglass saltmarsh core results reported by Livens *et al.* (1994) and (4) the two cores analysed by MacKenzie *et al.* (1994) are also used to estimate sediment mixing. The cores of Aston & Stanners (1981a, 1982a) were collected in 1978 while those of Kershaw *et al.* (1990), Livens *et al.* (1994) and MacKenzie *et al.* (1994) were collected almost a decade ago. For the results reported by Aston & Stanners (1981a, 1982a), all four cores are used for the estimation using ^{241}Am activities, however, only two cores are used for the calculation using Pu isotopes due to the large sampling intervals and lack of data for the other two cores. As shown in the Table 5-1, results agree very well with those of this work. The average mixing estimated from different radionuclides from all the studies is 90 % for ^{241}Am, 87 % for ^{137}Cs and 88 % for Pu isotopes.

Using the results in Table 5-1, it is possible to estimate the half-value period reported by MacKenzie *et al.* (1994). The half-value period is characteristic half-times for reduction of Sellafield derived radionuclides in contaminated sediments by dispersion and dilution. From the assumptions of this study's modelling, mixing is applied to the Sellafield discharge on an annual basis. Therefore once the degree of mixing is determined, it can be multiplied until we get the value of 50 % (i.e. $R^x = 0.5$ where R is the degree of mixing and x is the half-value period). For example, the average mixing for ^{241}Am is 90 % and the number of years that these value become 50 % is 6 ~ 7 years (i.e. $0.9^x = 0.5$). Using the same method, the half-value period for ^{137}Cs is approximately 5 years and that of Pu isotopes is also approximately 5 years. Values for ^{241}Am and Pu isotopes agree well with those of MacKenzie *et al.* (1994), although there is a poorer agreement for ^{137}Cs. The results from this study present longer half-value periods of approximately 5 years (3.3 years by

MacKenzie *et al.*, 1994), implying that the redissolution of ^{137}Cs suggested by them is not occurring.

	^{241}Am	^{137}Cs	^{238}Pu	$^{239,240}Pu$	^{241}Pu
R-96-000 Core	90 %	88 %	89 %	90 %	90 %
R-96-007 Core	88 %	83 %	83 %	86 %	83 %
R-97-003 Core	88 %	84 %	-	-	-
Aston & Stanners (1981a, 1982a)	91 %	-	93 %	92 %	-
Kershaw *et al.* (1990)	90 %	87 %	-	89 %	-
Livens *et al.* (1994) **Upper**	-	-	-	90 %	-
Livens *et al.* (1994) **Middle**	-	-	-	88 %	-
MacKenzie *et al.* (1994) **S1**	92 %	90 %	-	92 %	-
MacKenzie *et al.* (1994) **S2**	91 %	89 %	-	92 %	-
Average	90 %	87 %	88 %	90 %	87 %

Table 5-1. Estimated sediment mixing determined by the author

5.3. Conclusion

As described by MacKenzie *et al.* (1994), direct comparison of Sellafield discharge data with the vertical profiles of radionuclides measured in cores is not recommended because mixing of sediments labelled with Sellafield-derived radionuclides occurs. This can be seen by comparing Pu isotopic ratio profiles in cores with the ratios in the discharge which shows no correlation. Sediment mixing has been determined using simple mathematical modelling. ^{241}Am, ^{137}Cs and Pu isotopes were used for the estimation. The sediment mixing ranges from 87 % to 90 % were found using data from this study and also including data from earlier studies of other workers.

Chapter 6. Irish Sea sediments

6. Irish Sea sediments

6.1. Major and trace element data

Selected vertical profiles of major and trace elements for core I-96-002 are given in Figure 4-1. These show that the composition of sediments remain unchanged with depth. The average Al_2O_3 value (7.88 %) is lower than is found in the Ravenglass saltmarsh cores and SiO_2 is higher (73.02 %) which implies that this core is sandier and less clay rich than saltmarsh cores. No confirming evidence of early diagenesis was found in this core. This core was sub-sampled by MAFF, Lowestoft, and a visual observation of oxic and anoxic boundary was not recorded.

6.2. Vertical distribution of radionuclides

The I-96-002 core shows vertical profiles of steadily increasing activities with depth for the radionuclides measured (Figure 6-1). Cores collected from the Irish Sea often show vertical profiles of radionuclides consistent with active mixing (bioturbation and physical mixing). MacKenzie *et al.* (1998) analysed three cores collected from the Irish Sea for ^{241}Am, ^{137}Cs and Pu isotopes. Figure 6-2 and 6-3 show vertical profiles of Pu isotopes for these cores as well as for I-96-002 core and their sampling locations. None of their cores shows radionuclide profiles that resemble the Sellafield discharge and they concluded that complete mixing occurred. Since some vertical variation is seen for core I-96-002, it implies that incomplete mixing (the mixing discussed in Chapter 5) has occurred in the seabed where this core was collected. The sediment accumulation rates in one core collected from the western Irish Sea (west of the Isle of Man) are 0.07 ~ 0.018 cm/yr over the last 3000 - 4000 years (Kershaw, 1986 ; Kershaw *et al.*, 1988). Two other cores were collected from the eastern Irish Sea adjacent to the Sellafield effluent pipelines. No estimations of sediment accumulation rate were made in these two cores since almost constant ^{14}C ages were found in those two cores. Bioturbation was claimed to be responsible for the homogenous vertical distribution of ^{14}C in the eastern Irish Sea cores. Results from the current work suggest the possibility of higher sediment accumulation rates in this region. The activities of all the radionuclides measured show a steady increase with depth which one would expect based on the Sellafield discharge data. Assuming that the peaks of radionuclides would be found

below 28 cm, it could be concluded that higher sediment accumulation rate would be responsible for such vertical distribution of radionuclides. It is likely that once radionuclides are discharged from the Sellafield site they interact with particulate matter being continuously resuspended from and deposited onto the seabed. The I-96-002 core seemed to be collected from a less dynamic region of the Irish Sea where the mixing is less active. However, cores 1, 2, & 3 studied by MacKenzie *et al.* (1998) were sampled from regions subject to very dynamic circumstances where the complete homogenisation can be achieved showing incomparable vertical profiles of radionuclides with discharge record. This will be discussed further in the next section using the Pu isotopic ratios.

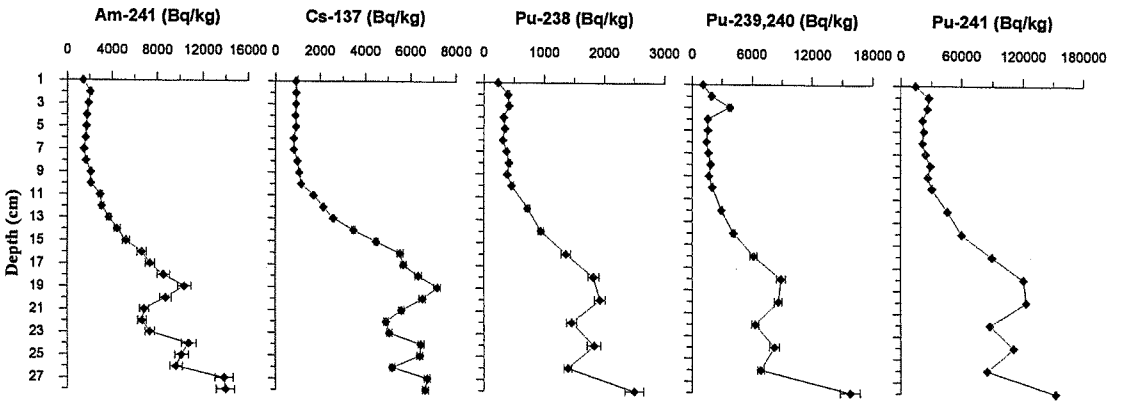

Figure 6-1. Vertical profiles of radionuclides in the Irish Sea core

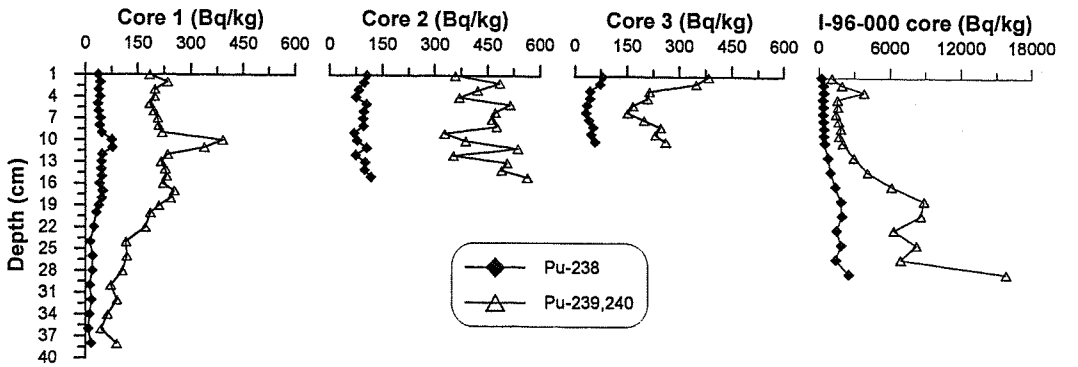

Figure 6-2. Vertical profiles of Pu isotopes in the Irish Sea cores (cores 1-3 ; MacKenzie *et al.*, 1998)

The Pu activities presented in Figure 6-2 show quite significant variations between cores studied by MacKenzie *et al.* (1998) and the one analysed for this work. The I-96-002 core was collected closest to the effluent pipelines and the other three cores were collected further from the effluent pipelines (Figure 6-3). It supports the findings by Hetherington (1978) that a major fraction of the Pu discharged is lost from the water to the sediment immediately after its release from Sellafield. These higher activities found in the I-96-002 core may be due to the different composition between cores but there are no geochemistry data available for the three cores investigated by MacKenzie *et al.* (1998).

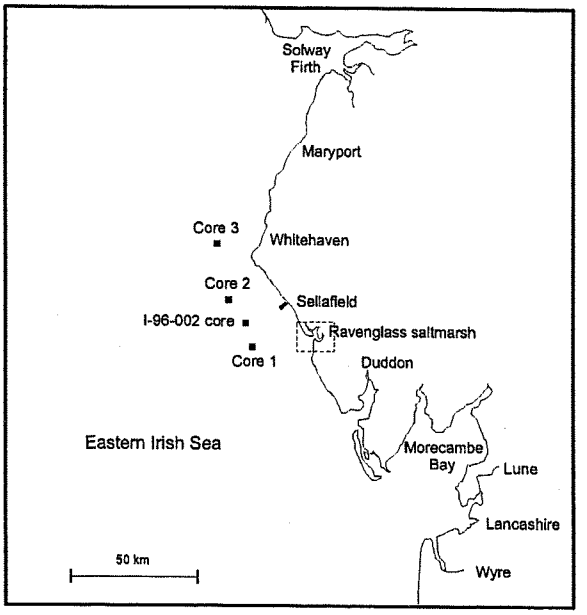

Figure 6-3. Sampling locations of Core 1, 2, 3 and I-96-002 core

6.3. Pu isotopic ratios in the core

Several authors have used Pu isotopic ratios (^{238}Pu and ^{239,240}Pu) to estimate sediment accumulation rates (Hetherington, 1978 ; Stanners & Aston, 1981a, 1984). Am is not involved in redox-induced geochemical processes, and consequently will preserve the isotopic composition characteristic of the discharge (Hamilton & Clifton, 1980 ; Aston & Stanners, 1981a). However, direct comparison of isotopic ratios involving different radionuclides (such as Am/Cs, Am/Pu, Cs/Pu etc.) may not be appropriate since each radionuclide will have different chemical behaviour in the environment. One of the major differences is the distribution coefficient (K_d) of various radionuclides. The use of isotopic

ratios of the same element is more reliable since environmental processes will not fractionate them.

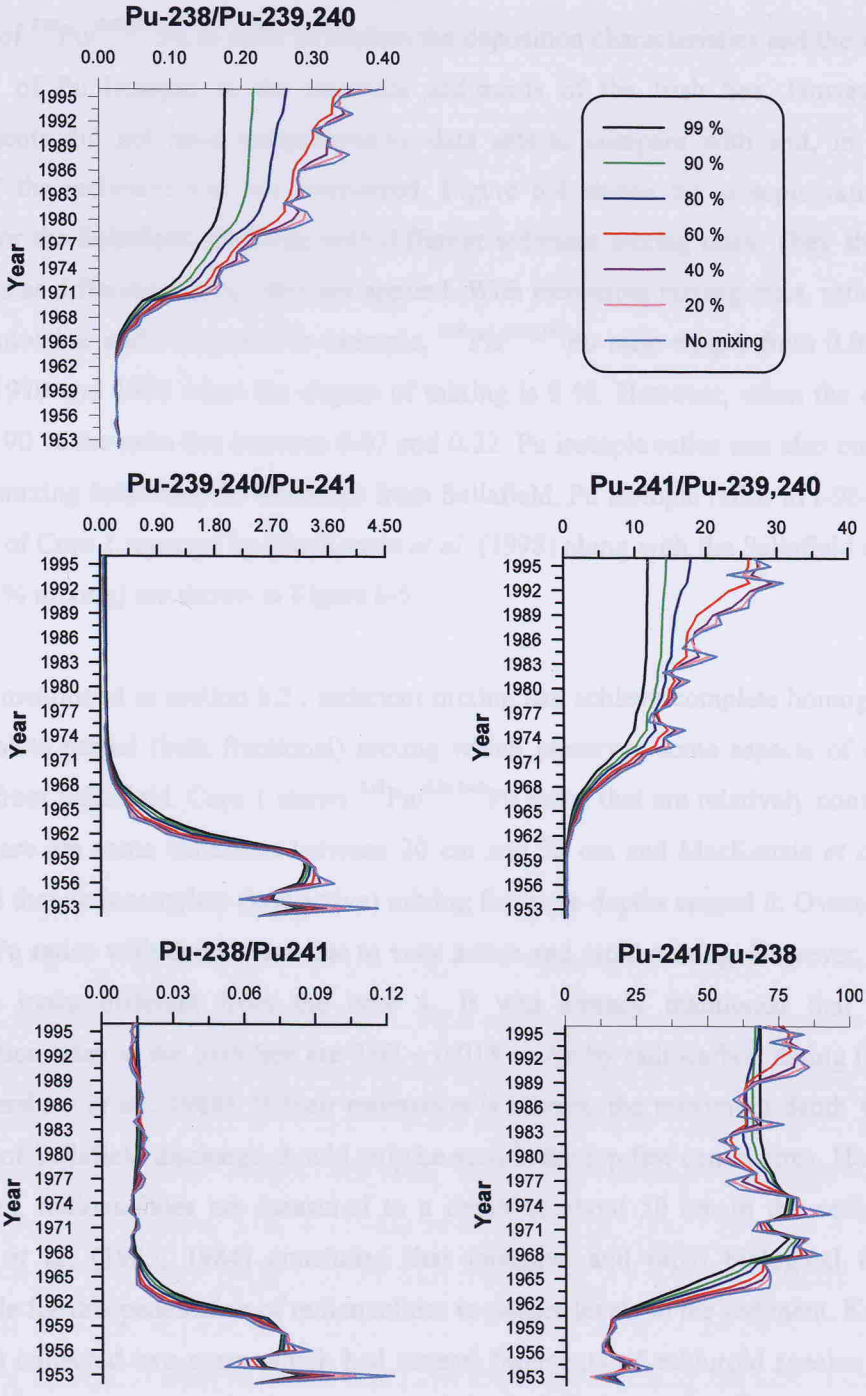

Figure 6-4. Pu isotopic ratios for the Sellafield discharges with various degrees of mixing

An important and distinctive feature of the Sellafield discharge profiles is the higher quantity of $^{alphas}Pu$ in the early years of the discharge resulting from the reprocessing of low "burn-up" fuel in the early to mid 1960s (Kershaw *et al.*, 1990). Direct use of these ratios without a consideration of sediment mixing is problematic. Aston & Stanners (1981a) used the ratios of $^{238}Pu/^{239,240}Pu$ in order to explain the deposition characteristics and the immobile behaviour of Pu isotopes in the intertidal sediments of the Irish Sea. However, their measurements did not have comprehensive data sets to compare with and, in addition, mixing of the sediment was not considered. Figure 6-4 shows the isotopic ratios of Pu isotopes for the Sellafield discharge with different sediment mixing rates. They show large differences as different mixing rates are applied. With increasing mixing rates, ratio profiles become smoother and constant. For example, $^{238}Pu/^{239,240}Pu$ ratio ranges from 0.08 to 0.39 between 1970 and 1996 when the degree of mixing is 0 %. However, when the degree of mixing is 90 % the ratio lies between 0.07 and 0.22. Pu isotopic ratios can also confirm the sediment mixing following the discharge from Sellafield. Pu isotopic ratios in I-96-002 core and those of Core 1 reported by MacKenzie *et al.* (1998) along with the Sellafield discharge ratios (85 % mixing) are shown in Figure 6-5.

As mentioned in section 6.2., sediment mixing can achieve complete homogenisation or incomplete partial (bulk fractional) mixing which preserves some aspects of discharge histories from Sellafield. Core 1 shows $^{238}Pu/^{239,240}Pu$ ratios that are relatively constant with depth. There are some variations between 20 cm and 30 cm and MacKenzie *et al.* (1998) concluded that an incomplete (less active) mixing for those depths caused it. Overall, almost constant Pu ratios with depth were due to very active and rapid mixing. However, the I-96-002 core looks different from the core 1. It was already mentioned that sediment accumulation rates in the Irish Sea are 0.07 ~ 0.018 cm/yr by radiocarbon dating (Kershaw, 1986 ; Kershaw *et al.*, 1988). If their estimation is correct, the maximum depth where the signature of Sellafield discharge should only be seen in the top few centimetres. However, in most cases, radionuclides are measured to a depth of about 50 cm in the sediment and Kershaw *et al.* (1983, 1984) concluded that intensive and rapid biological mixing is responsible for this penetration of radionuclides to deeper levels in the sediment. Kershaw *et al.* (1984) collected two cores which had several fragments of echiuroid species and their burrows. Two cores were then sub-sampled for the brown-coloured burrow linings and adjacent sediment. Pu isotopic ratio results clearly showed the migration of Pu in the burrow linings but it was not always seen in the adjacent sediment. This indicates that sediment

mixing by biological activity does not achieve complete mixing but is confined to the burrow linings and the vicinity of burrows. Therefore, bioturbation can achieve penetration of sediment but not uniformly. The high sediment accumulation may be another explanation. For the I-96-002 core, $^{238}Pu/^{239,240}Pu$ ratios are between 0.16 ~ 0.25 (except the ratio of 3 cm from surface) and this matches the ratios when the mixing rate is between 80 ~ 85 %.

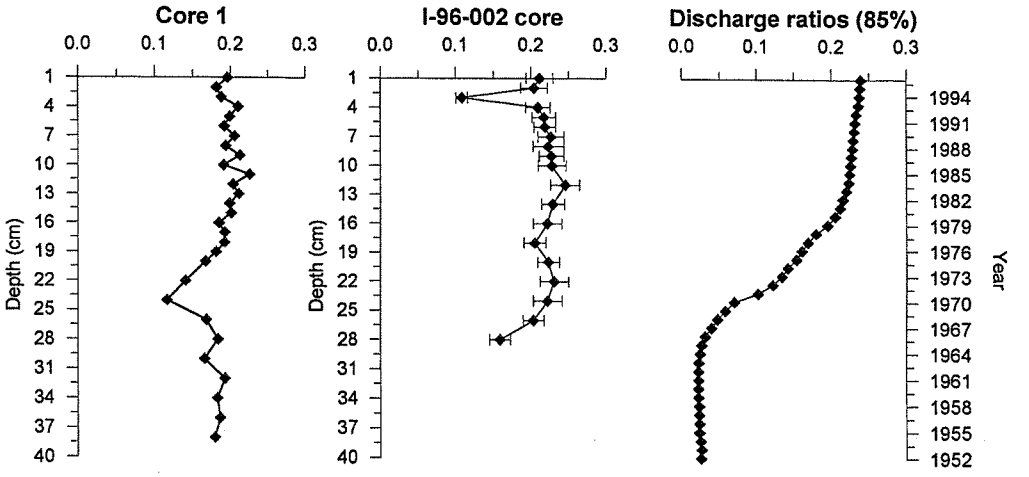

Figure 6-5. $^{238}Pu/^{239,240}Pu$ ratios in cores and Sellafield discharge (85 % mixing)

Considering that the mixing rate is 85 %, the $^{238}Pu/^{239,240}Pu$ ratio at 28 cm is 0.16 which corresponds to that of 1976. With these, we can estimate the sediment accumulation rate of the region where I-96-002 core was collected is approx. 1.5 cm/yr. At 3 cm from the surface, sudden change in $^{238}Pu/^{239,240}Pu$ is found. This may result from the reworking of the sediment, possibly bioturbation, associated with previously discharged Pu (possibly early 1970s) which could be found below 28 cm assuming the above hypothesis is right. Kershaw *et al.* (1984) also found such a Pu ratio change in one of their cores. They found the Pu isotopic ratio in the burrow linings with more recent origin in the deeper depth which was not measured in the adjacent sediment in the same depth. The $^{241}Pu/^{238}Pu$ ratios show similar pattern with the values comparable to the discharge ratios. As already discussed, a general increase of radionuclide vertical profiles suggests this core may preserve the history of Sellafield discharge. It must be remembered that above estimation of sediment accumulation rate is based on the Pu isotopic ratios of last two samples. It may be argued that those decreases in ratios may be due to the incomplete mixing also seen in Core 1. However, the

steady increase of radionuclide activities in the I-96-002 core implies that this core has preserved the history of Sellafield discharge in some extent which is not found in Core 1. Further work with a longer core, at least a metre long, would need to be carried out to fully understand this mixing process.

6.4. Ingrown ^{241}Am by the decay of ^{241}Pu

One of the earliest works concerning ^{241}Pu activities is reported by Livingston *et al.* (1975) in which they estimated ^{241}Pu activities along with ^{alphas}Pu in the environmental samples (sediment core, harbour sediment, beach sand, seaweed, starfish etc.). Their method used the measurement of ingrown ^{241}Am produced by the decay of ^{241}Pu previously plated on a disc for the alpha spectrometry with other ^{alphas}Pu. Day & Cross (1981) also estimated ^{241}Pu activities around the Sellafield site (i.e. Irish Sea). Although they did not measure ^{241}Pu activities directly from environmental samples, they used discharge data to estimate the ingrowth of ^{241}Am in the system. They reported that ^{241}Am resulted from the decay of ^{241}Pu and that up to 1980 this contributed approximately 27% of total sedimentary reservoir of ^{241}Am in the system. Currently, approximately 46 % of total ^{241}Am in the system originates from the decay of ^{241}Pu. Contributions from the two sources are shown in Figure 6-6 for individual years. These results have shown the importance of environmental ^{241}Pu in supplying ^{241}Am.

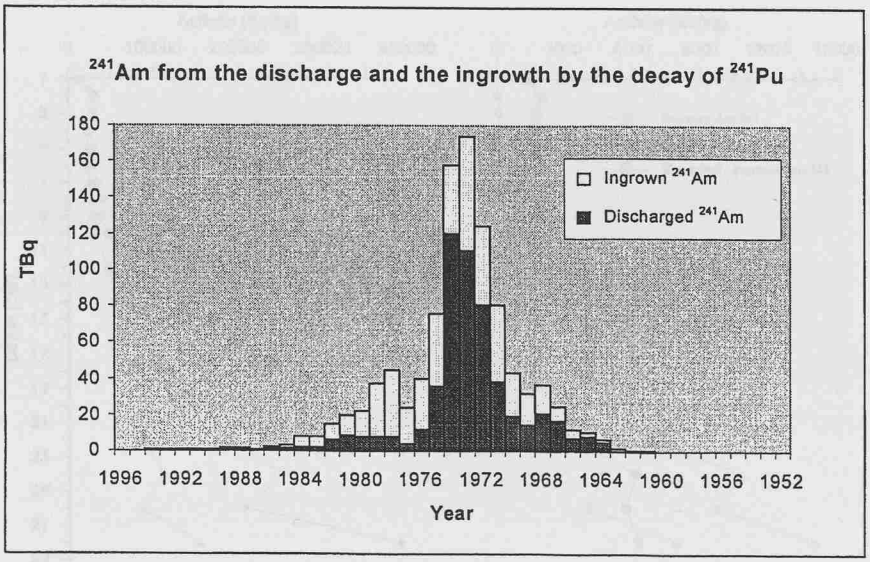

Figure 6-6. ^{241}Am activities from the Sellafield site and the decay of ^{241}Pu

Here, the activities of ^{241}Am ingrown from the decay of ^{241}Pu are estimated in the I-96-002 core. ^{241}Pu activities at the time of discharge ($[^{241}Pu]_0$) must be calculated in order to estimate ^{241}Am formed (Equation 1).

$$[^{241}Pu]_0 = \frac{[^{241}Pu]_t}{\exp\left(-\frac{t \ln 2}{T_{Pu}}\right)} \qquad \text{Equation (1)}$$

$$[^{241}Am]_t = [^{241}Pu]_0 \frac{T_{Pu}}{(T_{Am} - T_{Pu})}\left[\exp\left(-\frac{t \ln 2}{T_{Am}}\right) - \exp\left(-\frac{t \ln 2}{T_{Pu}}\right)\right] \qquad \text{Equation (2)}$$

The quantities of ^{241}Am formed after time t, following the decay of a given initial quantity of ^{241}Pu, are then estimated using equation 2 (Day & Cross, 1981), where T_{Am} and T_{Pu} are the half lives of ^{241}Am and ^{241}Pu which are 433 yr and 14.4 yr, respectively. It was reported in the previous section that the sediment accumulation rate is 1.5 cm/yr. The results are shown in Figure 6-7. The profiles on the left are the measured ^{241}Pu and the decay corrected ^{241}Pu activities to the time when sediment was deposited. It is estimated that the sum of measured ^{241}Pu activities are 52 % of their initial activities decay-corrected to the year of deposition. 48 % of ^{241}Pu deposited have decayed to ^{241}Am. The percentage of ingrown ^{241}Am activities tend to show a steady increase with depth starting from 3.3 % at the top to 56 % at 28 cm. The ingrown ^{241}Am contributes approximately 22 % of the total measured ^{241}Am.

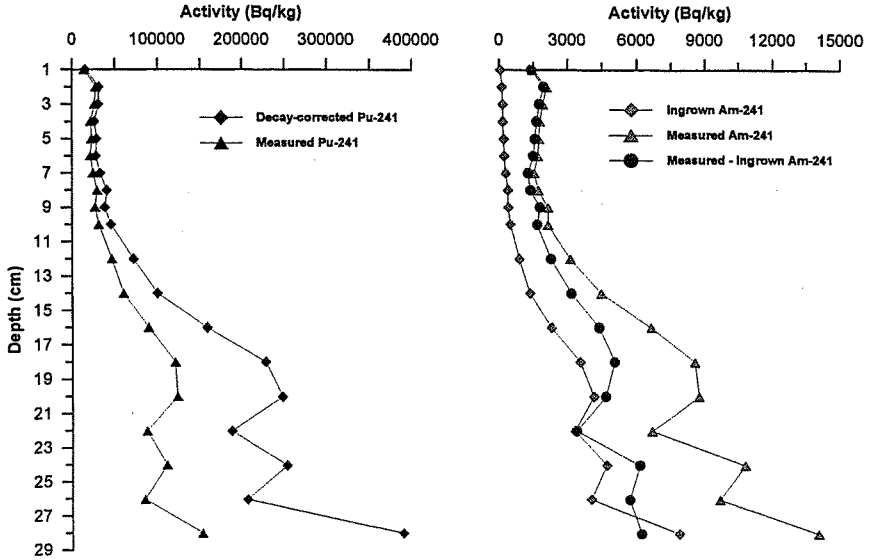

Figure 6-7. ^{241}Am and ^{241}Pu in I-96-002 core

6.5. Conclusions

It appears that the I-96-002 core has at least preserved the history of Sellafield discharge in terms of its radionuclide vertical profiles. However, Pu isotopic ratio profiles show that sediment mixing has occurred. No correlation is found between Pu isotopic ratios in the core and decay-corrected discharge ratios. A good agreement between both ratios is observed using the sediment mixing hypothesis. Although the levels of radionuclides released from Sellafield have reduced significantly since 1980s, those mixed sediments in the Irish Sea bed will play a major role as a source of radionuclides to the surrounding areas. It also is concluded that the Irish Sea bed where the I-96-002 core was collected possibly has experienced high sediment accumulation rates. Further work with a longer core, at least a metre long, would need to be carried out to fully understand this mixing process. Finally, the importance of the high activities of ^{241}Pu and its role in supplying ^{241}Am to the environment in situ should be noted, particularly when considering the long-term radiological impact of environmental ^{241}Am.

Chapter 7. Vertical variation of radionuclides in the Ravenglass saltmarsh

7. Vertical variations of radionuclides in the Ravenglass saltmarsh

7.1. Major and trace element data

From the major elements results (such as Al_2O_3, Fe_2O_3, K_2O and SiO_2), R-96-000 & R-97-003 cores show no significant changes in their composition with depth. However, R-96-007 & R-96-008 cores show variations near the bottom of the cores, especially Al_2O_3 and SiO_2 indicating a change in composition to sandy materials with depth. The same pattern was reported in a core collected from the same saltmarsh and analysed by Hamilton & Clarke (1984). The R-96-000 core shows lower clay contents (average Al_2O_3 9.18 % & SiO_2 69.93 %) than the R-96-007 core (average Al_2O_3 10.82 % & SiO_2 67.37 %). The average Al_2O_3 value for R-96-008 core is 8.45 % which is the lowest found in the saltmarsh cores and that of SiO_2 is 73.42 %. The mean Al_2O_3 content for R-97-003 core is 13.17 % and that of SiO_2 is 57.88 %. Therefore, the R-97-003 core has the highest clay contents which implies that high activities of radionuclides can be found in this core compared to other three cores. It is evident that this core was collected from the back of the marsh where finer size fractions can be transported and deposited during the tidal cycles. High CaO concentrations found from the top few centimetres of the R-96-007 core may have been caused by the presence of shelly fragments on the surface.

Variations in Mn concentration are observed in all the saltmarsh cores analysed (Figure 7-1). By comparing those changes in Mn concentration with those of Fe and S, no clear evidence has been found to support the redox sensitive behaviour of Mn resulted from oxic-anoxic changes. The changes in S concentration for R-96-008 core indicate there is a reducing zone below 32 cm (this reducing boundary was found by visual observation carried out before sectioning the core at one centimetre intervals), however, the changes in Mn concentration do not show variations big enough to be caused by the redox changes. The variations of Mn concentration measured in all saltmarsh cores may relate to the organic content in those fractions or to the water table which may result in localised reduction and oxidation. Such boundaries are also found visually for other cores (see Table 7-1) but no confirming evidence of oxic-anoxic boundary is found in the geochemistry data. Saltmarshes are regularly inundated and drained, therefore, there may be no real reduced zone overall.

Elevated concentrations of elements in the top fraction of the R-96-000 core appear to be caused by the higher clay contents in that fraction.

	Oxic-anoxic boundary by visual observation	Oxic-anoxic boundary by geochemical data
R-96-000 (saltmarsh) core	12 cm	Not found
R-96-007 (saltmarsh) core	25 cm	Uncertain
R-96-008 (saltmarsh) core	32 cm	32 cm
R-97-003 (saltmarsh) core	Not found	Not found

Table 7-1. Reducing-oxidising boundaries in saltmarsh cores.

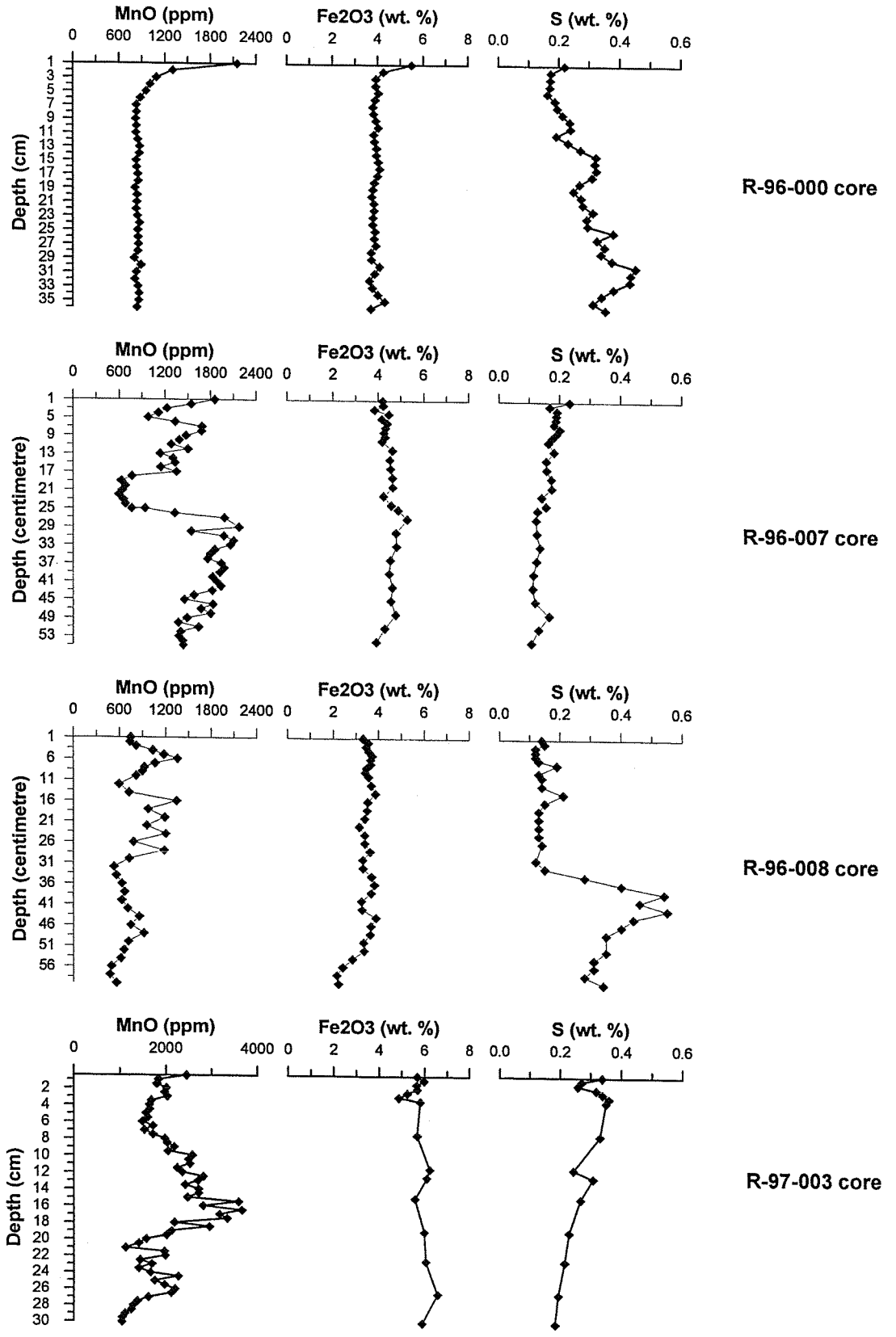

Figure 7-1. Vertical profiles of MnO, Fe_2O_3 and S in cores

7.2. Sediment accumulation rates in the saltmarsh

Sediment accumulation rates are determined using vertical profiles of radionuclides from the cores collected as well as the laminae found in one of the cores. Three cores are used to estimate the sediment accumulation rate. They are R-96-000, R-96-007 and R-97-003 (only ^{241}Am and ^{137}Cs were measured) cores. The R-96-008 core is not included since the top few centimetres are apparently missing. All the radionuclides (^{241}Am, ^{137}Cs, ^{238}Pu, ^{239,240}Pu and ^{241}Pu) measured are employed for the determination of sediment accumulation rates for this particular saltmarsh. Several assumptions are made for the estimation of sediment accumulation rate. They are ;

1. The inputs of the particles and the erosion of the once deposited particles are constant, therefore, the corresponding peak activity in a sediment core profile may be matched to the time of the peak discharge
2. The core compression during the sampling is assumed to be even throughout the cores
3. It is assumed that the transit time of radionuclides from the effluent pipelines to the saltmarsh is approximately 1 year (Aston & Stanners, 1982a,b,c)
4. Post-depositional migration of radionuclides is negligible

The curve fitting method is used for the estimation of sediment accumulation rate. Two approaches are made. The first approach does not incorporate sediment mixing and the second approach takes sediment mixing into consideration. The equation used is ;

$$A_C = C + \left[C \times \left(\frac{S}{100} \right) \right]$$

Where ;

$\mathbf{A_c}$ = Accumulation rate (cm/yr)

$$\mathbf{C} = \left[\frac{D}{(Y_S - Y_P)} \right]$$

$\mathbf{D}$ = Depth in cm where there is highest activity
$\mathbf{Y_p}$ = Year when there is highest discharge
$\mathbf{Y_s}$ = Year representing the top of the sample (1995)
$\mathbf{S}$ = Shortening (compression) occurred during the sampling (%)

The results are shown in Table 7-2 with and without sediment mixing. Both R-96-000 and R-96-007 cores were collected at the front of the saltmarsh and show similar sediment accumulation rates (approximately 1 cm/yr). However, R-97-003 core which was sampled at the back of the marsh shows a lower sediment accumulation rate (0.57 cm/yr considering no mixing and 0.66 cm/yr considering mixing, respectively). The lower sediment accumulation rate may be related to the quantity of particle input during the tidal cycles. The amount of particles deposited onto the saltmarsh would vary from site to site. It is likely that the front of the saltmarsh would have a higher particle input than the back of the marsh due to the frequency of inundation of the saltmarsh. In addition, coarser particles tend to deposit at the front of the marsh associated with less radionuclides. Stanners & Aston (1984) estimated both sediment accumulation rates and diffusion coefficients using Cs and Pu isotopes and the isotopic ratios of $^{134}Cs/^{137}Cs$ and $^{238}Pu/^{239,240}Pu$ in cores collected from the opposite side of the estuary (saltmarsh near Newbiggin). They obtained the diffusion coefficients for Cs and Pu isotopes using a mathematical model. They also modelled and plotted vertical profiles of radionuclides with different diffusion coefficients based on the Sellafield discharge data and compared them to the measured vertical profiles of radionuclides from the cores. The diffusion coefficients estimated are $< 10^{-8}$cm/yr for Cs and $< 10^{-12}$cm/yr for Pu, and the sediment accumulation rates range from 16 ~ 71 mm/yr. Their finding supports one of the assumptions made here, the negligible post-depositional migration of radionuclides in the saltmarsh. Clifton & Hamilton (1982) also carried out a study at the same saltmarsh as Stanners and Aston worked on and reported sediment accumulation rates of 5 ~ 34 mm/yr. It appears that the sediment accumulation rates of current research site are lower than their research site and, most importantly, sediment accumulation rates vary significantly within the same saltmarsh.

	R-96-000 Core		R-96-007 Core		R-97-003 Core	
	Without mixing	With mixing	Without mixing	With mixing	Without mixing	With mixing
^{241}Am	0.91 ± 0.05	0.95 ± 0.05	0.97 ± 0.05	1.01 ± 0.05	0.58 ± 0.05	0.61 ± 0.05
^{137}Cs	0.90 ± 0.05	1.20 ± 0.05	0.96 ± 0.05	1.20 ± 0.05	0.55 ± 0.05	0.70 ± 0.07
Pu isotopes	0.86 ± 0.05	1.06 ± 0.05	1.04 ± 0.05	1.27 ± 0.05	No Data	No Data
Mean	0.89 ± 0.05	1.07 ± 0.25	0.99 ± 0.09	1.16 ± 0.27	0.57 ± 0.02	0.66 ± 0.06
Laminae	No Data		0.97 ± 0.02		No Data	

Table 7-2. Estimated sediment accumulation rates using radionuclides (cm/yr)

7.3. ^{210}Pb dating for R-96-007 core

In addition to the use of anthropogenic radionuclides for the determination of sediment accumulation rates, the ^{210}Pb dating was also performed. ^{210}Pb in R-96-007 was measured but could not be used for conventional dating because of an input of anthropogenic ^{210}Pb. This originated from the Albright & Wilson phosphoric acid production plant, which is located in Whitehaven, approximately 18 km north of the Sellafield site. This had discharged wastes containing significant amounts of naturally occurring radionuclides (U series) into the Irish Sea (Allington *et al.*, 1995). ^{210}Pb from the plant affected the ^{210}Pb inventory around the area. A new raffinate treatment plant was built and primary processing of phosphate ore was changes to the use of importing of crude phosphoric acid in June 1992 resulting in a significant reduction of uranium series discharges from the plant. The same difficulties were also experienced in the use of ^{210}Pb dating by Kershaw *et al.* (1990) and McCartney *et al.* (1990). However, by looking at the prominent decrease of ^{210}Pb in the top 4 cm fractions in this study, it can also be estimated that the accumulation rate is about 1 cm/yr since the new process was introduced (Figure 7-2). This agrees with the accumulation rates obtained from the radionuclide vertical profiles. It also indicates the transit time of approximately 1 year applied in the previous section for the determination of sediment accumulation rates is acceptable.

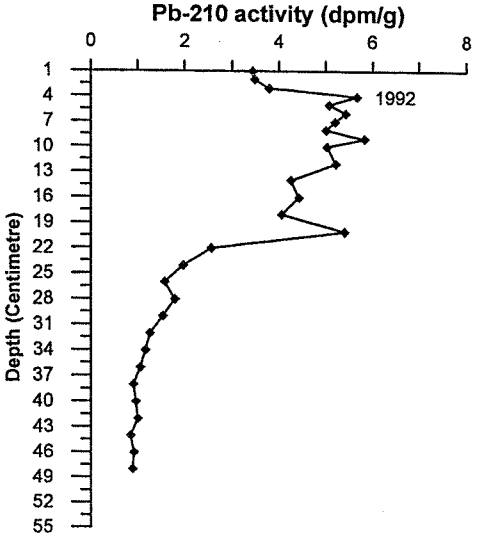

Figure 7-2. ^{210}Pb profiles (R-96-007 core)

7.4. Erosion of the saltmarsh

The R-96-008 core, collected from the right front of the saltmarsh, shows a rather different pattern compared to the other three (R-96-000, R-96-007 & R-97-003) cores. It shows an abnormally high activity of ^{241}Am (14250 Bq/kg) and a slight increase of Pu isotopes in the top cm fraction (see Figure 4-4), and all the radionuclides activities are approximately double those found in the other cores for the first few centimetres. Those high activities correspond to the 13-16 cm fractions for R-96-000 core and the 10-11cm fractions for R-96-007 core (R-97-003 core is not compared since it was collected at the back of the marsh). There are two possible explanations for this abnormality. The first explanation is the presence of "hot particles" reported by Hamilton (1981) and Kershaw *et al.* (1986). Hot particles are debris derived from the reprocessing of Magnox uranium fuel elements released together with liquid effluent from the Sellafield site. The presence of hot particles is important since their small size (~ 10 x 30 μm) enables them to enter human respiratory system through marine aerosols (Hamilton, 1981). This possibility is well supported by the finding of Cambray & Eakins (1982). They collected soil samples along two transects perpendicular to the Cumbrian coast and extending up to 20 km inland and found evidence of radionuclide transfer (^{241}Am and Pu isotopes in particular) inland associated with marine aerosols. Another explanation is the redistribution of particles associated with old discharges containing high levels of radionuclides. It may be bioturbation, the deposition of eroded sediments on the surface or the exposure of older sediments following the erosion of the marsh where the core was collected.

The R-96-008 core was taken from the saltmarsh adjacent to the main channel entrance. Therefore, the most probable explanation of higher activities in the top centimetre is that erosion of the upper sediment revealed earlier historical levels. If we assume that the top 10 to 15 centimetres had been eroded by some kind of physical processes (such as tidal currents or weathering), this could explain why there are higher activities in the top part of the core compared to the other three saltmarsh cores. One of the core results reported by Livens *et al.* (1994) also shows a similar pattern (see Figure 7-8). The highest activity (9890 Bq/kg) was found at the top of the lower zone core. It was not possible to identify the exact sampling location but it was possibly collected from the saltmarsh where erosion was taking place. Although erosion in the saltmarsh was not discussed, it is clear from the results of both studies that certain areas of the Ravenglass saltmarsh are being eroded and those eroded

sediments containing higher activities of radionuclides can be a local source of contaminated sediment in the Ravenglass saltmarsh and other surrounding areas. Considering that the samples investigated by Livens *et al.* (1994) were collected a decade ago, the saltmarsh has played a role of providing radionuclides to the local areas for a substantial period of time. Aston *et al.* (1981) also reported that the surface erosion was responsible for producing different vertical profiles (higher concentrations on the surface) of Pu and Hg in a Wyre estuary sediment core.

7.5. Vertical distribution of radionuclides in saltmarsh cores

Vertical profiles of all the radionuclides analysed are shown in Figures 7-3 ~ 7-7, together with annual discharge data (Gray *et al.*, 1995) from the Sellafield site since 1952 (decay corrected to 01/01/98). ^{241}Am and ^{137}Cs discharges from the Sellafield site peaked in the mid 1970s with ^{137}Cs discharges being approximately 40 times higher than those of ^{241}Am. However, ^{137}Cs activities found in sediment cores are generally lower than those of ^{241}Am. This trend is the same as that reported by Sanchez *et al.* (1998) for saltmarshes from Sellafield to S. Wales. This pattern is explained because ^{137}Cs, which has lower K_d than ^{241}Am, is more conservative in seawater with limited interaction with particulate. However, ^{241}Am has high K_d and can be associated with particles very rapidly. The reported K_d value for ^{137}Cs is 3×10^3 and for ^{241}Am is 2×10^6 in marine systems (IAEA, 1985).

For Pu isotopes, there are two discharge peaks in the 1970s, the first one was 1973 and the second one occurred in 1978. ^{241}Pu discharges are 20 ~ 40 times higher than total ^{alpha}Pu discharges since 1970. ^{238}Pu discharge data are not available before 1978 and the reported figures were estimated by Gray *et al.* (1995). They use the discharge ratios of ^{238}Pu/^{239,240}Pu after 1978 in order to extrapolate the activities of ^{238}Pu discharge between 1952 and 1978. In addition, some of the discharge records for radionuclides, such as ^{241}Am, ^{238}Pu, ^{241}Pu, were not available during the early years of site operation. Gray *et al.* (1995), therefore, estimated those early discharge records using SEAM (Sellafield Environmental Assessment Model) to correlate the discharge rates with the environmental monitoring data reported by BNFL, UKAEA and MAFF. They also used data for sediment cores collected from a disused dock basin in the Maryport harbour to assess their modelled calculations (Kershaw *et al.*, 1990). All the discharge data used in this study are based on their report.

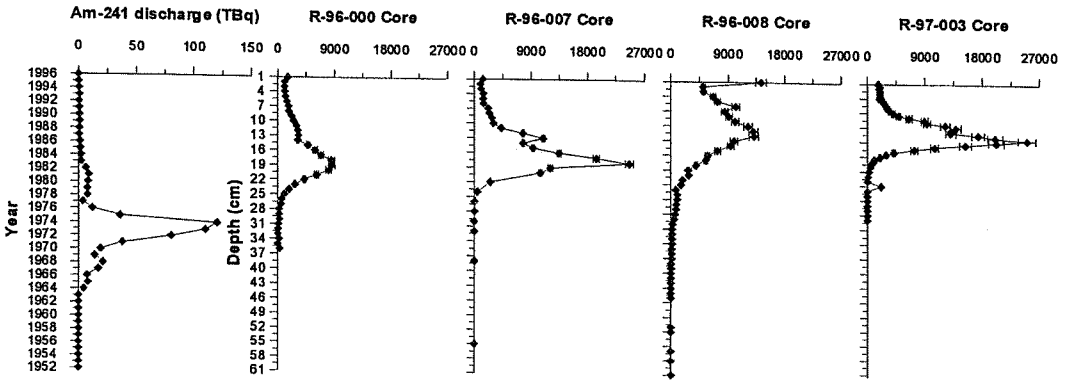

Figure 7-3. Vertical profiles of ^{241}Am for all the cores

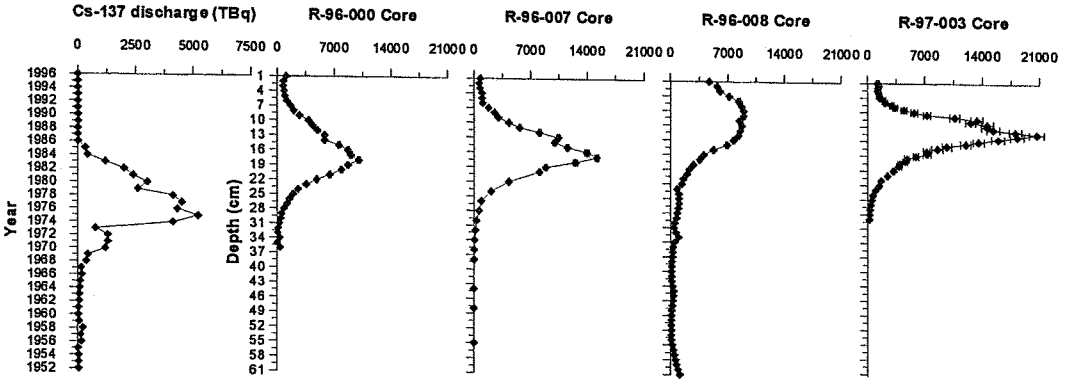

Figure 7-4. Vertical profiles of ^{137}Cs for all the cores

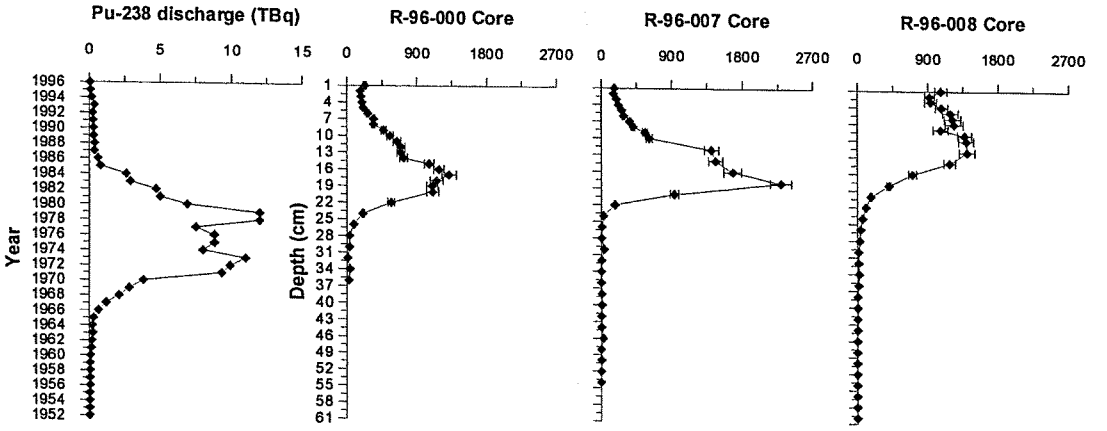

Figure 7-5. Vertical profiles of ^{238}Pu for all the cores

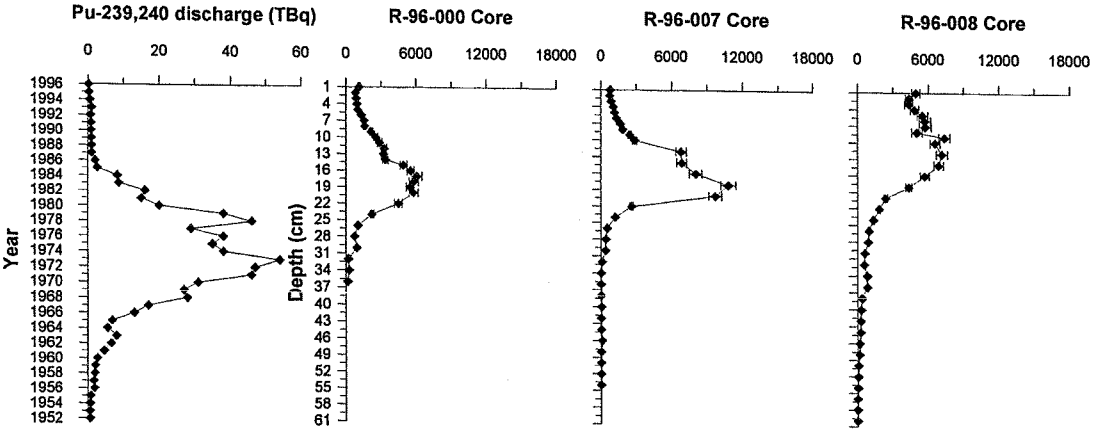

Figure 7-6. Vertical profiles of $^{239,240}Pu$ for all the cores

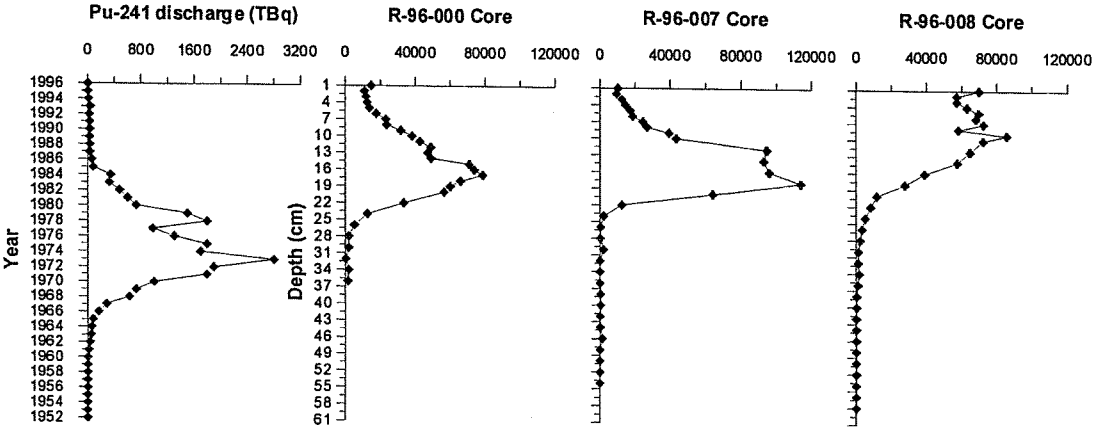

Figure 7-7. Vertical profiles of ^{241}Pu for all the cores

The R-96-000, R-96-007 & R-97-003 cores show similar radionuclide profiles. The main differences are the activities of radionuclides and the peak locations. For ^{241}Am and ^{137}Cs, vertical profiles are very similar to those of Sellafield discharges. These three cores show detailed histories of Sellafield discharges. However, Pu isotope profiles are different. Peaks of both ^{241}Am and ^{137}Cs are found at 17-19 cm for R-96-000 & R-96-007 cores which implies that both cores have similar accumulation rates. However, for R-97-003 core, the highest values of ^{241}Am and ^{137}Cs are measured at 11 and 12 cm implying a lower accumulation rate than for R-96-000 & R-96-007 cores. Since this core is collected at the back of the marsh where the inundation frequency of the tides is lower, a correspondingly small amount of sediment particles are introduced onto this part of the saltmarsh. The levels of activities measured vary with cores. For R-97-003 core ^{241}Am and ^{137}Cs (Pu isotopes were not measured) show the highest activities. From the geochemistry data, the clay content in this core is the highest among four saltmarsh cores and is probably responsible for the high levels of radionuclides. It also is well known that vegetation can act as a trap. Therefore, during the tidal cycle finer particles associated with radionuclides are transported and deposited farther to the back of the marsh than coarser particles.

Livens *et al.* (1994) reported the activities of $^{239,240}Pu$ in three cores from the same saltmarsh and they are shown in Figure 7-8 to be compared with the results from this work. The cores were collected from the upper, middle and lower parts of the marsh. Unfortunately, the exact sampling locations are not available although they were collected either at column W or column C on the grid shown in Chapter 3 (pers comm). The distribution of $^{239,240}Pu$ in the upper and middle zones is very similar to that of R-96-000 and R-96-007 cores. The highest activities were measured at 12.5 cm fractions in the upper and middle zone cores. This does not agree with the findings of this work that the sediment accumulation rate becomes lower towards the back of the marsh. This can be explained by the fact that their samples were sectioned every 2.5 cm intervals which means the activity peak can differ within 2.5 cm. Both the R-98-008 core and the one collected from the lower part of the marsh by Livens *et al.* (1994) also show similar distribution pattern which is caused by the erosion of the sampling locations as discussed in Chapter 7.4. They found no convincing evidence of any changes in redox potential, and the Eh/pH data showed that the chemical environment remained unchanged.

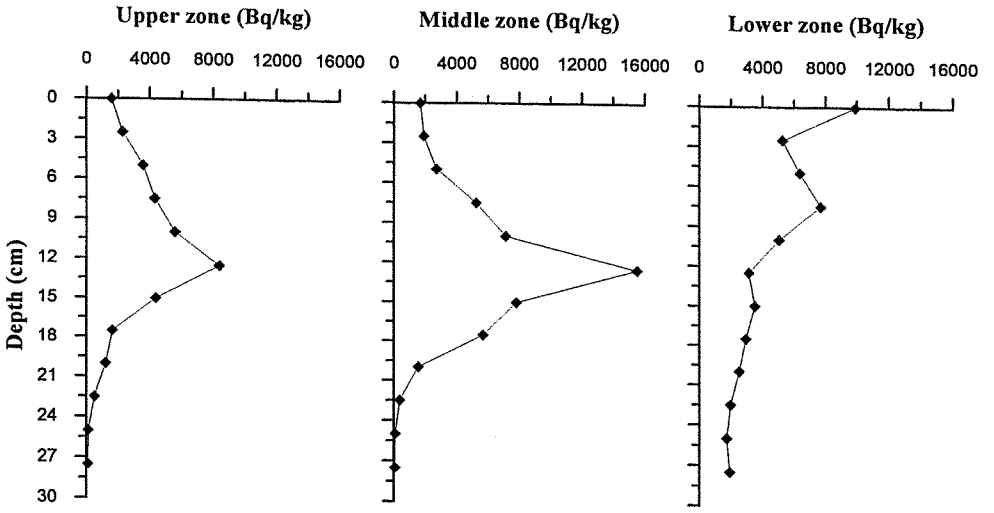

Figure 7-8. ^{239,240}Pu activity profiles reported by Livens *et al.* (1994)

It has been reported in the literature that the levels of Pu isotopes in the sediment were controlled due to changes in sediment composition and pre and post-depositional processes such as physical mixing, redox changes and bioturbation (Aston *et al*, 1981, 1985 ; Mudge, *et al.*, 1989 ; Hursthouse, *et al.*, 1991). This applies to the other radionuclides such as ^{241}Am and ^{137}Cs. From the results of this work, however, the redox changes and bioturbation do not seem to play an important role in remobilising radionuclides within the Ravenglass saltmarsh. Albert & Orlandini (1981) carried out an experiment to determine the relative mobilities of ^{239,240}Pu and ^{241}Am from the Lake Michigan sediments under oxic and anoxic conditions with respect to those of iron and manganese and organic contents such as humic and fulvic acids. It was concluded that the elements studied did not show remobilisation under both oxic and anoxic conditions. Carpenter & Beasley (1981) also reported the evidence against remobilisation of Am and Pu in oxic and anoxic sedimentary environments. In addition, bioturbation of sediments after deposition does not seem to be important for the Ravenglass saltmarsh. Biological activity seems to be confined only to the top few centimetres (Hetherington, 1978 ; Aston & Stanners, 1981a ; Hamilton & Clarke, 1984) and it is shown by the well preserved vertical profiles of radionuclides. Even if biological activity produces a blurring of the variation in activity down the core profile, it does not seem to redistribute the activity of radionuclides substantially. Therefore, the vertical and spatial distribution of radionuclides in the saltmarsh depends on the differing annual Sellafield discharge level and the sediment composition.

7.6. Variations in Pu isotopic ratios in saltmarsh cores

For the Ravenglass saltmarsh cores (see Figures 7-9 ~ 7-11), the Pu isotopic ratio up to 30 cm from the surface agree well with the modelled values using the Sellafield discharge data. Those values up to 30 cm from the surface indicate the sediment mixing rate lay between 85 ~ 95 % which agree with the findings already reported. However, below 30 cm from the surface, the shape of the ratio profiles become inconsistent with those estimated values. There are a number of possible explanations for this deviation.

1. The $^{238}Pu/^{239,240}Pu$ and $^{241}Pu/^{238}Pu$ ratios in R-96-007 and R-96-008 cores show high uncertainties towards the bottom of the cores which results from the higher measurement uncertainties for ^{238}Pu.
2. Contamination of the core and disturbance of the distribution of radionuclides during the sampling and the sample preparation, such as smearing. However, assuming the outer 1 mm was affected by smearing, the volume of smeared fractions is less than 5 % of the total volume in each subsamples, which could not results in such large alterations in ratios, and the contamination during the sample preparation is highly unlikely. Therefore it does not seem to influence much on the results.
3. The unreliability of ^{241}Pu discharge data reported by BNFL, Sellafield prior to 1972. Before 1972, ^{241}Pu activities in liquid effluent were not determined. ^{241}Pu discharged before 1972 was estimated using the Sellafield Environmental Assessment Model (SEAM) by Gray *et al.* (1995). The main difference of $^{241}Pu/^{239,240}Pu$ and $^{241}Pu/^{238}Pu$ ratios between measured and modelled data is found at the bottom of cores which represent the early years of discharge. Assuming the ^{238}Pu and $^{239,240}Pu$ discharge data are correct, it draws a conclusion that the discharged ^{241}Pu in the early years must have been higher than currently reported values.
4. Biological activity in the bottom of the cores. However, the bioturbation in the saltmarsh environment is not very active and limited to the top few centimetres. Therefore, it is unlikely that the bioturbation caused such variations in Pu isotopic ratios in such depths.
5. The last and most likely explanation is the presence of advective flows in the saltmarsh. The changes of Pu isotopic ratio showing the recent Sellafield

discharge ratios are detected for all the cores in some extent although uncertainties for some of them are relatively high. If there is advective flow allowing the migration of recent Sellafield radionuclides in the bottom of the saltmarsh where the sediment composition becomes sandier, such variations in Pu isotopic ratios can be explained. The increase of ^{137}Cs activities in the bottom of R-96-008 (Figure 7-4) core may also due to the presence of advective flows (lateral migration).

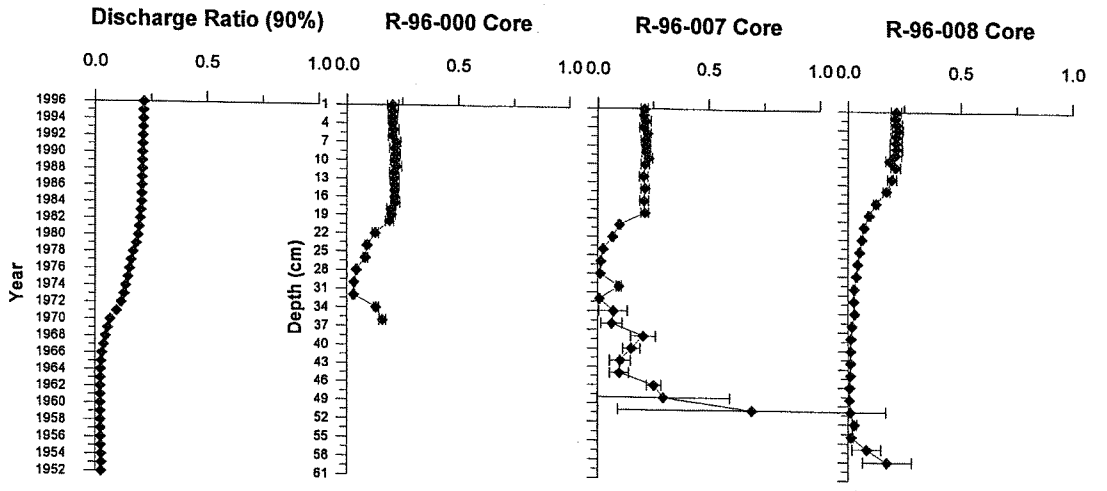

Figure 7-9. $^{238}Pu/^{239,240}Pu$ ratios in saltmarsh cores

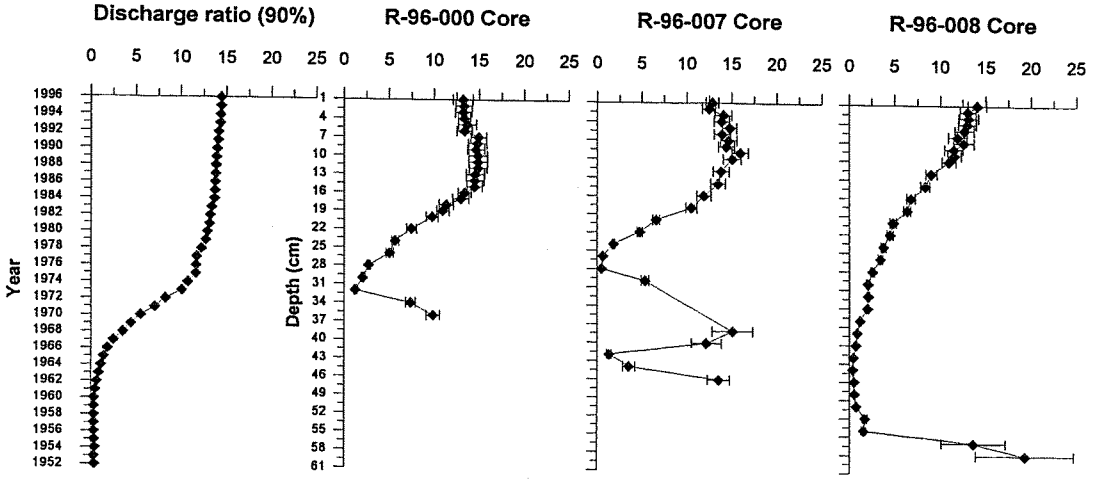

Figure 7-10. $^{241}Pu/^{239,240}Pu$ ratios in saltmarsh cores

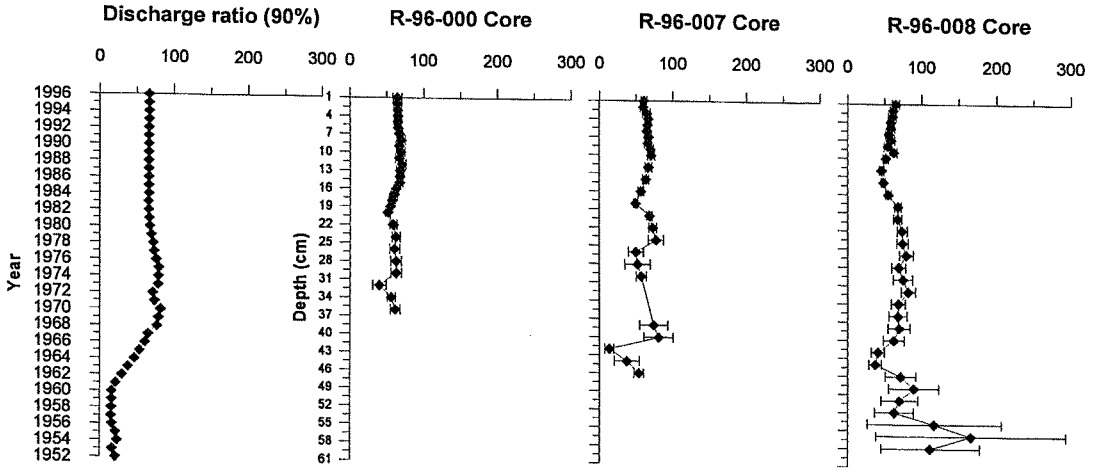

Figure 7-11. $^{241}Pu/^{238}Pu$ ratios in saltmarsh cores

7.7. Implication of ^{241}Pu activities in saltmarsh cores

Figures 7-12 and 7-13 show the ^{241}Pu and the ingrown ^{241}Am activities in R-96-000 and R-96-007 cores. The equations used are already presented in Chapter 6 and the sediment accumulation rates for both cores are based on 1 cm/yr as reported in section 7.2. According to the estimation, the sum of measured ^{241}Pu activities are 46 % (R-96-000 core) and 33 % (R-96-007 core) of their activities decay-corrected back to the year of the deposition. Therefore, between 54 % and 67 % of ^{241}Pu originally presented in these cores have decayed to ^{241}Am. The percentage of ingrown ^{241}Am activities tends to show a steady increase with depth starting from 3.1 % to the highest of 92 % for the R-96-000 core and from 2.5 % to the highest of 80 % for the R-96-007 core. For the R-96-000 core, the ingrown ^{241}Am contributes approximately 41 % of the total measured ^{241}Am and 28 % for the R-96-007 core, respectively. For the R-96-007 core, the estimation is based on the activities up to 30 cm below the surface since both ^{241}Am and ^{241}Pu activities are either negligible or undetected below this depth. As shown in Figure 7-12 and 7-13, the general vertical distribution of ^{241}Am does not differ too much before and after the subtraction of ingrown ^{241}Am. The depths where the peaks are found stay unchanged. From the above results, it is evident that the presence of ^{241}Pu contributes significantly to ^{241}Am activities and this contribution can be quantified when the chronology of the study area is known.

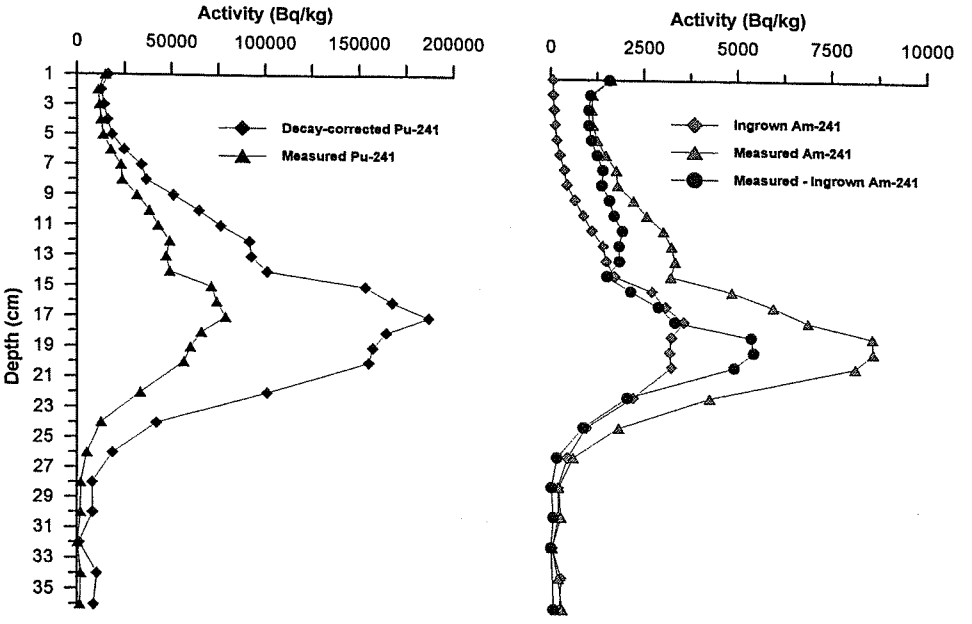

Figure 7-12. ^{241}Am and ^{241}Pu in R-96-000 core

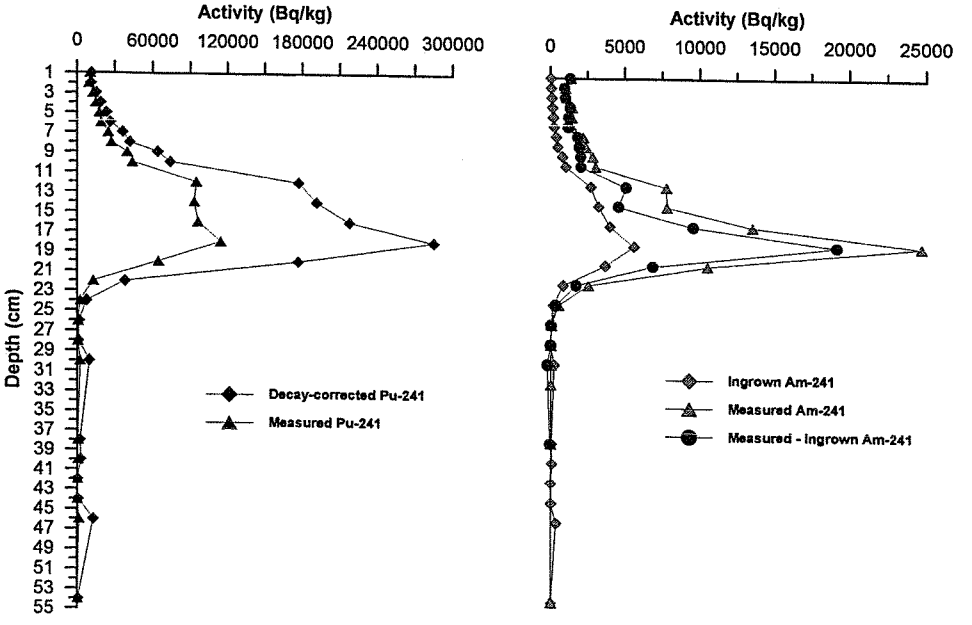

Figure 7-13. ^{241}Am and ^{241}Pu in R-96-007 core

7.8. Conclusions

All the saltmarsh cores show only small variations in sediment composition with depth although the clay contents vary with different cores. No clear evidence of oxic-anoxic boundaries are found. Activities of measured radionuclides depend on the sediment composition of each core but vertical profiles show that the differing annual Sellafield discharge determines their vertical distributions. Sediment accumulation rates (0.6 ~ 1.2 cm/yr) are estimated and vary with different locations of the saltmarsh. Determination of sediment accumulation rates using ^{210}Pb supports these estimations (It should be noted that the method used in this study is not conventional ^{210}Pb dating and based on one core). The rear of the marsh is inundated less frequently and is exposed to the lower tidal energy. Consequently, this area has lower sediment accumulation rates compared to the front of Ravenglass saltmarsh which is being eroded in certain locations. Pu isotopic ratios confirm the sediment mixing, however, there may be some processes below 30 cm from the surface which redistribute radionuclides. It is not exactly known what is responsible for the redistribution but the presence of advective flows in the bottom of the saltmarsh is the most likely explanation. Alternatively, the reported Sellafield discharge data are unreliable. The results also show the importance of ^{241}Pu as a new source term for ^{241}Am.

Chapter 8. Spatial variations across the Ravenglass saltmarsh

8. Spatial variations across the Ravenglass saltmarsh

8.1. Spatial distribution of radionuclides in the saltmarsh in 1980 and 1997

The spatial distribution of several radionuclides in the Ravenglass saltmarsh was reported by Horrill (1983). Both surface scrape and vegetation samples were collected in 1980 and analysed for gamma and alpha-emitting radionuclides. ^{241}Am and ^{137}Cs data in 1980 surface scrape samples are plotted in Figure 8-1 & 8-3 and are compared with the spatial distribution of ^{241}Am and ^{137}Cs from this work (Figure 8-2 & 8-4). The categorisation of the saltmarsh undertaken by Horrill with the dominating vegetation will not be taken into account for the comparison.

For ^{241}Am in 1980 samples, the lowest activity was found at F7, and the highest activity was from X6. It was the northern and western edges and some points in the middle of the marsh where relatively higher activities of ^{241}Am were found. ^{137}Cs data showed a similar pattern that the higher activities were found in the middle part and the northern and western edges of the marsh. The highest ^{137}Cs activity was measured at A6, and the lowest activity was found at E0. For the 1997 results, the lowest activity of ^{241}Am is measured from the sample collected at F5, and the highest activities are found from the samples collected at E0 and F6. Another two points showing relatively high activities of ^{241}Am are B0 and E6. For ^{137}Cs, the highest activity points are the same as those of ^{241}Am and the lowest activity is found at W10. The sampling points where the higher activities are found are the back, the north-west & north-east boundaries of the marsh and the south-east part of the marsh where there is a main channel entrance. These locations where higher activities are found, particularly the back and the north-west boundary of the marsh, are similar to those reported by Horrill (1983).

Although Horrill did measure Pu activities in his surface scrape samples, it was not as extensive as both ^{241}Am and ^{137}Cs. ^{239,240}Pu activities in 1980 samples ranged from 2190 Bq/kg to 15725 Bq/kg. The activities of Pu isotopes from this work (Figures 8-5 ~ 8-7) are between 101 Bq/kg and 823 Bq/kg for ^{238}Pu, from 499 Bq/kg to 3774 Bq/kg for ^{239,240}Pu and for ^{241}Pu, it ranges from 6670 Bq/kg to 55872 Bq/kg. ^{239,240}Pu activities from this work are lower because of the significant reduction in discharge. ^{241}Pu activities are approximately an

order of magnitude higher than those of $^{239,240}Pu$. The general distribution pattern of Pu isotopes in the Ravenglass saltmarsh is very similar to those of both ^{241}Am and ^{137}Cs.

The major differences found between the Horrill study and this work are the measured activity and the two sampling locations near the main channel entrance where higher activities are found. ^{241}Am, ^{137}Cs and Pu isotopes activities in the marsh have decreased significantly after the 17 year period because of the falling discharges from the Sellafield site. However, the general distribution pattern for measured radionuclides at the same sampling years is similar. It is believed that the edges of the marsh are the regions of low energy flow regimes during the tidal cycles so that the accumulation of the fine grain size sediment, which has not settled out of suspension at an initial stage of tidal cycles, takes place with the vegetation acting as a trap. In addition, the Ravenglass saltmarsh is only fully covered at spring tides ; that implies the rear and the edges of the marsh are less frequently covered than other part of the marsh. It was already reported (see Chapter 7.2) that A3 where the R-97-003 core was collected shows a sediment accumulation rate lower than measured at the front of the marsh. The preferential accumulation of fine grain size sediment at the rear of the marsh was evaluated by collecting samples from six sampling locations. The results are shown in Table 8-1 and they clearly show higher Al_2O_3 (lower SiO_2) contents for A3, B0 & E0 where higher activities of radionuclides are found compared with other three locations (E3, F5 & Y3) where lower activities were reported. Therefore, although the surface scrape samples from the top 1 cm were collected, samples from those slow sediment accumulation rate regions will contain a more compressed historical record of Sellafield discharges as well as higher activities of radionuclides associated with finer (more clay-rich) sediments. These conclusions are similar to those reported by Horrill (1983). He concluded that once the tide has flooded under the railway viaduct the river currents push the silt-laden water downstream against the embankment. However, since the Esk estuary is a macrotidal estuary, the influence of river currents may not reach to the saltmarsh unless there is significant rainfall. Tidal inundation combined with the presence of vegetation may be the processes responsible for the distribution of radionuclides in the Ravenglass saltmarsh. He also concluded that the higher activities of both ^{241}Am and ^{137}Cs found in the middle of the marsh resulted from the relatively good trapping efficiency of *Halimione portulacoides* (sea purslane).

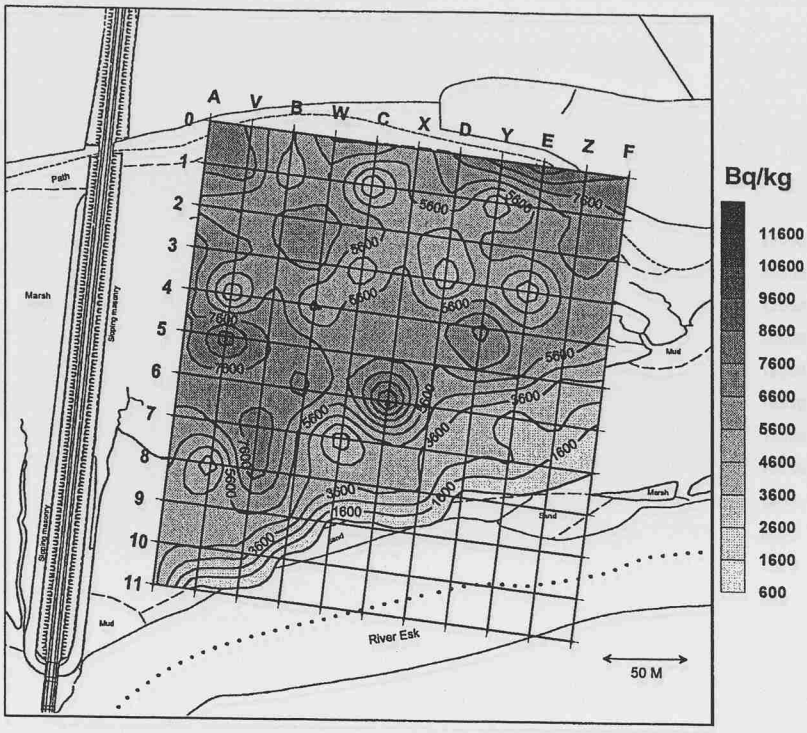

Figure 8-1. Spatial distribution of ^{241}Am in 1980 samples

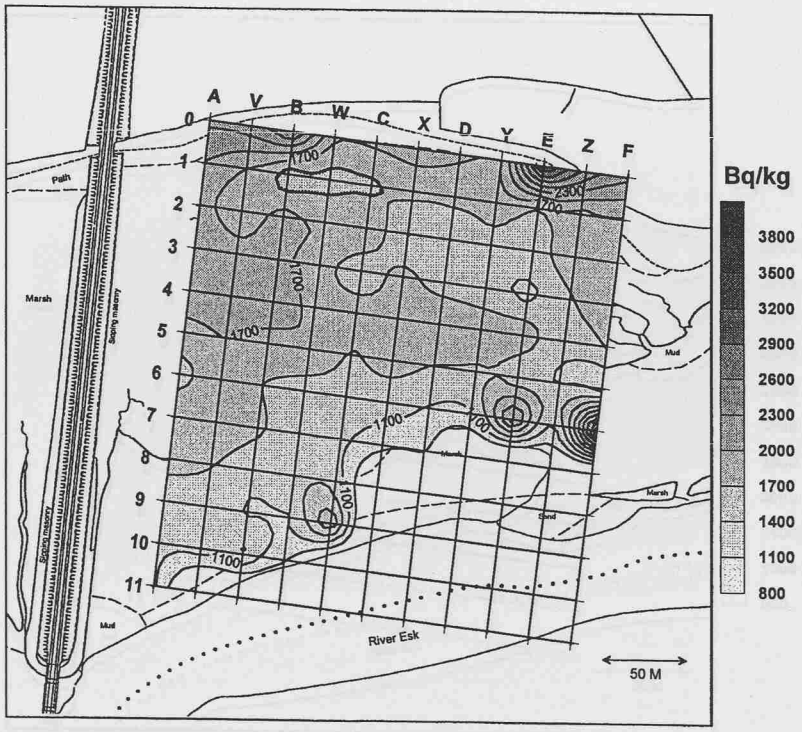

Figure 8-2. Spatial distribution of ^{241}Am in 1997 samples

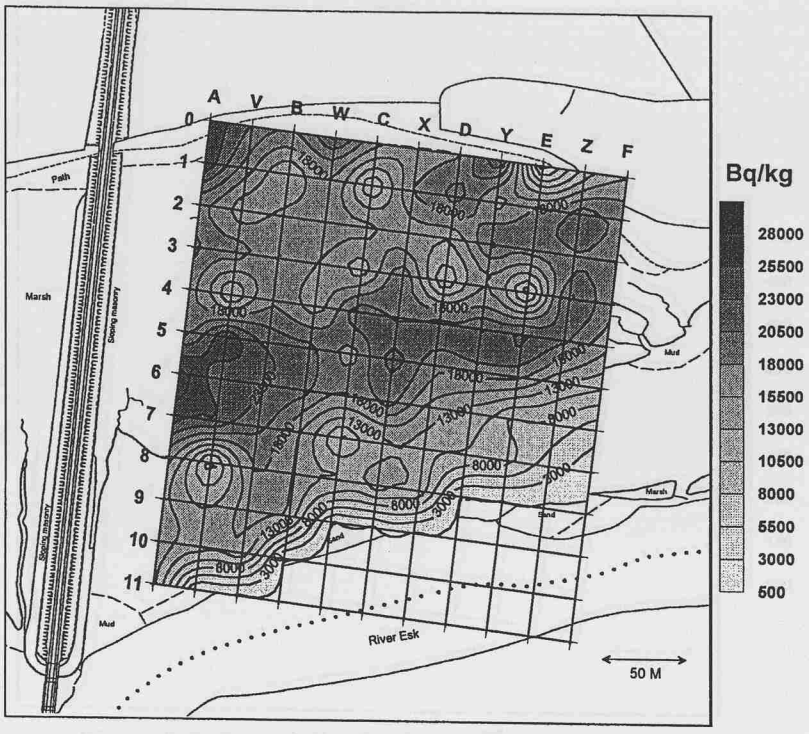

Figure 8-3. Spatial distribution of ^{137}Cs in 1980 samples

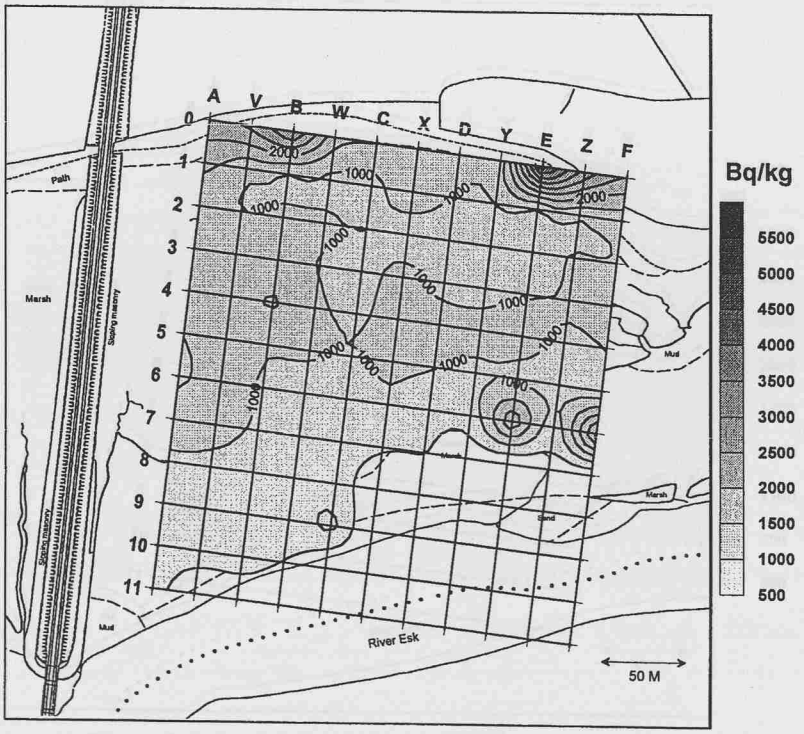

Figure 8-4. Spatial distribution of ^{137}Cs in 1997 samples

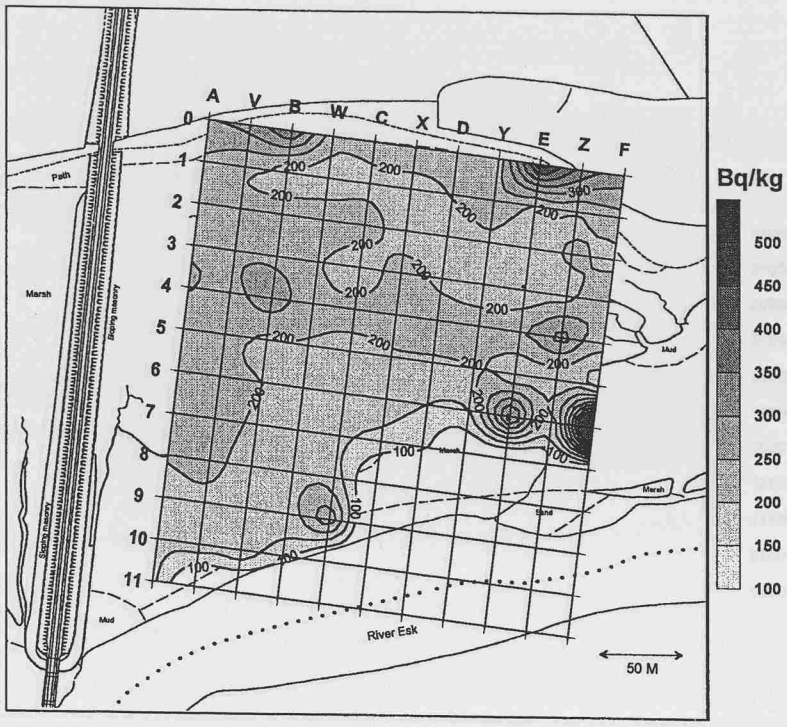

Figure 8-5. Spatial distribution of ^{238}Pu in 1997 samples

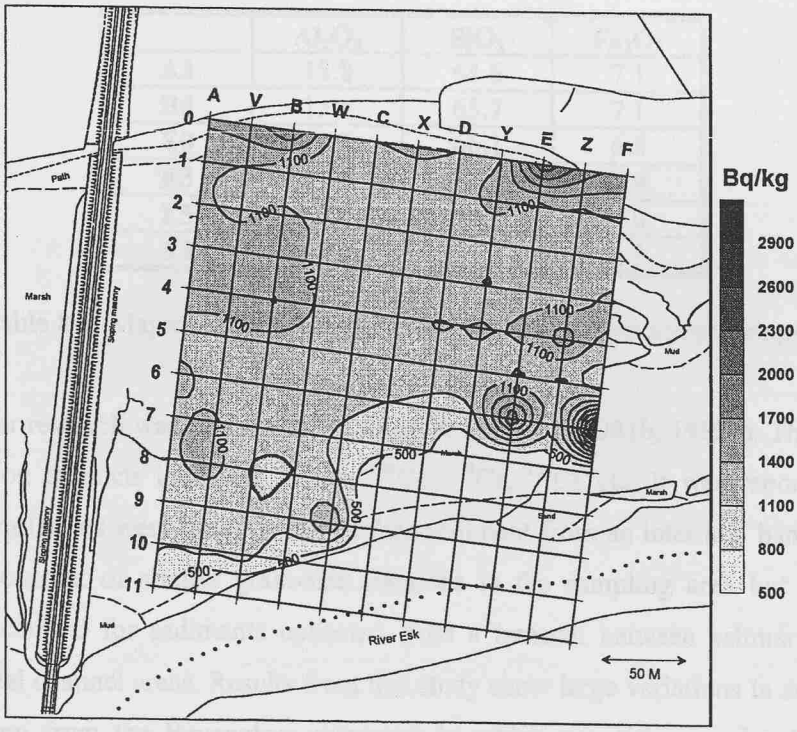

Figure 8-6. Spatial distribution of $^{239,240}Pu$ in 1997 samples

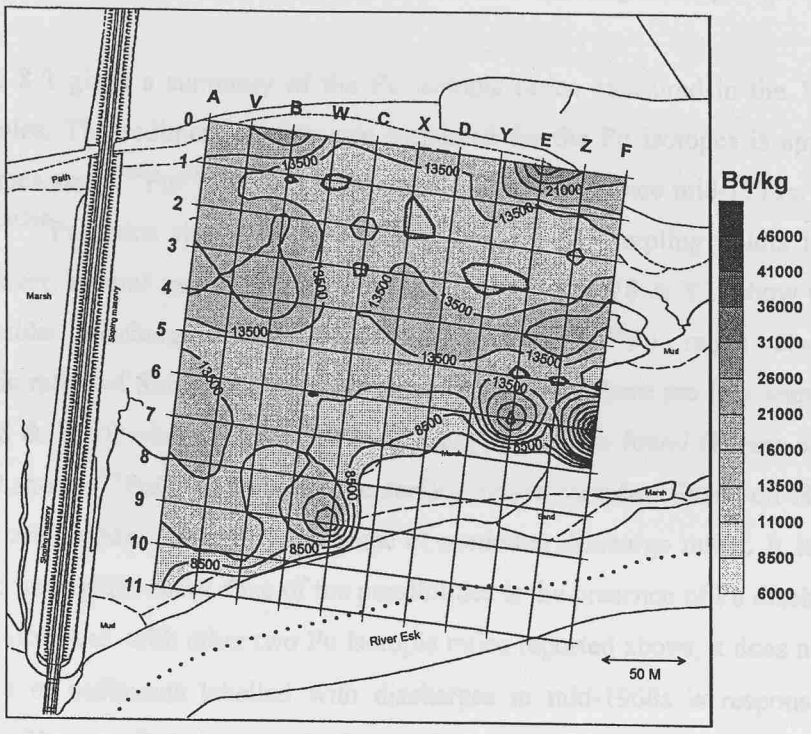

Figure 8-7. Spatial distribution of ^{241}Pu in 1997 samples

	Al_2O_3	SiO_2	Fe_2O_3
A3	15.8	64.6	7.1
B0	15.8	65.7	7.1
E0	15.5	66.1	6.5
E3	11.5	72.9	4.9
F5	10.0	74.3	4.0
Y3	11.5	71.3	4.9

Table 8-1. Major element results for some of the surface scrape samples

Similar research was performed by Aston & Stanners (1981b, 1982b). They measured several fission products including ^{241}Am, ^{144}Ce, ^{134}Cs, ^{137}Cs etc. It was reported that less significant variations were found in the surface sediment from an intertidal bank which was due to the content of similar grain-size fractions in the sampling area but considerable variations occurred for sediments collected from a transect between saltmarsh, intertidal bank and tidal channel areas. Results from this study show large variations in surface scrape samples taken from the Ravenglass saltmarsh in which vegetation, grain size and tides control migration and accumulation of radionuclides.

8.2. Variations in Pu isotopic ratios in 1997 surface scrape samples

Table 8-2 gives a summary of the Pu isotopic ratios measured in the 1997 surface scrape samples. The sediment mixing rate estimated for the Pu isotopes is approx. 90 %. Therefore, measured $^{238}Pu/^{239,240}Pu$ ratios represent discharges since mid-1970s. From Table 8-3, $^{238}Pu/^{239,240}Pu$ ratios since 1981 are 0.20 ~ 0.22. Most sampling points fall into this group, however, several sampling locations (B5, E3, E6, V1, V8 & Y1) show the ratios of relatively older discharge ratios (Figure 8-8). $^{241}Pu/^{239,240}Pu$ ratios also represent characteristic ratios of Sellafield discharge since mid-1970s. There are four sampling points (B5, E3, V8 & W10) where slightly older discharge ratios are found (Figure 8-9). Finally, Figure 8-10 shows $^{241}Pu/^{238}Pu$ ratios in the surface scrape samples. Based on 90 % mixing, these ratios are slightly different from those of modelled discharge ratios. It is not certain what caused these differences. One of the possibilities is the presence of Pu discharged in the mid-1960s. However, with other two Pu isotopic ratios reported above, it does not seem that the presence of sediments labelled with discharges in mid-1960s is responsible for the abnormality. The sampling points with abnormal ratios are B2, C1, C7, D5, E2, E3, V6, W2 & W10.

	$^{238}Pu/^{239,240}Pu$	$^{241}Pu/^{239,240}Pu$	$^{241}Pu/^{238}Pu$
Range	0.16 ~ 0.22	11.5 ~ 14.8	55.4 ~ 73.2
Average	0.20	13.1	64.4
Median	0.20	13.1	64.6
Average % ± 2SD	8.5 ± 2.4	6.0 ± 1.5	6.7 ± 1.9

Table 8-2. Various Pu isotopic ratios in the 1997 samples

Based on the above measured and reported ratios, it can be concluded that the radionuclides found in the surface scrape samples contain discharge history since mid-1970s. This may be caused by either the surface erosion of those particular areas of the marsh showing older discharge ratios (i.e. mid-1970s) or the redistribution of the reworked sediments associated with older discharges. The latter is more likely the cause in this case. The possible origin of those reworked sediments associated with older discharges will be discussed in the next section.

	$^{238}Pu/^{239,240}Pu$	$^{241}Pu/^{239,240}Pu$	$^{241}Pu/^{238}Pu$
1996	0.22	14.4	66.7
1995	0.22	14.4	66.7
1994	0.22	14.4	66.6
1993	0.22	14.3	66.6
1992	0.21	14.1	66.2
1991	0.21	14.1	66.0
1990	0.21	14.0	65.8
1989	0.21	13.9	65.7
1988	0.21	13.8	65.7
1987	0.21	13.8	65.7
1986	0.21	13.7	65.8
1985	0.21	13.7	65.8
1984	0.21	13.7	65.9
1983	0.20	13.4	65.3
1982	0.20	13.2	65.5
1981	0.20	13.1	66.5
1980	0.19	12.9	67.1
1979	0.18	12.7	69.0
1978	0.17	12.2	71.6
1977	0.16	11.7	72.8
1976	0.15	11.6	75.7
1975	0.15	11.6	79.1
1974	0.14	10.7	78.6
1973	0.13	10.0	78.0
1972	0.12	8.2	70.9
1971	0.10	7.0	72.9
1970	0.07	5.4	81.0
1969	0.06	4.4	78.3
1968	0.05	3.5	76.2
1967	0.04	2.5	64.3
1966	0.03	1.8	60.0
1965	0.03	1.4	52.6
1964	0.02	1.1	45.4
1963	0.02	0.8	36.7
1962	0.02	0.6	28.1
1961	0.02	0.4	19.6
1960	0.02	0.3	14.6
1959	0.02	0.3	13.7
1958	0.02	0.3	13.2
1957	0.02	0.3	13.3
1956	0.02	0.3	13.4
1955	0.02	0.4	15.3
1954	0.03	0.4	14.7
1953	0.03	0.3	11.7
1952	0.03	0.4	15.7

Table 8-3. Isotopic ratios of Pu isotopes at 90 % degree of mixing

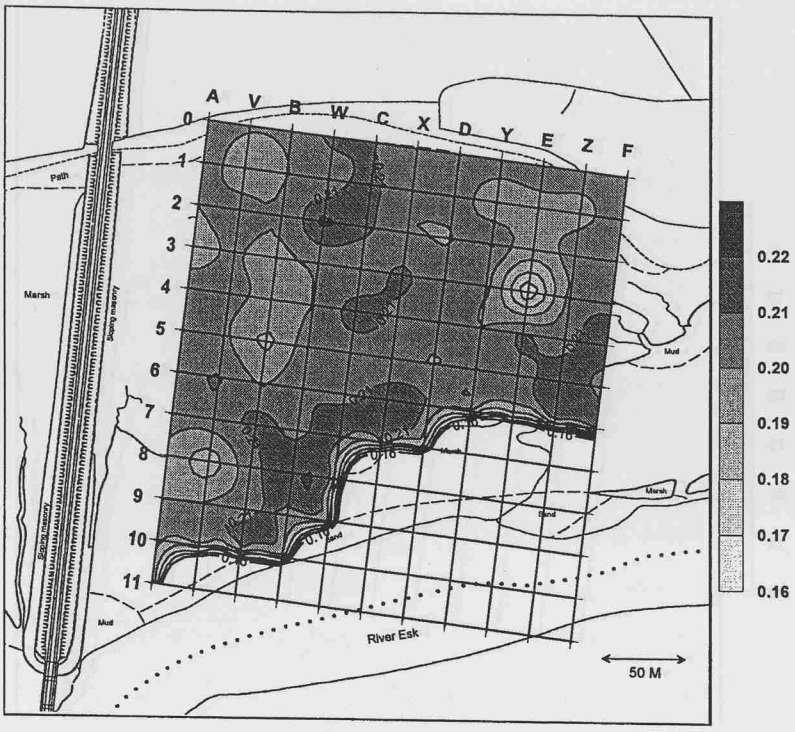

Figure 8-8. Ratios of $^{238}Pu/^{239,240}Pu$ in surface scrape samples

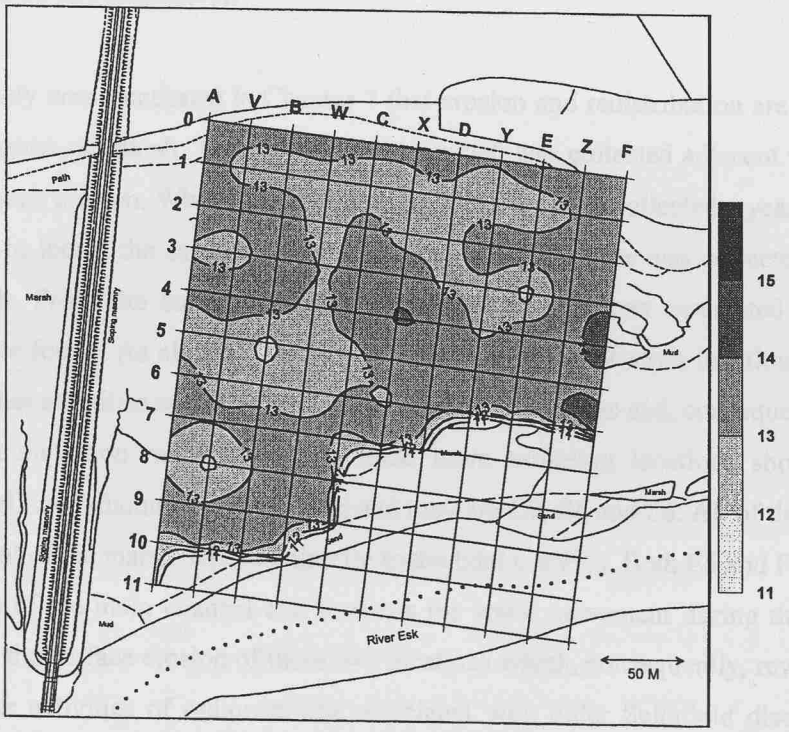

Figure 8-9. Ratios of $^{241}Pu/^{239,240}Pu$ in surface scrape samples

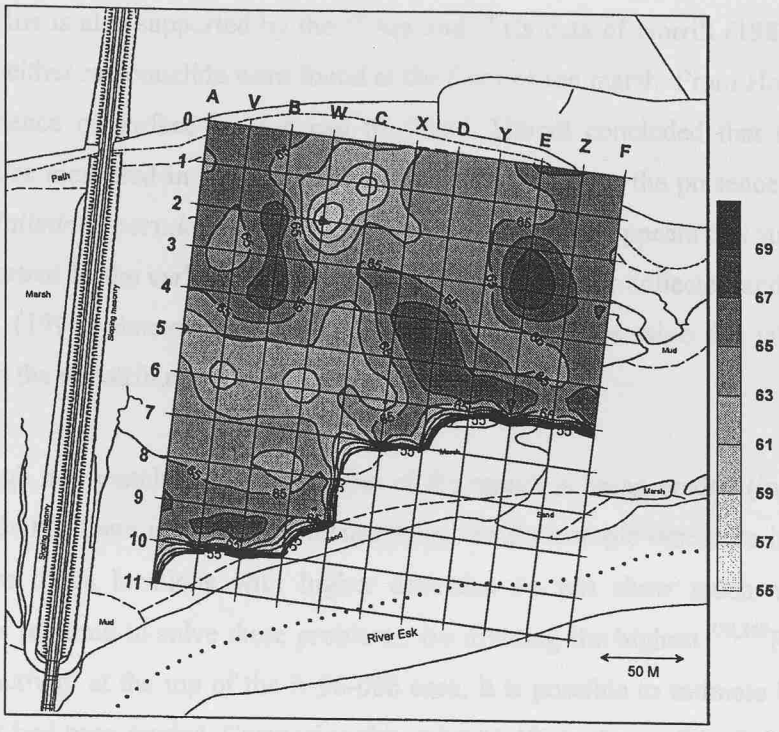

Figure 8-10. Ratios of $^{241}Pu/^{238}Pu$ in surface scrape samples

8.3. Erosion of the saltmarsh

It already was mentioned in Chapter 7 that erosion and redistribution are taking place in the Ravenglass saltmarsh. The R-96-008 core, which was collected adjacent to E7, shows evidence of such erosion. When the surface scrape samples were collected a year later, it was not possible to locate the sampling site where the R-96-008 core was collected. It was no longer marsh. From the surface scrape results, several locations associated with higher activities were found. As already shown in section 8.1., some of those locations (A3, B0 & E0) with higher activities correlated with the higher clay contents and, consequently, the low sediment accumulation rates. There are some more sampling locations showing higher activities of all the radionuclides measured and they are C9, E6 and F6. All of these locations are at the front of the marsh exposed directly to the tidal currents. Both E6 and F6 are located at the mouth of the main channel and it seems the water movement during the tidal cycle contribute to the surface erosion of these two locations which, consequently, reveal sediment having higher activities of radionuclides associated with older Sellafield discharges. It is unlikely that these parts of the marsh contain high clay contents since the stronger tidal

movement is dominating (see Table 8-1 for F5 and major element data for R-96-008 core in Chapter 4). This is also supported by the ^{241}Am and ^{137}Cs data of Horrill (1983) since high activities of neither radionuclide were found at the front of the marsh. From Horrill's results, no clear evidence of surface erosion can be found. Horrill concluded that the relatively higher activities measured in the middle of the marsh was due to the presence of particular vegetation, *Halimione portulacoides* (sea purslane). Therefore, it appears that surface erosion was not important in the early 1980s. However, one of the cores collected and analysed by Livens *et al.* (1994) almost a decade ago shows that surface erosion did take place and contributed to the redistribution of sediments in the saltmarsh.

Although it is concluded that the front of the marsh is being eroded (in terms of the measured activity), there is no clear evidence using the Pu isotopic ratios. Pu isotopic ratios reported from those locations with higher activities do not show much variation. An explanation is required to solve these problems. By dividing the highest ^{239,240}Pu activity by the ^{239,240}Pu activity at the top of the R-96-008 core, it is possible to estimate how much of the sediments had been eroded. Comparing this value (1.49) to those of the R-96-000 and R-96-007 cores indicates about 14 cm of the top sediments had been eroded. Using this estimation, the sediment accumulation rate for this core can be estimated and it is approximately 1.5 cm/yr. Consequently, the top fraction of the R-96-008 core represents discharges for 1985. Even if the top 14 - 15 cm have been eroded, no significant changes are seen for the Pu isotopic ratios and this is due to the relatively constant Pu isotopic ratios since the 1980s. It is obvious that the eroded sediments from the Ravenglass saltmarsh will be dispersed in the saltmarsh but there is a limitation in using the Pu isotopic ratios due to the above reason. There are sampling locations where Pu isotopic ratios from the surface scrape samples are more typical of the mid-1970s discharges. Based on the Pu isotopic ratios of surface scrape samples, no sign of the mid-1970s discharge ratios is found where surface erosion is taking place. Therefore, it seems surface material at those sampling locations showing the mid-1970s discharge ratios originated from elsewhere, not from the Ravenglass saltmarsh. This may be resuspended sediments in the River Esk during the tidal cycle.

8.4. Loss on ignition data

Figure 8-11 shows the loss on ignition (LOI) results in the surface scrape samples. The LOI represents not only organic matter content but also lattice bound -OH within clay,

carbonate and other volatile elements. Assinder (1983) and Livens & Baxter (1988) found no convincing evidence that the total organic carbon (organic matter) would have an influence on the radionuclide activity in soils collected near the Ravenglass saltmarsh. They reported that the sediments having a greater clay + silt size fractions (< 63 μm) show higher activities of radionuclides. From the surface contour plot of LOI (Figure 8-11), it is clear that the highest LOI are found at the back and the edges of the marsh which are low energy environments during the tidal cycles. The further from the main channel, the higher the LOI results. With the XRF results reported in Table 8-2, it appears that the presence of finer size fractions (i.e. clays) in these areas have caused such LOI distribution on the marsh. It also can be concluded that the main mechanism for the distribution of sediments associated Sellafield derived radionuclides is the regular flooding of main channel controlled by the tidal cycles.

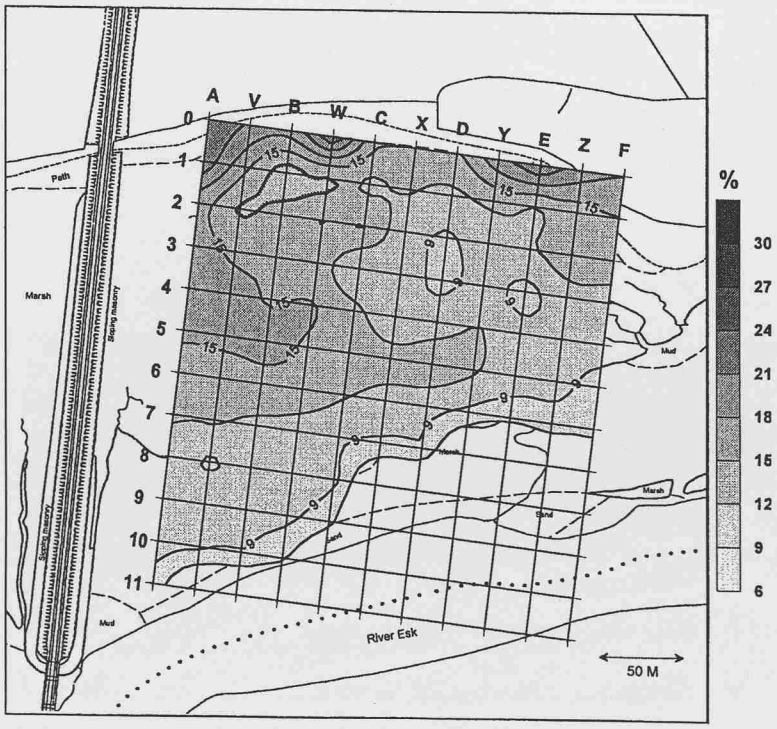

Figure 8-11. Loss on ignition data for the 1997 samples

8.5. Conclusions

The activities of ^{241}Am, ^{137}Cs and Pu isotopes in surface scrape samples in 1980 and 1997 samples show significant decrease over the 17 year period. It is expected due to the reduction of discharge levels from Sellafield. The spatial distribution of radionuclides in the Ravenglass saltmarsh appears to be controlled by tidal inundation of the saltmarsh, by the presence of vegetation acting as a baffle to trap sediment and by sediment composition. It appears that the southeast part of the marsh is continuously being eroded and keeps changing the morphology of the marsh. There is a evidence of sediment redistribution with the discharge history typical of the mid-1970s reflected in material originated both from resuspended sediments transported from the River Esk associated with tides and the Ravenglass saltmarsh itself as a result of surface erosion.

Chapter 9. Overall conclusions

9. Overall conclusions

1. It is believed that mixing of sediments largely contributes to the changes in isotopic ratios of radionuclides. The Irish Sea core has shown such mixing exists. Thus, it has been estimated, using various anthropogenic radionuclides originated from the Sellafield site, that mixing of sediments lies between 80 ~ 90 % from the Sellafield pipeline until the arrival at the Ravenglass saltmarsh. This hypothesis is supported by the comparison of Pu isotopic ratios in cores to those of a model.

2. From the radionuclide and geochemistry data, it is evident that particle size (i.e. clay contents) controls the relative levels of radionuclides in the saltmarsh. Different sediment accumulation rates over the saltmarsh combined with the presence of vegetation are also responsible for the spatial and vertical distributions of radionuclide in the Ravenglass saltmarsh. No significant sign of chemically or biologically-driven redistribution of radionuclides is observed, however, surface erosion as a post-depositional process is responsible for the redistribution of radionuclides. In addition, core profiles of radionuclides analysed are similar to the Sellafield discharge record implying the annual Sellafield discharge is one of the major factors to determine the vertical distribution of radionuclides in this saltmarsh.

3. Sediment accumulation rates have been estimated using data from three saltmarsh cores. Two of the cores collected at the front of the marsh show sediment accumulation rates of approximately 1 cm/yr. This agrees well with estimates based on counting sedimentary lamination from one core. A core collected from the north-west side of the marsh (rear of the marsh) reveals the sediment accumulation rate lower (approximately 0.6 cm/yr) than that of the front of the marsh. The tidal currents, deposition of fine grain size fractions and the less frequent inundation of this part of the marsh are responsible for the slow sediment accumulation rates. The ^{210}Pb results for R-96-007 core support this estimation.

4. Estimating ingrown ^{241}Am in cores has identified the importance of ^{241}Pu in the environment. Based on the Sellafield discharge record, it is estimated that approximately 46 % of total ^{241}Am in the system have originated from the decay of ^{241}Pu *in situ*. Estimation undertaken on two of the saltmarsh cores has revealed that 28 % and 41 % of the total ^{241}Am are generated by the decay of ^{241}Pu.

5. Although the profiles of radionuclides measured appear to preserve the discharge history from the Sellafield site, in terms of the Pu isotopic ratios, it only preserves the discharge history up to 30 cm from the surface. The ratios of $^{241}Pu/^{239,240}Pu$ and $^{241}Pu/^{238}Pu$ do not agree well with those of the modelled discharge ratios. This may be due to the unreliability of discharge data or most likely the presence of advective flows in the saltmarsh which may introduce more recent Pu isotopic ratios of Sellafield discharge into the deeper sediments.

6. Spatial distribution of radionuclides in the Ravenglass saltmarsh is controlled by the combination of tidal movement and the particle size (clay content) of the sediments. It is also observed that erosion of the saltmarsh is occurring and that the eroded sediments are redistributed in the Ravenglass saltmarsh along with sediments labelled with older Sellafield discharge originated from the River Esk.

Chapter 10. References

10. References

Albert, J. J. & Orlandini, K. A. (1981) Laboratory and field studied of the relative mobility of $^{239,240}Pu$ and ^{241}Am from the lake sediments under oxic and anoxic conditions. *Geochimica et Cosmochimica Acta* **45**, 1931 - 1939.

Allington, D. J., Baxter, A. J., Poole, A. J. & Young, A. K. (1995) The nature of phosphate ore and associated waste products discharged into the eastern Irish Sea from a phosphoric acid production plant. *The Science of the Total Environment* **173/174**, 137-149.

Appleby, P. G. & Oldfield, F. (1992) Application to lead-210 to sedimentation studies. In Uranium-Series Disequilibrium : Application to Earth, Marine and Environmental Sciences. (ed. Ivanovich, M. & Harmon, R. S.), Clarendon, Oxford, pp. 731-778.

Assinder, D. J. (1983) Behaviour of plutonium in the intertidal sediments of the eastern Irish Sea. *Ecological Aspects of Radionuclide Release* (Coughtrey, P. J., ed.). British Ecological Society Special Publication No. 3. Blackwell, Oxford. pp.189-197.

Assinder, D. J., Kelly, M. & Aston, S. R. (1984) Conservative and non-conservative behaviour of radionuclides in an estuarine environment, with particular respect to the behaviour of plutonium isotopes. *Environmental Technology Letters* **5**, 23-30.

Assinder, D. J., Kelly, M. & Aston, S. R. (1985) Tidal variations in dissolved and particulate phase radionuclide activities in the Esk estuary, England, and their distribution coefficients and particulate activity fractions. *Journal of Environmental Radioactivity* **2**, 1-22.

Assinder, D. J., Yamamoto, M., Kim, C. K., Seki, R., Takaku, Y., Yamauchi, Y., Igarashi, S., Komura, K. & Ueno, K. (1993) Radioisotopes of thirteen elements in intertidal coastal and estuarine sediments in the Irish Sea. *Journal of Radioanalytical and Nuclear Chemistry, Articles* **170**, 333-346.

Aston, S. R. (1980) Evaluation of the chemical forms of plutonium in seawater. *Marine Chemistry* **8**, 319-325.

Aston, S. R. & Stanners, D. A. (1979) The determination of estuarine sedimentation rates by $^{134}Cs/^{137}Cs$ and other artificial radionuclide profiles. *Estuarine, Coastal and Marine Science* **9**, 529-541.

Aston, S. R., Assinder, D. J., Stanners, D. A. & Rae, J. E. (1981) Plutonium occurrence and phase distribution in sediments of the Wyre estuary, Northwest England. *Marine Pollution Bulletin* **12**, 308-314.

Aston, S. R. & Stanners, D. A. (1981a.) Plutonium transport to and deposition and immobility in Irish Sea intertidal sediments. *Nature* **289**, 581-582.

Aston, S. R. & Stanners, D. A. (1981b.) Americium in intertidal sediments from the coastal environments of Windscale. *Marine Pollution Bulletin* **12**, 149-153.

Aston, S. R. & Stanners, D. A. (1981c) Observation on the deposition, mobility and chemical associations of plutonium in intertidal sediments. In *Techniques for Identifying Transuranic Speciation in Aquatic Environments*, pp. 209-217, IAEA, Vienna.

Aston, S. R. & Rae, J. E. (1982) The deposition of Windscale radiocaesium in the Wyre estuary and the measurement of sedimentation rates. *Marine Environmental Research* **7**, 83-90.

Aston, S. R. & Stanners, D. A. (1982a) The transport to and the deposition of americium in intertidal sediments of the Ravenglass estuary and its relationship to plutonium. *Environmental Pollution Series B.* **3**, 1-9.

Aston, S. R. & Stanners, D. A. (1982b) Local variability in the distribution of Windscale fission products in estuarine sediments. *Estuarine, Coastal and Shelf Science* **14**, 167-174.

Aston, S. R. & Stanners, D. A. (1982c) Gamma emitting fission products in surface sediments of the Ravenglass estuary. *Marine Pollution Bulletin* **13**, 135-138.

Aston, S. R., Assinder, D. J. & Kelly, M. (1985) Plutonium in intertidal, coastal and estuarine sediments in the northern Irish Sea. *Estuarine, Coastal and Shelf Science* **20**, 761-771.

Berner, R. A. (1980) *Early Diagenesis : A Theoretical Approach.* Princeton, NJ : Princeton University Press. 241pp.

BNFL (1997) *Annual Report*, BNF Ltd, Warrington, Cheshire.

Browne, E. & Firestone, R. (1986) *Table of Radioactive Isotopes.* Wiley, New York.

Burdige, D. J. & Gieskes, J. M. (1983) A pore-water/solid phase diagenetic model for Mn in marine sediments. *American Journal of Science* **283**, 29-47.

Burton, P. J. (1986) Laboratory studies on the remobilisation of actinides from Ravenglass estuary sediment. *The Science of the Total Environment* **52**, 123-145.

Cambray, R. S. & Eakins, J. D. (1982) Pu, ^{241}Am and ^{137}Cs in soil in West Cumbria and a maritime effect. *Nature* **300**, 46-48.

Carpenter, R. & Beasley, T. M. (1981) Plutonium and americium in anoxic marine sediments : Evidence against remobilisation. *Geochimica et Cosmochimica Acta* **45**, 1917-1930.

Carpenter, R., Peterson, M. L., Bennett, J. T. & Somayajulu, B. L. K. (1984) Mixing and cycling of uranium, thorium and Pb-210 in Puget Sound sediments. *Geochimica et Cosmochimica Acta* **48**, 1949-1963.

Casella, V. R., Bishop, C. T., Glosby, A. A. & Phillips, C. A. (1981) Anion exchange method for the sequential determination of uranium, thorium and lead-210 in coal and coal ash. *Journal of Radioanalytical Chemistry* **62**, 257-266.

Chester, R. (1990) *Marine Geochemistry*. Cambridge, Chapman & Hall, 698pp.

Choppin, G. R. & Kobashi, A. (1990) Distribution of Pu(V) and Pu(VI) in seawater. *Marine Chemistry* **30**, 241-247.

Choppin, G. R., Liljenzin, J. O. & Rydberg, J. (1996) *Radiochemistry and Nuclear Chemistry (2nd ed.)*. Oxford, Butterworth - Heinemann, 707pp.

Chung, Y. & Chang, W. C. (1995) Pb-210 fluxes and sedimentation rates on the lower continental slope between Taiwan and the South Okinawa Trough. *Continental Shelf Research* **15**, 149-164.

Clifton, R. J. & Hamilton, E. I. (1982) The application of radioisotopes in the study of estuarine sedimentary processes. *Estuarine, Coastal and Shelf Science* **14**, 433-446.

Croudace, I. W. (1991) A reliable and accurate procedure for preparing low activity efficiency calibration standards for germanium gamma-ray spectrometers. *Journal of Radioanalytical and Nuclear Chemistry, Letters* **153**, 151-162

Croudace, I. W. & Cundy, A. B. (1995) Heavy metal and hydrocarbon pollution in recent sediments from Southampton Water, Southern England: A geochemical and isotopic study. *Environmental Science and Technology* **29**, 1288-1296.

Croudace, I. W., Warwick, P. E., Taylor, R. N., Dee, S. J., Milton, J. A. & Oh, J.-S. (1998a) Borate fusion followed by ion-exchange/extraction chromatography for rapid determination of Pu and U in environmental materials. *Radioactivity & Radiochemistry* **9**, 41-48

Croudace, I. W., Warwick, P. E., Taylor, R. N. & Dee, S. J. (1998b) Rapid procedure for plutonium and uranium determination in soils using a borate fusion followed by ion-exchange and extraction chromatography. *Analytica Chimica Acta* **371**, 217-225.

Currie, L. A. (1968) Limits of qualitative detection and quantitative determination. *Analytical Chemistry* **40**, 586-593.

Darral, K. G., Hammond, G. C. M. & Tyler, J. F. C. (1973) The determination of ^{241}Pu in effluents. *Analyst* **98**, 358-363.

Day, J. P. & Cross, J. E. (1981) ^{241}Am from the decay of ^{241}Pu in the Irish Sea. *Nature* **292**, 33-35.

DeMaster, D. J., McKee, B. A., Nittrouer, C. A., Brewster, D. C. & Biscaye, P. E. (1985) Rates of sediment reworking at the Hebble site based on measurements of Th-234, Cs-137 and Pb-210. *Marine Geology* **66**, 133-148.

Edgington, D. N., Val Klump, J., Robbins, J. A., Kusner, Y. S., Pampura, V.D. & Sandimirov, I. V. (1991) Sedimentation rates, residence times and radionuclide inventories in Lake Baikal from ^{137}Cs and ^{210}Pb in sediment cores. *Nature* **350**, 601-604.

Fairbridge, R. W. (1980) The estuary : its identification and geodynamic cycle. In *Chemistry and Biochemistry of Estuaries* (ed. Olausson, E. & Cato, I.) New York, Wiley, 1-36.

Goldberg, E. D. (1963) Geochronology with ^{210}Pb. *Symposium on radioactive dating*, IAEA, Vienna, 121-130.

Gray, J., Jones, S. R. & Smith, A. D. (1995) Discharges to the environment from the Sellafield Site, 1951-1992. *Journal of Radiological Protection* **15**, 99-131.

Hamilton, E. I. & Clifton, R. J. (1980) Concentration and distribution of the transuranium radionuclides $^{239,240}Pu$, ^{238}Pu and ^{241}Am in *Mytilus edulis*, *Fucus vesiculosus* and surface sediment of Esk estuary. *Marine Ecology, Progress Series* **3**, 267-277.

Hamilton, E. I. (1981) Alpha-particle radioactivity of hot particles from the Esk Estuary. *Nature* **290**, 690-693.

Hamilton, E. I. & Clarke, K. R. (1984) The recent sedimentation history of the Esk estuary. Cumbria, U.K. : The application of radiochronology. *The Science of the Total Environment* **35**, 325-386.

Hamilton, E. I. & Stevens, H. E. (1985) Some observations on the geochemistry and isotopic composition of Uranium in relation to the reprocessing of nuclear fuels. *Journal of Environmental Radioactivity* **2**, 23-40.

Hamilton, E. I. (1989) Radionuclides and large particles in estuarine sediments. *Marine Pollution Bulletin* **20**, 603-607.

Hamilton, E. I. (1998) Marine environmental radioactivity - the missing science?. *Marine Pollution Bulletin* **36**, 8-18.

Hetherington, J. A. (1978) The uptake of plutonium nuclides by marine sediments. *Marine Science Communications* **4**, 239-274.

Horrill, A. D. (1983) Concentrations and spatial distribution of radioactivity in an ungrazed saltmarsh. *Ecological Aspects of Radionuclide Release* (Coughtrey, P. J., ed.). British Ecological Society Special Publication No. 3. Blackwell, Oxford. p.119-215.

Horrocks, D. L. & Studier, M. H. (1958) Low-level ^{241}Pu analysis by liquid scintillation techniques. *Analytical Chemistry* **30**, 1747-1750.

Horwitz, E. P., Dietz, M. L., Chiarizia, R. & Diamond, H. (1992) Separation and preconcentration of uranium from acidic media by extraction chromatography. *Analytica Chimica Acta* **266**, 25-37.

Horwitz, E. P., Dietz, M. L., Chiarizia, R., Diamond, H., Maxwell III, S. L. & Nelson, M. R. (1995) Separation and preconcentration of actinides by extraction chromatography using a supported liquid anion exchanger : application to the characterisation of high-level nuclear waste solutions. *Analytica Chimica Acta* **310**, 63-78.

Howorth, J. M. (1989) *Studies of Environmental Radioactivity in Cumbria. Part 17. A Revised Basis for Modelling Radionuclides Dispersion in the Irish Sea.* **AERE-R13448**, London, UKAEA.

Hursthouse, A. S., Baxter, M. S., Livens, F. R. & Duncan, H. J. (1991) The behaviour of Sellafield-derived neptunium and other nuclides during transfer to the terrestrial environment in Cumbria, UK, *Journal of Environmental Radioactivity* **14**, 147-174.

IAEA (1985) *Sediment Kds and concentrations factors for radionuclides in the marine environment.* Technical Report of the IAEA No. 247, Vienna.

IAEA (1986) *Summary report on the post-accident review meeting on the Chernobyl accident.* Safety Series Report No. 75, INSAG-1, Vienna, 106pp.

Jackson , D. I., Jackson, A. A., Evans, D., Wingfield, R. T. R., Barnes, R. P. & Arthur, M. J. (1995) *United Kingdom offshore regional report : The geology of the Irish Sea.* HMSO for the British Geological Survey, London, 123pp.

Jacobs, D. G. & Tamura, T. (1960) *The mechanism of ion fixation using radioisotope techniques.* Trans. 7th Internat. Cong. Soil Sci., Madison, Wisc., Vol. 2, 206-214.

Kanai, Y. (1986) Determination of $^{234}U/^{238}U$ activity ratios in geological reference materials by alpha spectrometry. *Radioisotopes* **35**, 601-604.

Kershaw, P. J., Swift, D. J., Pentreath, R. J. & Lovett, M. B. (1983) Plutonium redistribution by biological activity in Irish Sea sediments. *Nature* **306**, 774-775.

Kershaw, P. J., Swift, D. J., Pentreath, R. J. & Lovett, M. B. (1984) The incorporation of plutonium, americium and curium into the Irish Sea seabed by biological activity. *The Science of the Total Environment* **40**, 61-81.

Kershaw, P. J. (1986) Radiocarbon dating of Irish Sea sediments. *Estuarine, Coastal and Shelf Science* **23**, 295-303.

Kershaw, P. J., Brealey, J. H., Woodhead, D. S. & Lovett, M. B. (1986) Alpha-emitting, hot particles in the Irish Sea sediments. *The Science of the Total Environment* **53**, 77-87.

Kershaw, P. J., Swift, D. J. & Denoon, D. C. (1988) Evidence of recent sedimentation in the eastern Irish Sea. *Marine Geology* **85**, 1-14.

Kershaw, P. J., Woodhead, D. S., Malcolm, S. J., Allington, D. J. & Lovett, M. B. (1990) A sediment history of Sellafield discharges. *Journal of Environmental Radioactivity* **12**, 201-241.

Kershaw, P. J., Pentreath, R. J., Woodhead, D. S. & Hunt, G. J. (1992) *A review of radioactivity in the Irish Sea : A report prepared for the Marine Pollution Monitoring Management Group.* Aquatic Environment Monitoring Report No. 32, MAFF Direct. Fish. Res., Lowestoft.

Kershaw, P. J. & Baxter, A. J. (1993) Sellafield as a source of radioactivity to the Barent Sea. In *Proceedings of Radioactivity and Environmental Security in the Oceans : New Research and Policy Priorities in the Arctic and North Atlantic*, 91-104, WHOI, 647pp.

Kim, C. K., Morita, S., Seki, R., Takaku, Y., Ikeda, N. & Assinder, D. J. (1992) Distribution and behaviour of ^{99}Tc, ^{237}Np, $^{239+240}Pu$ and ^{241}Am in the coastal and estuarine sediments of the Irish Sea. *Journal of Radioanalytical Nuclear Chemistry* **156**, 201-213.

Koide, M., Soutar, A. & Goldberg, E. D. (1972) Marine geochronology with Pb-210. *Earth and Planetary Science Letters* **14**, 442-446.

Korkisch, J. & Tera, F. (1961) Separation of thorium by anion exchange. *Analytical Chemistry* **33**, 1264-1266.

Korkisch, J. & Hazan, I. (1964) Ion exchange determination of uranium in ferrous alloys. *Analytical Chemistry* **36**, 2464-2466.

Krishnaswami, S., Lal, D., Martin, J. M. & Meybeck, M. (1971) Geochronology of lake sediment. *Earth and Planetary Science Letters* **11**, 407-414.

Krishnaswami, S. & Sarin, M. M. (1976) The simultaneous determination of Th, Pu, Ra isotopes, ^{210}Pb, ^{55}Fe, ^{32}Si and ^{14}C in marine suspended phases. *Analytica Chimica Acta* **83**, 143-356.

Libes, S. M. (1992) *An Introduction to Marine Biogeochemistry.* Singapore, John Wiley & Sons, Inc. 734pp.

Livens, F. R., & Baxter, M. S. (1988) Particle size and radionuclide levels in some west Cumbrian soils. *The Science of the Total Environment* **70**, 1-17.

Livens, F. R., Horrill, A. D. & Singleton, D. L. (1994) Plutonium in estuarine sediments and the associated interstitial waters. *Estuarine Coastal and Shelf Science* **38**, 479-489.

Livingston, H. D., Schneider, D. L. & Bowen, V. T. (1975) ^{241}Pu in the marine environment by a radiochemical procedure. *Earth and Planetary Science Letters* **25**, 361-367.

Loring, D. H. and Rantala, R. T. T. (1992) Manual for the geochemical analyses of marine sediments and suspended particulate matter. *Earth Science Reviews* **32**, 235-283.

MacKenzie, A. B. & Scott, R. D. (1982) Radiocaesium and plutonium in intertidal sediments from southern Scotland. *Nature* **299**, 613-616.

MacKenzie, A. B., Scott, R. D., & Williams T. M. (1987) Mechanisms for northward dispersion of Sellafield waste. *Nature* **239**, 42-45.

MacKenzie, A. B. & Scott, R. D. (1993) Sellafield waste radionuclides in the Irish Sea intertidal and saltmarsh sediments. *Environmental Geochemistry and Health* **15**, 173-184.

MacKenzie, A. B., Scott, R. D., Allan, R. L., Ben Shaban, Y. A., Cook, G. T. & Pulford I. D. (1994) Sediment radionuclide profiles : implications for mechanisms of Sellafield waste dispersal in the Irish Sea. *Journal of Environmental Radioactivity* **23**, 36-69.

MacKenzie, A. B., Cook, G. T., McDonald, P. & Jones, S. R. (1998) The influence of mixing timescale and re-dissolution processes on the distribution of radionuclides in northeast Irish Sea sediments. *Journal of Environmental Radioactivity* **39**, 35-53.

MAFF (1993) *Radioactivity in surface and coastal waters of the British Isles, 1992.* Aquatic Environment Monitoring Report No. 38., MAFF Direct. Fish. Res., Lowestoft, 66pp.

Malcolm, S. J., Battersby, N. S., Stanley, S. O. and Brown, C. M. (1986) Organic degradation, sulphate reduction and ammonia production in the sediment of Loch Eil, Scotland. *Estuarine Coastal and Shelf Science* **23**, 689-706.

Malcolm, S. J., Kershaw, P. J., Lovett, M. B. & Harvey, B. R. (1990) The interstitial water chemistry of ^{239,240}Pu and ^{241}Am in the sediment of the north-east Irish Sea. *Geochimica et Cosmochimica Acta.* **54**, 29-35.

McCartney, M., Kershaw, P. J. & Allington, D. J. (1990) The behaviour of ^{210}Pb and ^{226}Ra in the eastern Irish Sea. *Journal of Environmental Radioactivity* **12**, 243-265.

McDonald, P., Cook, G. T., Baxter, M. S. & Thomson, J. C. (1990) Radionuclide transfer from Sellafield to south-west Scotland. *Journal of Environmental Radioactivity* **12**, 285-298

McDonald, P., Cook, G. T., Baxter, M. S. & Thomson, J. C. (1992) The terrestrial distribution of artificial radioactivity in south-west Scotland. *The Science of the Total Environment* **111**, 59-82.

McKay, W. A. & Pattenden, N. J. (1989) Radionuclides in shoreline waters of the northeast Irish Sea. *The Science of the Total Environment* **84**, 159-167.

McMurtry, G. M., Schneider, R. C., Colin, P. L., Buddemeier, R. W. & Suchanek, T. H. (1985) Redistribution of fallout radionuclides in Enewetak Atoll lagoon sediments by callianassid bioturbation. *Nature* **313**, 674-677.

Mitchell, P. I., Batlle, J. V., Ryan, T. P., McEnri, C., Long, S., O'Colmain, M., Cunningham, J. D., Caulfield, J. J., Larmour, R. A. & Ledgerwood, F. K. (1991) Plutonium, americium and radiocaecium in seawater, sediments and coastal soils in Carlingford Lough. In *Radionuclides in the study of marine processes* (Kershaw & Woodhead eds.), 265-275.

Morse, J. W. & Choppin, G. R. (1991) The chemistry of transuranic elements in natural waters. *Reviews in Aquatic Sciences* **4**, 1-22.

Mossop, I. A. (1960) Filtration of the gaseous effluent of an air-cooled reactor. *British Chemical Engineering* **June**, 420-426.

Mudge, S., Kelly, M., Hamilton-Taylor, J. & Bradshaw, K. (1989) *Behaviour of plutonium in estuarine environments*. Contract Report to UK Department of the Environment, No. DOE/HMIP/RR/91/0DI.

Navratil, J. D., Nelson, R. C. & Nixon, R. A. (1979) Anion exchange separation and radiometric determination of neptunium in plutonium. *Radiochemical Radioanalytical Letters* **40**, 37-40.

Nelson, F., Michelson, D. C. & Holloway, J. H. (1964). Ion exchange procedures III. Separation of uranium, neptunium and plutonium. *Journal of Chromatography* **14**, 258-260.

Nelson, D. M. & Lovett, M. B. (1978) Oxidation state of plutonium in the Irish Sea. *Nature* **276**, 599-601.

Nelson, D. M., Orlandini, K. A. & Penrose, W. R. (1989) Oxidation states of plutonium in carbonate rich natural waters. *Journal of Environmental Radioactivity* **9**, 189-198.

Nittrouer, C. A., Sternberg, R. W., Carpenter, R. & Bennett, J. T. (1979) The use of Pb-210 geochronology as a sedimentological tool : Application to the Washington continental shelf. *Marine Geology* **31**, 297-316.

Paatero, J. & Jaakkola, T. (1994) Determination of the ^{241}Pu deposition in Finland after the Chernobyl accident. *Radiochimica Acta* **64**, 139-144.

Parsa, B. (1992) A sequential radiochemical procedure for isotopic analysis of uranium and thorium in soil. *Journal of Radioanalytical Nuclear Chemistry* **157**, 65-73.

Pattenden, N. J., McKay, W. A. & Branson, J. R. (1989) Environmental radioactivity in Caithness and Sutherland, Part 5 : Radionuclide soil deposits associated with coastal inlets. *Nuclear Energy* **28**, 235-248.

Pattenden, N. J. & McKay, W. A. (1994) Studies of artificial radioactivity in the coastal environment of northern Scotland : A review. *Journal of Environmental Radioactivity* **24**, 1-51.

Peirson, D. H., Cambray, R. S., Cawse, P. A., Eakins, J. D. & Pattenden, N. J. (1982) Environmental radioactivity in Cumbria. *Nature* **300**, 27-31.

Pentreath, R. J. (1987) The interaction with suspended and settled sedimentary materials of long-lived radionuclides discharged into United Kingdom coastal waters. *Continental Shelf Research* 7, 1457-1469.

Pimpl, M. (1992) Increasing the sensitivity of ^{241}Pu determination for emission and immission control of nuclear installations by aid of liquid scintillation counting. *Journal of Radioanalytical and Nuclear Chemistry, Articles* **161**, 429-436.

Pimpl, M., Yoo, B. & Yordanova, I. (1992) Optimisation of a radioanalytical procedure for the determination of uranium isotopes in environmental samples. *Journal of Radioanalytical and Nuclear Chemistry, Articles* **161**, 437-441.

Pritchard, D. W. (1967) Observations of circulation in coastal plain estuaries. In *Estuaries* (ed. Lauff, G. H.) American Association for the Advancement of Science, Washington, D.C., 37-44.

Pulford, I. D., Allan, R. L., Cook, G. T. & MacKenzie, A. B. (1998) Geochemical association of Sellafield-derived radionuclides in saltmarsh deposits of the Solway Firth. *Environmental Geochemistry and Health* **20**, 95-101.

Radakovitch, O., Charmasson, S., Arnaud, M. & Bouisset, P. (1999) ^{210}Pb and caesium accumulation in the Rhone delta sediments. *Estuarine, Coastal and Shelf Science* **48**, 77-92.

Ritchie, J. C. & McHenry, J. R. (1990) Application of radioactive fallout cesium-137 for measuring soil erosion and sediment accumulation rates and patterns : a review. *Journal of Environmental Quality* **19**, 215-233.

Rosental, R., Eagle, G. A. & Orren, M. J. (1986) Trace metal distributions in different chemical fractions of nearshore marine sediments. *Estuarine, Coastal and Shelf Science* **22**, 303-324.

Ryan, T. P., Mitchell, P. I., Jordi Vives i Battle, Sanchez-Cabeza, J. A., McGarry, A. T. & Schell, W. R. (1993) Low-level ^{241}Pu analysis by supproted-disk liquid scintillation counting. In *Liquid Scintillation Spectrometry 1992* (Noakes, Schonhofer & Polach ed.), RADIOCARBON, Arizona, pp483 (pp. 75-82).

Saito, A. & Choppin, G. R. (1983) Separation of actinides in different oxidation states from neutral solutions by solvent extraction. *Analytical Chemistry* **55**, 2454-2457.

Sanchez, A. L., Murray, J. W., Schell, W. R. & Miller, L. G. (1986) Fallout plutonium in two oxic-anoxic environments. *Limnology and Oceanography* **31**, 1110-1121.

Sanchez, A. L., Gastaud, J., Noshkin, V. & Buesseler, K. O. (1991) Plutonium oxidation states in the southwestern Black Sea : evidence regarding the origin of the cold intermediate layer. *Deep-Sea Research* **38**, S845-S853.

Sanchez, A. L., Gastaud, J., Holm, E. & Roos, P. (1994) Distribution of plutonium and its oxidation states in Framvaren and Hellvik fjords, Norway. *Journal of Environmental Radioactivity* **22**, 205-217.

Sanchez, A. L., Horrill, A. D., Howard, B. J., Singleton, D. L. & Mondon, K. (1998) Anthropogenic radionuclides in tide-washed pastures bordering the Irish Sea coast of England and Wales. *Water, Air and Soil Pollution* **106**, 403-424.

Santschi, P. H. & Honeyman, B. D. (1989) Radionuclides in aquatic environments. *Radiation Physics and Chemistry* **34**, 213-240.

Seaborg, G. T., James, R. A., Ghiorso, A. & Morgan, L. O. (1949) *The Transuranium Elements* (eds. Seaborg, G. T., Katz, J. J. & Manning, W. M.) McGraw-Hill, New York, 1525-1553.

Sholkovitz, E. R. (1983) The geochemistry of plutonium in fresh and marine water environments. *Earth Science Reviews* **19**, 95-161.

Sholkovitz, E. R. & Mann, D. R. (1984) The pore water chemistry of $^{239,240}Pu$ and ^{137}Cs in sediments of Buzzard Bay, Massachusetts. *Geochimica et Cosmochimica Acta.* **48**, 1107-1114.

Shukla, J. P., Kumar, A. & Singh, R. K. (1993) Liquid-liquid extraction of plutonium (IV) by dicyclohexano-18-crown-6 from aqueous-organic solutions. *Radiochimica Acta* **60**, 103-107.

Sill, C. W. & Sill, D. W. (1995). Sample dissolution. *Radioactivity & Radiochemistry* **6**, 8-14.

Silverberg, N., Nguyen, H. V., Delibrias, G., Koide, M., Sundby, B. Yokohama, Y. & Chesselet, R. (1986) Radionuclide profiles, sedimentation rates, and bioturbation in modern sediments of the Laurential Trough, Gulf of St. Lawrence. *Oceanologica Acta* **9**, 285-290.

Smith, L. L., Crain, J. S., Yaeger, J. S., Horwitz, E. P., Diamond, H. & Chiarizia, R. (1995). Improved separation method for determining actinides in soil samples. *Journal of Radioanalytical and Nuclear Chemistry* **194**, 151-156.

Stanners, D. A. & Aston, S. R. (1981a) An improved method of determining sedimentation rates by the use of artificial radionuclides. *Estuarine, Coastal and Shelf Science* **13**, 101-106.

Stanners, D. A. & Aston, S. R. (1981b) ^{134}Cs : ^{137}Cs and ^{106}Ru : ^{137}Cs ratios in intertidal sediments from the Cumbria and Lancashire coasts, England. *Estuarine, Coastal and Shelf Science* **13**, 409-417.

Stanners, D. A. & Aston, S. R. (1984) The use of reprocessing effluent radionuclides in the geochronology of recent sediments. *Chemical Geology* **44**, 19-32.

Stather J. W., Dionian, J., Brown, J., Fell, T. P. & Muirhead, C. (1986) The risks of Leukaemia and other cancers in Seascale from radiation exposure. NRPB-R171, London, HMSO.

Thomson, J. (1982) A total dissolution method for determination of the alpha-emitting isotopes of uranium and thorium in deep-sea sediments. *Analytica Chimica Acta* **142**, 259-268.

Woodhead, D. S. (1988) Mixing processes in near-shore marine sediments as inferred from the distributions of radionuclides discharged into the northeast Irish Sea from BNFL, Sellafield. In *Radionuclides - A Tool for Oceanography* (ed. Guary, J.C., Guegueniat, P. & Pentreath, R.J.), Elsevier Applied Science, London, 331-340.

Yang, D., Zhu, Y. & Mobius, S. (1991) Rapid method for alpha counting with extractive scintillator and pulse shape analysis. *Journal of Radioanalytical and Nuclear Chemistry* **147**, 177-189.

Appendices

A.1. Details of cores analysed

	Date	Location	Length	XRF	^{241}Am & ^{137}Cs	Pu-alpha	^{241}Pu
I-96-002 Core	Dec-95	Irish Sea	28 cm	Done	Done	Done	Done
R-96-000 Core	Apr-96	Between B7 and W7	36 cm	Done	Done	Done	Done
R-96-007 Core	Jul-96	5 m south of X6	55 cm	Done	Done	Done	Done
R-96-008 Core	Jul-96	40 cm east of E7	61 cm	Done	Done	Done	Done
R-97-003 Core	June-97	A3	30 cm	Done	Done	-	-

A.2. Analytical methods

A.2.1. Sampling and storage

1) I-96-002 core was collected by MAFF in the Irish Sea adjacent to the effluent discharge pipe in 1995. It was 2.5 km to the west of Sellafield and was subsampled from the box core at centimetre intervals.
2) R-96-000 core was taken in April 1996 using a one metre long plastic drainage pipe.
3) R-96-007 & R-96-008 cores were collected in July 1996 using the same kind of plastic pipes.
4) R-97-003 core was collected in June 1997
5) The surface scrape (1 cm) samples were collected in March 1997.

Samples collected were transferred to the Southampton Oceanography Centre on the following day, and stored in a refrigerator at ~ 4°C to limit biological and chemical activity (Loring & Rantala, 1992).

A.2.2. Sample preparation

Core samples were split and X-radiographed in order to investigate any internal structures. Both surface scrape and sectioned core samples were freeze-dried until a constant mass was obtained. Dried samples were then ground to a fine powder and transferred into

scintillation vials for gamma-spectrometry. The remaining ground samples were stored until required.

A.2.3. ^{210}Pb determination

Apparatus

Glass beakers (250ml) & watch glass to fit
Plating cells
Silver plating discs and disc holders
Crystallising dishes
Centrifuge

Reagents

6M hydrochloric acid
8M nitric acid
Aqua Regia (3 parts c.HCl + 1 part c.HNO_3)
^{209}Po internal standard (approx. 4.86 dpm/ml or 4.02 dpm/g)
Ascorbic acid

Procedure

1. Weigh 5g of ignited sediment sample into a 250ml beaker and moisten with distilled water.
2. Add 10ml of Aqua Regia slowly with caution and check if there is vigorous reaction. If not, add another 20ml of Aqua Regia and add 1ml of ^{209}Po tracer. Then reflux the sample on a hotplate for 4 hours.
3. Evaporate the sample to dryness and add another 30ml of Aqua Regia. Then reflux the sample again for 3-4 hours.
4. Allow to cool and then centrifuge for 20 minutes at 3500 rpm.
5. Collecting the supernatant, retrieve the sediment and reflux on a hotplate with a fresh charge of Aqua Regia for a further 3 hours.
6. Allow to cool, centrifuge, and mix supernatants.
7. Evaporate the sample to dryness and redissolve the sample in 5.5ml of 6M hydrochloric acid. Transfer the solution to a Polonium plating cell. Wash the beaker several times

with distilled water and add the washings to the cell. Make the volume of liquid in the cell up to 40ml at which point the molarity of the acid will be approximately 0.8M.

8. Add approximately 1.5g of ascorbic acid (reducing agent) to the cell and stir until the solution changes to a pale yellow colour.
9. Add the disc holder with a freshly burnished silver disc inserted.
10. Leave to plate for 36 hours or more, on a warm (<40°C) hotplate.
11. Inspect the disc regularly in the early stages to ensure that the disc is not discolouring (i.e. turning black). If it does, replace the disc with a fresh one.
12. At the end of the plating, remove the disc, wash with distilled water followed by acetone, mark the sample number on the back and leave covered by crystallising dish for a minimum of 24 hours before counting.

A.2.4. Electrodeposition of Pu & U

The EDP (electrodeposition) cell was prepared by placing a new stainless steel disc into the base of the EDP cell, a new insert into the top of the EDP cell and screwing on the top. The cells were checked for any leaks by doing an initial test using distilled water. 1ml of 10% hydrochloric acid was added to the beaker followed by 5ml of 4% ammonium oxalate solution and the solution was transferred to the electrodeposition cell. A further 5ml of water was then added to the electrodeposition cell and the cathode connection was attached. The platinum anode was lowered into the solution, the current was adjusted to 400 mA and electrodeposition was carried out for 100 minutes. The current and sample level in the cell were checked at regular intervals. The current was adjusted accordingly and the cell was topped up with water if the level dropped significantly. After 100 minutes of electrodeposition, a few drops of ammonia solution were added. Deposition was continued for another 30 seconds and then the power supply was disconnected. The cell was rinsed several times with water and the stainless steel disc was removed. The disc was washed with water again and dried on a hot plate. The disc was then counted by alpha spectrometry.

A.2.5. Detection limits in routine XRF analysis using a Rh anode X-ray tube

Element	X-Ray	Possible interferences*	L.L.D. (ppm)**
As	As K	Pb	2 (200 s)
Ba	Ba L	Ce, high As	10
Bi	Bi L	W	5
Br	Br K		30
Ce	Ce L		10
Cl	Cl K		50
Cr	Cr K	V	4
Cu	Cu K	Cu from the tube	3
Ga	Ga K		1.5
I	I K		3 (200 s)
La	La K		5
Mo	Mo K		5
Ni	Ni K		1.5
Nb	Nb K	Y	1.5
P	P K		30
Pb	Pb L	Bi	1.5
Rb	Rb K	high U	1.5
S	S K		50
Sb	Sb K		5
Sn	Sn K		4
Sr	Sr K		1.5
Th	Th L	High Pb	2
U	U L	High Rb	1.4 (400 s)
V	V K		4
W	W L	High Zn, Ga	8
Y	Y K	Rb	1.5
Zn	Zn K		1.5
Zr	Zr K	Sr	1.5

The detection limits are calculated assuming a count-time of 100 seconds on the background unless otherwise stated.

* Note that most of these interferences are already dealt with automatically.

** Better DLs may be obtained by using longer count times.

A.3. Geochemical data, I-96-002 (subtidal) core

Depth	1	2	3	4	5	6	7	8	9	10	11	12	13	14	15	16	17	18	19	20	21	22	23	24	25	26	27	28
Major elements (wt. %)																												
SiO_2	74.01	71.98	72.65	73.10	73.09	74.12	74.96	75.23	75.04	73.68	72.50	72.57	71.77	71.60	72.18	72.04	71.91	71.79	71.93	71.63	72.47	73.64	73.03	73.28	73.61	73.57	73.80	73.32
TiO_2	0.44	0.50	0.51	0.48	0.48	0.45	0.43	0.43	0.44	0.45	0.49	0.48	0.49	0.47	0.47	0.49	0.48	0.48	0.47	0.49	0.46	0.44	0.45	0.46	0.45	0.43	0.44	0.45
Al_2O_3	7.38	7.89	7.67	7.47	7.58	7.31	7.38	7.12	7.09	7.71	8.20	8.22	8.48	8.62	7.94	8.26	8.26	8.32	8.37	8.41	8.02	7.78	8.15	7.91	7.75	7.77	7.58	7.87
Fe_2O_3	2.83	3.17	3.08	2.96	3.00	2.84	2.72	2.70	2.74	2.96	3.14	3.07	3.15	3.10	3.13	3.17	3.09	3.22	3.20	3.15	3.04	2.92	3.01	3.12	2.96	3.00	2.89	2.95
MnO	0.08	0.07	0.06	0.06	0.06	0.05	0.05	0.05	0.05	0.05	0.06	0.06	0.06	0.06	0.06	0.06	0.06	0.06	0.06	0.06	0.06	0.05	0.05	0.05	0.05	0.06	0.05	0.05
MgO	1.36	1.51	1.42	1.42	1.36	1.33	1.29	1.26	1.28	1.40	1.45	1.41	1.53	1.50	1.59	1.48	1.53	1.51	1.48	1.50	1.44	1.41	1.40	1.42	1.30	1.37	1.35	1.40
CaO	3.43	3.48	3.53	3.59	3.68	3.53	3.44	3.38	3.48	3.48	3.64	3.52	3.62	3.63	3.80	3.56	3.60	3.53	3.48	3.43	3.44	3.38	3.39	3.19	3.38	3.34	3.28	3.45
Na_2O	1.38	1.45	1.37	1.33	1.30	1.37	1.31	1.20	1.19	1.23	1.33	1.32	1.37	1.43	1.24	1.30	1.42	1.43	1.36	1.41	1.33	1.26	1.35	1.29	1.24	1.42	1.32	1.39
K_2O	1.44	1.60	1.53	1.50	1.52	1.55	1.45	1.37	1.58	1.54	1.69	1.66	1.72	1.71	1.66	1.65	1.67	1.61	1.63	1.62	1.59	1.55	1.59	1.58	1.59	1.54	1.58	1.60
P_2O_5	0.12	0.13	0.13	0.12	0.12	0.10	0.09	0.10	0.10	0.11	0.11	0.12	0.11	0.11	0.11	0.11	0.11	0.12	0.11	0.12	0.12	0.11	0.11	0.11	0.11	0.13	0.11	0.10
LOI	7.5	8.2	8.1	8.0	7.8	7.3	6.9	7.2	7.0	7.4	7.4	7.6	7.7	7.8	7.8	7.9	7.9	7.9	7.9	8.2	8.0	7.5	7.5	7.6	7.6	7.4	7.6	7.4
S	0.26	0.24	0.24	0.25	0.25	0.25	0.24	0.26	0.25	0.25	0.26	0.25	0.26	0.26	0.26	0.29	0.28	0.30	0.29	0.29	0.26	0.25	0.27	0.28	0.27	0.27	0.28	0.29
Cl	3.00	2.32	1.99	2.33	2.33	2.34	2.01	2.01	2.01	1.67	1.66	1.66	1.66	1.66	1.66	1.66	1.66	1.66	1.66	1.66	1.66	1.67	1.67	1.67	1.67	1.67	1.67	1.67
Trace elements (ppm)																												
Br	106	103	93	101	93	88	81	82	80	77	79	77	79	79	77	83	82	82	77	81	69	68	78	73	75	73	75	82
I	67	65	56	54	60	72	55	73	51	45	58	68	58	56	60	48	44	48	44	65	52	57	51	48	52	51	48	54
Rb	67	67	67	67	66	63	64	64	64	67	69	70	70	70	71	70	71	71	72	72	68	66	67	67	68	67	67	71
Sr	131	129	137	131	129	126	125	129	126	128	131	128	133	132	132	132	130	129	129	132	125	125	127	125	130	127	124	127
Y	17	20	21	20	21	19	18	19	20	21	22	22	22	22	23	23	22	25	24	26	22	22	23	23	22	22	23	24
Zr	321	363	443	406	361	335	335	306	278	309	329	332	321	281	275	289	290	277	256	261	300	279	313	290	280	276	277	271
Nb	10	11	12	12	11	11	11	10	10	10	11	12	11	11	11	11	12	11	11	11	11	11	11	11	11	11	10	11
Pb	35	38	38	36	36	35	35	35	35	36	41	38	36	40	39	40	39	39	38	42	37	36	39	37	38	37	39	43
Zn	84	90	91	90	88	86	80	86	86	93	99	99	97	97	98	96	100	104	101	107	91	89	90	92	94	91	94	103
Ni	23	24	23	23	23	23	21	23	22	26	26	26	27	29	25	24	25	27	26	27	24	23	23	23	24	22	24	26
Cr	89	105	115	96	92	105	93	106	94	125	111	110	114	116	103	98	104	100	110	112	94	98	100	101	103	93	102	100
Ba	280	274	288	294	273	273	275	266	261	273	279	291	279	265	289	279	279	257	250	294	292	281	255	268	293	273	277	289
La	24	27	28	24	29	25	27	25	31	25	28	29	24	29	27	34	32	34	35	32	26	29	29	26	27	27	23	29
Ce	29	25	32	41	33	33	43	36	44	34	37	30	57	39	43	40	41	52	51	42	28	26	59	37	38	44	45	41
MnO	1271	1126	941	923	854	828	771	865	833	849	868	857	876	868	862	856	840	895	860	889	831	811	850	855	828	811	835	851
TiO_2	5227	5301	5557	5535	5327	5246	5167	4970	5062	5356	5507	5743	5611	5647	5597	5446	5596	5696	5436	5744	5553	5317	5419	5223	5264	5222	5061	5357
Radionuclides (Bq/kg)																												
^{241}Am	1459	2078	1910	1785	1742	1677	1512	1702	2120	2110	2953	3097	3715	4446	5229	6605	7344	8531	10372	8712	6820	6631	7319	10741	10105	9623	13846	13966
^{137}Cs	905	919	904	888	905	813	820	973	1070	1154	1705	2143	2573	3475	4476	5527	5671	6314	7159	6496	5580	4909	5046	6436	6386	5176	6706	6634
^{238}Pu	231	398	412	326	344	313	371	411	383	457		722		940		1361		1819		1921		1458		1825		1396		2500
$^{239,240}Pu$	1093	1952	3801	1559	1583	1431	1637	1844	1683	2006		2941		4105		6133		8877		8610		6316		8225		6882		15780
^{241}Pu	14305	27565	26117	21532	22615	21283	24319	28954	26510	30488		45753		59852		89287		120364		122969		87259		110582		84610		152389

* All the data are based on the dry weight

A.4. Geochemical data, R-96-000 (saltmarsh) core

Depth	1	2	3	4	5	6	7	8	9	10	11	12	13	14	15	16	17	18
Major elements (wt. %)																		
SiO_2	60.73	67.97	69.07	69.76	69.70	69.38	70.41	70.22	70.06	69.55	70.01	70.21	70.11	69.72	69.61	69.67	69.82	70.73
TiO_2	0.68	0.65	0.64	0.65	0.66	0.65	0.65	0.65	0.64	0.66	0.65	0.66	0.66	0.64	0.65	0.65	0.64	0.63
Al_2O_3	11.24	9.33	9.06	9.00	9.04	9.18	9.02	9.16	9.20	9.40	9.50	9.22	9.22	9.31	9.45	9.34	9.32	9.02
Fe_2O_3	4.88	3.90	3.62	3.62	3.73	3.58	3.51	3.54	3.63	3.72	3.56	3.58	3.68	3.66	3.74	3.79	3.71	3.60
MnO	0.19	0.10	0.08	0.07	0.07	0.06	0.06	0.06	0.06	0.06	0.06	0.06	0.06	0.06	0.06	0.06	0.06	0.06
MgO	2.45	1.94	1.89	1.86	1.89	1.86	1.82	1.86	1.86	1.90	1.86	1.83	1.85	1.87	1.87	1.90	1.84	1.79
CaO	4.01	3.67	3.62	3.48	3.43	3.22	3.16	3.17	3.16	3.24	3.39	3.26	3.42	3.48	3.33	3.37	3.38	3.27
Na_2O	2.11	1.85	1.85	1.83	1.83	1.84	1.79	1.87	1.81	1.83	1.77	1.75	1.81	1.84	1.75	1.81	1.80	1.81
K_2O	2.45	2.13	2.11	2.11	2.06	2.14	2.09	2.06	2.02	2.11	2.06	2.14	2.11	2.04	2.19	2.12	2.10	2.12
P_2O_5	0.21	0.17	0.18	0.18	0.19	0.17	0.15	0.16	0.17	0.16	0.15	0.15	0.15	0.14	0.14	0.15	0.16	0.15
LOI	11.0	8.3	7.9	7.4	7.4	7.9	7.3	7.2	7.4	7.4	7.0	7.1	6.9	7.2	7.2	7.1	7.2	6.8
S	0.22	0.17	0.17	0.17	0.16	0.19	0.19	0.21	0.24	0.24	0.19	0.23	0.27	0.32	0.32	0.32	0.31	0.27
Cl	1.69	1.27	1.20	1.15	1.03	1.07	1.04	1.01	0.97	0.98	0.92	0.98	0.96	0.95	0.91	0.94	0.91	0.92
Trace elements (ppm)																		
Br	147	97	89	87	82	90	89	82	82	80	74	76	66	63	66	64	64	63
I	118	67	60	54	58	51	49	45	34	54	45	42	49	51	63	58	49	51
Rb	69	75	71	72	73	71	71	71	72	74	72	73	72	70	71	73	74	71
Sr	148	131	127	124	124	118	116	115	119	117	120	121	122	122	116	120	122	121
Y	26	24	26	26	28	29	28	28	30	29	29	30	29	29	30	32	33	32
Zr	227	298	330	322	321	325	318	314	306	298	305	299	297	294	286	297	304	304
Nb	15	14	13	14	14	14	14	14	15	14	14	15	14	14	13	13	13	13
Pb	84	50	49	49	48	49	45	44	45	48	45	46	44	42	44	47	49	47
Zn	141	109	104	108	106	112	108	107	113	107	102	112	107	104	103	113	112	110
Ni	34	27	28	26	26	25	27	27	27	26	27	27	29	27	26	29	27	26
Cr	109	102	102	105	98	101	96	95	107	96	96	104	102	100	112	113	110	109
Ba	309	299	302	297	292	296	303	302	302	314	307	300	314	299	300	294	304	296
La	26	23	25	25	26	26	25	26	27	25	19	27	26	26	26	26	29	30
Ce	46	39	35	43	38	37	40	49	38	43	42	45	39	36	41	41	50	36
MnO	2149	1304	1090	1010	955	880	826	831	817	826	820	844	868	866	823	830	845	850
TiO_2	6564	6081	6222	6304	5986	6271	5987	6082	6067	6102	5965	6161	6363	5972	6178	6170	6031	5992
Radionuclides (Bq/kg)																		
^{241}Am	1619	1125	1098	1135	1238	1472	1752	1791	2210	2567	3013	3226	3322	3205	4833	5934	6854	8566
^{137}Cs	1121	779	725	873	950	1219	1655	2025	2721	3848	4333	4921	5820	5830	7599	8712	9064	10011
^{238}Pu	230	170	179	191	210	269	343	340	472	552	641	694	693	727	1058	1183	1315	1154
$^{239,240}Pu$	1121	821	878	934	998	1320	1545	1595	2154	2557	2876	3292	3239	3377	4909	5526	6074	5800
^{241}Pu	14765	10928	11628	12458	13630	17595	23047	23576	31486	38032	42686	48898	47051	48992	70941	73867	78548	65819

* All the data are based on the dry weight

Depth	19	20	21	22	23	24	25	26	27	28	29	30	31	32	33	34	35	36
Major elements (wt. %)																		
SiO_2	70.69	71.06	70.74	70.69	70.65	70.92	70.36	70.43	70.06	71.24	71.12	69.21	70.59	71.78	71.67	69.89	67.92	71.79
TiO_2	0.63	0.62	0.63	0.64	0.64	0.65	0.67	0.65	0.63	0.63	0.62	0.63	0.62	0.59	0.59	0.59	0.63	0.57
Al_2O_3	8.97	8.83	9.07	8.97	9.03	8.83	9.01	9.15	9.15	8.80	8.84	9.43	8.96	8.78	8.83	9.22	9.83	8.73
Fe_2O_3	3.51	3.47	3.55	3.56	3.52	3.51	3.60	3.56	3.62	3.45	3.46	3.76	3.58	3.38	3.50	3.69	3.94	3.43
MnO	0.06	0.06	0.06	0.06	0.06	0.06	0.06	0.06	0.06	0.06	0.06	0.06	0.06	0.06	0.06	0.06	0.06	0.06
MgO	1.72	1.74	1.76	1.76	1.76	1.73	1.79	1.82	1.82	1.75	1.75	1.90	1.78	1.72	1.72	1.79	1.91	1.65
CaO	3.17	3.04	3.05	3.01	3.17	3.15	3.26	3.21	3.17	3.23	3.25	3.34	3.27	3.06	3.05	3.30	3.55	3.09
Na_2O	1.71	1.74	1.71	1.74	1.70	1.73	1.82	1.72	1.74	1.78	1.82	1.82	1.78	1.71	1.73	1.75	1.81	1.67
K_2O	2.13	2.08	1.94	2.15	2.09	2.03	2.04	2.03	2.12	2.09	2.07	2.15	2.10	1.99	1.97	2.10	2.22	2.02
P_2O_5	0.15	0.14	0.14	0.14	0.14	0.14	0.13	0.13	0.12	0.12	0.12	0.12	0.12	0.11	0.10	0.11	0.11	0.10
LOI	7.3	7.2	7.3	7.3	7.2	7.3	7.3	7.3	7.5	6.8	6.9	7.6	7.1	6.8	6.8	7.5	8.0	6.9
S	0.25	0.27	0.28	0.31	0.29	0.29	0.36	0.32	0.35	0.34	0.37	0.45	0.43	0.43	0.38	0.34	0.31	0.35
Cl	0.88	0.96	0.90	0.96	0.90	0.86	1.01	0.94	0.97	0.90	0.95	1.06	0.90	0.91	0.95	0.95	0.89	0.93
Trace elements (ppm)																		
Br	60	57	64	60	60	59	59	62	64	56	59	66	60	53	52	59	59	52
I	60	78	58	63	60	72	78	76	85	58	80	74	60	60	65	80	67	58
Rb	70	70	71	71	71	69	69	70	73	70	70	75	72	69	71	75	79	71
Sr	118	114	115	114	118	118	117	117	122	119	119	121	120	115	115	125	130	121
Y	31	31	31	30	29	29	27	26	24	23	22	23	21	22	16	20	20	19
Zr	299	307	325	319	323	329	349	321	280	294	301	282	290	290	242	232	228	249
Nb	14	14	14	13	13	15	15	13	14	13	14	14	14	13	13	13	14	13
Pb	46	48	48	49	49	48	48	49	54	49	49	55	53	49	47	46	49	43
Zn	108	112	115	117	113	108	107	110	116	103	106	121	113	102	93	94	98	88
Ni	25	27	27	28	24	26	25	26	28	26	24	28	25	27	28	26	29	26
Cr	102	105	109	100	103	98	108	93	103	90	97	104	94	97	94	93	97	88
Ba	291	305	309	302	306	307	317	303	313	322	303	310	302	288	285	285	287	284
La	25	24	27	23	29	27	22	25	24	26	22	26	23	21	20	22	22	18
Ce	38	36	31	33	27	36	27	25	35	39	49	48	39	37	36	32	36	37
MnO	810	835	833	823	840	866	845	848	853	844	799	885	827	807	847	862	857	832
TiO_2	5654	5991	6063	6045	6153	6214	6302	6060	6168	6116	6094	6248	5924	5850	5807	5905	6196	5752
Radionuclides (Bq/kg)																		
^{241}Am	8583	8101	6149	4231	2736	1815	1040	595	544	207	194	267	83	34	15	186	2	297
^{137}Cs	8699	7908	6440	4828	3561	2533	1939	1504	1214	808	545	440	244	118	43	258	4	352
^{238}Pu	1098	1103		568		202		84		31		29		6		34		23
$^{239,240}Pu$	5486	5779		4470		2225		1018		731		920		205		261		147
^{241}Pu	60016	56424		33266		12539		5087		1952		1846		244		1912		1446

* All the data are based on the dry weight

A.5. Geochemical data, R-96-007 (saltmarsh) core

Depth	1	2	3	4	5	6	7	8	9	10	11	12	13	14	15	16	17	18	19	20	21	22	23	24	25	26	27
Major elements (wt. %)																											
SiO_2	62.75	64.83	67.65	64.25	67.08	67.23	66.32	67.89	67.14	68.99		65.68		67.26		67.03		65.76		65.64		68.15		68.83		67.22	
TiO_2	0.64	0.67	0.63	0.70	0.68	0.67	0.68	0.67	0.69	0.69		0.73		0.70		0.71		0.70		0.71		0.70		0.69		0.73	
Al_2O_3	10.14	10.46	9.69	11.31	10.76	10.77	10.66	10.32	10.71	10.29		11.24		11.02		10.81		11.09		11.01		10.76		10.59		11.06	
Fe_2O_3	4.19	4.22	3.84	4.47	4.16	4.40	4.32	4.25	4.30	4.17		4.62		4.51		4.54		4.63		4.64		4.23		4.57		4.88	
MnO	0.16	0.13	0.11	0.10	0.09	0.15	0.12	0.15	0.12	0.12		0.14		0.13		0.11		0.07		0.06		0.05		0.06		0.09	
MgO	2.16	2.11	1.95	2.20	2.04	2.05	2.07	1.93	2.02	1.93		2.08		2.08		2.05		2.12		2.02		1.99		1.95		2.10	
CaO	3.82	3.03	1.89	1.59	1.38	1.26	1.28	1.22	1.24	1.26		1.24		1.29		1.26		1.24		1.23		1.26		1.23		1.24	
Na_2O	2.02	1.92	1.93	2.03	2.05	2.04	2.03	1.95	1.89	1.86		1.97		1.94		1.94		2.01		1.92		1.82		1.76		1.81	
K_2O	2.22	2.36	2.23	2.48	2.47	2.44	2.45	2.35	2.42	2.23		2.44		2.38		2.36		2.37		2.44		2.37		2.33		2.44	
P_2O_5	0.20	0.19	0.18	0.18	0.18	0.18	0.18	0.17	0.17	0.17		0.18		0.18		0.20		0.20		0.21		0.17		0.18		0.16	
LOI	11.7	10.1	9.9	10.7	9.1	8.8	9.9	9.1	9.3	8.3		9.7		8.5		9		9.8		10.1		8.5		7.8		8.3	
S	0.23	0.17	0.19	0.19	0.19	0.18	0.20	0.19	0.18	0.16		0.18		0.16		0.16		0.17		0.18		0.14		0.16		0.13	
Cl	1.70	1.40	1.49	1.56	1.37	1.54	1.63	1.56	1.47	1.35		1.44		1.30		1.33		1.36		1.34		1.18		1.20		1.04	
Trace elements (ppm)																											
Br	157	154	200	226	179	220	204	196	170	156	159	172	159	152	168	167	182	195	201	195	190	158	166	148	142	136	140
I	93	89	109	114	91	105	95	93	81	70	70	62	66	68	85	70	74	62	72	70	62	60	68	58	66	64	69
Rb	85	85	83	92	90	91	90	88	90	88	88	92	89	91	91	92	93	91	92	94	94	89	87	89	95	94	97
Sr	151	124	105	103	100	101	100	98	100	101	97	102	100	100	102	100	102	100	101	103	101	99	98	97	98	101	103
Y	25	26	26	33	32	32	31	30	36	35	35	37	37	38	40	42	41	40	44	53	36	31	33	30	27	29	29
Zr	253	291	293	266	293	268	259	262	280	301	285	294	297	279	270	286	284	299	293	287	284	306	312	301	298	296	291
Nb	15	15	14	14	16	15	15	15	15	15	16	16	16	16	16	15	15	15	16	15	16	16	16	16	16	16	17
Pb	64	55	55	67	58	59	59	55	57	57	54	59	57	58	62	63	68	67	69	78	72	62	63	67	78	80	78
Zn	129	123	117	142	125	134	133	125	129	121	119	134	123	128	136	139	152	144	150	164	156	136	138	138	149	152	165
Ni	30	29	29	32	31	32	32	30	33	32	31	34	32	33	33	34	34	32	33	35	34	32	31	32	34	34	37
Cr	106	110	112	119	123	122	115	112	115	115	112	124	119	123	121	133	140	129	138	156	136	121	119	117	123	122	122
Ba	335	337	357	340	349	347	330	336	338	340	329	351	330	352	344	362	352	349	355	356	348	347	353	352	367	371	385
La	26	29	28	34	34	32	33	30	33	31	32	36	35	36	38	36	37	37	38	41	33	32	31	32	33	34	34
Ce	49	48	41	52	52	53	53	52	53	51	59	46	53	50	53	52	53	52	55	55	57	51	53	51	57	55	52
MnO	1855	1543	1226	1115	983	1335	1685	1679	1477	1389	1279	1501	1136	1304	1331	1142	1348	765	629	679	641	600	651	680	762	938	1324
TiO_2	6579	6519	6600	6986	7057	7093	6794	6874	7168	7053	6905	7323	7045	7107	7187	7359	7206	7373	7143	7232	7288	7084	7342	7251	7479	7375	7695
Radionuclides (Bq/kg)																											
^{241}Am	1367	1004	1110	1458	1430	1438	2197	2394	2836	3040	4285	7762	10956	7785	9374	13511	19419	24673	12100	10492		2538		516		58	
^{137}Cs	803	647	762	1016	1013	1109	1810	2537	3009	4309	5642	8107	10463	9983	11596	13969	15224	12540	8884	8085		4292		2122		915	
^{238}Pu	167	157	193	217	262	287	364	407	564	615		1410		1464		1679		2294		938		172		28		7	
$^{239,240}Pu$	790	753	882	1044	1171	1336	1665	1867	2464	2883		6827		6886		8045		10824		9749		2626		1204		536	
^{241}Pu	10145	9407	12422	14496	17328	18659	24447	26904	39386	43489		94584		92942		95922		114060		64158		12483		2156		332	

* All the data are based on the dry weight

Depth	28	29	30	31	32	33	34	35	36	37	38	39	40	41	42	43	44	45	46	47	48	49	50	51	52	53	54	55
Major elements (wt. %)																												
SiO_2	65.86		67.18			66.66			67.99			68.85			68.51			68.68			69.16			71.19			72.48	
TiO_2	0.74		0.73			0.71			0.68			0.70			0.71			0.69			0.70			0.66			0.63	
Al_2O_3	11.78		11.40			11.50			11.44			10.73			10.93			11.06			11.37			10.32			9.64	
Fe_2O_3	5.27		4.78			4.81			4.52			4.48			4.61			4.54			4.76			4.27			3.90	
MnO	0.21		0.16			0.21			0.18			0.17			0.18			0.15			0.17			0.14			0.13	
MgO	2.28		2.05			2.14			2.07			2.02			2.06			2.05			2.14			1.89			1.77	
CaO	1.32		1.22			1.27			1.28			1.27			1.24			1.28			1.30			1.22			1.16	
Na_2O	1.93		1.76			1.77			1.80			1.81			1.77			1.77			1.79			1.72			1.65	
K_2O	2.43		2.47			2.49			2.38			2.34			2.44			2.35			2.47			2.34			2.31	
P_2O_5	0.17		0.15			0.15			0.16			0.15			0.15			0.15			0.15			0.15			0.13	
LOI	8.0		8.1			8.3			7.5			7.5			7.4			7.3			6			6.1			6.2	
S	0.12		0.13			0.14			0.12			0.11			0.11			0.12			0.17			0.13			0.11	
Cl	1.00		0.93			0.96			0.97			0.90			0.90			0.86			0.91			0.95			0.91	
Trace elements (ppm)																												
Br	127	125	116	116	121	121	115	105	106	95	82	88	95	84	79	79	75	80	82	80	95	89	74	80	67	64	62	61
I	74	81	62	74	78	74	72	74	79	83	62	78	70	68	78	66	60	68	62	78	72	78	64	68	56	62	64	58
Rb	96	96	92	92	94	95	94	92	94	91	87	91	92	91	93	91	86	92	95	90	91	91	88	89	85	81	82	79
Sr	101	102	101	101	102	101	101	101	97	98	98	100	98	98	98	98	96	98	98	96	98	99	97	94	94	92	94	91
Y	28	27	27	25	26	26	26	24	25	25	24	24	24	25	25	24	24	24	25	24	24	25	24	23	23	23	23	22
Zr	284	293	293	291	284	281	274	290	270	278	313	295	283	295	296	290	294	284	281	304	289	296	309	310	316	311	297	312
Nb	17	17	16	17	16	16	16	16	15	16	16	15	16	15	16	16	15	16	16	15	17	15	15	15	14	15	14	15
Pb	82	81	75	71	73	70	73	65	66	67	68	71	74	69	68	64	60	65	69	64	69	64	57	60	57	55	54	55
Zn	164	165	146	147	153	150	148	137	135	130	122	126	129	126	126	123	112	125	131	121	128	126	114	119	107	104	102	102
Ni	36	37	34	35	36	36	34	33	32	34	32	33	33	32	34	33	30	32	33	32	34	32	30	32	28	28	28	27
Cr	125	121	119	111	114	124	113	108	107	110	111	101	107	106	108	102	103	113	113	110	106	103	105	110	107	97	101	101
Ba	386	400	390	371	376	372	386	376	370	375	383	380	386	375	375	362	358	357	367	349	361	359	349	343	356	345	350	353
La	34	29	31	31	30	31	31	29	32	30	28	31	30	26	32	31	23	24	29	28	29	28	27	29	29	25	26	25
Ce	53	52	49	50	52	57	51	56	48	52	44	52	56	44	60	54	49	52	50	54	47	46	46	54	48	44	41	41
MnO	1980	2171	1539	1971	2099	2056	1848	1790	1756	1934	1973	1916	1820	1874	1930	1814	1574	1449	1825	1665	1794	1484	1366	1632	1400	1374	1426	1431
TiO_2	7521	7704	7358	7351	7463	7500	7310	7394	7145	7300	7013	7242	7474	7147	7370	7284	6720	7241	7258	7147	7385	7329	6959	7254	6870	6639	6665	6768
Radionuclides (Bq/kg)																												
^{241}Am	24		9		4						3																	10
^{137}Cs	627		316		182		90		61		34						10				3							11
^{238}Pu	4		36		1						4		5		1		1		24				1		0		0	
$^{239,240}Pu$	408		384		99		5		8		20		30		10		13		96		1		1		0		0	
^{241}Pu	197		2057								304		368		13		46		1300								21	

* All the data are based on the dry weight

A.5.1. X – radiograph of core R-96-007

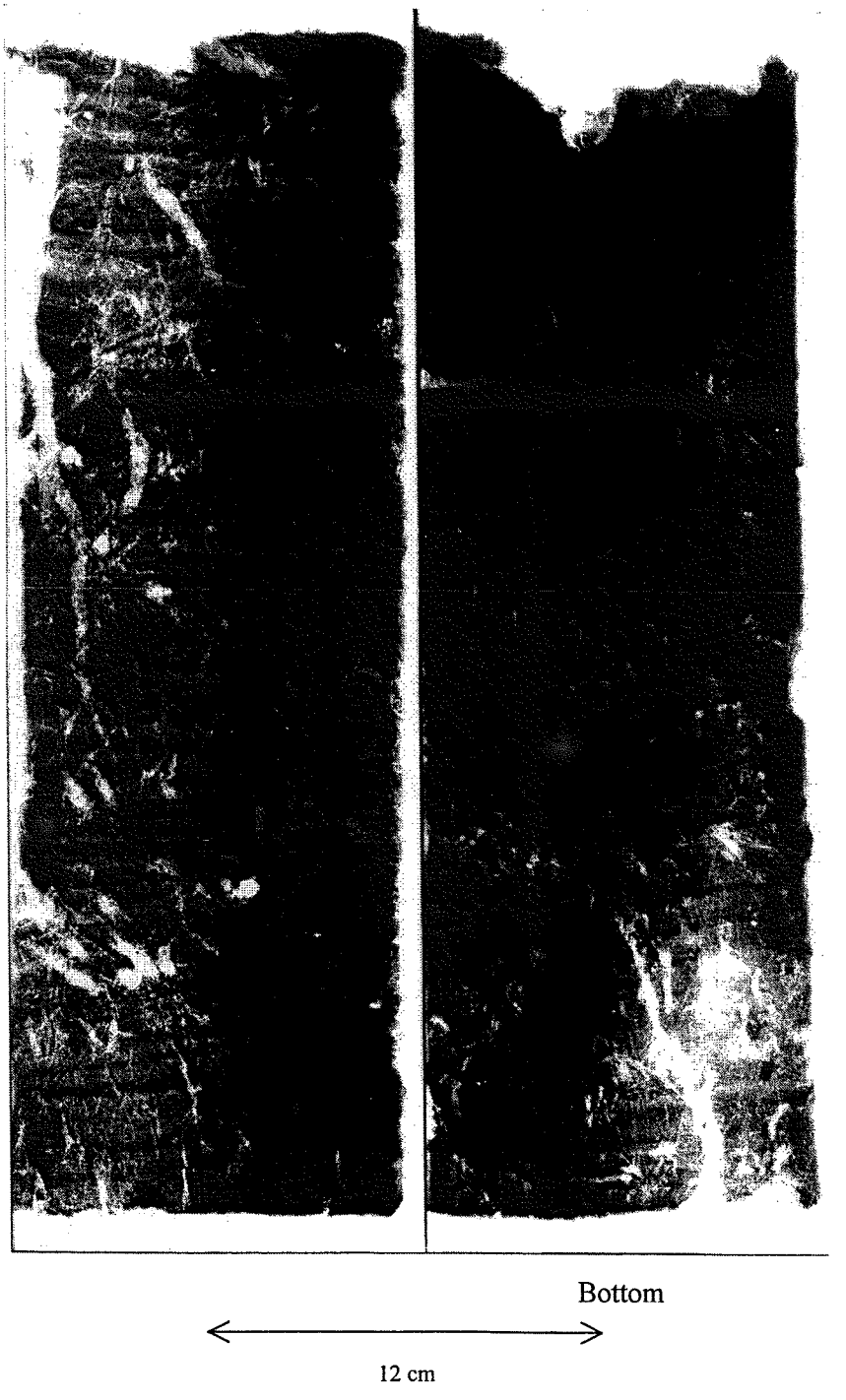

A.6. Geochemical data, R-96-008 (saltmarsh) core

Depth	1	2	3	4	5	6	7	8	9	10	11	12	13	14	15	16	17	18	19	20	21	22	23	24	25	26	27	28	29	30
Major elements (wt. %)																														
SiO_2	74.57	72.87	74.27	72.93	72.18	72.18	72.26	73.11	73.37	72.84		71.97		71.20		73.37		73.20		73.21		74.30		73.30		72.58		72.63		73.94
TiO_2	0.54	0.55	0.54	0.53	0.57	0.56	0.55	0.54	0.54	0.54		0.57		0.58		0.54		0.53		0.52		0.51		0.53		0.53		0.52		0.50
Al_2O_3	7.85	8.74	8.20	8.75	8.69	8.79	8.67	8.57	8.39	8.59		8.97		9.32		8.57		8.70		8.63		8.10		8.50		8.59		8.89		8.33
Fe_2O_3	3.12	3.32	3.25	3.35	3.47	3.41	3.40	3.24	3.19	3.33		3.42		3.58		3.30		3.27		3.18		2.95		3.17		3.15		3.38		3.10
MnO	0.07	0.07	0.08	0.09	0.10	0.11	0.09	0.08	0.07	0.07		0.06		0.08		0.11		0.09		0.10		0.08		0.11		0.07		0.11		0.07
MgO	1.43	1.58	1.47	1.60	1.58	1.58	1.56	1.50	1.48	1.51		1.58		1.66		1.45		1.47		1.46		1.39		1.44		1.51		1.51		1.43
CaO	2.77	2.88	2.63	2.82	2.84	2.95	2.91	2.93	2.92	2.96		2.83		2.69		2.59		2.67		2.77		2.73		2.70		2.72		2.53		2.73
Na_2O	1.47	1.51	1.47	1.54	1.49	1.57	1.56	1.54	1.55	1.57		1.57		1.63		1.55		1.57		1.60		1.58		1.64		1.68		1.63		1.57
K_2O	1.93	2.00	2.03	2.07	2.14	2.09	2.08	2.06	1.97	2.06		2.13		2.12		1.95		1.99		2.03		2.03		2.01		2.07		2.06		2.04
P_2O_5	0.14	0.15	0.16	0.16	0.17	0.17	0.17	0.16	0.17	0.17		0.16		0.17		0.17		0.16		0.15		0.13		0.15		0.14		0.15		0.14
LOI	6.1	6.3	5.9	6.2	6.8	6.6	6.7	6.2	6.3	6.4		6.7		7.0		6.4		6.3		6.3		6.2		6.4		7.0		6.6		6.2
S	0.14	0.15	0.12	0.12	0.12	0.13	0.19	0.41	0.13	0.14		0.14		0.21		0.15		0.13		0.13		0.13		0.13		0.14		0.46		0.12
Cl	1.54	1.23	0.78	1.17	2.11	1.23	2.27	0.94	1.35	1.87		0.92		0.97		1.50		1.12		0.62		0.62		0.72		0.70		5.85		0.62
Trace elements (ppm)																														
Br	73	86	72	75	78	75	84	75	78	81		93		109		90		91		91		83		105		120		139		101
I	44	48	44	61	61	61	70	46	55	44		48		51		67		53		53		57		59		46		61		42
Rb	71	76	74	75	75	74	75	72	71	73		76		78		72		71		72		69		69		71		74		72
Sr	116	119	115	118	120	123	124	121	119	121		119		118		118		116		119		116		115		116		112		116
Y	25	28	27	27	30	33	31	28	30	29		30		31		34		28		25		22		26		25		23		21
Zr	411	346	358	367	347	342	360	366	374	359		347		317		355		343		327		309		301		284		300		282
Nb	12	12	12	12	12	12	13	12	12	12		13		13		12		12		12		12		12		12		11		11
Pb	43	47	47	47	48	51	47	46	47	49		52		54		51		50		48		44		47		51		53		48
Zn	88	99	95	101	107	108	104	99	96	103		111		120		110		103		100		93		97		100		107		93
Ni	23	26	23	23	25	25	25	23	23	23		24		26		24		22		23		22		23		25		24		22
Cr	102	98	99	101	105	116	112	110	102	106		119		121		120		111		104		94		95		105		106		96
Ba	301	308	298	303	304	303	314	316	312	313		299		306		316		312		296		300		310		310		325		319
La	27	29	27	26	30	34	29	27	26	27		25		29		31		26		23		22		20		23		24		23
Ce	50	45	45	37	43	58	41	29	28	35		41		37		35		39		50		44		28		34		24		27
MnO	746	737	817	1035	1176	1355	1064	923	900	815		594		723		1342		973		1186		955		1198		780		1178		722
TiO_2	6135	5995	5780	5915	6110	6208	6114	5878	5594	6079		5960		6115		6016		5889		5813		5533		5611		5923		5968		5579
Radionuclides (Bq/kg)																														
^{241}Am	14250	5091	5151	6674	7327	10200	8471	9168	10105	12160	13029	13106	9924	9417	7370	5822	5504	3947	2730	2799	1858	1599	803	1027	1017	887	848	685	556	308
^{137}Cs	4745	5728	6072	7168	8356	8671	8961	8933	8418	8729	8499	8284	7694	6904	5255	4062	3540	2786	2284	1985	1556	1365	802	1026	1026	1039	943	829	736	503
^{238}Pu	1071	924	940	1079	1192	1218	1240	1068	1374	1394		1405		1183		707		406		172		111		68		42		33		17
$^{239,240}Pu$	4970	4377	4349	4851	5508	5712	5744	5048	7400	6587		7177		6897		5719		4345		2397		1825		1336		970		896		615
^{241}Pu	69884	57090	57058	62962	69692	68080	72339	58032	85579	72197		64633		57418		38869		27693		11623		8222		5091		3345		2296		1271

* All the data are based on the dry weight

Depth	31	32	33	34	35	36	37	38	39	40	41	42	43	44	45	46	47	48	49	50	51	52	53	54	55	56	57	58	59	60
Major elements (wt. %)																														
SiO_2		73.64		70.54		69.70		70.57		73.53		73.04		70.05		71.02		71.93		73.59		73.55		76.76		79.43		81.39		80.67
TiO_2		0.51		0.54		0.56		0.53		0.51		0.50		0.58		0.56		0.56		0.53		0.52		0.44		0.36		0.35		0.35
Al_2O_3		8.36		9.43		9.53		9.05		8.26		8.38		9.48		8.99		8.88		8.46		8.35		7.56		6.74		6.06		6.35
Fe_2O_3		3.11		3.42		3.53		3.40		3.03		3.05		3.59		3.40		3.39		3.12		3.15		2.68		2.29		2.06		2.12
MnO		0.05		0.05		0.06		0.06		0.06		0.07		0.07		0.07		0.07		0.07		0.06		0.05		0.04		0.04		0.05
MgO		1.42		1.63		1.69		1.62		1.43		1.45		1.69		1.61		1.56		1.44		1.45		1.21		1.04		0.93		0.96
CaO		2.73		3.27		3.52		3.50		3.14		3.22		3.49		3.43		3.16		3.02		2.93		2.62		2.31		2.24		2.38
Na_2O		1.55		1.61		1.68		1.68		1.59		1.65		1.68		1.68		1.66		1.62		1.63		1.47		1.38		1.27		1.27
K_2O		2.03		2.14		2.16		2.05		1.98		1.97		2.07		2.07		2.06		1.89		1.98		1.95		1.84		1.74		1.68
P_2O_5		0.14		0.15		0.13		0.11		0.10		0.10		0.11		0.11		0.11		0.10		0.10		0.09		0.08		0.08		0.08
LOI		6.5		7.2		7.4		7.4		6.4		6.6		7.2		7.1		6.6		6.2		6.3		5.2		4.5		3.9		4.1
S		0.15		0.28		0.40		0.54		0.46		0.55		0.44		0.40		0.35		1.27		0.35		0.31		0.31		0.28		0.34
Cl		0.67		1.00		1.17		0.73		1.17		1.03		1.93		1.35		1.77		9.19		1.46		0.78		0.74		0.65		0.91
Trace elements (ppm)																														
Br		69		67		61		58		54		58		61		55		52		70		51		42		37		31		32
I		29		44		46		46		40		44		44		32		30		30		36		17		19		15		23
Rb		71		77		78		74		70		70		78		73		73		69		70		65		62		58		
Sr		118		130		135		137		128		128		137		136		127		124		122		112		103		99		
Y		21		21		22		20		19		18		20		20		19		19		18		15		12		13		
Zr		266		288		267		259		292		290		301		285		307		313		290		262		217		217		
Nb		12		13		12		12		12		12		13		12		13		11		12		10		9		10		
Pb		52		57		59		59		51		51		56		55		55		49		46		41		34		31		
Zn		105		118		124		125		103		99		118		112		109		97		97		84		70		59		
Ni		24		26		27		25		24		22		27		25		25		23		24		21		17		15		
Cr		103		104		100		95		83		91		100		96		98		83		96		74		71		77		69
Ba		313		318		331		326		301		299		326		303		323		297		297		293		255		249		270
La		23		25		20		21		22		20		20		23		22		18		22		19		17		13		13
Ce		30		41		31		33		36		41		40		41		40		41		37		23		31		23		23
MnO		526		557		627		662		625		700		855		740		913		710		653		613		493		472		559
TiO_2		5727		6085		6254		5764		5700		5693		6332		5963		6179		5742		5770		5005		4358		4006		4307
Radionuclides (Bq/kg)																														
^{241}Am	192	200	207	211	151	141	148	57	41	32	28	27	24	20	15						2	7				4		3		
^{137}Cs	441	679	994	466	329	295	238	176	157	137	167	156	225	402	375	299	239	170	140	105	93	116	94	120	228	372	462	631	752	923
^{238}Pu		14		24		14		5		4		3		3		1		1		1		2						1		
$^{239,240}Pu$		548		810		820		385		304		262		248		176		146		67		57		25		6		3		6
^{241}Pu		1147		1636		966		338		221		119		93		91		80		49		96		39		79		61		59

* All the data are based on the dry weight

A.7. Geochemical data, R-97-003 (saltmarsh) core.

Depth	0.5	1	1.5	2	2.5	3	3.5	4	4.5	5	5.5	6	6.5	7	7.5	8	8.5	9	9.5	10	10.5	11	11.5	12	12.5	13	13.5	14	14.5	15
Major elements (wt. %)																														
SiO_2	55.54	55.24	56.94	56.04	56.38	58.13	53.69							57.58									56.11		58.22					59.26
TiO_2	0.75	0.51	0.76	0.75	0.73	0.71	0.81							0.81									0.81		0.08					0.84
Al_2O_3	12.25	12.40	12.64	12.48	11.89	11.37	13.84							12.88									13.18		13.54					13.60
Fe_2O_3	5.67	5.97	5.65	5.67	5.23	4.86	5.79							5.66									6.22		6.09					5.57
MnO	0.17	0.16	0.09	0.15	0.15	0.14	0.13							0.18									0.35		0.31					0.10
MgO	2.09	2.16	2.08	2.12	2.02	1.96	2.72							2.22									2.22		2.38					2.36
CaO	0.66	0.68	0.66	0.64	0.64	0.68	1.34							0.71									0.64		0.75					0.79
Na_2O	1.76	1.84	1.77	1.85	1.66	1.61	2.70							2.76									2.23		2.21					2.41
K_2O	2.58	2.62	2.67	2.62	2.52	2.46	2.66							2.72									2.78		2.68					2.79
P_2O_5	0.17	0.17	0.18	0.17	0.15	0.16	0.29							0.25									0.22		0.22					0.21
LOI	18.4	18.0	16.6	17.5	18.6	17.9	16.0							14.2									15.2		12.7					12.1
S	0.34	0.27	0.26	0.32	0.34	0.36	0.35							0.33									0.24		0.31					0.26
Cl	3.06	2.33	2.13	2.89	3.06	3.38	2.91							2.53									1.93		2.34					2.04
Trace elements (ppm)																														
Br	415	356	331	372	399	423	425	383	383	424	403	410	366	337	352	337	308	300	284	283	239	263	277	319	374	317	275	264	251	266
I	121	134	137	153	142	130	128	111	120	122	124	126	118	114	114	126	132	142	131	124	122	129	144	140	160	134	128	129	126	123
Rb	94	104	108	103	99	98	98	97	101	99	103	101	100	104	106	108	108	110	110	107	97	110	111	109	104	106	109	110	109	111
Sr	140	111	108	106	106	108	107	106	105	107	106	105	103	103	107	106	105	105	105	105	95	106	105	105	107	106	106	105	107	105
Y	26	29	30	29	30	32	34	35	34	33	34	36	38	38	40	41	41	42	42	42	40	44	43	44	47	46	43	40	38	36
Zr	171	185	194	188	185	188	199	199	193	187	205	205	213	221	217	216	211	214	217	227	207	228	225	229	220	219	234	228	234	229
Nb	14	15	16	15	15	15	16	15	15	15	16	15	15	16	17	17	16	16	16	17	16	17	17	16	16	17	16	17	16	17
Pb	99	78	82	79	76	77	74	75	77	73	77	75	77	78	80	81	81	83	84	85	67	88	92	93	96	95	96	95	90	97
Zn	177	178	180	178	170	171	160	163	168	165	162	161	162	160	168	190	176	177	176	179	157	187	187	186	192	190	191	193	189	192
Ni	36	37	39	38	37	36	36	36	37	36	38	37	38	38	40	41	39	41	41	41	33	41	39	41	42	42	41	41	42	43
Cr	94	97	106	97	98	99	107	105	107	103	108	103	102	102	107	112	107	114	114	113	105	120	123	126	125	137	127	122	120	119
Ba	312	318	324	324	308	301	307	298	297	286	311	296	301	308	319	367	326	323	322	322	294	327	336	331	318	326	333	328	328	334
La	31	33	35	36	36	34	36	32	33	33	37	36	37	37	38	40	42	40	43	42	38	42	40	41	42	39	39	42	39	39
Ce	47	57	63	49	60	55	56	60	57	58	56	51	54	66	57	58	58	63	65	55	51	61	62	63	64	57	56	58	63	61
MnO	2447	1840	1804	2005	1968	2023	1683	1640	1648	1564	1604	1484	1717	1532	1718	1971	2025	2176	2040	2577	2495	2520	2247	2361	2815	2699	2423	2713	2716	2476
TiO_2	6647	7068	7305	6876	6663	6474	6731	6641	6699	6546	7129	7009	7034	7344	7374	7418	7480	7519	7387	7344	6799	7640	7595	7579	7375	7627	7749	7672	7696	7767
Radionuclides (Bq/kg)																														
^{241}Am	1728	1952	1819	2019	1973	2023	1862	2470	2610	3040	3110	3570	4100	4950	6550	9010	9410	12290	13860	13180	13150	17410	20050	25080	20220	15400	10620	7390	4230	2980
^{137}Cs	1262	1385	1315	1268	1386	1474	1512	2020	2240	3000	3400	4460	5720	7310	10670	13340	12570	14590	14630	15300	18020	20670	18250	15910	13540	11990	9750	8600	7260	7300

Depth	15.5	16	16.5	17	17.5	18	18.5	19	19.5	20	20.5	21	21.5	22	22.5	23	23.5	24	24.5	25	25.5	26	26.5	27	27.5	28	28.5	29	29.5	30
Major elements (wt. %)																														
SiO_2								58.09							61.45								61.55							64.02
TiO_2								0.78							0.86								0.91							0.84
Al_2O_3								15.43							13.57								14.86							13.62
Fe_2O_3								5.97							6.04								6.57							5.87
MnO								0.18							0.10								0.14							0.14
MgO								2.21							2.36								2.51							2.36
CaO								0.24							0.84								0.82							0.79
Na_2O								1.96							1.91								2.22							2.16
K_2O								2.66							2.72								2.84							2.74
P_2O_5								0.19							0.19								0.24							0.19
LOI								11.8							10.0								7.4							7.3
S								0.23							0.21								0.19							0.18
Cl								1.76							1.67								1.45							1.38
Trace elements (ppm)																														
Br	288	273	259	262	317	274	286	274	272	250	252	228	254	265	247	258	248	219	220	217	217	215	206	193	189	207	194	212	221	235
I	143	147	134	149	158	140	152	147	113	140	123	116	122	138	126	132	129	112	125	122	127	132	126	118	123	99	95	101	110	104
Rb	111	112	111	112	110	110	107	110	110	111	110	107	113	113	109	110	108	109	108	105	110	114	110	108	105	104	105	105	103	105
Sr	105	105	104	106	106	103	104	103	104	103	102	99	104	104	103	102	102	103	105	103	103	104	103	100	97	97	96	97	102	102
Y	36	33	32	31	30	31	30	29	30	28	27	25	27	28	27	28	27	28	28	27	28	29	28	26	25	25	25	26	27	27
Zr	221	226	225	224	229	229	228	232	227	225	230	229	225	227	229	229	237	237	249	245	240	235	237	253	241	241	244	238	258	247
Nb	16	16	17	17	17	17	17	17	17	17	17	16	17	16	17	17	17	17	17	16	18	17	17	16	16	16	16	15	17	17
Pb	99	94	102	98	96	99	97	103	99	100	90	85	88	87	96	88	84	85	94	89	98	98	96	81	78	75	74	79	79	79
Zn	205	192	204	197	198	187	191	195	193	183	182	168	185	188	178	180	171	173	175	167	175	185	179	170	153	153	150	151	155	158
Ni	43	42	44	42	42	40	41	40	42	39	39	38	40	42	41	41	38	41	40	39	42	42	42	40	35	36	36	37	38	38
Cr	115	116	114	114	113	105	104	104	103	110	103	106	110	106	109	104	100	102	107	108	102	106	108	103	95	102	99	97	101	100
Ba	325	336	342	340	338	351	340	361	356	356	353	346	343	348	341	351	354	362	372	369	369	387	373	354	353	343	355	349	349	341
La	41	35	36	35	35	32	35	37	33	34	33	33	34	35	32	33	32	32	31	36	33	35	36	34	32	32	36	33	31	31
Ce	66	61	64	57	59	56	55	56	60	60	57	58	66	61	63	58	57	60	66	57	61	61	62	69	62	58	53	55	55	61
MnO	3594	2810	3662	3177	3343	2185	2951	2123	2007	1575	1416	1128	1961	1981	1441	1695	1416	1666	2269	1758	1967	2192	2113	1621	1381	1286	1245	1106	1050	1038
TiO_2	7570	7709	7815	7667	7602	7807	7577	7801	7792	7809	7759	7672	7816	7738	7802	7789	7771	7810	7856	7869	7925	8102	8030	7959	7831	7696	7660	7731	7765	7769
Radionuclides (Bq/kg)																														
^{241}Am	1999	1148	925	640	496		260		152		65		2141		40		21		23		21		8		9		6			
^{137}Cs	5920	4830	4600	4010	3850		3211		2476		1676		1443		968		677		529		417		322		254		259			

A.8.1. Cumulative activities of ^{241}Am with various mixing rates

YEAR	99%	95%	90%	85%	80%	75%	70%	60%	50%	40%	30%	20%	10%	0%
1996														
1995	419.4	173.9	57.9	20.0	7.7	3.6	2.1	1.1	0.7	0.5	0.3	0.2	0.2	0.1
1994	423.5	182.9	64.3	23.5	9.5	4.6	2.8	1.6	1.1	0.9	0.7	0.6	0.5	0.4
1993	427.4	192.2	71.0	27.1	11.4	5.7	3.4	2.0	1.5	1.3	1.1	1.0	0.9	0.9
1992	430.8	201.4	77.9	30.9	13.2	6.4	3.7	1.9	1.3	1.1	0.9	0.7	0.6	0.5
1991	434.7	211.4	86.0	35.7	15.8	7.8	4.5	2.3	1.6	1.3	1.1	0.9	0.8	0.7
1990	438.3	221.8	94.7	41.2	18.8	9.4	5.4	2.6	1.8	1.4	1.2	1.0	0.9	0.7
1989	442.0	232.7	104.4	47.6	22.6	11.6	6.6	3.1	2.1	1.7	1.4	1.3	1.2	1.1
1988	445.4	243.8	114.8	54.7	26.9	14.0	7.9	3.4	2.0	1.4	1.1	0.9	0.8	0.7
1987	449.1	255.8	126.7	63.5	32.7	17.7	10.3	4.5	2.6	1.7	1.3	1.0	0.8	0.6
1986	453.0	268.6	140.1	74.0	40.1	22.7	13.8	6.4	3.8	2.7	2.1	1.7	1.5	1.3
1985	456.3	281.4	154.3	85.5	48.5	28.6	17.9	8.5	5.1	3.6	2.7	2.2	1.8	1.6
1984	459.3	294.6	169.7	98.8	58.7	36.1	23.3	11.6	7.1	5.0	3.8	3.0	2.5	2.2
1983	461.7	307.7	186.0	113.5	70.5	45.1	30.0	15.6	9.8	6.9	5.1	3.8	2.9	2.1
1982	464.2	321.6	204.3	131.0	85.5	57.3	39.8	22.3	15.3	11.9	9.8	8.3	7.2	6.2
1981	462.6	332.0	220.1	146.8	99.1	68.0	48.0	26.8	18.0	14.1	12.0	10.5	9.4	8.6
1980	458.6	340.5	235.0	162.7	113.1	79.3	56.3	30.5	19.0	13.8	11.3	9.9	8.8	8.0
1979	455.2	350.0	252.3	182.0	131.4	95.1	69.1	37.5	22.0	14.6	11.2	9.4	8.4	7.6
1978	452.1	360.4	271.9	205.2	154.8	116.7	87.9	49.9	28.8	17.6	12.0	9.3	8.2	7.7
1977	449.0	371.4	293.6	232.4	184.0	145.4	114.7	70.4	42.3	24.8	14.4	8.4	5.2	3.6
1976	449.9	387.1	322.3	269.2	225.5	189.2	158.7	111.4	77.5	53.2	36.0	24.1	16.3	11.6
1975	442.7	395.3	345.2	303.1	267.4	236.8	210.2	166.3	131.7	103.9	81.3	62.7	47.4	34.7
1974	412.2	379.6	345.0	315.8	290.9	269.4	250.7	219.4	194.1	173.1	155.3	140.0	126.8	115.5
1973	299.7	278.0	255.0	235.7	219.3	205.3	193.1	173.2	157.2	144.0	132.6	122.7	113.7	105.7
1972	195.9	181.4	165.9	152.9	142.0	132.8	124.9	112.5	103.1	95.8	89.9	84.9	80.6	76.7
1971	120.4	110.2	99.1	89.7	81.6	74.7	68.9	59.6	52.7	47.6	43.7	40.7	38.4	36.4
1970	84.9	77.7	69.7	62.7	56.5	51.1	46.4	38.6	32.6	28.0	24.5	21.8	19.7	18.2
1969	67.4	62.6	57.2	52.3	47.9	43.9	40.3	34.1	28.9	24.7	21.1	18.1	15.5	13.4
1968	54.6	51.9	48.7	45.9	43.2	40.7	38.5	34.5	31.1	28.2	25.8	23.6	21.7	20.0
1967	34.9	33.5	31.9	30.4	29.0	27.6	26.4	24.1	22.2	20.5	19.1	17.9	17.0	16.2
1966	18.9	18.3	17.5	16.7	16.0	15.3	14.6	13.3	12.0	10.9	9.8	8.8	7.9	7.1
1965	11.9	11.7	11.5	11.3	11.1	10.9	10.7	10.2	9.8	9.4	9.0	8.5	8.1	7.7
1964	4.3	4.3	4.3	4.3	4.3	4.3	4.3	4.3	4.3	4.3	4.3	4.3	4.3	4.3
1963	0	0	0	0	0	0	0	0	0	0	0	0	0	0
1962	0	0	0	0	0	0	0	0	0	0	0	0	0	0
1961	0	0	0	0	0	0	0	0	0	0	0	0	0	0
1960	0	0	0	0	0	0	0	0	0	0	0	0	0	0
1959	0	0	0	0	0	0	0	0	0	0	0	0	0	0
1958	0	0	0	0	0	0	0	0	0	0	0	0	0	0
1957	0	0	0	0	0	0	0	0	0	0	0	0	0	0
1956	0	0	0	0	0	0	0	0	0	0	0	0	0	0
1955	0	0	0	0	0	0	0	0	0	0	0	0	0	0
1954	0	0	0	0	0	0	0	0	0	0	0	0	0	0
1953	0	0	0	0	0	0	0	0	0	0	0	0	0	0
1952	0	0	0	0	0	0	0	0	0	0	0	0	0	0

*A.8.2. Cumulative activities of ^{241}Am with various mixing rates**

YEAR	99%	95%	90%	85%	80%	75%	70%	60%	50%	40%	30%	20%	10%	0%
1996	790.1	321.9	104.8	34.9	12.4	5.1	2.5	1.0	0.5	0.3	0.2	0.1	0.1	0.1
1995	798.1	338.8	116.4	41.0	15.5	6.6	3.4	1.5	0.9	0.6	0.4	0.3	0.2	0.1
1994	806.0	356.5	129.2	48.1	19.2	8.7	4.7	2.2	1.5	1.1	0.9	0.7	0.6	0.5
1993	813.7	374.8	143.0	56.0	23.4	10.9	6.0	3.0	2.1	1.7	1.5	1.3	1.2	1.1
1992	820.7	393.3	157.6	64.6	27.8	13.1	7.0	3.0	1.9	1.5	1.2	1.0	0.9	0.7
1991	828.3	413.2	174.3	75.1	33.8	16.5	8.9	3.8	2.4	1.8	1.5	1.3	1.1	1.0
1990	835.6	433.9	192.6	87.2	41.0	20.6	11.3	4.7	2.8	2.1	1.7	1.4	1.2	1.1
1989	843.0	455.6	212.8	101.3	49.9	26.0	14.6	6.0	3.4	2.5	2.0	1.7	1.6	1.4
1988	850.0	478.1	234.8	117.5	60.6	32.8	18.8	7.6	4.0	2.6	1.9	1.5	1.3	1.2
1987	857.4	502.0	259.6	136.8	74.3	42.1	25.2	10.7	5.6	3.4	2.3	1.7	1.3	1.1
1986	865.0	527.3	287.2	159.7	91.5	54.7	34.4	16.0	9.0	5.8	4.1	3.2	2.6	2.2
1985	871.5	552.7	316.7	185.3	111.7	70.0	46.0	23.1	13.7	9.1	6.5	4.8	3.7	2.8
1984	877.5	578.9	348.8	214.7	136.1	89.6	61.8	33.8	21.8	15.8	12.4	10.2	8.8	7.9
1983	878.4	601.0	378.8	243.3	160.3	109.0	77.0	43.2	27.9	19.8	14.9	11.7	9.4	7.7
1982	879.5	624.6	412.3	277.1	190.7	135.1	99.0	59.2	40.3	30.2	24.0	19.8	16.9	14.7
1981	873.5	642.0	441.8	308.7	220.0	160.5	120.4	74.1	51.3	38.7	31.0	25.8	22.1	19.5
1980	862.6	655.2	469.1	340.2	250.6	188.0	144.1	91.0	63.4	47.9	38.1	31.2	26.0	21.8
1979	849.3	666.7	497.0	374.6	286.0	221.5	174.6	115.3	83.3	65.3	54.5	47.2	41.6	36.9
1978	820.5	662.9	511.2	397.3	311.3	246.1	196.7	130.6	92.6	70.9	58.4	51.2	46.8	44.0
1977	784.4	651.5	519.2	415.6	334.1	269.5	218.2	144.5	97.3	67.2	48.2	36.3	28.7	23.9
1976	768.2	660.7	550.3	460.9	387.8	327.5	277.6	200.9	146.8	108.3	81.0	61.7	48.4	39.2
1975	736.3	654.1	567.8	496.0	435.6	384.4	340.4	269.5	215.1	172.7	139.2	112.5	91.1	73.9
1974	669.1	610.7	548.8	496.6	452.2	413.9	380.8	325.9	282.4	247.0	217.6	192.7	171.5	153.3
1973	521.0	481.5	439.4	403.8	373.5	347.5	324.9	287.7	258.2	234.2	214.1	197.0	182.2	169.3
1972	355.2	328.6	300.1	275.9	255.3	237.6	222.3	197.3	177.8	162.2	149.4	138.5	129.1	120.7
1971	236.9	218.8	199.3	182.6	168.2	155.8	145.1	127.5	114.1	103.7	95.4	88.8	83.4	78.8
1970	159.7	147.4	133.9	122.1	111.8	102.7	94.6	81.2	70.6	62.2	55.4	50.0	45.6	42.1
1969	118.7	110.8	102.0	94.1	87.0	80.7	75.0	65.2	57.0	50.1	44.3	39.3	34.9	31.1
1968	88.5	83.9	78.7	74.1	69.9	66.1	62.7	56.8	51.8	47.5	43.9	40.8	38.0	35.6
1967	53.5	50.9	48.0	45.3	42.9	40.8	38.8	35.4	32.4	30.0	27.9	26.2	24.7	23.4
1966	30.3	28.9	27.2	25.8	24.4	23.1	22.0	19.9	18.0	16.4	14.9	13.6	12.5	11.4
1965	19.1	18.4	17.6	16.9	16.2	15.6	15.1	14.1	13.2	12.4	11.7	11.0	10.4	9.8
1964	9.4	9.1	8.7	8.4	8.1	7.8	7.6	7.2	6.9	6.6	6.4	6.2	6.0	5.9
1963	3.6	3.4	3.1	2.9	2.8	2.6	2.5	2.3	2.1	1.9	1.8	1.7	1.5	1.4
1962	2.2	2.0	1.9	1.8	1.7	1.6	1.5	1.4	1.3	1.2	1.1	1.1	1.0	1.0
1961	1.2	1.1	1.0	0.9	0.9	0.8	0.7	0.7	0.6	0.6	0.5	0.5	0.5	0.5
1960	0.8	0.7	0.6	0.5	0.5	0.4	0.4	0.3	0.3	0.2	0.2	0.2	0.2	0.2
1959	0.6	0.5	0.5	0.4	0.4	0.3	0.3	0.3	0.2	0.2	0.2	0.1	0.1	0.1
1958	0.5	0.4	0.4	0.4	0.3	0.3	0.3	0.2	0.2	0.2	0.1	0.1	0.1	0.1
1957	0.4	0.4	0.3	0.3	0.3	0.2	0.2	0.2	0.2	0.1	0.1	0.1	0.1	0.1
1956	0.3	0.3	0.3	0.2	0.2	0.2	0.2	0.2	0.2	0.1	0.1	0.1	0.1	0.1
1955	0.2	0.2	0.2	0.2	0.2	0.1	0.1	0.1	0.1	0.1	0.1	0.1	0.1	0.1
1954	0.1	0.1	0.1	0.1	0.1	0.1	0.1	0.1	0.1	0.1	0.1	0.1	0.1	0.1
1953	0.1	0.1	0.1	0.1	0.1	0.1	0.1	0.1	0.1	0.1	0.0	0.0	0.0	0.0
1952	0.1	0.1	0.1	0.1	0.1	0.1	0.1	0.1	0.1	0.1	0.1	0.1	0.1	0.1

** considering the ingrown ^{241}Am by the decay of ^{241}Pu)*

A.9. Cumulative activities of ^{137}Cs with various mixing rates

YEAR	99%	95%	90%	85%	80%	75%	70%	60%	50%	40%	30%	20%	10%	0%
1996														
1995	21003	10115	4054	1626	660	278	128	44	27	21	18	15	13	11
1994	21204	10636	4491	1899	810	356	167	54	32	25	20	17	15	13
1993	21405	11182	4976	2219	997	457	220	69	38	30	26	23	21	20
1992	21601	11750	5507	2588	1222	584	286	83	37	25	20	17	15	13
1991	21806	12355	6105	3029	1511	761	390	116	48	29	22	19	16	14
1990	22013	12990	6768	3547	1871	996	538	171	68	39	30	25	22	20
1989	22215	13653	7498	4150	2314	1302	740	251	96	47	32	27	25	24
1988	22415	14347	8305	4854	2863	1704	1023	379	146	59	27	16	12	10
1987	22631	15091	9216	5699	3566	2258	1447	614	271	122	56	26	14	9
1986	22851	15875	10230	6694	4446	2998	2054	1009	523	282	156	85	42	14
1985	23068	16697	11351	7859	5540	3980	2914	1658	1018	671	473	356	286	245
1984	23053	17317	12340	8957	6619	4979	3813	2355	1546	1065	759	555	413	312
1983	22971	17900	13364	10171	7884	6223	5001	3405	2468	1882	1491	1214	1009	852
1982	22342	17946	13903	10964	8790	7162	5928	4255	3233	2576	2130	1811	1572	1387
1981	21167	17430	13906	11267	9254	7699	6488	4781	3692	2972	2476	2118	1845	1627
1980	19738	16635	13644	11341	9533	8097	6944	5256	4130	3364	2832	2456	2185	1988
1979	17929	15419	12952	11004	9432	8145	7081	5448	4285	3440	2814	2340	1974	1684
1978	16410	14458	12520	10965	9686	8616	7710	6273	5202	4391	3768	3284	2903	2595
1977	13954	12487	11028	9847	8864	8028	7307	6131	5215	4489	3910	3447	3077	2784
1976	11283	10214	9160	8310	7600	6992	6462	5578	4862	4264	3755	3314	2931	2600
1975	8771	8015	7289	6718	6250	5856	5518	4964	4524	4161	3849	3571	3315	3073
1974	5756	5203	4685	4288	3972	3711	3493	3151	2903	2721	2588	2490	2419	2368
1973	3422	2984	2574	2259	2004	1790	1607	1306	1070	882	732	612	514	435
1972	3018	2683	2377	2146	1962	1808	1674	1452	1270	1119	992	885	794	717
1971	2324	2069	1844	1681	1556	1454	1367	1224	1106	1005	917	838	767	701
1970	1639	1440	1270	1153	1069	1004	952	871	810	761	720	686	657	633
1969	1017	850	708	613	545	495	456	398	355	321	292	268	246	227
1968	798	656	535	454	398	358	328	285	256	235	218	205	195	186
1967	618	495	388	315	265	229	202	165	140	121	106	94	83	74
1966	549	443	349	284	239	207	183	152	132	118	108	99	92	87
1965	468	375	291	232	190	160	138	109	91	79	70	63	57	52
1964	420	341	266	212	173	144	123	96	79	69	61	55	50	46
1963	378	310	245	196	159	131	110	83	67	57	50	46	42	38
1962	343	286	230	185	151	124	103	74	57	47	41	37	34	32
1961	314	267	219	180	148	122	101	70	49	36	27	22	19	17
1960	300	263	224	191	163	140	119	87	64	46	34	24	18	14
1959	288	262	233	208	186	167	150	122	99	80	64	51	40	30
1958	261	244	226	210	196	183	172	153	138	125	114	106	98	92
1957	171	160	149	139	129	121	114	101	91	82	75	68	61	55
1956	117	111	104	99	93	89	84	78	72	69	66	64	62	61
1955	56	52	48	44	40	36	33	27	22	18	15	12	10	8
1954	49	47	45	42	40	38	36	32	29	26	23	21	19	17
1953	32	32	31	30	29	28	28	26	24	23	21	20	18	16
1952	16	16	16	16	16	16	16	16	16	16	16	16	16	16

A.10. Cumulative activities of ^{238}Pu with various mixing rates

YEAR	99%	95%	90%	85%	80%	75%	70%	60%	50%	40%	30%	20%	10%	0%
1996	86.49	39.37	15.03	6.00	2.59	1.27	0.72	0.34	0.22	0.15	0.11	0.08	0.07	0.06
1995	87.30	41.38	16.63	6.99	3.17	1.61	0.95	0.47	0.31	0.23	0.17	0.13	0.10	0.08
1994	88.10	43.47	18.39	8.13	3.86	2.04	1.24	0.66	0.47	0.37	0.30	0.25	0.20	0.16
1993	88.83	45.59	20.25	9.37	4.62	2.51	1.53	0.83	0.61	0.51	0.45	0.40	0.37	0.35
1992	89.37	47.62	22.12	10.61	5.34	2.88	1.70	0.80	0.53	0.41	0.34	0.29	0.26	0.23
1991	90.05	49.89	24.32	12.22	6.39	3.53	2.10	0.96	0.60	0.45	0.37	0.32	0.28	0.25
1990	90.71	52.25	26.75	14.08	7.68	4.38	2.65	1.18	0.70	0.51	0.41	0.35	0.31	0.27
1989	91.35	54.72	29.42	16.25	9.26	5.48	3.39	1.52	0.85	0.58	0.45	0.38	0.33	0.29
1988	91.98	57.29	32.37	18.77	11.21	6.92	4.43	2.05	1.13	0.73	0.55	0.45	0.39	0.35
1987	92.55	59.94	35.58	21.67	13.58	8.76	5.83	2.83	1.55	0.96	0.65	0.49	0.39	0.32
1986	93.16	62.75	39.17	25.12	16.57	11.25	7.87	4.18	2.47	1.59	1.11	0.83	0.66	0.56
1985	93.54	65.46	42.90	28.89	20.01	14.25	10.43	6.03	3.80	2.57	1.82	1.33	0.99	0.72
1984	93.75	68.15	46.86	33.14	24.11	18.04	13.87	8.85	6.16	4.62	3.67	3.06	2.63	2.33
1983	92.35	69.29	49.48	36.25	27.23	20.95	16.50	10.86	7.67	5.73	4.49	3.65	3.04	2.58
1982	90.68	70.22	52.12	39.61	30.82	24.50	19.88	13.81	10.18	7.89	6.38	5.36	4.65	4.14
1981	87.41	69.56	53.31	41.73	33.34	27.15	22.49	16.12	12.08	9.36	7.45	6.08	5.08	4.37
1980	83.88	68.62	54.37	43.95	36.21	30.37	25.88	19.58	15.42	12.48	10.26	8.53	7.13	5.99
1979	78.68	65.93	53.76	44.67	37.78	32.51	28.42	22.65	18.87	16.23	14.26	12.70	11.42	10.33
1978	69.04	58.52	48.26	40.40	34.32	29.58	25.85	20.54	17.09	14.75	13.10	11.89	10.96	10.25
1977	59.39	50.82	42.24	35.47	30.09	25.78	22.29	17.16	13.68	11.26	9.51	8.20	7.17	6.35
1976	53.57	46.81	39.87	34.26	29.67	25.90	22.77	18.01	14.66	12.27	10.52	9.22	8.21	7.40
1975	46.64	41.48	36.09	31.60	27.84	24.67	21.97	17.69	14.53	12.18	10.42	9.10	8.10	7.34
1974	39.70	35.94	31.94	28.55	25.63	23.10	20.90	17.25	14.38	12.11	10.29	8.81	7.61	6.62
1973	33.41	30.87	28.14	25.80	23.77	21.98	20.40	17.71	15.53	13.73	12.23	10.97	9.91	9.03
1972	24.63	22.99	21.23	19.73	18.42	17.27	16.24	14.47	13.00	11.75	10.67	9.71	8.85	8.06
1971	16.74	15.71	14.63	13.73	12.95	12.28	11.68	10.68	9.88	9.23	8.68	8.23	7.84	7.51
1970	9.32	8.63	7.91	7.31	6.80	6.35	5.95	5.28	4.74	4.28	3.89	3.57	3.29	3.05
1969	6.33	5.88	5.41	5.02	4.69	4.40	4.15	3.73	3.38	3.08	2.82	2.60	2.40	2.23
1968	4.15	3.84	3.53	3.28	3.08	2.90	2.75	2.50	2.30	2.14	1.99	1.87	1.76	1.66
1967	2.52	2.30	2.08	1.91	1.77	1.66	1.56	1.41	1.29	1.20	1.12	1.05	0.99	0.94
1966	1.59	1.43	1.27	1.14	1.04	0.96	0.89	0.79	0.71	0.65	0.60	0.57	0.54	0.51
1965	1.09	0.97	0.84	0.74	0.66	0.60	0.54	0.46	0.39	0.34	0.30	0.27	0.25	0.23
1964	0.87	0.78	0.68	0.60	0.54	0.49	0.44	0.37	0.32	0.28	0.24	0.21	0.19	0.17
1963	0.71	0.64	0.57	0.51	0.47	0.43	0.39	0.34	0.30	0.27	0.25	0.22	0.21	0.19
1962	0.52	0.47	0.42	0.38	0.34	0.32	0.29	0.26	0.23	0.21	0.19	0.17	0.16	0.15
1961	0.38	0.34	0.30	0.27	0.24	0.22	0.20	0.17	0.15	0.14	0.13	0.12	0.11	0.10
1960	0.27	0.25	0.22	0.19	0.17	0.15	0.14	0.12	0.10	0.09	0.08	0.07	0.06	0.06
1959	0.22	0.20	0.18	0.16	0.14	0.13	0.12	0.10	0.08	0.07	0.06	0.05	0.05	0.04
1958	0.18	0.16	0.15	0.13	0.12	0.11	0.10	0.09	0.08	0.07	0.06	0.05	0.05	0.04
1957	0.13	0.12	0.11	0.11	0.10	0.09	0.08	0.07	0.06	0.06	0.05	0.05	0.04	0.04
1956	0.10	0.09	0.09	0.08	0.08	0.07	0.07	0.06	0.06	0.05	0.05	0.05	0.04	0.04
1955	0.06	0.05	0.05	0.04	0.04	0.04	0.04	0.03	0.03	0.02	0.02	0.02	0.02	0.01
1954	0.04	0.04	0.04	0.04	0.03	0.03	0.03	0.03	0.02	0.02	0.02	0.02	0.02	0.01
1953	0.03	0.03	0.03	0.03	0.03	0.02	0.02	0.02	0.02	0.02	0.02	0.02	0.02	0.01
1952	0.01	0.01	0.01	0.01	0.01	0.01	0.01	0.01	0.01	0.01	0.01	0.01	0.01	0.01

A.11. Cumulative activities of $^{239,240}Pu$ with various mixing rates

YEAR	99%	95%	90%	85%	80%	75%	70%	60%	50%	40%	30%	20%	10%	0%
1996	488.59	202.40	69.41	25.05	9.83	4.39	2.31	1.01	0.61	0.42	0.30	0.23	0.18	0.15
1995	493.38	212.89	76.96	29.30	12.10	5.65	3.09	1.44	0.93	0.67	0.50	0.38	0.29	0.23
1994	498.13	223.85	85.25	34.20	14.83	7.23	4.09	2.02	1.40	1.09	0.89	0.73	0.60	0.50
1993	502.66	235.11	94.17	39.64	17.92	8.97	5.12	2.53	1.80	1.48	1.28	1.15	1.05	0.97
1992	506.75	246.46	103.55	45.50	21.18	10.66	5.93	2.60	1.65	1.27	1.05	0.90	0.78	0.69
1991	511.18	258.71	114.29	52.71	25.62	13.30	7.49	3.18	1.93	1.45	1.20	1.03	0.91	0.82
1990	515.51	271.46	126.08	61.05	31.00	16.64	9.53	3.93	2.21	1.57	1.26	1.07	0.94	0.84
1989	519.87	284.86	139.16	70.84	37.70	21.06	12.41	5.16	2.75	1.82	1.39	1.16	1.01	0.90
1988	524.21	298.91	153.62	82.28	46.00	26.88	16.45	7.10	3.70	2.30	1.65	1.31	1.12	1.00
1987	528.50	313.59	169.58	95.62	56.24	34.51	22.07	10.16	5.40	3.24	2.16	1.56	1.21	0.97
1986	532.85	329.07	187.34	111.35	69.09	44.72	30.14	15.32	8.85	5.68	3.95	2.95	2.35	2.00
1985	536.22	344.29	205.93	128.65	83.87	56.96	40.20	22.19	13.70	9.19	6.52	4.77	3.53	2.60
1984	539.01	359.67	225.92	148.30	101.58	72.48	53.72	32.65	22.21	16.48	13.05	10.85	9.35	8.30
1983	536.07	369.86	241.81	164.70	116.60	85.57	64.88	40.59	27.82	20.45	15.84	12.74	10.47	8.70
1982	532.69	380.17	259.01	183.53	134.88	102.49	80.26	53.15	38.23	29.37	23.81	20.19	17.74	16.00
1981	521.91	383.34	270.01	197.10	148.60	115.32	91.80	61.92	44.47	33.42	26.03	20.95	17.43	15.00
1980	512.03	387.73	283.34	214.23	167.00	133.76	109.72	78.19	58.94	46.04	36.76	29.75	24.29	20.00
1979	497.00	387.08	292.60	228.51	183.75	151.69	128.17	96.99	77.87	65.10	55.87	48.74	42.93	38.00
1978	463.64	367.45	282.89	224.13	182.19	151.58	128.81	98.32	79.75	67.74	59.55	53.68	49.32	46.00
1977	421.86	338.37	263.21	209.56	170.23	140.78	118.30	87.19	67.49	54.36	45.17	38.41	33.19	29.00
1976	396.83	325.65	260.23	212.42	176.54	149.03	127.57	96.99	76.98	63.41	53.90	47.04	41.94	38.00
1975	362.45	302.79	246.93	205.20	173.18	148.04	127.96	98.32	77.96	63.52	53.00	45.22	39.39	35.00
1974	330.76	281.89	235.47	200.24	172.72	150.73	132.81	105.53	85.93	71.29	60.01	51.11	43.92	38.00
1973	295.72	256.72	219.42	190.87	168.40	150.30	135.44	112.55	95.86	83.22	73.38	65.54	59.19	54.00
1972	244.16	213.39	183.80	161.02	143.00	128.40	116.34	97.58	83.71	73.05	64.60	57.71	51.94	47.00
1971	199.15	175.15	152.00	134.15	120.00	108.54	99.05	84.31	73.42	65.13	58.66	53.54	49.40	46.00
1970	154.70	135.95	117.77	103.70	92.51	83.38	75.79	63.85	54.84	47.81	42.21	37.68	34.00	31.00
1969	124.95	110.47	96.41	85.53	76.88	69.84	63.99	54.74	47.68	42.03	37.36	33.40	29.98	27.00
1968	98.94	87.87	77.13	68.86	62.35	57.12	52.84	46.24	41.37	37.58	34.53	31.99	29.84	28.00
1967	71.65	63.02	54.58	48.07	42.94	38.83	35.49	30.40	26.73	23.96	21.76	19.94	18.38	17.00
1966	55.20	48.44	41.76	36.55	32.43	29.11	26.41	22.33	19.47	17.39	15.85	14.68	13.75	13.00
1965	42.63	37.30	31.96	27.71	24.28	21.48	19.15	15.55	12.93	10.98	9.50	8.39	7.54	6.90
1964	36.09	32.00	27.84	24.48	21.73	19.44	17.50	14.42	12.06	10.19	8.68	7.43	6.38	5.50
1963	30.90	27.90	24.82	22.33	20.28	18.58	17.15	14.87	13.12	11.73	10.59	9.63	8.81	8.10
1962	23.03	20.84	18.58	16.74	15.23	13.98	12.93	11.28	10.04	9.08	8.30	7.65	7.09	6.60
1961	16.60	14.99	13.31	11.93	10.79	9.84	9.04	7.80	6.89	6.20	5.67	5.24	4.89	4.60
1960	12.12	10.94	9.68	8.62	7.73	6.98	6.34	5.33	4.57	4.00	3.56	3.21	2.93	2.70
1959	9.51	8.67	7.76	6.97	6.29	5.71	5.20	4.38	3.75	3.26	2.87	2.56	2.31	2.10
1958	7.49	6.92	6.28	5.73	5.24	4.81	4.43	3.80	3.30	2.90	2.57	2.30	2.08	1.90
1957	5.64	5.28	4.87	4.50	4.18	3.88	3.62	3.17	2.80	2.49	2.22	1.99	1.79	1.60
1956	4.08	3.88	3.63	3.42	3.22	3.04	2.89	2.61	2.40	2.22	2.08	1.97	1.88	1.80
1955	2.31	2.18	2.04	1.90	1.78	1.66	1.55	1.36	1.19	1.05	0.94	0.84	0.77	0.70
1954	1.62	1.56	1.49	1.42	1.35	1.28	1.21	1.09	0.99	0.89	0.80	0.72	0.66	0.60
1953	1.03	1.01	0.99	0.96	0.93	0.91	0.88	0.82	0.77	0.72	0.66	0.61	0.55	0.50
1952	0.54	0.54	0.54	0.54	0.54	0.54	0.54	0.54	0.54	0.54	0.54	0.54	0.54	0.54

A.12. Cumulative activities of ^{241}Pu with various mixing rates

YEAR	99%	95%	90%	85%	80%	75%	70%	60%	50%	40%	30%	20%	10%	0%
1996	5912	2657	1002	400	176	89	53	26	17	11	8	6	5	4
1995	5968	2792	1109	465	215	113	70	37	25	18	14	10	8	7
1994	6022	2932	1225	540	260	142	90	51	37	29	23	18	15	12
1993	6071	3074	1348	621	311	175	112	66	51	43	38	35	32	30
1992	6102	3205	1464	696	351	193	118	60	42	33	28	24	21	19
1991	6145	3354	1606	797	416	232	141	69	46	36	31	27	24	21
1990	6185	3508	1761	912	493	281	171	80	49	37	31	27	24	22
1989	6226	3669	1933	1047	589	346	213	97	55	38	30	25	22	19
1988	6269	3842	2126	1209	711	435	277	129	71	46	34	28	25	22
1987	6310	4021	2337	1397	862	550	364	177	98	60	40	29	23	19
1986	6354	4212	2576	1621	1053	708	493	264	158	103	72	53	42	35
1985	6383	4397	2823	1865	1273	898	654	381	245	169	121	88	63	43
1984	6404	4583	3088	2144	1536	1139	873	562	403	313	258	222	197	178
1983	6288	4636	3233	2312	1698	1281	992	640	449	337	266	219	186	160
1982	6190	4711	3414	2531	1922	1494	1188	799	577	440	352	294	252	222
1981	6028	4725	3547	2716	2124	1695	1380	962	709	546	434	356	302	265
1980	5821	4695	3647	2884	2324	1907	1593	1162	889	702	565	459	374	307
1979	5570	4619	3711	3032	2522	2134	1837	1425	1164	988	859	758	674	601
1978	5019	4230	3455	2860	2401	2044	1765	1374	1127	966	858	783	728	687
1977	4375	3729	3075	2556	2141	1808	1540	1144	878	696	569	477	408	357
1976	4059	3549	3020	2587	2231	1935	1690	1312	1043	849	706	599	517	451
1975	3644	3261	2855	2513	2225	1979	1770	1435	1184	995	851	741	658	595
1974	3080	2807	2511	2257	2037	1846	1678	1399	1178	1000	853	730	626	536
1973	2570	2391	2195	2025	1877	1747	1632	1439	1285	1160	1057	972	900	841
1972	1747	1632	1504	1393	1295	1208	1130	998	889	798	721	654	596	544
1971	1215	1145	1067	999	939	886	838	757	690	635	590	551	519	491
1970	732	689	641	598	561	527	496	443	399	361	330	303	280	260
1969	477	451	423	398	376	356	337	305	278	254	232	213	196	181
1968	299	285	269	256	244	233	224	207	194	182	172	163	156	149
1967	152	143	134	126	119	113	107	98	90	84	78	73	69	65
1966	87	82	76	71	67	63	60	54	50	46	43	40	38	36
1965	52	48	44	41	38	36	33	29	26	24	21	19	18	17
1964	35	33	31	29	27	25	24	21	19	17	16	14	13	12
1963	23	22	21	20	19	18	17	16	14	13	12	12	11	10
1962	13	13	12	11	11	10	10	9	8	8	8	7	7	7
1961	7	6	6	5	5	5	5	4	4	4	3	3	3	3
1960	4	4	3	3	3	2	2	2	2	1	1	1	1	1
1959	3	3	2	2	2	2	2	1	1	1	1	1	1	1
1958	2	2	2	2	2	1	1	1	1	1	1	1	1	1
1957	2	2	2	1	1	1	1	1	1	1	1	1	1	0
1956	1	1	1	1	1	1	1	1	1	1	1	1	1	0
1955	1	1	1	1	1	1	1	0	0	0	0	0	0	0
1954	1	1	1	1	1	0	0	0	0	0	0	0	0	0
1953	0	0	0	0	0	0	0	0	0	0	0	0	0	0
1952	0	0	0	0	0	0	0	0	0	0	0	0	0	0

A.13. Ratios of $^{238}Pu/^{239,240}Pu$ in discharges with various mixing rates

YEAR	99%	95%	90%	85%	80%	75%	70%	60%	50%	40%	30%	20%	10%	0%
1996	0.18	0.19	0.22	0.24	0.26	0.29	0.31	0.34	0.35	0.36	0.37	0.38	0.38	0.39
1995	0.18	0.19	0.22	0.24	0.26	0.29	0.31	0.33	0.34	0.34	0.34	0.34	0.34	0.34
1994	0.18	0.19	0.22	0.24	0.26	0.28	0.30	0.33	0.34	0.34	0.34	0.34	0.33	0.33
1993	0.18	0.19	0.22	0.24	0.26	0.28	0.30	0.33	0.34	0.34	0.35	0.35	0.35	0.36
1992	0.18	0.19	0.21	0.23	0.25	0.27	0.29	0.31	0.32	0.32	0.32	0.33	0.33	0.33
1991	0.18	0.19	0.21	0.23	0.25	0.27	0.28	0.30	0.31	0.31	0.31	0.31	0.30	0.30
1990	0.18	0.19	0.21	0.23	0.25	0.26	0.28	0.30	0.32	0.32	0.32	0.32	0.32	0.32
1989	0.18	0.19	0.21	0.23	0.25	0.26	0.27	0.29	0.31	0.32	0.32	0.33	0.32	0.32
1988	0.18	0.19	0.21	0.23	0.24	0.26	0.27	0.29	0.31	0.32	0.33	0.34	0.35	0.35
1987	0.18	0.19	0.21	0.23	0.24	0.25	0.26	0.28	0.29	0.30	0.30	0.31	0.32	0.33
1986	0.17	0.19	0.21	0.23	0.24	0.25	0.26	0.27	0.28	0.28	0.28	0.28	0.28	0.28
1985	0.17	0.19	0.21	0.22	0.24	0.25	0.26	0.27	0.28	0.28	0.28	0.28	0.28	0.28
1984	0.17	0.19	0.21	0.22	0.24	0.25	0.26	0.27	0.28	0.28	0.28	0.28	0.28	0.28
1983	0.17	0.19	0.20	0.22	0.23	0.24	0.25	0.27	0.28	0.28	0.28	0.29	0.29	0.30
1982	0.17	0.18	0.20	0.22	0.23	0.24	0.25	0.26	0.27	0.27	0.27	0.27	0.26	0.26
1981	0.17	0.18	0.20	0.21	0.22	0.24	0.24	0.26	0.27	0.28	0.29	0.29	0.29	0.29
1980	0.16	0.18	0.19	0.21	0.22	0.23	0.24	0.25	0.26	0.27	0.28	0.29	0.29	0.30
1979	0.16	0.17	0.18	0.20	0.21	0.21	0.22	0.23	0.24	0.25	0.26	0.26	0.27	0.27
1978	0.15	0.16	0.17	0.18	0.19	0.20	0.20	0.21	0.21	0.22	0.22	0.22	0.22	0.22
1977	0.14	0.15	0.16	0.17	0.18	0.18	0.19	0.20	0.20	0.21	0.21	0.21	0.22	0.22
1976	0.13	0.14	0.15	0.16	0.17	0.17	0.18	0.19	0.19	0.19	0.20	0.20	0.20	0.19
1975	0.13	0.14	0.15	0.15	0.16	0.17	0.17	0.18	0.19	0.19	0.20	0.20	0.21	0.21
1974	0.12	0.13	0.14	0.14	0.15	0.15	0.16	0.16	0.17	0.17	0.17	0.17	0.17	0.17
1973	0.11	0.12	0.13	0.14	0.14	0.15	0.15	0.16	0.16	0.16	0.17	0.17	0.17	0.17
1972	0.10	0.11	0.12	0.12	0.13	0.13	0.14	0.15	0.16	0.16	0.17	0.17	0.17	0.17
1971	0.08	0.09	0.10	0.10	0.11	0.11	0.12	0.13	0.13	0.14	0.15	0.15	0.16	0.16
1970	0.06	0.06	0.07	0.07	0.07	0.08	0.08	0.08	0.09	0.09	0.09	0.09	0.10	0.10
1969	0.05	0.05	0.06	0.06	0.06	0.06	0.06	0.07	0.07	0.07	0.08	0.08	0.08	0.08
1968	0.04	0.04	0.05	0.05	0.05	0.05	0.05	0.05	0.06	0.06	0.06	0.06	0.06	0.06
1967	0.04	0.04	0.04	0.04	0.04	0.04	0.04	0.05	0.05	0.05	0.05	0.05	0.05	0.06
1966	0.03	0.03	0.03	0.03	0.03	0.03	0.03	0.04	0.04	0.04	0.04	0.04	0.04	0.04
1965	0.03	0.03	0.03	0.03	0.03	0.03	0.03	0.03	0.03	0.03	0.03	0.03	0.03	0.03
1964	0.02	0.02	0.02	0.02	0.02	0.03	0.03	0.03	0.03	0.03	0.03	0.03	0.03	0.03
1963	0.02	0.02	0.02	0.02	0.02	0.02	0.02	0.02	0.02	0.02	0.02	0.02	0.02	0.02
1962	0.02	0.02	0.02	0.02	0.02	0.02	0.02	0.02	0.02	0.02	0.02	0.02	0.02	0.02
1961	0.02	0.02	0.02	0.02	0.02	0.02	0.02	0.02	0.02	0.02	0.02	0.02	0.02	0.02
1960	0.02	0.02	0.02	0.02	0.02	0.02	0.02	0.02	0.02	0.02	0.02	0.02	0.02	0.02
1959	0.02	0.02	0.02	0.02	0.02	0.02	0.02	0.02	0.02	0.02	0.02	0.02	0.02	0.02
1958	0.02	0.02	0.02	0.02	0.02	0.02	0.02	0.02	0.02	0.02	0.02	0.02	0.02	0.02
1957	0.02	0.02	0.02	0.02	0.02	0.02	0.02	0.02	0.02	0.02	0.02	0.02	0.02	0.02
1956	0.02	0.02	0.02	0.02	0.02	0.02	0.02	0.02	0.02	0.02	0.02	0.02	0.02	0.02
1955	0.02	0.02	0.02	0.02	0.02	0.02	0.02	0.02	0.02	0.02	0.02	0.02	0.02	0.02
1954	0.03	0.03	0.03	0.03	0.03	0.03	0.03	0.03	0.02	0.02	0.02	0.02	0.02	0.02
1953	0.03	0.03	0.03	0.03	0.03	0.03	0.03	0.03	0.03	0.03	0.03	0.03	0.03	0.03
1952	0.03	0.03	0.03	0.03	0.03	0.03	0.03	0.03	0.03	0.03	0.03	0.03	0.03	0.03

A.14. Ratios of $^{241}Pu/^{239,240}Pu$ with various mixing rates

YEAR	99%	95%	90%	85%	80%	75%	70%	60%	50%	40%	30%	20%	10%	0%
1996	12.1	13.1	14.4	16.0	17.9	20.3	22.8	26.0	26.9	27.1	27.0	26.9	26.9	26.6
1995	12.1	13.1	14.4	15.9	17.8	20.1	22.6	25.9	27.0	27.3	27.4	27.6	28.0	29.0
1994	12.1	13.1	14.4	15.8	17.5	19.7	22.0	25.4	26.4	26.4	26.0	25.3	24.4	23.1
1993	12.1	13.1	14.3	15.7	17.3	19.5	21.9	26.1	28.2	29.2	29.8	30.2	30.5	30.8
1992	12.0	13.0	14.1	15.3	16.6	18.1	19.8	23.2	25.3	26.2	26.6	26.9	27.0	27.1
1991	12.0	13.0	14.1	15.1	16.2	17.5	18.9	21.8	23.9	25.0	25.6	25.9	26.1	26.1
1990	12.0	12.9	14.0	14.9	15.9	16.9	18.0	20.3	22.3	23.6	24.4	25.0	25.5	25.9
1989	12.0	12.9	13.9	14.8	15.6	16.4	17.2	18.7	20.0	20.9	21.3	21.6	21.6	21.6
1988	12.0	12.9	13.8	14.7	15.5	16.2	16.9	18.1	19.2	20.1	20.9	21.4	21.9	22.2
1987	11.9	12.8	13.8	14.6	15.3	15.9	16.5	17.4	18.1	18.5	18.7	18.9	19.1	19.4
1986	11.9	12.8	13.7	14.6	15.2	15.8	16.4	17.2	17.8	18.1	18.1	17.9	17.7	17.7
1985	11.9	12.8	13.7	14.5	15.2	15.8	16.3	17.2	17.9	18.3	18.5	18.4	17.8	16.7
1984	11.9	12.7	13.7	14.5	15.1	15.7	16.2	17.2	18.1	19.0	19.8	20.5	21.1	21.5
1983	11.7	12.5	13.4	14.0	14.6	15.0	15.3	15.8	16.1	16.5	16.8	17.2	17.7	18.4
1982	11.6	12.4	13.2	13.8	14.2	14.6	14.8	15.0	15.1	15.0	14.8	14.5	14.2	13.9
1981	11.5	12.3	13.1	13.8	14.3	14.7	15.0	15.5	16.0	16.3	16.7	17.0	17.3	17.7
1980	11.4	12.1	12.9	13.5	13.9	14.3	14.5	14.9	15.1	15.2	15.4	15.4	15.4	15.3
1979	11.2	11.9	12.7	13.3	13.7	14.1	14.3	14.7	15.0	15.2	15.4	15.5	15.7	15.8
1978	10.8	11.5	12.2	12.8	13.2	13.5	13.7	14.0	14.1	14.3	14.4	14.6	14.8	14.9
1977	10.4	11.0	11.7	12.2	12.6	12.8	13.0	13.1	13.0	12.8	12.6	12.4	12.3	12.3
1976	10.2	10.9	11.6	12.2	12.6	13.0	13.2	13.5	13.5	13.4	13.1	12.7	12.3	11.9
1975	10.1	10.8	11.6	12.2	12.8	13.4	13.8	14.6	15.2	15.7	16.1	16.4	16.7	17.0
1974	9.3	10.0	10.7	11.3	11.8	12.2	12.6	13.3	13.7	14.0	14.2	14.3	14.2	14.1
1973	8.7	9.3	10.0	10.6	11.1	11.6	12.0	12.8	13.4	13.9	14.4	14.8	15.2	15.6
1972	7.2	7.6	8.2	8.7	9.1	9.4	9.7	10.2	10.6	10.9	11.2	11.3	11.5	11.6
1971	6.1	6.5	7.0	7.5	7.8	8.2	8.5	9.0	9.4	9.8	10.1	10.3	10.5	10.7
1970	4.7	5.1	5.4	5.8	6.1	6.3	6.5	6.9	7.3	7.6	7.8	8.0	8.2	8.4
1969	3.8	4.1	4.4	4.7	4.9	5.1	5.3	5.6	5.8	6.0	6.2	6.4	6.5	6.7
1968	3.0	3.2	3.5	3.7	3.9	4.1	4.2	4.5	4.7	4.8	5.0	5.1	5.2	5.3
1967	2.1	2.3	2.5	2.6	2.8	2.9	3.0	3.2	3.4	3.5	3.6	3.7	3.8	3.8
1966	1.6	1.7	1.8	2.0	2.1	2.2	2.3	2.4	2.5	2.6	2.7	2.7	2.8	2.8
1965	1.2	1.3	1.4	1.5	1.6	1.7	1.7	1.9	2.0	2.1	2.2	2.3	2.4	2.4
1964	1.0	1.0	1.1	1.2	1.2	1.3	1.4	1.5	1.6	1.7	1.8	1.9	2.1	2.2
1963	0.8	0.8	0.8	0.9	0.9	1.0	1.0	1.1	1.1	1.1	1.2	1.2	1.2	1.3
1962	0.6	0.6	0.6	0.7	0.7	0.7	0.8	0.8	0.8	0.9	0.9	0.9	1.0	1.0
1961	0.4	0.4	0.4	0.5	0.5	0.5	0.5	0.5	0.6	0.6	0.6	0.6	0.6	0.7
1960	0.3	0.3	0.3	0.3	0.3	0.3	0.3	0.3	0.3	0.4	0.4	0.4	0.4	0.4
1959	0.3	0.3	0.3	0.3	0.3	0.3	0.3	0.3	0.3	0.3	0.3	0.3	0.3	0.3
1958	0.3	0.3	0.3	0.3	0.3	0.3	0.3	0.3	0.3	0.3	0.3	0.3	0.3	0.3
1957	0.3	0.3	0.3	0.3	0.3	0.3	0.3	0.3	0.3	0.3	0.3	0.3	0.3	0.3
1956	0.3	0.3	0.3	0.3	0.3	0.3	0.3	0.3	0.3	0.3	0.3	0.3	0.3	0.3
1955	0.4	0.4	0.4	0.4	0.4	0.4	0.4	0.4	0.4	0.4	0.4	0.4	0.4	0.3
1954	0.4	0.4	0.4	0.4	0.4	0.4	0.4	0.4	0.4	0.4	0.4	0.4	0.4	0.5
1953	0.3	0.3	0.3	0.3	0.3	0.3	0.3	0.3	0.3	0.3	0.3	0.3	0.2	0.2
1952	0.4	0.4	0.4	0.4	0.4	0.4	0.4	0.4	0.4	0.4	0.4	0.4	0.4	0.4

A.15. Ratios of $^{241}Pu/^{238}Pu$ with various mixing rates

YEAR	99%	95%	90%	85%	80%	75%	70%	60%	50%	40%	30%	20%	10%	0%
1996	68.4	67.5	66.7	66.6	67.9	70.3	73.3	76.8	76.9	75.5	73.7	71.8	69.8	67.7
1995	68.4	67.5	66.7	66.6	67.9	70.5	73.8	78.7	80.3	80.7	80.9	81.4	82.8	85.3
1994	68.3	67.4	66.6	66.4	67.4	69.7	72.7	77.4	78.7	78.2	77.0	75.3	73.0	70.1
1993	68.3	67.4	66.6	66.3	67.3	69.7	73.1	79.8	83.3	84.7	85.4	85.8	86.0	86.3
1992	68.3	67.3	66.2	65.6	65.8	67.0	69.3	75.1	79.3	81.4	82.3	82.5	82.3	81.8
1991	68.2	67.2	66.0	65.2	65.0	65.7	67.3	72.4	77.4	80.8	83.1	84.8	86.1	87.1
1990	68.2	67.1	65.8	64.8	64.2	64.1	64.7	67.4	70.5	73.1	75.2	77.0	78.6	80.0
1989	68.2	67.1	65.7	64.5	63.6	63.1	63.0	63.6	64.5	65.2	65.7	66.3	66.9	67.4
1988	68.2	67.1	65.7	64.4	63.4	62.8	62.6	62.7	63.0	63.0	62.7	62.7	63.0	63.4
1987	68.2	67.1	65.7	64.4	63.4	62.8	62.5	62.6	62.9	62.6	61.6	60.4	59.4	58.7
1986	68.2	67.1	65.8	64.5	63.6	63.0	62.7	63.1	64.0	64.6	64.4	63.7	62.9	62.7
1985	68.2	67.2	65.8	64.6	63.6	63.0	62.7	63.2	64.4	65.6	66.2	65.8	64.0	60.0
1984	68.3	67.2	65.9	64.7	63.7	63.1	62.9	63.6	65.4	67.8	70.3	72.7	74.8	76.6
1983	68.1	66.9	65.3	63.8	62.3	61.1	60.1	58.9	58.5	58.7	59.3	60.1	61.0	62.2
1982	68.3	67.1	65.5	63.9	62.4	61.0	59.7	57.9	56.7	55.8	55.3	54.8	54.3	53.7
1981	69.0	67.9	66.5	65.1	63.7	62.4	61.3	59.7	58.7	58.3	58.3	58.7	59.4	60.6
1980	69.4	68.4	67.1	65.6	64.2	62.8	61.5	59.4	57.7	56.3	55.0	53.8	52.5	51.3
1979	70.8	70.1	69.0	67.9	66.7	65.6	64.6	62.9	61.7	60.9	60.2	59.6	59.0	58.2
1978	72.7	72.3	71.6	70.8	69.9	69.1	68.3	66.9	65.9	65.5	65.5	65.9	66.4	67.1
1977	73.7	73.4	72.8	72.0	71.2	70.2	69.1	66.7	64.2	61.8	59.8	58.1	56.9	56.1
1976	75.8	75.8	75.7	75.5	75.2	74.7	74.2	72.8	71.1	69.2	67.1	65.0	63.0	61.0
1975	78.1	78.6	79.1	79.5	79.9	80.2	80.6	81.1	81.5	81.7	81.6	81.4	81.2	81.1
1974	77.6	78.1	78.6	79.1	79.5	79.9	80.3	81.1	81.9	82.5	82.9	82.8	82.2	80.9
1973	76.9	77.5	78.0	78.5	79.0	79.5	80.0	81.3	82.7	84.5	86.4	88.6	90.8	93.1
1972	70.9	71.0	70.9	70.6	70.3	70.0	69.6	68.9	68.4	67.9	67.6	67.4	67.3	67.4
1971	72.6	72.9	72.9	72.8	72.5	72.2	71.7	70.8	69.8	68.9	67.9	67.0	66.2	65.3
1970	78.6	79.8	81.0	81.8	82.5	83.0	83.3	83.8	84.2	84.5	84.7	84.8	85.1	85.3
1969	75.3	76.8	78.3	79.4	80.2	80.8	81.2	81.8	82.2	82.3	82.3	82.1	81.7	81.2
1968	72.1	74.1	76.2	77.9	79.2	80.3	81.3	82.8	84.1	85.2	86.4	87.5	88.6	89.7
1967	60.3	62.3	64.3	65.8	67.0	67.8	68.5	69.2	69.6	69.7	69.7	69.6	69.5	69.4
1966	54.9	57.4	60.0	62.3	64.2	65.7	67.0	68.8	70.0	70.6	70.9	71.1	71.1	71.1
1965	47.2	49.7	52.6	55.2	57.5	59.6	61.5	64.6	67.0	68.8	70.1	71.0	71.4	71.6
1964	40.6	42.8	45.4	47.8	50.0	52.1	54.0	57.3	60.3	62.9	65.3	67.6	69.7	71.8
1963	33.2	34.8	36.7	38.5	40.2	41.7	43.1	45.5	47.5	49.2	50.7	51.9	52.9	53.8
1962	25.6	26.7	28.1	29.5	30.8	32.0	33.2	35.3	37.1	38.7	40.1	41.3	42.4	43.5
1961	18.4	18.9	19.6	20.3	20.9	21.6	22.3	23.6	24.7	25.8	26.7	27.5	28.3	29.0
1960	14.4	14.4	14.6	14.7	14.8	15.0	15.1	15.4	15.7	16.0	16.3	16.5	16.7	16.8
1959	13.7	13.7	13.7	13.7	13.8	13.8	13.9	14.0	14.2	14.4	14.6	14.8	15.1	15.3
1958	13.3	13.2	13.2	13.1	13.1	13.1	13.0	13.0	12.9	12.9	12.9	13.0	13.0	13.0
1957	13.4	13.3	13.3	13.2	13.1	13.1	13.0	12.9	12.8	12.8	12.8	12.8	12.9	13.1
1956	13.5	13.4	13.4	13.3	13.2	13.1	13.0	12.8	12.6	12.3	12.1	11.8	11.6	11.4
1955	15.1	15.2	15.3	15.4	15.5	15.7	15.8	16.1	16.4	16.6	16.9	17.0	17.0	16.8
1954	14.5	14.6	14.7	14.7	14.8	15.0	15.1	15.4	15.8	16.3	16.9	17.6	18.5	19.6
1953	11.9	11.8	11.7	11.6	11.5	11.4	11.3	11.0	10.7	10.3	9.9	9.4	8.9	8.2
1952	15.7	15.7	15.7	15.7	15.7	15.7	15.7	15.7	15.7	15.7	15.7	15.7	15.7	15.7

A.16. $^{238}Pu/^{239,240}Pu$ ratios in cores

Depth (cm)	I-96-002 Core	R-96-000 Core	R-96-007 Core	R-96-008 Core
1	0.21	0.20	0.21	0.22
2	0.20	0.21	0.21	0.21
3	0.11	0.20	0.22	0.22
4	0.21	0.20	0.21	0.22
5	0.22	0.21	0.22	0.22
6	0.22	0.20	0.22	0.21
7	0.23	0.22	0.22	0.22
8	0.22	0.21	0.22	0.21
9	0.23	0.22	0.23	0.19
10	0.23	0.22	0.21	0.21
11		0.22		
12	0.25	0.21	0.21	0.20
13		0.21		
14	0.23	0.22	0.21	0.17
15		0.22		
16	0.22	0.21	0.21	0.12
17		0.22		
18	0.20	0.20	0.21	0.09
19		0.20		
20	0.22	0.19	0.10	0.07
21				
22	0.23	0.13	0.07	0.06
23				
24	0.22	0.09	0.02	0.05
25				
26	0.20	0.08	0.01	0.04
27				
28	0.16	0.04	0.01	0.04
29				
30		0.03	0.09	0.03
31				
32		0.03	0.01	0.03
33				
34		0.13	0.07	0.03
35				
36		0.16	0.06	0.02
37				
38			0.20	0.01
39				
40			0.15	0.01
41				
42			0.10	0.01
43				
44			0.10	0.01
45				
46			0.25	0.01
47				
48			0.29	0.01
49				
50			0.69	0.01
51				
52			1.33	0.03
53				
54			1.00	0.01
55				
56				0.08
57				
58				0.17
59				
60				0.02

A.17. $^{241}Pu/^{239,240}Pu$ ratios in cores

Depth (cm)	I-96-002 Core	R-96-000 Core	R-96-007 Core	R-96-008 Core
1	13.1	13.2	12.8	14.1
2	14.1	13.3	12.5	13.0
3	6.9	13.2	14.1	13.1
4	13.8	13.3	13.9	13.0
5	14.3	13.7	14.8	12.7
6	14.9	13.3	14.0	11.9
7	14.9	14.9	14.7	12.6
8	15.7	14.8	14.4	11.5
9	15.8	14.6	16.0	11.6
10	15.2	14.9	15.1	11.0
11		14.8		
12	15.6	14.9	13.9	9.0
13		14.5		
14	14.6	14.5	13.5	8.3
15		14.5		
16	14.6	13.4	11.9	6.8
17		12.9		
18	13.6	11.3	10.5	6.4
19		10.9		
20	14.3	9.8	6.6	4.8
21				
22	13.8	7.4	4.8	4.5
23				
24	13.4	5.6	1.8	3.8
25				
26	12.3	5.0	0.6	3.4
27				
28	9.7	2.7	0.5	2.6
29				
30		2.0	5.4	2.1
31				
32		1.2		2.1
33				
34		7.3		2.0
35				
36		9.8		1.2
37				
38			15.1	0.9
39				
40			12.2	0.7
41				
42			1.3	0.5
43				
44			3.6	0.4
45				
46			13.5	0.5
47				
48				0.5
49				
50				0.7
51				
52				1.7
53				
54			80.0	1.6
55				
56				13.6
57				
58				19.3
59				
60				9.2

A.18. $^{241}Pu/^{238}Pu$ ratios in cores

Depth (cm)	I-96-002 Core	R-96-000 Core	R-96-007 Core	R-96-008 Core
1	61.9	64.3	60.8	65.3
2	69.2	64.2	59.9	61.8
3	63.4	64.8	64.4	60.7
4	66.0	65.1	66.7	58.4
5	65.8	65.0	66.0	58.5
6	68.0	65.4	65.0	55.9
7	65.6	67.2	67.1	58.4
8	70.4	69.3	66.1	54.3
9	69.3	66.7	69.8	62.3
10	66.7	68.9	70.7	51.8
11		66.6		
12	63.4	70.4	67.1	46.0
13		67.9		
14	63.7	67.4	63.5	48.5
15		67.0		
16	65.6	62.4	57.1	55.0
17		59.8		
18	66.2	57.1	49.7	68.2
19		54.7		
20	64.0	51.2	68.4	67.7
21				
22	59.9	58.6	72.6	73.9
23				
24	60.6	62.2	77.1	74.4
25				
26	60.6	60.4	50.0	79.6
27				
28	61.0	62.2	51.8	69.2
29				
30		62.6	57.1	75.0
31				
32		39.8		82.2
33				
34		56.2		68.7
35				
36		61.6		68.2
37				
38			74.0	69.8
39				
40			80.5	62.4
41				
42			13.3	41.0
43				
44			37.4	37.3
45				
46			53.6	71.7
47				
48				89.3
49				
50				69.9
51				
52				62.6
53				
54			80.0	116.5
55				
56				165.1
57				
58				111.0
59				
60				517.6

A.19. Ratios of $^{238}Pu/^{239,240}Pu$ in 1997 surface scrape samples

	A	V	B	W	C	X	D	Y	E	Z	F
0			0.20	0.21	0.21	0.21	0.21	0.21	0.21		
1	0.21	0.19	0.20	0.20	0.21	0.20	0.21	0.19	0.20	0.20	0.20
2	0.20	0.21	0.20	0.22	0.21	0.20	0.20	0.21	0.20	0.21	0.20
3	0.20	0.20	0.20	0.20	0.20	0.21	0.20	0.20	0.16	0.20	0.21
4	0.20	0.20	0.20	0.20	0.22	0.21	0.20	0.20	0.21	0.21	0.22
5	0.21	0.20	0.19	0.21	0.20	0.21	0.20	0.21	0.20	0.21	0.20
6	0.21	0.21	0.20	0.21	0.21	0.21	0.21	0.20	0.18	0.21	0.22
7	0.21	0.21	0.21	0.21	0.21	0.21	0.20				
8	0.20	0.18	0.21	0.22	0.21						
9	0.20	0.20	0.20	0.20	0.21						
10	0.20	0.20	0.21	0.20							
11	0.21										

A.20. Ratios of $^{241}Pu/^{239,240}Pu$ in 1997 surface scrape samples

	A	V	B	W	C	X	D	Y	E	Z	F
0			13.5	13.5	13.4	13.1	13.2	13.1	14.1		
1	13.3	12.8	12.6	12.7	12.3	12.9	13.0	12.4	12.3	13.0	13.4
2	13.4	13.3	13.9	12.4	13.6	12.4	12.8	13.7	13.5	13.6	13.1
3	12.9	12.6	13.2	13.0	13.1	13.9	12.7	12.8	11.5	13.7	13.9
4	13.2	13.6	13.6	12.7	13.4	14.1	13.9	12.7	13.7	13.5	14.7
5	12.4	12.7	11.6	13.0	12.7	13.4	13.7	13.6	13.1	13.4	13.4
6	13.4	12.6	12.4	12.3	13.1	12.7	13.6	13.3	12.6	13.2	14.8
7	13.3	13.1	13.6	13.3	12.8	13.8	12.3				
8	12.8	11.7	12.9	13.1	13.2						
9	13.5	13.0	13.4	13.3	13.8						
10	12.6	13.1	13.2	11.8							
11	13.0										

A.21. Ratios of $^{241}Pu/^{238}Pu$ in 1997 surface scrape samples

	A	V	B	W	C	X	D	Y	E	Z	F
0			66.4	63.3	63.9	62.8	63.7	63.6	67.9		
1	64.2	66.6	62.9	62.9	57.5	64.6	63.2	65.0	62.5	66.5	65.6
2	67.1	64.6	69.5	55.4	63.8	62.2	64.2	64.8	69.3	65.6	64.8
3	65.8	62.7	67.6	64.6	65.5	65.1	63.3	63.0	73.2	67.1	67.0
4	65.2	66.6	68.5	63.7	62.2	67.8	68.6	63.8	64.3	65.3	66.9
5	60.3	63.2	62.6	63.2	62.1	65.0	69.1	66.0	64.7	63.3	66.2
6	64.9	59.7	62.3	58.8	63.6	60.0	65.3	65.1	68.2	62.7	67.9
7	65.0	63.6	63.4	64.7	60.1	66.1	62.9				
8	64.7	64.2	62.9	60.3	64.1						
9	67.4	65.2	65.9	65.4	66.2						
10	62.6	65.1	64.2	57.8							
11	63.5										

A.22. Loss on ignition data for surface scrape samples (%)

	A	V	B	W	C	X	D	Y	E	Z	F
0			19.1	27.3	15.6	15.0	14.4	20.2	24.0		
1	23.5	15.7	9.7	11.1	11.1	12.3	11.1	12.8	11.4	13.5	14.8
2	16.1	11.3	13.4	15.3	15.6	10.2	8.5	10.9	11.9	14.7	14.1
3	17.1	14.4	15.0	12.8	8.4	11.0	8.1	10.0	7.6	10.8	10.2
4	16.1	15.8	14.7	15.4	13.0	9.3	10.4	12.2	9.8	9.8	10.3
5	15.5	15.8	15.8	14.6	13.7	12.9	14.1	12.4	10.3	9.8	7.7
6	13.7	13.1	14.2	14.1	12.3	10.8	10.0	8.3	6.7	7.8	7.4
7	12.5	12.5	11.3	10.6	9.5	8.5	8.9				
8	10.3	8.3	9.9	9.8	10.1						
9	10.0	11.7	9.2	9.8	6.9						
10	10.5	9.7	8.9	6.5							
11	8.0										

A.23. Publications

PAPER

Borate Fusion Followed by Ion-Exchange/Extraction Chromatography for the Rapid Determination of Pu and U in Environmental Materials

Ian W. Croudace, Phillip E. Warwick, Rex N. Taylor, Stephen J. Dee, James A. Milton and Jung-Suk Oh
School of Ocean and Earth Science, Southampton Oceanography Centre, UK

A method for actinide determinations has been established which has considerable advantages over currently described procedures. The benefits are rapid sample throughput, good safety features with no compromise in data quality. A borate fusion is used for the sample digestion. Chemical separation is optimised by using a column of anion-exchange resin column stacked on a UTEVA column. Uranium was measured using thermal ionisation mass spectrometry with a precision of 0.2% 2 sigma. Pu measurements were made using alpha-particle spectrometry. The procedure has been applied successfully to a wide range of sample types and other actinide elements (Th, Am, etc.) could also be included in the analytical scheme. The method has been thoroughly evaluated by measuring international reference samples. The method lends itself very well to large-scale environmental surveys.

Introduction

Numerous methods have been published for the determination of plutonium and uranium in soils and other environmental samples. These frequently involve an acid attack to leach or dissolve the sample or a fusion whereby the complete sample is opened-out.

Acid digestions

The initial digestion of soil by fusion or with one or more mineral acids (nitric, hydrochloric and hydrofluoric acids) is intended to dissolve any refractory PuO_2 present in soils or other matrices. Dissolution of any intractable PuO_2 prior to chemical separation is imperative but is not always effected by acid attack. In soil samples, it is important that any dissolution/digestion procedure should open-out the minerals present. Extraction of Pu and U can be achieved by leaching the sample with mineral acids (Talvitie, 1971; Meadows et al., 1975). Leaching allows large sample sizes to be processed although comparison of results obtained following preparation by either acid leaching and complete dissolution have shown that leaching is not appropriate for soils contaminated with refractory PuO_2 (Smith et al., 1992). Leaching with HF and HNO_3 (Talvitie 1971)) or with aqua regia followed by an attack on the residue with HF is more effective than simple leaching but is time-consuming and potentially very hazardous. The use of HF for the dissolution of PuO_2 in soils can result in up to 50% of the Pu remaining with insoluble fluorides and these residues must be attacked further with nitric/perchloric acids followed by boric acid to ensure complete dissolution of the fluorides. Microwave digestion of the sample under pressure with various mineral acids has also proved effective in the analysis of geological samples but can only treat a small sample size (up to 1 g). A high-pressure microwave digestion technique for the dissolution of PuO_2 in 2-g soil samples has been described (Smith and Yaeger, 1996).

Sample fusion

The problems associated with the partial dissolution of Pu during leaching can be overcome via a complete dissolution of the sample by fusion with an appropriate flux. Fusion with alkali hydroxides (Smith et al., 1995) can be suitable for reasonable sample sizes (up to 5 g) but sample composition can seriously affect the efficiency of this technique. Fusion of 1 g

Borate Fusion Followed by Ion-Exchange/Extraction Chromatography for the Rapid Determination of Pu and U in Environmental Materials

I.W. Croudace, P.E. Warwick, R.N. Taylor, S.J. Dee, J.A. Milton and J-S Oh

of soil with sodium carbonate resulted in an average of 1.8% of the Pu remaining in the insoluble siliceous fraction (Levine and Lamanna, 1965). Potassium fluoride, mixed fluoride/bifluoride fusions (Sill and Sill, 1995) and mixed potassium fluoride and potassium pyrosulphate fusions (Sill et al., 1974; Thomson, 1982) are very effective but liberate significant quantities of HF and sulphuric acid fumes and require great care and appropriate laboratory fume-extraction/-scrubbing for safe application. Most of the above fusion methods (except for the fluoride-only fusions) cause significant attack of the fusion vessel which can be a significant cost issue.

Borate fusions

The effective analysis of ceramics and geological samples (Bennett and Oliver, 1992) using borate fluxes is long established but does not seem to have received attention in the radiochemical field. High-purity fluxes containing negligible levels of U and Pu are readily available and are widely used in x-ray fluorescence analysis for trace element determinations. These fluxes rapidly dissolve most silicates, carbonates, sulphates, oxides etc. at a range of sample:flux ratios producing fluid melts at 1100-1200 °C. Opening-out of minerals and dissolution of silicate-oxide materials is readily achieved in 5-10 minutes. The resulting glass (plus any excess calcined carbonate) can be dissolved in dilute or strong acid with the precipitation of boric acid and silica gel. The ratio of sample to flux can be controlled thereby permitting larger sample sizes to be analysed.

Chemical separations

Most techniques for the purification of Pu and U have used anion-exchange chromatography (Talvitie, 1971), solvent extraction (Levine and Lamanna, 1965) and extraction chromatography (Jia et al., 1989; Delle Site et al., 1989; Smith et al., 1995; Horwitz et al., 1995).

Measurements

Pu is normally measured using alpha-particle spectrometry, although mass-spectrometric techniques have been published which have the advantage of providing separate information on ^{239}Pu and ^{240}Pu (McCormick 1992; Fassett and Kelly, 1984; Toole et al., 1990). U measurements can be made using either alpha-particle spectrometry (for ^{238}U, ^{234}U and to a lesser extent ^{235}U) or a mass spectrometric technique (for ^{238}U, ^{235}U and possibly ^{234}U although this isotope is present at very low concentrations). Since the mass spectrometric methods count ions rather than decays they are able to measure lower concentrations of ^{235}U and ^{238}U in samples than radiometric determinations and with greater precision. Thermal ionisation mass spectrometry, TIMS provides precision of nominally 0.1% (95% uncertainty) compared with approximately 1-2% for ICP-MS. TIMS precision and sensitivity depends to a certain extent on whether the instrument has a single-sector, a single-sector with an energy filter or double-sector. The precision tends to increase slightly in the order stated.

Experimental

A VG Sector-54 single-sector, thermal ionisation mass spectrometer was used to measure U isotopic ratios and concentrations using a single Daly detector. All sample and standard measurements were made by ensuring that at least 350 ng U was loaded onto single Re filaments coated with colloidal graphite. This loading was found to be the minimum that could be used to limit and control within-run mass fractionation effects. Each turret was loaded with two natural U standards to monitor accuracy. In addition, 235/238 ratios were corrected for non-linearity of the Daly detector by 0.12% per 10^{-11} Amps. Measurement uncertainty is better than 0.4% 2S.E. for 236/238, and better than 0.09% for 235/238. The precision, assessed on multiple runs of the CANMET natural uranium standard (CCRMP BL-1a), is better than 0.175% 2 s.d. (n = 78) on 235/238. Further details of the methodology have been published separately (Taylor et al., 1998).

Pu was measured using an EG&G Octete alpha-particle spectrometry system. Electrodepositing of the Pu onto stainless steel planchettes was achieved using a 2% ammonium oxalate electrolyte solution. Count-times of 2-3 days provided uncertainties of 5% at the 95% confidence level for ^{239,240}Pu.

Choice of isotopic spikes

^{234}U was chosen as the spike for the U determinations (concentrations and isotope ratio determinations). Uranium-233 would have been equally suitable. Plutonium-242 was chosen as the spike for Pu determinations. Plutonium-242 and ^{236}U standards of known activity were supplied by Amersham International Plc. Samples were spiked with the appropriate amount of ^{242}Pu and ^{236}U tracers (equivalent to 700 ng ^{236}U and 50 mBq ^{242}Pu) prior to fusion.

The fusion procedure

Seven g of Lithium borate flux (ICPH, France) was mixed with 5 g of soil. Fusions were performed in 35-mL grain-stabilised Pt-Au (95%-5%) dishes (Englehardt Industries) at 1200 °C in a resistance furnace. Eight 35-mL dishes at a time were inserted into the furnace and left for at least 15 minutes with periodic swirling using long Pt-tipped furnace tongs. The dishes were removed, one at a time, from the furnace and the melt poured into 250-mL beakers containing 75 mL of MilliQ water. The Pt dish is also placed in the beaker thus ensuring that any small amounts of melt quench and fall off the dish into the water. A watch glass was quickly placed on the beaker to prevent spitting out of the beaker. Since the method uses

Radioactivity & Radiochemistry
Vol. 9, No. 3, 1998

internal standards however, any losses were not important. To prevent shattering of the beaker by the melt a Pt-dish lid was placed in the bottom of the beaker containing the water and the melt was poured onto this. The Pt lid was then removed and the resulting low-density frothy glass was broken up easily with a glass rod. The dish was removed with rinsing. The mixture was acidified with 50 mL of concentrated nitric acid and was placed with 14 other beakers on a 15-position multi-block heater/magnetic stirrer (Labortechnik, Germany). This was heated to 40 °C with constant stirring for 8 hours. The glass dissolves readily with boric acid and silica gel forming during the dissolution.

Removal of silica and boric acid

With the borate fusion technique all the silica remains in the melt and subsequently forms a gelatinous precipitate when the glass is digested with nitric acid. This is not the case with HF digestions of samples where any silica produces the volatile SiF_4. Polyethylene glycol (PEG-2000, M.Wt. 2000) was used to flocculate silica (Smith et al., 1995) which could otherwise impair the column chromatography. The PEG-2000 solution was added as 1 mL of a 0.2 M solution to each digestion mixture (nominally 100 mL 4 M HNO_3) prior to digestion of the glass. Digestion took approximately 4 hours and each sample was filtered under suction using Whatman GF-C filters. A smooth precipitate consisting of most of the silica and excess boric acid was effectively retained by the filter was washed with 30 mL of 8 M HNO_3.

Chromatographic separation of Pu and U

The chemical separation of Pu and U is based on the separation used by Warwick et al. (1998) for the determination of Pu and U in aqueous samples. The technique uses the commercial extraction material, UTEVA™ resin that extracts all tetravalent actinides including U and Pu from nitric acid solutions. Fe(III) is not extracted (K_d for U(VI) is a maximum of 200 in >8 M nitric acid). The resin can therefore be used to separate U from Fe. However, as Pu and Th will also be extracted, separation of these elements from U must be achieved using a separate stage prior to the UTEVA™ column separation. This is achieved by isolating Pu and Th on an anion-exchange column prior to passing the U fraction through the UTEVA™ column. The combination of anion-exchange resin columns and the UTEVA™ resin columns allows the efficient separation and purification of U and Pu from Fe and other actinides as well as from the sample matrix. The technique was further streamlined by operating the anion-exchange and UTEVA™ columns in tandem, i.e. the eluate from the anion column passed immediately onto the UTEVA™ column.

Following filtration, the sample (as an 8 M HNO_3 solution) was loaded directly onto a 5 x 1 cm ID Eichrom (100-200 #) anion-exchange resin column. Plutonium, Th and to a lesser extent U were retained on the ion-exchange column. The eluent from the anion column was passed directly onto a 1.0 x 0.5 cm ID UTEVA™ column. Any U eluting from the anion-exchange column was retained on the UTEVA™ column. Tests show that up to 150 mL of sample solution can be passed through both columns without significant breakthrough of Pu of U. The stacked anion/UTEVA™ columns were rinsed with 8 M HNO_3 and 3 M HNO_3 to ensure that all the U had been eluted onto the UTEVA™ column. The two columns were then separated. The anion-exchange column was washed with concentrated HCl to remove Th and Pu was eluted with NH_4I/HCl. Any residual U remaining on the column was not eluted with the Pu unless the HCl concentration in the NH_4I/HCl reagent was greater than 10 M (Nelson et al., 1964). The Pu fraction was evaporated to dryness and the residue treated with HNO_3 to decompose excess NH_4I. Plutonium was then electro-deposited from 2% ammonium oxalate solution and the source counted using alpha-particle spectrometry. Uranium was eluted from the UTEVA column with 5 mL of 0.02 M HCl. The U fraction from the UTEVA column contained organic residues following evaporation and this was unsuitable for mounting onto a TIMS filament. The U fraction was further purified by using a small anion-exchange column with the U being retained from 8 M HCl and eluted with 0.02 M HCl. If the U were being measured by alpha-particle spectrometry this clean-up stage would not be required.

Results and Discussion

The two NIST certified SRMs (Appendix 1), Rocky Flats soil SRM 4353 and Marine sediment SRM 4357 were analysed following sample attack by either leaching with aqua regia (double-attack), fusion using the fluoride/pyrosulphate technique or fusion using the borate technique as described above. The results for these analyses (Table 1) show that the borate fusion method is effective in quantitatively extracting U and Pu from soil and sediment samples.

Borate Fusion Followed by Ion-Exchange/Extraction Chromatography for the Rapid Determination of Pu and U in Environmental Materials

I.W. Croudace, P.E. Warwick, R.N. Taylor, S.J. Dee, J.A. Milton and J-S Oh

Process	Productivity Work Rate	Staff days
Sample preparation	20 samples per day	1
Fusions / digestions	24 samples per day	0.6
Chemical separation	16 samples per day	1
Pu -counting	24 samples per week	0.1
U mass spectrometry	70 samples per week	0.6

Table 1 Comparison of sample digestion methods.

Notes: The constraints on the above rates are the use of 8 Pt-Au dishes, one 8-channel alpha-particle spectrometer, and a 20-position turret on the TIMS.

Overall accuracy

The accuracy of the method was determined through the analysis of a number of certified reference materials. The results for this evaluation are shown in Table 2. A set of NIST depleted and enriched uranium standards (Appendix 1) were prepared and measured by TIMS (Table 3).

Precision of replicate analyses

Isotope ratios measurement

The precision of the borate fusion technique was determined through replicate analysis of the two reference materials supplied by NIST (Table 4). The uncertainty of a single filament loading on a TIMS is better than 0.3% whereas for replicate determinations precision is approximately 1% for SRM 4357 and 0.5% for SRM 4353 at the 95% confidence level. It should be noted that measurements on single filaments are made by ion counting five blocks of ten measurement sequences on the masses of interest (i.e., 234, 235, 236 and 238).

The measurement of ^{235}U is not normally performed on its own and any assessment of ^{235}U enrichment is more routinely performed by measuring the ratio of ^{235}U(or ^{234}U) to ^{238}U. In general the precision achievable at the 95% confidence level is approximately 10% (alpha-particle spectrometry), 1% (ICP-MS) and 0.2% (TIMS).

Concentration measurements

The overall method uncertainty for U concentration measurement by TIMS is calculated as 1.4-1.6% (at the 95% limit) and is mostly associated with the certified calibration uncertainty of the ^{236}U spike.

Blanks and method uncertainties

The procedural blank was determined by analysing 7 g of the eutectic borate flux using the method described above. In addition the blank associated with the column separations and the TIMS filament loading were also determined by either passing blank acids through the ion-exchange columns or loading filaments with blank acids again following standard procedures. The overall method blank was found to correspond to 50 ng ^{238}U compared with 100 ng ^{238}U for the fluoride/pyrosulphate method.

Sample throughput for the method

The following chart shows the rate at which various processes can occur. The constraints on throughput are mostly linked to the availability of equipment.

Conclusions

An accurate and highly precise method has been developed for the rapid and effective determination of uranium and plutonium isotope compositions in soils and other environmental materials. The procedure is novel in two ways, firstly for its borate fusion and secondly for its use of two stacked columns (ion-exchange and extraction chromatography) for the rapid separation of U and Pu. Measurement of U is by thermal ionisation mass spectrometry whereas Pu is measured using alpha-particle spectrometry. Over seven hundred soil, other environmental samples and reference samples have been processed and measured over a 10-week period (for U) showing the method to be very rapid when compared with more conventional approaches. The high precision isotopic ratio determinations of uranium and the safety benefits of the sample attack are a positive feature of the analytical scheme. The technique described has recently been extended to include the determination of other actinides (Th, Am, Np).

Acknowledgements

The authors thank the following for their help during this study: Prof. R.W. Nesbitt (Dept. of Geology, University of Southampton) for his generous donation of the TIMS for 3 months and L. Janes for sample preparation. This study was performed as part of a contract to survey the former USAF airbase at Greenham Common, Berkshire, UK and the surrounding area for alleged U and Pu contamination. It was funded by Newbury District Council and Basingstoke and Deane Borough Council. Any interest in the original published final technical report should be addressed to the lead author.

Radioactivity & Radiochemistry
Vol. 9, No. 3, 1998

Comparison of Sample Digestion methods
(in Bq/kg with 2s errors)

Sample	Double Aqua regia leach		Fluoride/pyrosulphate fusion		Borate fusion	
	$^{238+240}Pu$	^{238}U	$^{238+240}Pu$	^{238}U	$^{238+240}Pu$	^{238}U
NIST 4353	6.97 ± 0.50	20.60 ± 0.09	-	39.78 ± 0.14	7.84 ± 0.67	37.90 ± 0.16
NIST 4353	11.93 ± 0.83	20.70 ± 0.09	7.30 ± 0.70	40.01 ± 0.19	7.69 ± 0.58	38.32 ± 0.22
NIST 4357	10.89 ± 0.80	6.29 ± 0.01	-	15.15 ± 0.01	10.40 ± 0.73	14.46 ± 0.03
NIST 4357	7.22 ± 0.43	6.78 ± 0.01	9.30 ± 0.72	15.24 ± 0.02	11.05 ± 0.91	14.26 ± 0.03

Summary of method accuracy
(in Bq/kg with 2s errors)

	$^{238+240}Pu$		^{238}Pu		^{238}U	
Sample	Measured	Certified	Measured	Certified	Measured	Certified
NIST 4353	7.93 ± 0.62	8.03 ± 0.60	-	0.17	37.77 ± 0.40	38.9 ± 1.32
NIST 4357	9.9 ± 0.8	10.4 ± 0.1	2.29 ± 0.35	2.32 ± 0.06	14.41 ± 0.39	12
IAEA 134	16.8 ± 1.2	15	3.31 ± 0.45	3.1	n.a.	
IAEA 135	221 ± 10	213	43.4 ± 2.2	43	2.45 ± 0.05	2.4

Table 2 Summary of method accuracy.

Sample	Certified $^{238}U/^{235}U$ ratio	Measured $^{238}U/^{235}U$ ratio
NIST U-010	98.62	98.97 0.05
NIST U-005	196.46	196.65 0.15

Table 3 Uranium-238/235 ratios for U standards.

	NIST SRM 4353 Rocky Flats Soil	
	$^{239+240}Pu$ Bq/kg	^{238}U Bq/kg
Mean SD	7.93 0.62	37.77 0.40
N=6		

	NIST SRM 4357 Ocean Sediment		
	$^{239+240}Pu$	^{238}Pu	^{238}U
Mean SD	9.90 0.8	2.29 0.35	14.41 0.10
n=7			

Table 4 Precision determined on replicate analyses NIST standards.

References

1. H. Bennett and G. Oliver, *XRF analysis of ceramics, minerals and allied materials.* John Wiley, Chichester, UK., (1992).
2. Site A. Delle, V. Marchionni, C. Testa and C. Triulzi, "Radiochemical determination of plutonium in marine samples by extraction chromatography," *Anal. Chim. Acta*, 117, 217-224, (1989).
3. J.D. Fassett and W.R. Kelly, "Interlaboratory isotopic ratio measurement of nanogram quantities of uranium and plutonium on resin beads by thermal ionisation mass spectrometry," *Anal. Chem.*, 56, 550-556, (1984).
4. E.P. Horwitz, M.L. Dietz, R. Chiarizia., H. Diamond, S.L. Maxwell and M.R. Nelson, "Separation and preconcentration of actinides by extraction chromatography using a supported liquid anion exchanger: application to the characterization of high-level waste solutions," *Anal. Chim. Acta*, 310, 63-78, (1995).
5. G. Jia, C. Testa, D. Desideri and M.A. Meli, "Extraction-chromatographic method for the determination of plutonium-239+240 and plutonium-238 in soils with high natural radioactivity," *Anal. Chim. Acta*, 220, 103-110, (1989).
6. H. Levine, and A. Lamanna, "Radiochemical determination of plutonium-239 in low-level environmental samples by electrodeposition," *Health Physics*, 11, 117-125, (1965).
7. McCormick, "Thermal-ionisation mass spectrometry for small sample analysis of uranium and plutonium," *Appl. Radiat. Isot.*, 43, 271-278, (1992).
8. J.W.T. Meadows, J.S. Schweiger, B. Mendoza and R. Stone, "Procedure for plutonium analysis in large (100g) soil and sediment samples. In: Reference methods for marine radioactivity studies II. IAEA, Vienna, pp89-90, (1975).
9. F. Nelson, D.C. Michelson and J.H. Holloway, "Ion exchange procedures III. Separation of uranium, neptunium and plutonium," *J. Chromatog.*, 14, 258-260, (1964).
10. C.W. Sill, K.W. Puphal, F.D. Hindman, "Simultaneous determination of alpha-emitting nuclides of radium through californium in soil," *Anal. Chem.*, 46, 1725-1737, (1974).
11. L.L. Smith and J.S. Yaeger, "High-Pressure Microwave Digestion: A waste-minimization tool for the radiochemistry laboratory," *Radioact. Radiochem.*, 7 (2), 35-38, (1996).
12. L.L. Smith, F. Markun and Kate T. Ten, "Comparison of acid leachate and fusion methods to determine plutonium and americium in environmental samples," *Anal. Chem. Lab.*, Argonne National Laboratory. Argonne Report ANL/ACL 92/2; order number DE92019413, (1992).
13. L.L. Smith, J.S. Crain, J.S. Yaeger, E.P. Horwitz, H. Diamond and R. Chiarizia, "Improved separation method for determining actinides in soil samples," *J. Radioanal. Nucl. Chem., Articles*, 194, 151-156, (1995).
14. N.A. Talvitie, "Radiochemical determination of plutonium in environmental and biological samples by ion-exchange," *Anal. Chem.*, 43, 1827-1830, (1971).
15. R.N. Taylor, I.W. Croudace, P.E. Warwick and S.J. Dee, "Precise and rapid determination of $^{238}U/^{235}U$ and uranium concentration in soil samples using thermal ionisation mass spectrometry," *Chemical Geology*, 144, 73-80, (1998).
16. J. Thomson, "A total dissolution method for determination of the α-emitting isotopes of uranium and thorium in deep-sea sediments," *Anal. Chim. Acta.*, 142, 259-268, (1982).
17. J. Toole, A.S. Hursthouse, P. McDonald, K. Sampson, M.S. Baxter, R.D. Scott and K. McKay. *The determination of actinides in environmental samples by ICP-MS. In: Plasma Source Mass Spectrometry.* Eds. Jarvis, Gray, Williams and Jarvis., Royal Society Chemistry Special Pub., 85, 155-162, (1990).
18. P.E. Warwick, I.W. Croudace and A.A. Dale, "An optimised and robust method for the determination of uranium and plutonium in aqueous samples," *Applied Radiation & Isotopes*, (in press, 1998).

Radioactivity & Radiochemistry
Vol. 9, No. 3, 1998

Biographies

The Southampton Oceanography Centre

was formed through a partnership between the Natural Environmental Research Council and the University of Southampton. The Centre has brought together the university former departments of Oceanography and Geology, now the School of Ocean and Earth Science SOES, and the various branches of the former NERC Institute of Oceanographic Sciences.

Ian W. Croudace

is a Senior Research Fellow in SOES and has 25 years research experience and over 50 scientific publications and reports. He is the founding director of the Geosciences Advisory Unit, a consultancy group in SOES that specialises in environmental radioactivity research. He obtained his PhD in geochemistry from the University of Birmingham and subsequently undertook post-doctoral research at the University of Paris VI and at CEN Saclay before arriving at the Southampton to carry out research and teaching in analytical geochemistry in the earth sciences.

Southampton Oceanography Centre
Department of Geology
Geosciences Advisory Unit
European Way
Southampton, SO14 3ZH
United Kingdom
Phone: 44-1703-592780
Fax: 44-1703-596450
Email: iwc@soc.soton.ac.uk

Philip Warwick

is the senior radiochemist for the Geosciences Advisory Unit. He previously managed the Environmental and Biological Chemistry laboratory for the Atomic Energy Authority at Winfrith. He is a specialist in radiochemistry, has over 9 years research experience in environmental radiochemistry and is currently completing a doctoral thesis at the University of Southampton. He has written over 20 scientific papers and numerous scientific reports.

Rex Taylor

is a senior research fellow in SOES and has 10 years research experience and has published over 35 scientific papers. He obtained his PhD in geochemistry at Southampton and subsequently worked at the Universities of London and Southampton on petrological processes and analytical techniques in geochemistry. Research interests include the geochemistry of the ocean basalts, radiogenic isotope systematics of island arc magmatism and the development of thermal and plasma-source mass spectrometry techniques in the measurement of uranium and lead.

Steve Dee

currently works in the petroleum industry. He obtained a PhD in geochemistry from the University of Southampton. He has over 10 years research experience and has been involved in major departmental research programmes funded by the EEC and industry. He also works as a consultant to industry specialising in data processing. He has co-authored over 20 reports, has 8 scientific research papers and has held positions at the University of Southampton and the University of Leeds.

J. Andy Milton

is a post-doctoral research fellow and is currently the manager of the laser ICP-MS facility at the Southampton Oceanography Centre. He obtained a PhD in organic chemistry in 1993 from the University of Southampton. His interests are primarily concerned with analytical geochemistry.

Jung-Suk Oh

is a graduate student working towards a PhD on the accumulation and migration of transuranic and other radionuclides in the Ravenglass saltmarsh. He holds an MSc in oceanography from Southampton and a BS from South Korea.

SOUTHAMPTON UNIVERSITY LIBRARY

USER'S DECLARATION

AUTHOR: JUNG-SUK OH

TITLE: THE MIGRATION AND ACCUMULATION OF RADIONUCLIDES IN THE RAVENGLASS SALTMARSH, CUMBRIA, U.K

DATE: 1999

I undertake not to reproduce this thesis, or any substantial portion of it, or to quote extensively from it without first obtaining the permission, in writing, of the Librarian of the University of Southampton.

To be signed by each user of this thesis

DATE	SIGNATURE	ADDRESS